UNIVERSIDAD NACIONAL AUTÓNOMA DE MÉXICO
POSGRADO EN CIENCIAS FÍSICAS
INSTITUTO DE FÍSICA

Divisibility classes of qubit maps and singular Gaussian channels

TESIS

QUE PARA OPTAR POR EL GRADO DE:
DOCTOR EN CIENCIAS (FÍSICA)

PRESENTA:
DAVID DÁVALOS GONZÁLEZ

Director de Tesis:
Dr. Carlos Francisco Pineda Zorrilla
Instituto de Física
Codirector de Tesis:
Dr. Mario Ziman
Instituto de Física, Academia Eslovaca de Ciencias

Miembros del comité tutor:
Dr. Carlos Francisco Pineda Zorrilla
Instituto de Física
Dr. Luis Benet Fernández
Instituto de Ciencias Físicas
Thomas Henry Seligman Schurch
Instituto de Ciencias Físicas

Ciudad Universitaria, Ciudad de México, Enero 2020

pcf
posgrado en ciencias físicas
u n a m

UNIVERSIDAD NACIONAL AUTÓNOMA DE MÉXICO
POSGRADO EN CIENCIAS FÍSICAS

Divisibility classes of qubit maps and singular Gaussian channels

TESIS

Que para obtener el grado de:	Doctor en Ciencias (Física)
Presenta:	David Dávalos González
Director de tesis:	Dr. Carlos Francisco Pineda Zorrilla
Codirector:	Dr. Mario Ziman

Miembros del Comité Tutoral:
Dr. Carlos Pineda, Dr. Luis Benet, y Dr. Thomas H. Seligman

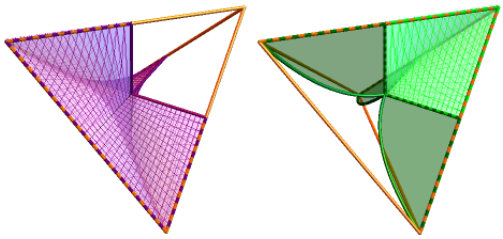

México D. F., 2019

pcf
posgrado en ciencias físicas
u n a m

UNIVERSIDAD NACIONAL AUTÓNOMA DE MÉXICO
POSGRADO EN CIENCIAS FÍSICAS

Divisibility classes of qubit maps and singular Gaussian channels

THESIS

To obtain the degree:	Doctor en Ciencias (Física)
Presents:	David Dávalos González
Director:	Dr. Carlos Francisco Pineda Zorrilla
Co-director:	Dr. Mario Ziman

Members of the Tutorial Committee:
Dr. Carlos Pineda, Dr. Luis Benet, and Dr. Thomas H. Seligman

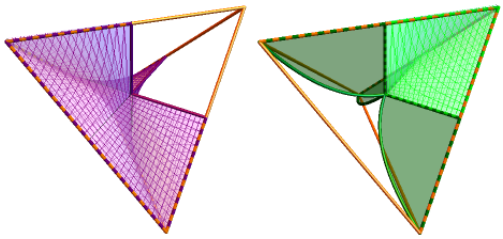

México D. F., 2019

Truth is ever to be found in simplicity, and not in the multiplicity and confusion of things.
Isaac Newton

Gracias

La idea que nació cuando cursaba la secundaría, la de convertirme algún día en científico, no habría sido posible de no haber nacido en el seno de una familia estable, funcional y de sólidos valores. Por eso les agradezco infinitamente a mis queridos Padres. A mi Madre, Sara, por dedicarme tanto de su tiempo y energía, por ser una Madre muy amorosa, llena de valores y por ser la persona mas paciente del mundo. Le agradezco a mi Padre, Juan Manuel, por siempre estar atento a que fuera una persona de principios y un buen ciudadano, por ser un padre amoroso y por darme su confianza. Le agradezco que siempre se haya preocupado por tener una computadora en casa y por ser un entusiasta de la tecnología, eso aportó fundamentalmente a quien soy hoy. A mis hermanas y hermanos por preocuparse por mi y por regalarme tantas veces su tiempo. A mi compañera de vida, a mi esposa Lorena, gracias por tenerme tanta paciencia, por creer en mi y por quererme tanto. A mi tutor y amigo, Carlos, le agradezco su paciencia, sus valiosas enseñanzas, su gran apoyo y su amistad. A Thomas Seligman y Luis Benet por siempre apoyarme. Le agradezco a mis amigos Luis Juarez, Arturo Carranza, Thomas Gorin, Mario Ziman, Diego Wisniacki, Ignacio García Mata, Juan Diego Urbina, Peter Rapčan, Tomáš Rybár, Edgar Aguilar, David Amaro, Alvaro Díaz, Miguel Cardona, Chayo Camarena, Antonio Rosado, Sergio Sánchez, Nephtalí Garrido, Sergio Pallaleo, Samuel Rosalio. A mis gatitos Lola y Dalí por hacerme feliz el poco tiempo que estuvieron en este mundo. A mi querida gatita Lulú por hacer de mi hogar siempre un lugar feliz. Les agradezco a todos los seres queridos que hicieron de esta parte de mi trayectoria algo memorable.

Agradezco el apoyo brindado por los proyectos PAPIIT número IG100518 y CONACYT CB-285754.

SYNOPSIS

We present two projects concerning the main part of my PhD work. In the first one we study quantum channels, which are the most general operations mapping quantum states into quantum states, from the point of view of their divisibility properties. We introduced tools to test if a given quantum channel can be implemented by a process described by a Lindblad master equation. This in turn defines channels that can be divided in such a way that they form a one-parameter semigroup, thus introducing the most restricted studied divisibility type of this work. Using our results, together the study of other types of divisibility that can be found in the literature, we characterized the space of qubit quantum channels. We found interesting results connecting the concept of entanglement-breaking channel and infinitesimal divisibility. Additionally we proved that infinitely divisible channels are equivalent to the ones that are implementable by one-parameter semigroups, opening this question for more general channel spaces. In the second project we study the functional forms of one-mode Gaussian quantum channels in the position state representation, beyond Gaussian functional forms. We perform a *black-box* characterization using complete positivity and trace preserving conditions, and report the existence of two subsets that do not have a functional Gaussian form. The study covers as particular limit the case of singular channels, thus connecting our results with the known classification scheme based on canonical forms. Our full characterization of Gaussian channels without Gaussian functional form is completed by showing how Gaussian states are transformed under these operations, and by deriving the conditions for the existence of master equations for the non-singular cases.

Keywords: divisibility, qubit channels, open quantum systems.

RESUMEN

En esta tesis se presentan dos proyectos realizados durante mis estudios de doctorado. En el primero se estudian los canales cuánticos, que son las operaciones más generales que transforman estados cuánticos en estados cuánticos, desde el punto de vista de sus propiedades de divisibilidad. Introducimos herramientas para probar si un canal cuántico dado puede ser implementado por un proceso descrito por una ecuación maestra de Lindblad. Ésto a su vez define a los canales que pueden ser divididos de tal manera que ellos forman semigrupos de un parámetro, introduciendo entonces el tipo más restringido de divisibilidad estudiado de este trabajo. Usando nuestros resultados, junto con el estudio de otros tipos de divisibilidad que pueden ser encontrados en la literatura, caracterizamos el espacio de canales cuánticos de un qubit. Encontramos resultados interesantes que conectan el concepto de canales que rompen el entrelazamiento (del sistema con cualquier sistema auxiliar) y el de divisibilidad infinitesimal. Además probamos que el conjunto de canales infinitamente divisibles es equivalente al de los canales implementables por semigrupos de un parámetro. Ésto abre la pregunta sobre si esto sucede para espacios de canales más generales. En el segundo proyecto estudiamos las formas funcionales de canales Gaussianos de un solo modo, más allá de la forma funcional Gaussiana. Se hace una caracterización de *caja negra* utilizando las condiciones de completa positividad y preservación de la traza, y se reporta la existencia de dos subconjuntos que no poseen forma funcional Gaussiana. El estudio cubre en particular el límite de los canales singulares, conectando entonces nuestros resultados con la la clasificación basada en formas canónicas. Nuestra caracterización de canales Gaussianos sin forma funcional Gaussiana es completada mostrando como los estados Gaussianos se transforman bajo esas operaciones, así como al derivar las condiciones para la existencia de ecuaciones maestras para los casos no singulares.

Contents

Chapter 1

Introduction

In questions of science, the authority of a thousand is not worth the humble reasoning of a single individual.
Galileo Galilei

The advent of quantum technologies opens questions aiming for deeper understanding of the fundamental physics beyond the idealized case of isolated quantum systems. Also the well established Born-Markov approximation used to describe open quantum systems (e.g. relaxation process such as spontaneous decay and decoherence) is of limited use and a more general framework of open system dynamics is required. Recent efforts in this area have given rise to relatively novel research subjects - non-markovianity and divisibility.

A central object of study in quantum information theory and open quantum systems are quantum channels, also called quantum operations. They describe, for instance, the noisy communication between Alice and Bob or the changes that an open quantum system undergoes at some fixed time. They can also be seen as the basic building blocks of time-dependent quantum processes (also called quantum dynamical maps). Conversely, families of quantum channels arise naturally given a quantum dynamical map.

Given a quantum channel, for instance an spin flip or the approximation of the universal NOT gate, one can wonder about how it can be implemented. The latter in the sense of, being quantum channels discrete operations, can we find a continuous time-dependent processes that at some time it implements the given channel?, or, does process such that we "just wait for a relaxation of the physical system" implements such channel? It turns that this question is related with the

one of finding simpler operations such that their concatenation equals the given quantum channel [WC08]. Such operations are simpler in the sense that they are closer to the subset of unitary operations, or even "smaller" in the sense that they are closer to the identity channel.

This thesis encompasses the results of two works developed during my PhD.

The first and the most extended one was devoted to study the divisibility properties of quantum channels (discrete evolutions of quantum systems), for the particular case of qubits. We revise the divisibility types introduced in the seminal paper by Wolf et al. [WC08] and derived several useful relations to decide each type of divisibility. In particular, we characterize channels that can be divided in such a way that they belong to one-parameter semigroups (dynamics described by Lindblad master equations), and extended the analysis of [WECC08] for channels with negative eigenvalues. We did this using the results by Evans et al. [EL77] and Culver [Cul66].

Beyond the mentioned characterization tools, the principal aim of the work was to understand the forms of non-markovianity standing behind the observed quantum channels. The non-markovianity character describe the back-action of the system's environment on the system's future time evolution. Such phenomena is identified as emergence of memory effects [ARHP14, VSL$^+$11, PGD$^+$16]. On the other side, divisibility questions the possibility of splitting a given quantum channel into a concatenation of other quantum channels. In this work we will investigate the relation between these two notions. Thus, we related features of of continuous time evolutions of quantum systems, and the concept of divisibility of quantum maps, which are discrete evolutions. A very first example of this is the well known identification of one-parameter semigroups with Linbladian dynamics [Lin76].

The second project is devoted to representation theory of continuous-variable quantum systems, which is a central topic of study given its role in the description of physical systems like the electromagnetic field [CLP07], solids and nanomechanical systems [AKM14] and atomic ensembles [HSP10]. In this theory the simplest states, both from a theoretical an experimental point of view, are the so-called Gaussian states. An operation that transforms such family of states into itself is called a Gaussian quantum channel (GQC). Even though Gaussian states and channels form small subsets among general states and channels, they have proven to be useful in a variate of tasks such as quantum communication [GVAW$^+$03], quantum computation [LB99] and the study of quantum entanglement in simple [BvL05] and complicated scenarios [LRW$^+$18]. In this project we study the possible functional forms that one-mode Gaussian quantum channels can have

in the position state representation, and characterize the particular case of singular channels. Although they are already characterized by their action on the first and second moments of Gaussian states [Hol07, WPGP$^+$12], we connect our framework to such known results. Additionally we give an insight of the possible functional forms of, for instance, Gaussian unitaries.

The thesis is organized as follows: In chapter 2 we discuss the most widely adopted scheme to study open quantum systems, introducing the formalism of bipartite systems and useful tools for it. Later on we present the general setting for system plus reservoir dynamics and its formal solution. As a paradigmatic example of open system dynamics, we present briefly the microscopic derivation of the Lindblad master equation using the well known Born-Markov approximation, and discuss the properties of the generator of the dynamics. Subsequently we introduce the formalism of quantum channels, being the most general operations over quantum systems (excluding post-selection), by introducing some useful mathematical definitions and contrasting with its classical analog. Additionally we discuss briefly the concept of *local operations and classical communications* (LOCC), also known as filtering operations. Finally we give a very brief introduction to continuous variable systems, giving special attention to Gaussian states and channels.

In chapter 3 we discuss the different available representations for quantum channels and their relation with the concept of complete positivity. In particular we introduce the well known Kraus representation and discuss the Choi-Jamiołkowski theorem which in turn defines a very useful representation to study quantum channels and their divisibility properties. Later on we introduce various matrix representations of quantum channels, paying special attention to hermitian and traceless bases types (without taking into account the component proportional to identity). Furthermore we introduce useful decompositions of qubit channels into unitary conjugations and one-way stochastic local operations, and classical communication, both being analogous to the well known singular value decomposition. Finally we give an introduction to representations of Gaussian channels and a detailed derivation of the position-state representations for Gaussian channels without Gaussian functional form.

In chapter 4 we give the definition of divisible quantum channel, as well the definition of various subclasses of divisible channels concerning additional properties. In particular we discuss the concepts of infinitesimal and infinitely divisible channels and some relations and inclusions between them. Among infinitesimal divisible channels we identify two subclasses, being the set of infinitesimal divisible channels in complete positive and positive (but not complete positive) maps.

Later on we introduce the concept of L-divisible channels, defining the set of channels which are members of one-parameter semigroups. We show that the set of infinitely divisible channels is the same of the L-divisible Pauli channels.

In chapter 5 we study one-mode Gaussian quantum channels in continuous-variable systems by performing a *black-box* characterization using complete positivity and trace preserving conditions, and report the existence of two subsets that do not have a functional Gaussian form. Our study covers as particular limit the case of singular channels, thus connecting our results with their known classification scheme based on canonical forms. Our full characterization of Gaussian channels without Gaussian functional form is completed by showing how Gaussian states are transformed under these operations, and by deriving the conditions for the existence of master equations for the non-singular cases.

In chapter 6 we give a summary of the two projects introduced in this work and conclusions.

Finally, in the appendix A we prove that the exact reduced dynamics of an open quantum system never follow a Lindblad master equation unless they are unitary, given a bounded global Hamiltonian. In appendix B we give an example that shows that the set of Lorentz normal forms introduced in the literature, is incomplete. In the appendix C we attach copies of the articles produced during my PhD.

Chapter 2

Open quantum systems and quantum channels

When we talk mathematics, we may be discussing a secondary language built on the primary language of the nervous system.
John Von Neumann

In this chapter we introduce the usual scheme to study open quantum systems, the widely known Born-Markov approximation and the concept of CP-divisibility. Later on and based on the idea of *(classical) stochastic map*, we discuss the axiomatic formulation of quantum channels and its connection with the usual construction of open quantum systems. Finally, for continuous variable systems, we discuss the paradigmatic example of Gaussian channels.

2.1 Introduction to the scheme of open quantum systems

The most widely used scheme to study open quantum systems is based on the idea of study a closed system composed by the *central system* and its *environment*, see fig. 2.1 for an schematic explanation. Thus, concepts as bipartite Hilbert spaces, density matrix and partial trace are useful tools to study open systems. In what follows we give a brief review of them.

Bipartite Hilbert space. Consider a bipartite closed quantum system described by a Hilbert space with the structure $\mathscr{H} = \mathscr{H}_{\mathrm{S}} \otimes \mathscr{H}_{\mathrm{E}}$, where $\mathscr{H}_{\mathrm{S}}$ is the Hilbert

space of the open system and $\mathscr{H}_{\mathrm{E}}$ is the Hilbert space of the *environment*. If $\{|\phi_i^{\mathrm{S}}\rangle\}_{i=1}^{\dim(\mathscr{H}_{\mathrm{S}})}$ and $\{|\phi_i^{\mathrm{E}}\rangle\}_{i=1}^{\dim(\mathscr{H}_{\mathrm{E}})}$ are basis for the spaces $\mathscr{H}_{\mathrm{S}}$ and $\mathscr{H}_{\mathrm{E}}$, respectively, a basis for $\mathscr{H}$ is simply $\{|\phi_i^{\mathrm{S}}\rangle \otimes |\phi_j^{\mathrm{E}}\rangle\}_{i=1,j=1}^{\dim(\mathscr{H}_{\mathrm{S}}),\dim(\mathscr{H}_{\mathrm{E}})}$. It is typical that for finite dimensional systems one has that $\dim(\mathscr{H}_{\mathrm{E}}) \gg \dim(\mathscr{H}_{\mathrm{S}})$ as the environment is usually "bigger" than the central system.

To describe the states of open quantum systems it is necessary to model the *ignorance* that the observer has with respect to the open system. Since the experimentalist cannot access the degrees of freedom of the environment, they are simply ignored. To do this we need the two following concepts.

Density matrix. Let a quantum system that has probability p_i to be in the state $|\phi_i\rangle$, and let the operator A an observable over such system. Using the average formula $\langle A\rangle = \sum_i p_i \langle\phi_i|A|\phi_i\rangle$ it is straightforward to show that $\langle A\rangle = \mathrm{tr}\,(A\rho)$ with

$$\rho = \sum_i p_i |\phi_i\rangle\langle\phi_i|, \tag{2.1}$$

and $\sum_i p_i = 1$. ρ is called *density operator* or *density matrix*. Note that ρ is a positive-semidefinite operator given that $p_i \geq 0$, and the states $|\phi_i\rangle$ don't need to be orthogonal. Also note that since ρ is hermitian, together with positive-semidefiniteness, implies that we can always write any density matrix as in eq. (2.1) with the states $|\phi_i\rangle$ being orthogonal. Thus, every operator ρ acting on a Hilbert space $\mathscr{H}$, fulfilling $\rho \geq 0$, $\rho = \rho^\dagger$ and $\mathrm{tr}(\rho) = 1$ is a density matrix. The set of density matrices will be denoted along this work as $\mathscr{S}(\mathscr{H})$.

Comparing the notion of density matrices with the notion of state vectors in the Hilbert space $|\psi\rangle \in \mathscr{H}$, density matrices describe physical systems where the observer has an *incomplete* knowledge of the system's state. Thus, while state vectors are naturally equipped with *intrinsic* or *quantum* probabilities, density operators are additionally equipped with *classical* probabilities. The density matrices enjoying the form $\rho = |\psi\rangle\langle\psi|$, or equivalently $\rho^2 = \rho$, i.e. projectors, are *pure states*. It is clear that in this case the system is prepared in the state $|\psi\rangle$ with probability one.

A useful quantity to characterize quantum states is the *purity*, defined as

$$P(\rho) = \mathrm{tr}\left(\rho^2\right). \tag{2.2}$$

It ranges from $\dim(\mathscr{H})^{-1}$ to 1; 1 is obtained for pure states and $\dim(\mathscr{H})^{-1}$ for the complete mixture $\mathbb{1}/\dim(\mathscr{H})$.

Additionally the set $\mathscr{S}$ is convex, i.e. any convex combination of density matrices is another density matrix, in the same way as classical distributions do. In fact, mixed states ($P(\rho) < 1$) can be written always as convex combinations of pure states, see eq. (2.1). Furthermore the set $\mathscr{S}(\mathscr{H})$ is a subset of the bigger set of *trace-class* operators, $\mathscr{T}(\mathscr{H})$, defined as the ones containing operators with finite trace norm. The latter is defined as $|\Delta|_{\text{tr}} = \text{tr}\sqrt{A^\dagger A}$. This set is in turn a subset of the set of bounded operators $\mathscr{B}(\mathscr{H})$, containing operators with finite *operator norm*, defined as $|A|_{\text{op}} = \sup_{|\psi\rangle} |A|\psi\rangle|$, where $|A|\psi\rangle| = \sqrt{(\langle A\psi|A\psi\rangle)}$, i.e. the standard Hilbert space norm, with normalized vectors $|\psi\rangle$.

It is worth to note that for the finite dimensional, bounded operators always have finite trace norm and vice versa, thus $\mathscr{T}(\mathscr{H}) = \mathscr{B}(\mathscr{H})$. But the identification of such sets is relevant for infinite dimensional systems, where counter-examples of the non-equivalence of such sets exist [HZ12]. Additionally $\mathscr{B}(\mathscr{H})$ is the dual space of $\mathscr{T}(\mathscr{H})$ under the Hilbert-Schmidt product, defined as $\langle A, B\rangle = \text{tr}(A^\dagger B)$ [Hol01].

Now, to ignore the degrees of freedom of the unaccessible part of the system, we have to perform an operation in a very analogous way as computing marginal distributions in classical probability theory. For density operators this introduces the concept of partial trace.

Partial trace. Let $\rho \in \mathscr{S}(\mathscr{H}_\text{A} \otimes \mathscr{H}_\text{B})$ and $\mathscr{H}_\text{A,B}$ the Hilbert spaces of systems A and B. Thus, ρ describes a state of a bipartite system composed by A and B. If we want to know the state of the system A alone, one performs a partial trace over B defined as

$$\rho_A = \text{tr}_B(\rho_{AB}) = \sum_{i=1}^{d_\text{B}} \left(\mathbb{1} \otimes \langle \phi_i^\text{B}|\right) \rho_{AB} \left(\mathbb{1} \otimes |\phi_i^\text{B}\rangle\right),$$

where $\{|\phi_i^\text{B}\rangle\}_{i=1}^{d_\text{B}}$ is a complete orthonormal basis on $\mathscr{H}_\text{B}$. The resulting operator ρ_A is a density matrix describing the state of the system A alone. It is trivial to show that it is a density operator. A similar formula holds for ρ_B. An alternative definition is $\text{tr}_B(A \otimes B) = A\,\text{tr}(B)$ plus linearity.

In general for composite systems, in a pure state, knowing the reduced states (for instance for bipartite systems, ρ_A and ρ_B) is in general not enough to know the whole state of a system. This captures the *non-local* nature of quantum correlations, demanding simultaneous measurements on both parts of the system. In such case we say that the subsystems A and B are entangled. To see this, consider the example of the Bell state $|\Omega\rangle = 1/\sqrt{2}\,(|00\rangle + |11\rangle)$, where $\{|0\rangle, |1\rangle\}$ is an orthogonal basis of a qubit system. It is trivial to show that $|\Omega\rangle$ cannot be written

as $|\phi\rangle \otimes |\psi\rangle$, a factorizable state, prohibiting the observer to know the state of the whole system only by non-simultaneous measurements on A and B (described by reduced density matrices). In fact it is easy to show that $\rho_{A,B} = \mathbb{1}/2$ are the reduced density matrices, appearing also when the total state is $\rho_{AB} = \mathbb{1}/4$. For composite systems in mixed states the situation is quite different. In this case simultaneous measurements are needed to access classical correlations. To see this consider the state

$$\rho_{\mathrm{AB}} = \sum_i p_i \rho_{\mathrm{A}}^i \otimes \rho_{\mathrm{B}}^i, \tag{2.3}$$

being a convex combination of factorizable mixed states. This state is a mixed separable state [HHHH09], i.e. subsystems A and B are not entangled. Notice now that performing only local non-simultaneous measurements, the accessible reduced states are $\rho'_{A,B} = \sum p_i \rho^i_{A,B}$. This state also arise when the total system is in the factorizable state $\rho'_{\mathrm{A}} \otimes \rho'_{\mathrm{B}}$. Therefore local simultaneous measurements are needed.

2.1.1 System plus reservoir dynamics

The most widely used scheme to study open quantum systems is to consider a bipartite system, where the central system S, is interacting with its environment, E. The full system $\mathrm{S}+\mathrm{E}$ undergoes a closed system evolution, i.e. Hamiltonian dynamics, see fig. 2.1. The *total Hamiltonian* H, describing the whole system, has the following general structure

$$H = H_{\mathrm{S}} + H_{\mathrm{E}} + V, \tag{2.4}$$

where $H_{\mathrm{S,E}}$ are the free Hamiltonians of the central system and the environment, respectively, and V is the interaction Hamiltonian among them. Now let $\rho_{\mathrm{SE}}(0)$ be the state of the total system at the time $t = 0$. Thus, the state of the system S at the time t is simply:

$$\rho_{\mathrm{S}}(t) = \mathrm{tr}_{\mathrm{E}} \left(U(t) \rho_{\mathrm{SE}}(0) U^{\dagger}(t) \right), \tag{2.5}$$

where $U(t) = e^{-\mathrm{i}Ht}$ (taking $\hbar = 1$) and tr_{E} is the partial trace over the environmental degrees of freedom. Note that for a general initial state $\rho_{\mathrm{SE}}(0)$, where one allows classical and quantum correlations, $\rho_{\mathrm{SE}}(t)$ depends on general on initial information about the environment and its correlations with the central system S. Thus, to compute the dynamics of the central system such that we end up to universal reduced dynamics, i.e. the same for every initial state and independent of the initial information in the environment, we take a factorized initial

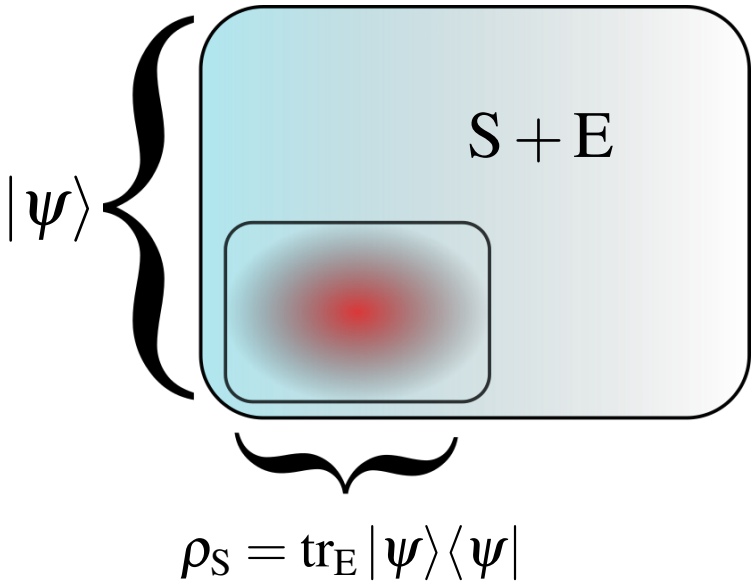

Figure 2.1: Diagram of the scheme to study open quantum systems. The letters S and E state for the *open (or central) system* and *environment* parts of the total closed system, $S+E$. The latter is described (typically) by a pure state $|\psi\rangle \in \mathscr{H}_S \otimes \mathscr{H}_E$ and the central system is described by the reduced state computed using the partial trace over the environmental degrees of freedom, see main text.

state $\rho_{SE}(0) = \rho_S(0) \otimes \rho_E$ [BP07, RH12]. We don't write explicitly the time-dependence of the environmental state since one is not usually interested on its evolution. With the choice of a factorizable total initial state and using equation eq. (2.5), we have the following expression for the evolution of the central system,

$$\rho_S(t) = \mathrm{tr}_E \left[U(t) \left(\rho_S(0) \otimes \rho_E \right) U^\dagger(t) \right]. \tag{2.6}$$

Therefore we have that the dynamics over S only depend on the total Hamiltonian H and the environmental initial state ρ_E, whereas $\rho_S(t)$ depends only on its initial condition.

Hence the equation eq. (2.6) defines a dynamical map, $\mathscr{E}_t$, parametrized by t. . Thus, we have

$$\mathscr{E}_t[\rho(0)] = \mathrm{tr}_E \left[U(t) \left(\rho_S(0) \otimes \rho_E \right) U^\dagger(t) \right]. \tag{2.7}$$

Such map possesses all the information concerning the dynamics of the system S, thus knowing $\mathscr{E}_t$ one can know entirely the evolution of the system S. The map

$$\begin{array}{ccc} \rho_{\mathrm{S}}(0)\otimes\rho_{\mathrm{E}} & \xrightarrow{U(t)\cdot U^{\dagger}(t)} & \rho_{\mathrm{SE}}(t) \\ \big\downarrow{\scriptstyle \mathrm{tr}_{\mathrm{E}}(\cdot)} & & \big\downarrow{\scriptstyle \mathrm{tr}_{\mathrm{E}}(\cdot)} \\ \rho_{\mathrm{S}}(0) & \xrightarrow{\quad\mathscr{E}_t\quad} & \rho_{\mathrm{S}}(t) \end{array}$$

Figure 2.2: Scheme of the equivalences between the concept of dynamical map and the theory of open quantum systems.

$\mathscr{E}_t$ can be obtained numerically or experimentally (depending on the context) by measuring only the system S by *quantum process tomography* [NC11]. In fig. 2.2 we present a schematic description of the two equivalent schemes under which the system S evolves, and their connection throughout tr_{E}.

Eq. (2.7) can be reduced, by writing $\rho_{\mathrm{E}} = \sum_j p_j^{\mathrm{E}} |\phi_j^{\mathrm{E}}\rangle\langle\phi_j^{\mathrm{E}}|$, in the following way,

$$\mathscr{E}_t[\rho_{\mathrm{S}}(0)] = \sum_{i,j} K(t)_{i,j}\rho_{\mathrm{S}}(0)K(t)_{i,j}^{\dagger}, \tag{2.8}$$

where the operators $K(t)_{ij} = \sqrt{p_j^{\mathrm{E}}}\langle\phi_i^{\mathrm{E}}|U(t)|\phi_j^{\mathrm{E}}\rangle$ are called Kraus operators and act upon the system S alone [RH12]. The expression of eq. (2.8) is called *sum represention*, also called Kraus representation of the map $\mathscr{E}_t$, this will be retaken on chapter 3.

Now let us discuss the differential equation for the density matrix of an open quantum system. The total state of the system evolves according to the *Von Neumann equation* [BP07],

$$\frac{d\rho_{\mathrm{SE}}}{dt} = -\mathrm{i}[H, \rho_{\mathrm{SE}}], \tag{2.9}$$

which is the analog of the Liouville equation describing the evolution of a classical distribution in the phase space.

Taking the partial trace on both sides of eq. (2.9) one arrives to the following:

$$\begin{aligned} \frac{d\rho_{\mathrm{S}}}{dt} &= -\mathrm{i}\,\mathrm{tr}[H, \rho_{\mathrm{SE}}] \\ &= L_t[\rho_{\mathrm{S}}], \end{aligned} \tag{2.10}$$

where L_t is the generator of the master equation of the system S. Integrating time in both sides from $\tau = 0$ to $\tau = t$, we arrive to the equivalent integral equation:

$$\rho_{\mathrm{S}}(t) = \rho_{\mathrm{S}}(0) + \int_0^t d\tau L_\tau[\rho_{\mathrm{S}}(t)]. \tag{2.11}$$

To compute the formal solution of this equation, we use the method of successive approximations. This consists on substituting the whole expression for $\rho_{\mathrm{S}}(t)$ defined by the right hand side of eq. (2.11). A first iteration leads to

$$\rho_{\mathrm{S}}(t) = \rho_{\mathrm{S}}(0) + \int_0^t d\tau_1 L_{\tau_1}[\rho_{\mathrm{S}}(0)] + \int_0^t d\tau_1 \int_0^t d\tau_2 L_{\tau_1}[L_{\tau_2}[\rho_{\mathrm{S}}(t)]]. \tag{2.12}$$

Repeating this procedure infinite times, i.e. substituting $\rho_{\mathrm{S}}(t)$ defined by the right hand side of the last equation in its second integrand several times, we arrive to a power series solution for $\rho_{\mathrm{S}}(t)$ (powers of L_t). This leads to the well known Dyson series for L_t. Compactly,

$$\rho(t) = \vec{\mathrm{T}} \exp\left(\int_0^t ds L_s\right) \rho(0) \tag{2.13}$$

with $\vec{\mathrm{T}}$ the time-ordering operator, defined as

$$\vec{\mathrm{T}}[H(\tau_1)H(\tau_2)] = \theta(\tau_1 - \tau_2)H(\tau_1)H(\tau_2) + \theta(\tau_2 - \tau_1)H(\tau_2)H(\tau_1),$$

with $\theta(x)$ the Heaviside step function. Eq. (2.13) constitutes the formal solution to the Von Neumann equation with generator L_t, and we can easily identify $\mathscr{E}_t = \vec{\mathrm{T}} \exp\left(\int_0^t ds L_s\right)$.

2.1.2 Born-Markov approach: microscopic derivation

In general the form of the generator L_t, given a global Hamiltonian, can be quite involved [BP07], but in the limit of *weak coupling* and *short memory* we can perform the very widely known *Born-Markov approximation*. A brief discussion is presented in this subsection.

The Born-Markov approximation leads to the *Lindblad master equation*. We will briefly overview its usual textbook derivation. The first step is to use the interaction picture, hence the total Hamiltonian becomes $H_I(t) = e^{\mathrm{i}H_0 t} H e^{-\mathrm{i}H_0 t}$, where $H_0 = H_{\mathrm{S}} + H_{\mathrm{E}}$ is the *free* Hamiltonian. Assuming that the dimension of $\mathscr{H}_{\mathrm{E}}$ is big compared with the dimension of $\mathscr{H}_{\mathrm{S}}$, the weak coupling limit leads to negligible changes in the environmental state. Thus, at time t we can approximate

$$\rho_{\mathrm{SE}}(t) \approx \rho_{\mathrm{S}}(t) \otimes \rho_E.$$

In other words, the state of the total system is left always approximately uncorrelated, while the state of the environment is never updated. Therefore the environment *forgets* any information about the central system, while the state of the

latter undergoes a non-trivial evolution. Additionally to simplify the derivation we choose ρ_{E} a stationary state of H_{E}, i.e. $[H_{\mathrm{E}}, \rho_{\mathrm{E}}] = 0$ [RH12]. ρ_{E} is typically chosen as a thermal state of the environmental Hamiltonian, $\rho_{\mathrm{E}} \propto \exp(-\beta H_{\mathrm{E}})$, with $\beta = 1/(k_{\mathrm{B}}T)$, k_{B} the Boltzmann constant and T the environment temperature.

Now, in the interaction picture the Von Neumann equation becomes

$$\frac{d\rho_{\mathrm{S}}}{dt} = -\mathrm{i}\,\mathrm{tr}_{\mathrm{E}}[V_{\mathrm{I}}(t), \rho_{\mathrm{S}}], \tag{2.14}$$

where $V_{\mathrm{I}}(t) = e^{\mathrm{i}H_0 t} V e^{-\mathrm{i}H_0 t}$ and the state $\rho_{\mathrm{S}}(t)$ are now written in the interaction picture. Inserting $\rho_{\mathrm{S}}(t)$ from its integral equation eq. (2.11) in the differential equation (2.14) and assuming $\mathrm{tr}_{\mathrm{E}}[V_{\mathrm{I}}(t), \rho_{\mathrm{S}} \otimes \rho_{\mathrm{E}}] = 0$ [BP07], we obtain

$$\frac{d\rho_{\mathrm{S}}}{dt} = -\int_0^t d\tau\, \mathrm{tr}_{\mathrm{E}}[V_{\mathrm{I}}(t), [V_{\mathrm{I}}(\tau), \rho_{\mathrm{S}}(\tau) \otimes \rho_{\mathrm{E}}]]. \tag{2.15}$$

If we assume that the dynamics of the state of the central system does not depend on its past, we can change $\rho_{\mathrm{S}}(\tau)$ to $\rho_{\mathrm{S}}(t)$, this is called the *Markovian approximation*. Additionally doing the variable change $\tau' = t - \tau$, we arrive to

$$\frac{d\rho_{\mathrm{S}}}{dt} = -\int_0^t d\tau'\, \mathrm{tr}_{\mathrm{E}}[V_{\mathrm{I}}(t), [V_{\mathrm{I}}(t-\tau'), \rho_{\mathrm{S}}(t) \otimes \rho_{\mathrm{E}}]], \tag{2.16}$$

this equation is known as Redfield equation [Red65] and it is local in time [BP07]. Assuming that the time scale on which the central system varies appreciably is much larger than the time on which the correlations of the environment decay (say τ_{E}), the integrand decays to zero rapidly for $\tau' \gg \tau_{\mathrm{E}}$. Then we can safely replace t by ∞ in the integrand limits, obtaining

$$\frac{d\rho_{\mathrm{S}}}{dt} = -\int_0^\infty d\tau'\, \mathrm{tr}_{\mathrm{E}}[V_{\mathrm{I}}(t), [V_{\mathrm{I}}(t-\tau'), \rho_{\mathrm{S}}(t) \otimes \rho_{\mathrm{E}}]]. \tag{2.17}$$

Up to this point, eq. (2.17) has in general fast oscillating terms coming from the explicit dependence on $V_{\mathrm{I}}(t)$, this in turn can bring a generator that leads to a quantum process that violates complete positivity [ARHP14, RH12]. In order to get rid of such fast oscillations, one uses the aforementioned assumption that the environment is initialized in a stationary state, and perform the so called *secular approximation* [ARHP14]. A detailed derivation is outside of the scope of this thesis, but it can be consulted on references [BP07, RH12]. After performing the Markov, Born and secular approximations and changing back to the Schrödinger

picture, the resulting master equation can be written in the following forms

$$\frac{d\rho_{\rm S}}{dt} = {\rm i}[\rho_{\rm S}, \tilde{H}_{\rm S}] + \sum_{i,j=1}^{d_{\rm S}^2-1} G_{ij}\left(F_i\rho_{\rm S}F_j^\dagger - \frac{1}{2}\{F_j^\dagger F_i, \rho_{\rm S}\}\right), \tag{2.18}$$

$$= {\rm i}[\rho_{\rm S}, \tilde{H}_{\rm S}] + \sum_{j=1}^{d_{\rm S}^2-1} \gamma_j\left(A_j\rho_{\rm S}A_j^\dagger - \frac{1}{2}\{A_j^\dagger A_j, \rho_{\rm S}\}\right), \tag{2.19}$$

$$= L[\rho_S]. \tag{2.20}$$

F_j ($j = 0, \cdots, d_{\rm S}^2 - 1$) are operators acting on the central system that additionally form an orthonormal basis under Hilbert-Schmidt inner product, such that $F_0 = \mathbb{1}/\sqrt{d_{\rm S}}$ and ${\rm tr}\,F_j = 0\ \forall j > 0$ (this will be revised in subsection 3.3.1); the matrix G is called dissipator matrix. In the second inequality we have used the singular value decomposition of matrix G, thus operators A_i are linear combinations of F_i. The scalars $\gamma_j > 0$ are called *relaxation rates* and the operator $\tilde{H}_{\rm S}$ is the shifted free Hamiltonian of the central system. The first term on both equations, the commutator, is called *Hamiltonian part*, while the second, the superoperator defined with the summations, is called *dissipator*. Note that if $\gamma_j = 0$ $\forall j$ (uncoupled limit), one recovers the Hamiltonian dynamics over the system S. The operator L is called *Lindblad operator* or *Lindbladian* and eq. (2.20) is called *Lindblad master equation*. We will use along the work the notation L for Lindblad operators.

Note that L is independent of time, hence the formal solution of the master equation eq. (2.20) equation is simply the exponentiation of L [see eq. (2.13)], i.e.

$$\rho_{\rm S}(t) = e^{Lt}\rho_{\rm S}(0). \tag{2.21}$$

Therefore the dynamics is homogeneous in time and, together with the fact that $\mathscr{E}_t = \exp(Lt)$, we have $\mathscr{E}_{t+s} = \mathscr{E}_t\mathscr{E}_s$, i.e. the quantum process $\mathscr{E}_t$ resulting from a Lindblad master equation forms a one-parameter semigroup. In fact, Lindblad has proven the converse, including the case of infinite dimension [Lin76]:

Theorem 1 (One-parameter quantum semigroups)**.** *Let $\mathscr{E}_t$ with $\mathscr{E}_0 = id$ and $t \geq 0$ a quantum process, it is a one-parameter quantum semigroup if and only if it has a generator with the form presented in eq. (2.20).*

It is worth to point out that starting from global dynamics governed by a bounded Hamiltonian, the reduced dynamics are never of Lindblad form. This can be stated as the following,

Theorem 2 (Exact dynamics with Lindblad master equation)**.** *Let $\mathscr{E}_t = e^{tL}$ a quantum process generated by a Lindblad operator L. The equation*

$$\mathscr{E}_t[\rho] = \mathrm{tr}_E\left[e^{-\mathrm{i}Ht}\left(\rho\otimes\rho_E\right)e^{\mathrm{i}Ht}\right],$$

where H has finite dimension, holds if and only if $\mathscr{E}_t$ is an unitary conjugation for every t.

A proof made jointly with Sergey Filippov is given in the appendix A. It was made using an specific matrix representation for operators that will be introduced in the next chapter. But a more general proof can be found in [Exn85].

Let us point out that this is not the case for global unbounded Hamiltonians, they can lead to Lindblad master equations for the reduced dynamics. This is shown below together other illustrative examples.

Examples. To illustrate Lindblad dynamics we present several examples. The first one, depolarizing dynamics, is constructed via a continuous and monotonic contraction of the Bloch sphere. The second one corresponds to a system for which the exact reduced dynamics have Lindblad generator.

Example 1 (Dephasing dynamics)**.** *Let $\rho(0) = \begin{pmatrix} \rho_{00} & \rho_{01} \\ \rho_{01}^* & \rho_{11} \end{pmatrix}$ be the initial state, written in a basis called decoherence basis, of a system that undergoes depolarizing dynamics. This is, only coherence terms (in this basis) are modified in the following way:*

$$\mathscr{E}_t : \rho(0) \mapsto \begin{pmatrix} \rho_{00} & \rho_{01}e^{-\gamma t} \\ \rho_{01}^* e^{-\gamma t} & \rho_{11} \end{pmatrix} =: \rho(t),$$

with $\gamma > 0$. It is trivial to check that $\mathscr{E}_t$ is a one-parameter semigroup with $\mathscr{E}_0 = id$. For $t \to \infty$, we get $\rho(0) \to diag(\rho_{00}, \rho_{11})$. For this process it is easy to prove, by taking $0 < t \ll 1$, that its generator is $L[\rho] = \gamma/2\,(\sigma_z\rho\sigma_z - \rho)$, which has Lindblad form. It has null Hamiltonian part and only one operator $A_0 = \sigma_z$ and one relaxation ration, $\gamma/2$.

Example 2 (Dynamics from global unbounded Hamiltonian)**.** *Consider a bipartite system composed by a qubit interacting with a particle in a line, with global Hamiltonian $H = \sigma_z \otimes \hat{x}$, where $\hat{x}$ is position operator. Notice that H is unbounded since the configuration space of the particle is the entire real line. Initializing the environment in the state $|\psi\rangle$ with*

$$\langle x|\psi\rangle = \sqrt{\frac{\gamma}{\pi}}\frac{1}{x+\mathrm{i}\gamma},$$

it can be shown that the exact reduced dynamics for the qubit, without any approximation, is $L[\rho] = \gamma/2\,(\sigma_z \rho \sigma_z - \rho)$ *[AHFB15]. The same generator as in the first example.*

2.2 Quantum channels

In this section we give a brief introduction to classical stochastic processes, this motivates the definition of quantum channel. We first give an overview of stochastic processes; based on this we review the construction steps of quantum channels and discuss several of their properties. Additionally we introduce the simplest example of local operations and classical communication. Later on one we discuss the definition of CP-divisible processes based on the definition of classical Markovianity. Finally we give a brief revision of Gaussian quantum states and channels.

2.2.1 A classical analog

The classical analog of quantum channels are the widely known *stochastic matrices* or *stochastic maps* which propagate classical probability distributions. To introduce them consider, for sake of simplicity, a finite dimensional stochastic system whose state x_t (at time t) is described by the probability distribution (or probability vector) $\vec{p}(t)$, i.e. $x_t \sim \vec{p}(t)$ [with $\sum_i p_i(t) = 1$ and $p_i(t) \geq 0$]. Note that probability vectors form a convex space in the very same way that density matrices do. The distribution $\vec{p}(t)$ is the classical analogous object to density matrices. They serve as the tool to model the accessible information of the observer about the state of the classical stochastic system.

Consider now the most general linear transformation on probability vectors that takes, for instance $\vec{p}(0)$ to $\vec{p}(t)$ and let us write it explicitly as a matrix multiplication, $\vec{p}(t) = \Lambda_{(t,0)}\vec{p}(0)$. We have to impose further constrictions over $\Lambda_{(t,0)}$ in order to preserve the normalization of $\vec{p}(t)$ and the non-negativity of its elements. Since $p_i(t) = \sum_j \left(\Lambda_{(t,0)}\right)_{ij} \vec{p}_j(0)$, simple algebra leads us to note that $\sum_i \left(\Lambda_{(t,0)}\right)_{ij} = 1 \;\; \forall j$ and $\left(\Lambda_{(t,0)}\right)_{ij} \geq 0$. Matrices that fulfill these conditions are widely known as *stochastic matrices*, and form a convex set following the convexity of the space of probability distributions.

A remarkable property of stochastic maps is that they are contractive with respect to the Kolmogorov distance.

Theorem 3 (Contractivity of stochastic maps)**.** *The matrix Λ is a stochastic matrix if and only if*

$$\mathscr{D}_K(\Lambda\vec{p},\Lambda\vec{q}) \leq \mathscr{D}_K(\vec{p},\vec{q}), \tag{2.22}$$

where $\mathscr{D}_K(\vec{p},\vec{q}) = \sum_k |p_k - q_k|$ is the Kolmogorov distance.

It is worth to note Kolmogorov distance is a measure of distinguishability between classical distributions. A detailed proof of this theorem can be found in Ref. [ARHP14].

A particular and interesting class of stochastic matrices are *bistochastic matrices*. They are defined as the transformations that leave invariant the probability distribution with maximum entropy, given by $\vec{m} = (1/N,\ldots,1/N)^{\mathrm{T}}$, where N is the number that the system can have. Therefore a bistochastic matrix fulfills $\vec{m} = \Lambda_{(0,t)}\vec{m}$. Doing simple algebra lead us to note that bistochastic matrices additionally fulfill $\sum_j \left(\Lambda_{(t,0)}\right)_{ij} = 1 \ \ \forall i$. This implies that they are also stochastic matrix *acting from the right*, i.e. mapping row probability vectors. This is also the origin of the name bistochastic.

In the previous section we have introduced the concept of Markovianity in the context of open quantum systems, the so called Markovian approximation. It consisted on assuming that the system 'forgets the information about its previous states'. This concept comes from the theory of classical stochastic processes. Let us introduce the following definition [BP07, ARHP14],

Definition 1 (Classical Markovian process)**.** *Let x_t be the state of a stochastic system where $t \in [0,\tau]$, and $\chi = \{t_0,\ldots t_n\}$ any ordered set of times such that $0 < t_0 < t_1 < \cdots < t_n < \tau$, the process is Markovian if*

$$P(x_{t_n},t_n|x_{t_{n-1}},t_{n-1};\ldots;x_{t_0},t_0) = P(x_{t_n},t_n|x_{t_{n-1}},t_{n-1}) \ \ \forall n > 0, \tag{2.23}$$

where $P(\cdot|\cdot)$ denotes conditional probability.

According to this definition, the conditional probability of the system to be at the state x_{t_n} at the time t_n, given the history of events $\{x_{t_{n-1}},t_{n-1};\ldots;x_{t_0},t_0\}$, depends only on the previous state. This definition captures the memoryless character of Markovian processes.

Consider now a stochastic process and $\{\Lambda_{(t,0)}\}_{t\in\chi}$ its set of stochastic matrices given some ordered set of times χ. If the process is Markovian then the matrices $\Lambda_{(t_m,t_n)}$ are stochastic matrices for any χ, where $t_m > t_n \in \chi$. The converse is not true [ARHP14, BP07]. This condition implies that the map $\Lambda_{(t,0)}$ is divisible in

the sense that it can always be written as

$$\Lambda_{(t_1,t_0)} = \Lambda_{(t_1,s)}\Lambda_{(s,t_0)} \ \ \forall \ \ t_1 > s > t_0, \tag{2.24}$$

with $\Lambda_{(t_1,s)}$, $\Lambda_{(s,t_0)}$ and $\Lambda_{(t_1,t_0)}$ stochastic matrices, the latter two by definition. Intermediate maps can be constructed as $\Lambda_{(t_1,s)} = \Lambda_{(t_1,t_0)}\Lambda^{-1}_{(s,t_0)}$ if $\Lambda^{-1}_{(s,t_0)}$ exists. Note that theorem 3 implies that Markovian stochastic processes do not increase the Kolmogorov distance.

2.2.2 Construction of quantum channels

The concept of quantum channel, also known as quantum operation, captures the idea of stochastic map in the quantum setting. Thus, being the density matrices the analogous objects to probability vectors, we seek for linear operations that transform density matrices into density matrices. The operations that do such job are defined as follows:

Definition 2 (Positive and trace preserving linear operations (PTP))**.** *A linear operation $\mathscr{E} : \mathscr{T}(\mathscr{H}) \to \mathscr{T}(\mathscr{H})$ is positive and trace preserving if, for all $\Delta \in \mathscr{H}$, we have the following*

- $\mathscr{E}[\Delta] \geq 0 \ \ \forall \Delta \geq 0$,
- $\mathrm{tr}\,(\mathscr{E}[\Delta]) = \mathrm{tr}\,(\Delta)$.

A remarkable property of linear positive maps is that they are contractive respect to the trace norm [ARHP14]. This is leads to a decrease of the distinguishability of quantum states, similar to the classical case.

Theorem 4 (Contractivity of positive maps)**.** *A linear map $\mathscr{E}$ is PTP if and only if $|\mathscr{E}[\Delta]|_{tr} \leq |\Delta|_{tr} \ \ \forall \Delta^\dagger = \Delta \in \mathscr{B}(\mathscr{H})$.*

A simple proof for the finite dimensional case can be found in Ref. [ARHP14].

Now, given that any hermitian operator can be written as

$$\Delta = (\mathrm{tr}\,\Delta)\, H_p, \text{ for } \mathrm{tr}\,\Delta \neq 0,$$
$$\Delta = \mathrm{tr}\,\Delta^+\,(\rho_1 - \rho_2)\,, \text{ for } \mathrm{tr}\,\Delta = 0,$$

where $H_p = p\rho_1 - (1-p)\rho_2$ a Helstrom matrix and $p \in [0,1]$, by theorem 4 the generalized trace distance defined as $\mathscr{D}_p(\rho_1,\rho_2) = |p\rho_1 - (1-p)\rho_2|_{\mathrm{tr}}$ decreases after the application of a positive map $\mathscr{E}$, i.e.

$$\mathscr{D}_p\,(\mathscr{E}[\rho_1], \mathscr{E}[\rho_2]) \leq \mathscr{D}_p\,(\rho_1,\rho_2)\,.$$

It is worth to point out that this is directly related to the two-state discrimination problem where we have, for instance, probability p of erroneously identify ρ_1 with ρ_2 [NC11, ARHP14]. In this setting the probability of failing with such identification is

$$P_{\text{err}} = \frac{1 - \mathscr{D}_p(\rho_1, \rho_2)}{2}.$$

Therefore if the distance is zero, the probability of correctly identify ρ_1 is the same as choosing randomly between ρ_1 and ρ_2, but if it is 1, we identify ρ_1 from ρ_2 with certainty. For $p = 1/2$ we recover the standard unbiased trace distance.

It is well known that any quantum system can be entangled with another, for instance a central system can be entangled with its environment. Thus, in the context of quantum operations we must handle this fact carefully. Let us define the following:

Definition 3 (k-positive operations)**.** *A linear map $\mathscr{E}$ is k-positive if*

$$id_k \otimes \mathscr{E}[\tilde{\Delta}] \geq 0 \;\; \forall \tilde{\Delta} \geq 0 \in \mathscr{B}(\mathscr{H}_k \otimes \mathscr{H}),$$

with k a positive integer, being the dimension of $\mathscr{H}_k$ and id_k the identity map in that space.

Therefore a positive map is k-positive if the expended map $\text{id}_k \otimes \mathscr{E}$ is positive, the trace preserving of k-positive maps follows immediately from the trace preserving of $\mathscr{E}$. Such maps transform properly density matrices of the extended system (with ancilla of dimension k) into density matrices, apart from the fact that they transform properly the density matrices of the system, hence handling quantum entanglement correctly for this ancilla.

Since the dimension of any other quantum system is arbitrary, being for example the rest of the universe, one must have that quantum maps must transform quantum states for every positive integer k. Therefore one defines *complete positive* and trace preserving linear maps as the following,

Definition 4 (Complete positive and trace preserving operations (CPTP))**.** *A trace preserving linear operation $\mathscr{E} : \mathscr{T}(\mathscr{H}) \to \mathscr{T}(\mathscr{H})$ is complete positive if*

$$id_k \otimes \mathscr{E}[\tilde{\Delta}] \geq 0 \;\; \forall \tilde{\Delta} \geq 0 \in \mathscr{B}(\mathscr{H}_k \otimes \mathscr{H}), \forall k \in \mathbb{Z}_0^+,$$

where $\mathbb{Z}^+$ is the set of the positive integers.

It will be shown later in chapter 3, that deciding complete positivity is straightforward using the so called Choi matrix.

It is trivial to check that unitary operations, $\mathscr{U}[\rho] = U\rho U^\dagger$, are CPTP maps as expected. Additionally they leave invariant the maximally mixed state, $\mathbb{1}/\dim(\mathscr{H})$. In fact, unitary operations belong to a wider class of CPTP maps called *unital quantum maps*, similar to its classical counterpart. The set of unital channels is defined simply as the one containing CPTP maps $\mathscr{E}$ that additionally fulfill $\mathscr{E}[\mathbb{1}] = \mathbb{1}$.

Additionally notice that due to the trace preserving property the adjoint operator of $\mathscr{E}$ is always unital. The adjoint is defined in the usual way,

$$\langle A, \mathscr{E}[B]\rangle = \langle \mathscr{E}^*[A], B\rangle, \tag{2.25}$$

where the inner product is the Hilbert-Schmidt product and $A \in \mathscr{T}(\mathscr{H})$ and $B \in \mathscr{B}(\mathscr{H})$ [Hol01, HZ12]. Now, $\forall \Delta \in \mathscr{T}(\mathscr{H})$ we write the trace preserving condition as $\mathrm{tr}\,\Delta = \mathrm{tr}\,\mathscr{E}[\Delta] = \langle \mathbb{1}, \mathscr{E}[\Delta]\rangle = \langle \mathscr{E}^*[\mathbb{1}], \Delta\rangle$, therefore $\mathscr{E}^*[\mathbb{1}] = \mathbb{1}$.

Let us now illustrate the connection of the concept of quantum channel with the scheme of open quantum systems introduced above. Consider the following theorem [Sti06]:

Theorem 5 (Stinespring dilation theorem)**.** *Let $\mathscr{E}$ a CPTP map, there exist an environmental Hilbert space $\mathscr{H}_E$ and $\rho_E \in \mathscr{S}(\mathscr{H}_E)$ such that*

$$\mathscr{E}[\rho] = \mathrm{tr}_E\left[U\left(\rho \otimes \rho_E\right)U^\dagger\right],$$

with the unitary matrix $U : \mathscr{H} \otimes \mathscr{H}_E \to \mathscr{H} \otimes \mathscr{H}_E$.

The unitary U and the state ρ_E are not unique [HZ12]. Stinespring theorem is an important result given that one can always understand a CPTP operation as a Hamiltonian evolution in a bigger space, such that we recover the given operation at some fixed time and by performing a partial trace over the environmental degrees of freedom. Later in this chapter we will discuss an important implication of this theorem for Markovian processes.

Along the work we will also denote the set of CPTP linear maps simply as C.

A remarkable property of C is its convexity. To show this consider the following convex combination of CPTP maps: $\mathscr{E} = p\mathscr{E}_1 + (1-p)\mathscr{E}_2$, acting upon the density matrix ρ_0. By linearity we have $\mathscr{E}[\rho_0] = p\mathscr{E}_1[\rho_0] + (1-p)\mathscr{E}_2[\rho_0]$. Defining the density matrices $\rho_i = \mathscr{E}_i[\rho_0] \in \mathscr{S}(\mathscr{H})$, it follows from the convexity of $\mathscr{S}(\mathscr{H})$ that $\mathscr{E}$ is another CPTP map. Therefore the set C is convex.

Unitary maps are extremal channels of C i.e. they cannot be written as convex combinations of other channels, but they can be used to construct other maps,

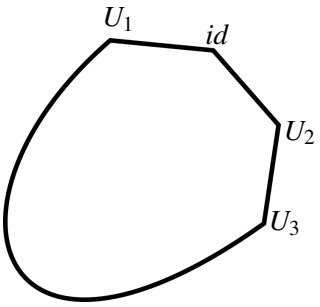

Figure 2.3: The figure shows an schematic slice of CPTP maps, one can see the identity map and other extremal channels. The straight lines are convex combinations of those channels, the curve contains channels in the boundary that cannot be written as convex combinations of unitary channels.

see fig.2.3. For instance consider a simple convex combination of unitary maps $\mathscr{E}[\rho] = \sum_i p_i U \rho U^\dagger$, with $\sum_i p_i = 1$ and $p_i \geq 0$. This channel is a more general example of a unital channel, in fact it turns that every unital qubit channel has such form. This can be shown easily using the Ruskai's decomposition that will be introduced in the next chapter. Convex combinations of unitary channels can be implemented in the laboratory, for instance choosing unitaries randomly by tossing a die.

Regarding the algebraic properties of the set C, it enjoys the structure of a semigroup. It is closed under the composition operation, i.e. $\mathscr{E}_1\mathscr{E}_2 \in \mathsf{C}$, $\forall \mathscr{E}_1, \mathscr{E}_2 \in \mathsf{C}$, and is associative, $(\mathscr{E}_1\mathscr{E}_2)\,\mathscr{E}_3 = \mathscr{E}_1\,(\mathscr{E}_2\mathscr{E}_3)$. Additionally it contains an identity element. C does not contain the inverse elements, this captures the irreversible character of general quantum operations, being only the unitaries the ones their inverse elements in C. Furthermore, C contains another remarkable convex structure,

Definition 5 (Entanglement-breaking channels)**.** *A map $\mathscr{E} \in \mathsf{C}$ is entanglement-breaking if it breaks the entanglement of the system with any ancilla, i.e. $\forall k \in \mathbb{Z}^+$ and $\forall \sigma \in \mathscr{S}(\mathscr{H}_k \otimes \mathscr{H})$, the state $(id_k \otimes \mathscr{E})[\sigma]$ is separable.*

This set is convex given that convex combinations of separable states is separable [HHHH09].

Quantum channels can be seen as the basic building of time-dependent quantum processes, also called quantum dynamical maps.

Definition 6 (Quantum dynamical maps)**.** *A continuous family of channels $\{\mathscr{E}_t \in \mathsf{C} : \mathsf{t} \geq 0, \mathscr{E}_0 = id\}$ is called quantum dynamical map.*

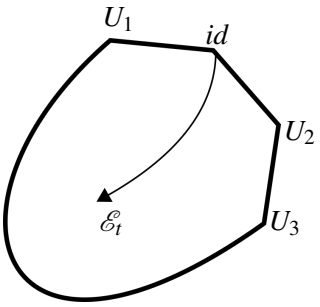

Figure 2.4: Scheme of an smooth dynamical map inside a slice of the set C.

Given some interval $\mathscr{I}$, if the family is smooth respect to $t \in \mathscr{I}$ and invertible, it admits a master equation

$$\dot{\rho}(t) = A_t[\rho(t)] \text{ with } A_t = \dot{\mathscr{E}}_t \mathscr{E}_t^{-1}.$$

An schematic description is shown in fig. 2.4. Note that the standard scheme open quantum systems, introduced at the beginning of this chapter, leads to quantum dynamical maps.

2.2.3 Non-Linear CPTP operations

Notice that the set C does not contain everything that can be performed on a quantum system; it contains only linear operations. Therefore C do not contain *post-seletion* procedures, i.e. updating the state once a measurement is done and the result is known. For instance, let ρ the state of some system and $\{M_i\}$ a collection of *measurement operators* over it, where the index i refers to the measurement outcome. The probability of measuring i is $p(i) = \text{tr}\left(M_i \rho M_i^\dagger\right)$, while the operation performed over the state is

$$\rho \mapsto \frac{M_i \rho M_i^\dagger}{\text{tr}\left(M_i \rho M_i^\dagger\right)}.$$

This operation is explicitly non-linear but it is trivially complete positive and trace preserving. Note that if the action of the measurement apparatus is performed but the experimentalist do not read the outcome, or it is simply forgotten, the resulting map belongs to C [NC11]. This is shown by noting that the operation $M_i \rho M_i^\dagger$ is applied with probability $p(i)$, then the performed operation is $\sum_i p(i) M_i \rho M_i^\dagger$ and it is linear and CPTP by construction. Complete positivity follows immediately

from the complete positivity of $\rho \mapsto M_i \rho M_i^\dagger$ and the trace preserving property from the weighted summation.

A more general set of operations including measurements, postselection and exchange of classical information will be introduced in the next subsection.

2.2.4 Local operations and classical communication

Several types of quantum operations can be found and studied, in particular in Ref. [HZ12] there is a classification mainly based on its *locality*. A paradigmatic and widely studied type are the so called *local operations and classical communication* [HHHH09]. A surprising feature of this operations is that they can increase the entanglement of entangled states of a system (at the cost of throwing some members of the ensemble), but cannot create them from non-entangled ones [VDD01, HHHH09].

In this work we are particularly interested in *one-way stochastic local operations and classical communication* channels (1wSLOCC). Consider a bipartite system where one part is controlled by Alice and the other by Bob. Alice performs an operation which includes measurements with postselection, and then she communicates its outcome to Bob. Then Bob performs a local operation that can be again a measurement with postselection, finishing the protocol. The stochasticity comes from the fact that this operation, for each particular set of measurement outcomes, has a certain probability generally less than 1 of occurrence. And the one-way comes from the fact that no feedback is given to Alice and no more operations and classical communications are performed. This operations can be written in the following way:

$$\rho \mapsto \rho' = \frac{(X \otimes Y)\,\rho\,(X \otimes Y)^\dagger}{\mathrm{tr}\left[(X \otimes Y)\,\rho\,(X \otimes Y)^\dagger\right]}. \tag{2.26}$$

Additionally we will consider $\det X \neq 0$ and $\det Y \neq 0$, this is the usual choice as projective measurements destroy entanglement [VDD01]. This operations are complete positive and trace preserving, but non-linear unless X and Y are unitaries. Additional notice that given ρ and ρ', the matrices X and Y can always be chosen such that $\det X = \det Y = 1$ (for the invertible case). Therefore for two-level systems it is enough to consider $X, Y \in \mathrm{SL}(2,\mathbb{C})$ [Tun85], where the latter is the *special linear group* of 2×2 matrices with complex entries. Furthermore notice that the operation

$$\rho \mapsto (X \otimes Y)\,\rho\,(X \otimes Y)^\dagger \tag{2.27}$$

preserves the determinant, i.e. $\det\rho = \det\rho'$. In the next chapter we will exploit this to show that there is a correspondence between 1wSLOCC and Lorentz transformations. We use this to introduce a decomposition analogous to the singular value decomposition, but using the Lorentz metric instead of the Euclidean, enjoying an useful physical meaning.

2.3 Quantum channels of continuous variable systems

Many of the definitions and tools introduced in the previous sections are also relevant for the infinite dimensional case. Although we can always choose countable basis for the Hilbert space as long it is separable [HZ12], it is often of interest to consider non-countable bases, typically phase-space variables. This introduces the theory of continuous variable systems. It is a central topic of study given that they appear naturally in the description of many physical systems. A few examples are the electromagnetic field [CLP07], solids and nano-mechanical systems [AKM14] and atomic ensembles [HSP10]. In particular, in this section we introduce and discuss a set of continuous variable channels called *Gaussian quantum channels*.

2.3.1 Gaussian quantum states

To introduce the definition of Gaussian quantum channel, consider first the simplest state type of quantum states in continuous variable, both from a theoretical an experimental point of view, the so-called *Gaussian states*. The operations that transform such family of states into itself are called Gaussian quantum channels (GQC). Even though Gaussian states and channels are small subsets of all possible states/channels, they have proven to be useful in a very wide variate of tasks such as quantum communication [GVAW$^+$03], quantum computation [LB99] and the study of quantum entanglement in simple [BvL05] and complicated scenarios [LRW$^+$18].

Gaussian states are defined as those having Gaussian Wigner function. In particular, for one-mode the Wigner function is

$$W(\vec{u}) = \frac{1}{2\pi\sqrt{\det\sigma}} e^{-\frac{1}{2}\left(\vec{u}-\vec{d}\right)^{\mathrm{T}}\sigma^{-1}\left(\vec{u}-\vec{d}\right)}, \tag{2.28}$$

where $\vec{u} = (q,p)^{\mathrm{T}}$ [EW07]. The *mean vector* $\vec{d}$ and the *covariance matrix* σ are

the first and second moments, respectively. They are given by

$$\sigma = \begin{pmatrix} \langle \hat{q}^2 \rangle - \langle \hat{q} \rangle^2 & \frac{1}{2}\langle \hat{q}\hat{p} + \hat{p}\hat{q} \rangle - \langle \hat{q} \rangle \langle \hat{p} \rangle \\ \frac{1}{2}\langle \hat{q}\hat{p} + \hat{p}\hat{q} \rangle - \langle \hat{q} \rangle \langle \hat{p} \rangle & \langle \hat{p}^2 \rangle - \langle \hat{p} \rangle^2 \end{pmatrix},$$
$$\vec{d} = \left(\langle \hat{q} \rangle, \langle \hat{p} \rangle \right)^{\mathrm{T}}.$$

The observables $\hat{q}$ and $\hat{p}$ are the standard canonical conjugate position and momentum variables. As for any other Gaussian variable, Gaussian quantum states are characterized completely by first and second probabilistic moments. Therefore a Gaussian state S can be denoted as $S = S\left(\sigma, \vec{d}\right)$.

2.3.2 Gaussian quantum channels

To start with, we recall the following definition [WPGP$^+$12]:

Definition 7 (Gaussian quantum channels)**.** *A quantum channel is Gaussian (GQC) if it transforms Gaussian states into Gaussian states.*

This definition is strictly equivalent to the statement that any GQC, say $\mathscr{A}$, can be written as

$$\mathscr{A}[\rho] = \mathrm{tr}_{\mathrm{E}} \left[U \left(\rho \otimes \rho_{\mathrm{E}} \right) U^{\dagger} \right] \tag{2.29}$$

where U is a unitary transformation, acting on a combined global state obtained from enlarging the system with an environment E, that is generated by a quadratic bosonic Hamiltonian (i.e. U is a *Gaussian unitary*) [WPGP$^+$12]. The environmental initial state ρ_E is a Gaussian state and the trace is taken over the environmental degrees of freedom.

Following definition 7, a GQC is fully characterized by its action over Gaussian states, and this action is in turn defined by *affine transformations* [WPGP$^+$12]. Specifically, $\mathscr{A} = \mathscr{A}\left(\mathbf{T}, \mathbf{N}, \vec{\tau}\right)$ is given by a tuple $\left(\mathbf{T}, \mathbf{N}, \vec{\tau}\right)$ where $\mathbf{T}$ and $\mathbf{N}$ are 2×2 real matrices with $\mathbf{N} = \mathbf{N}^{\mathrm{T}}$ [WPGP$^+$12] acting on Gaussian states according to

$$\mathscr{A}\left(\mathbf{T}, \mathbf{N}, \vec{\tau}\right) \left[S\left(\sigma, \vec{d}\right) \right] = S\left(\mathbf{T}\sigma\mathbf{T}^{\mathrm{T}} + \mathbf{N}, \mathbf{T}\vec{d} + \vec{\tau} \right).$$

In the particular case of closed systems we have $\mathbf{N} = \mathbf{0}$ and $\mathbf{T}$ is a symplectic matrix. The particular form and properties of Gaussian quantum channels in the continuous variable representations, as well their connection the mentioned affine transformations, will be given in chapter 3.

In this work we explore GQCs without Gaussian functional form in the position state representation. In particular we study channels that can arise when singularities on the coefficients of Gaussian forms GF occur (they will be denoted by δGQC). Such channels can lead immediately to singular Gaussian operations. Thus, we characterize which forms in δGQC lead to valid quantum channels, and under which conditions singular operations lead to valid *singular Gaussian quantum channels* (SGQC).

Let us note that although channels with Gaussian form trivially transform Gaussian states into Gaussian states, the definition goes beyond GF. We will use the typical *difference* and *sum* coordinates, $x = q_2 - q_1$ and $r = (q_1 + q_2)/2$, respectively. Defining $\rho(x,r) = \left\langle r - \frac{x}{2} \right| \hat{\rho} \left| r + \frac{x}{2} \right\rangle$, a quantum channel in this representation is defined such that

$$\rho_f(x_f, r_f) = \int_{\mathbb{R}^2} dx_i dr_i J(x_f, x_i; r_f, r_i) \rho_i(x_i, r_i), \tag{2.30}$$

where $\hat{\rho}_i$ and $\hat{\rho}_f$ are the initial and final states, respectively, and $J(x_f, x_i; r_f, r_i)$ is the representation of the quantum channel in the aforementioned variables. An example of a channel without GF can be constructed from the general form of Gaussian quantum channel with GF [MP12]:

$$J_{\mathrm{G}}(x_f, x_i; r_f, r_i) = \frac{b_3}{2\pi} \exp\Big[\imath\Big(b_1 x_f r_f + b_2 x_f r_i + b_3 x_i r_f + b_4 x_i r_i + c_1 x_f + c_2 x_i\Big) - a_1 x_f^2 - a_2 x_f x_i - a_3 x_i^2\Big], \tag{2.31}$$

where all coefficients are real and no quadratic terms in $r_{i,f}$ are allowed. Choosing

$$a_n = \alpha_n \varepsilon^{-1} + \tilde{a}_n$$

and

$$b_n = \beta_n \varepsilon^{-1/2} + \tilde{b}_n,$$

with $\varepsilon > 0$, $\alpha_n, \beta_n, \tilde{a}_n, \tilde{b}_n \in \mathbb{R} \ \ \forall n$ and $\tilde{b}_3 = 0$. Taking the limit $\varepsilon \to 0$ and using the formula

$$\delta(x) = \lim_{\varepsilon \to 0} \frac{1}{2\sqrt{\pi\varepsilon}} e^{\frac{-x^2}{4\varepsilon}}, \tag{2.32}$$

we arrive to

$$\lim_{\varepsilon \to 0} J_{\mathrm{G}}(x_f, x_i; r_f, r_i) = \mathscr{N} \delta(\alpha x_f - \beta x_i) e^{\Sigma'(x_f, x_i; r_f, r_i)}, \tag{2.33}$$

where $\alpha, \beta \in \mathbb{R}$ and $\Sigma'(x_f, x_i; r_f, r_i)$ is a quadratic form that now admits quadratic terms in $r_{i,f}$, arising from the completion of the square of the exponent of eq. (2.31)

to take the limit of eq. (2.32). This is the first example of a δGQC. This channel is still a GQC according to the definition. A physical, but complicated realization occurs in the system of one Brownian quantum particle with harmonic potential and linearly coupled to the bath. In such system, channels with the functional form of eq. (2.33) are realized at isolated points in time, see equations 6.71-75 of Ref. [GSI88].

Since the form of eq. (2.33) admits quadratic terms in $r_{i,f}$ in the exponent, it suggest that a form with two deltas exist and can be defined using the same limit, see eq. (2.32). In fact, the identity map is a particular case; it is realized setting $J(x_f,x_i;r_f,r_i) = \delta(x_f - x_i)\delta(r_f - r_i)$. In any case, to avoid working with such limits, it is convenient to perform a *black-box* characterization of general forms involving Dirac's deltas, which will be done in the next chapter. This will lead to explicit relations between position state representation and affine representations of Gaussian quantum channels without Gaussian functional form.

Chapter 3

Representations of quantum channels

Simplicity is the ultimate sophistication.
Leonardo da Vinci

In this chapter we introduce several and useful representations of quantum channels for the finite dimensional case. We start with the Kraus representation, already mentioned in the previous chapter, but additionally we will show that quantum channels always have this form. Later on we introduce Choi's theorem (and the so called Choi-Jamiołkowski representation) which is cornerstone tool to study many properties of quantum channels. We also discuss operational representations by introducing two types of basis. These representations are useful to prove several results in this work. Next, we apply the introduced tools to the qubit case. Additionally we discuss two decomposition of qubit channels, leading to two *normal forms* that are essential to study divisibility properties of quantum channels.

3.1 Kraus representation

In the previous chapter we have shown that starting from the usual scheme of open quantum systems, we arrive to the *Kraus representation*, see eq. (2.8). Later on, using the Stinespring dilation theorem, see Theorem 5, we show that CPTP maps can always fit in the scheme of open quantum systems for some global

unitary evolution. Since the latter scheme always has a Kraus representation, one concludes that CPTP maps always have a Kraus representation. It turns out that the converse also holds [KBDW83].

Theorem 6 (Kraus)**.** *A linear operation $\mathscr{E} : \mathscr{T}(\mathscr{H}) \to \mathscr{T}(\mathscr{H})$ belongs to* C *if and only if there exist a set of bounded operators $\{K_i\}$ such that*

$$\mathscr{E}[\Delta] = \sum_i K_i \Delta K^\dagger{}_i \;\; \forall \Delta \in \mathscr{T}(\mathscr{H}),$$

with $\sum_i K_i^\dagger K_i = \mathbb{1}$.

Proof. The 'only if' part is already commented in the main text and follows the logic: every $\mathscr{E} \in \mathsf{C}$ has a dilation such that it has the familiar form of the open quantum systems dynamics, i.e. there exists U and ρ_E such that $\mathscr{E}[\rho] = \mathrm{tr}_\mathrm{E}\left[U\left(\rho \otimes \rho_\mathrm{E}\right)U^\dagger\right]$. We already showed that writing ρ_E in terms of its eigenbasis, the latter expression leads to the Kraus representation, see eq. (2.8). To prove the 'if' part, we only have to construct the extended map to test its complete positivity. Let $k > 0 \in \mathbb{Z}$ and $\tau_k = (\mathrm{id}_k \otimes \mathscr{E})\left[\tilde{\Delta}_k\right]$, where $\tilde{\Delta}_k \in \mathscr{B}(\mathscr{H}_k \otimes \mathscr{H})$ and $\tilde{\Delta}_k \geq 0$, using Kraus decomposition and evaluating $\langle\phi|\tau_k|\phi\rangle$ with $|\phi\rangle \in \mathscr{H}_k \otimes \mathscr{H}$, one arrives to

$$\begin{aligned}
\langle\phi|\tau_k|\phi\rangle &= \sum_i \langle\phi|\left(\mathbb{1}_k \otimes K_i\right)\tilde{\Delta}_k\left(\mathbb{1} \otimes K_i^\dagger\right)|\phi\rangle \\
&= \sum_i \langle\phi_i|\tilde{\Delta}_k|\phi_i\rangle \\
&\geq 0.
\end{aligned}$$

The latter follows immediately from the positive-semidefinitiveness of $\tilde{\Delta}_k$, i.e. $\langle\phi_i|\tilde{\Delta}_k|\phi_i\rangle \geq 0$. The condition $\sum_i K_i^\dagger K_i = \mathbb{1}$ comes from the trace-preserving of $\mathscr{E}$ and the cyclic property of the trace,

$$\begin{aligned}
\mathrm{tr}\,\mathscr{E}[\Delta] &= \sum_i \mathrm{tr}\left[K_i \Delta K_i^\dagger\right] \\
&= \sum_i \mathrm{tr}\left[K_i^\dagger K_i \Delta\right] \\
&= \mathrm{tr}\left[\left(\sum_i K_i^\dagger K_i\right)\Delta\right] \\
&= \mathrm{tr}\,\Delta,
\end{aligned}$$

□

Therefore $\sum_i K_i^\dagger K_i = \mathbb{1}$. It is worth to note that Kraus operators are not unique. Defining a new set of operators, $A_k = \sum_l u_{kl} K_l$, it is easy to show that $\sum_i K_i \Delta K_i^\dagger = \sum_k A_k \Delta A_k^\dagger$ if and only if u_{kl} are the components of an unitary matrix. Therefore different Kraus representations are related by unitary conjugations.

3.2 Choi-Jamiołkowski representation

The Choi-Jamiołkowski representation arises as part of a very useful theorem in quantum information theory, the so called Choi's theorem [Cho75, HZ12].

Theorem 7 (Choi)**.** *Let $\mathscr{E} : \mathbb{C}^{n\times n} \to \mathbb{C}^{m\times m}$ be a linear map. The following statements are equivalent:*
i) $\mathscr{E}$ is $n-$positive.
ii) The matrix

$$C_{\mathscr{E}} = \sum_{i,j=1}^{n} |\varphi_i\rangle\langle\varphi_j| \otimes \mathscr{E}[|\varphi_i\rangle\langle\varphi_j|] \in \mathbb{C}^{n\times m} \otimes \mathbb{C}^{n\times m}$$

is positive-semidefinite with $\{|\varphi_i\rangle\}_{i=1}^n$ an orthonormal basis in $\mathbb{C}^n$.
iii) $\mathscr{E}$ is completely positive.

Proof. The proof of *iii)* $\to$ *i)* is trivial, if $\mathscr{E}$ is completely positive then it is $n-$positive. The implication *i)* $\to$ *ii)* can be proved easily by noticing that normalizing $C_{\mathscr{E}} \to C_{\mathscr{E}}/n =: \tau_{\mathscr{E}}$, where $\tau_{\mathscr{E}}$ can be obtained as the application $\tau_{\mathscr{E}} = (\mathrm{id}_n \otimes \mathscr{E})[\omega]$, where $\omega = |\Omega\rangle\langle\Omega|$ with $|\Omega\rangle = 1/\sqrt{n}\sum_i^n |\varphi_i\rangle \otimes |\varphi_i\rangle$ a Bell state between two copies of $\mathbb{C}^n$. Therefore, by the $n-$positivity of $\mathscr{E}$ it follows that $\tau_{\mathscr{E}}$ is positive-semidefinite.

What remains to prove is *ii)* $\to$ *iii)*. To do this observe that the space $\mathbb{C}^{n\times m}$ is isomorphic to the direct sum of n copies of $\mathbb{C}^m$, i.e. $\mathbb{C}^{n\times m} \cong \mathbb{C}_1^m \oplus \mathbb{C}_2^m \oplus \cdots \oplus \mathbb{C}_n^m$, and define the projector into the kth copy as $P_k = \langle\varphi_k| \otimes \mathbb{1}$, such that $P_k C_{\mathscr{E}} P_l = \mathscr{E}[|\varphi_k\rangle\langle\varphi_l|]$. Now, given that $C_{\mathscr{E}}$ is positive-semidefinite, it can be written as $C_{\mathscr{E}} = \sum_i^{nm} |\Psi_i\rangle\langle\Psi_i|$, where $|\Psi_i\rangle \in \mathbb{C}^{n\times m}$ are generally unnormalized vectors. Thus, we have that $\mathscr{E}[|\varphi_k\rangle\langle\varphi_l|] = \sum_i P_k|\Psi_i\rangle\langle\Psi_i|P_l$, where $P_k|\Psi_i\rangle \in \mathbb{C}_k^m$. Defining the operators $\{K_i : \mathbb{C}^n \to \mathbb{C}^m\}_i$ via the equation $P_k|\Psi_i\rangle = K_i|\varphi_k\rangle$, where choosing for example $|\varphi_k\rangle$ as the canonical basis, the columns of K_i contain the n projections of $|\Psi_i\rangle$ into the copies of $\mathbb{C}^m$. Finally we arrive to $\mathscr{E}[|\varphi_k\rangle\langle\varphi_l|] = \sum_i K_i|\varphi_k\rangle\langle\varphi_l|K_i^\dagger \;\; \forall k,l = 1,\ldots,n$. In conclusion, since $\{|\varphi_k\rangle\langle\varphi_l|\}_{k,l}$ is a complete basis of $\mathbb{C}^{n\times n}$, by linearity and by theorem 6, the map $\mathscr{E}$ is completely positive. □

The matrix $C_{\mathscr{E}}$ is commonly known as Choi matrix and $\tau_{\mathscr{E}}$ as Choi-Jamiołkowski state. Both define the Choi-Jamiołkowski representation, in this work labeled as $\tau_{\mathscr{E}}$ since it is normalized.

Choi's theorem provides a simple test of complete positivity, which I find beautiful. For instance, if we want to know if a given PTP map $\mathscr{E}$ is a valid quantum map, we just have to consider two copies of our system in only one state, the Bell state, then apply $\mathscr{E}$ to one of the copies and check if the result, $\tau_{\mathscr{E}} = (\mathrm{id}_n \otimes \mathscr{E})[\omega]$, is a density matrix.

The Choi-Jamiołkowski representation enjoys other useful properties, if $\mathscr{E}$ preserves the trace, the matrix

$$\tau_{\mathscr{E}} = \frac{1}{n} \begin{pmatrix} \mathscr{E}[|\varphi_1\rangle\langle\varphi_1|] & \dots & \mathscr{E}[|\varphi_1\rangle\langle\varphi_n|] \\ \vdots & \ddots & \vdots \\ \mathscr{E}[|\varphi_n\rangle\langle\varphi_1|] & \dots & \mathscr{E}[|\varphi_n\rangle\langle\varphi_n|] \end{pmatrix} \tag{3.1}$$

has blocks of trace $1/n$ and 0, since $\mathrm{tr}\,\mathscr{E}[|\varphi_i\rangle\langle\varphi_j|] = \delta_{ij}$. This property additionally means that not every density matrix in $\mathbb{C}^{n\times m} \otimes \mathbb{C}^{n\times m}$ has a corresponding CPTP map.

The matrix rank of $\tau_{\mathscr{E}}$ coincides with the so called *Kraus rank*, i.e. the number of linearly independent Kraus operators required to write the channel. This can be shown easily noticing that computing $\tau_{\mathscr{E}}$ from the Kraus sum, one arrives to the equality $|\Psi_i\rangle = 1/\sqrt{n}\mathbb{1} \otimes K_i|\Omega\rangle$, therefore the linear independence of $\{|\Psi_i\rangle\}_i$ follows immediately from the linear independence of $\{K_i\}_i$. Therefore the maximum Kraus rank is *mn* and the minimum 1. Channels with Kraus rank equal to 1 are trivially unitary channels given that $\mathscr{E}[\Delta] = K\Delta K^\dagger$ with $K^\dagger K = \mathbb{1}$. Channels with the maximum rank are called *full Kraus rank channels*.

Another interesting property is that if $\tau_{\mathscr{E}}$ is separable (i.e. not entangled) , then $\mathscr{E}$ is entanglement-breaking, see definition 5. For qubit channels it is enough to test that the concurrence is zero [RFZB12].

3.3 Operational representations

It has been shown that the Choi-Jamiołkowski representation is useful to test several properties of quantum channels. In this section we will introduce other representations, this time with operational meanings. They are basically operator basis that give matrix and vector forms to channels and density matrices, respectively.

The vectorization of density matrices can be achieved simply "making them flat", this is,

$$\begin{pmatrix} \rho_{11} & \cdots & \rho_{1d} \\ \vdots & \ddots & \vdots \\ \rho_{d1} & \cdots & \rho_{dd} \end{pmatrix} \mapsto \begin{pmatrix} \rho_{11} \\ \rho_{12} \\ \vdots \\ \rho_{dd} \end{pmatrix} =: \vec{\rho}.$$

Using this mapping, the matrix form of operators acting on $\mathscr{T}(\mathscr{H})$ is build using the simple rule [GTW09]

$$A\rho B \mapsto \left(A \otimes B^{\mathrm{T}}\right) \vec{\rho}. \tag{3.2}$$

For instance applying this rule to a commutator, $[H,\rho] \mapsto \left(H \otimes \mathbb{1} - \mathbb{1} \otimes H^{\mathrm{T}}\right) \vec{\rho}$. This representation is useful to prove various results involving operators acting on the space of density matrices, see for instance the appendix A. Additionally it is simple to prove that the Hilbert-Schmidt inner product is mapped to $\langle \gamma, \rho \rangle \mapsto \vec{\gamma}^{\dagger} \vec{\rho}$.

One can use other operator basis accordingly to our purposes. In general we have the following, consider $\{A_i\}_i$ an orthonormal operator basis in the space $\mathscr{T}(\mathscr{H})$, the components of the density matrix are

$$\alpha_i = \langle A_i, \rho \rangle = \mathrm{tr}\left[A_i^{\dagger} \rho\right],$$

so

$$\rho = \sum_i \alpha_i A_i.$$

Correspondingly, the components of operators acting on $\mathscr{B}(\mathscr{H})$, for instance $\mathscr{E}$, are simply

$$\hat{\mathscr{E}}_{ij} = \langle A_i, \mathscr{E}[A_j] \rangle = \mathrm{tr}\left[A_i^{\dagger} \mathscr{E}[A_j]\right].$$

Using this equation it is easy to prove that the representation of the adjoint operator of $\mathscr{E}$, see eq. (2.25), is simply $\hat{\mathscr{E}}^{*} = \hat{\mathscr{E}}^{\dagger}$.

3.3.1 Hermitian and traceless basis

Two types of basis are specially useful in this work, the first one are the hermitian basis. This is, every orthonormal basis $\{A_i\}_i$ that fulfills $A_i = A_i^{\dagger}$, $\forall i$. To show the utility of this kind of basis, let us introduce the following definition,

Definition 8 (Hermiticity preserving operators)**.** *A linear operator $\mathscr{E} : \mathscr{B}(\mathscr{H}) \to \mathscr{B}(\mathscr{H})$ preserves hermiticity if*

$$\mathscr{E}[\Delta]^{\dagger} = \mathscr{E}[\Delta^{\dagger}],\ \forall \Delta \in \mathscr{B}(\mathscr{H}).$$

Using the Kraus representation is trivial to prove that linear CPTP maps preserve hermiticity, using complete positivity. Furthermore, hermiticity preserving maps enjoy an hermitian Choi-Jamiołkowski representation, i.e. $\tau_{\mathscr{E}} = \tau_{\mathscr{E}}^{\dagger}$ [Wol11].

Using an hermitian basis it is straightforward to prove the following,

Proposition 1 (Representation with real entries)**.** *Let $\mathscr{E}$ be a linear and hermiticity preserving map. Its matrix representation using an hermitian basis $\{A_i\}$ has real entries.*

Proof. Let $\overline{\hat{\mathscr{E}}_{ij}} = \overline{\mathrm{tr}\left[A_i \mathscr{E}[A_j]\right]}$, where the line over denotes complex conjugation. Distributing the latter inside the argument of the trace and using the hermiticity of A_i, we get $\overline{\hat{\mathscr{E}}_{ij}} = \mathrm{tr}\left[A_i \mathscr{E}[A_j]^{\dagger}\right]$, finally stressing that $\mathscr{E}[A_j]^{\dagger} = \mathscr{E}[A_j^{\dagger}] = \mathscr{E}[A_j]$, we arrive to $\overline{\hat{\mathscr{E}}_{ij}} = \hat{\mathscr{E}}_{ij}$. □

This simple property will be used later to prove the equivalence of the problem of finding channels that can be written as $\mathscr{E} = \exp(L)$, with L a Lindblad operator.

The second useful type of basis are the so called traceless bases. They are defined as follows. Let $\{F_i\}_{i=0}^{d^2-1}$ be an orthogonal basis, where we have indicated the dimension of the space $\mathscr{T}(\mathscr{H})$ as d^2 with $d = \dim(\mathscr{H})$, it is traceless if $F_0 = \mathbb{1}/\sqrt{n}$ and $\mathrm{tr}\, F_i = 0 \;\; \forall i > 0$. The traceless property comes from the fact that only one element has non-zero trace, it is easy to prove that it must be proportional to the identity, given that one can write the identity matrix using such basis.

This basis is useful to prove that generators of quantum dynamical maps, L_t, defined with $\mathscr{E}_{(t+\varepsilon,t)}[\rho] = \rho + \varepsilon L_t[\rho] + \mathscr{O}(\varepsilon^2)$, have the following specific structure.

Theorem 8 (Specific form of generators of dynamical maps)**.** *Let $L : \mathscr{T}(\mathscr{H}) \to \mathscr{T}(\mathscr{H})$ be a linear operator fulfilling $L[\Delta]^{\dagger} = L[\Delta^{\dagger}]$ and $\mathrm{tr}\,[L[\Delta]] = 0$ (or equivalently $L^*[\mathbb{1}] = 0$), then it has the following form,*

$$L[\rho] = \mathrm{i}[\rho, H] + \sum_{i,j=1}^{d^2-1} G_{ij}\left(F_i \rho F_j^{\dagger} - \frac{1}{2}\{F_j^{\dagger} F_i, \rho\}\right), \tag{3.3}$$

where $d = \dim(\mathscr{H})$, $H \in \mathbb{C}^{d\times d}$ and $G \in \mathbb{C}^{\left(d^2-1\right)\times\left(d^2-1\right)}$ are hermitian, and $\{F_i\}_{i=0}^{d^2-1}$ is an orthonormal traceless basis of $\mathscr{B}(\mathscr{H})$.

Notice that Lindblad operators enjoy such form with the additional condition that $G \geq 0$, see eq. (2.20). A proof of this is given in Ref. [EL77] for the infinite dimensional case using technicalities beyond this work. Here we will prove it for

the finite dimensional case, using the notation of an incomplete proof given in Ref. [WECC08].

Proof. Since L preserves hermiticity, it has an hermitian Choi-Jamiołkowski matrix, $\tau_L \in \mathbb{C}^{d^2\times d^2}$. We can write such matrix always as

$$\tau_L = \tau_\phi - |\Psi\rangle\langle\Omega| - |\Omega\rangle\langle\Psi|, \tag{3.4}$$

where $|\Psi\rangle = -\omega_\perp \tau_L |\Omega\rangle - (\lambda/2)|\Omega\rangle$, $\lambda = \langle\Omega|\tau_L|\Omega\rangle$, $\omega_\perp \tau_L \omega_\perp = \omega_\perp \tau_\phi \omega_\perp = \tau_\phi$ and $\omega_\perp = \mathbb{1} - \omega$. Observe that choosing the traceless operator basis $\{F_i\}_{i=0}^{d^2-1}$, it is simple to prove that the matrix τ_ϕ can be understood also as the Choi-Jamiołkowski matrix of the following operator:

$$\phi[\rho] = \sum_{i,j=1}^{d^2-1} G_{ij} F_i \rho F_j^\dagger, \tag{3.5}$$

with G hermitian, i.e. $\tau_\phi = (\mathrm{id}_{d^2} \otimes \phi)[\omega]$. This can be shown noticing that the summation $\sum_{i,j=1}^{d^2-1}$ goes over only traceless operators, therefore the projections into the one-dimensional space of $|\Omega\rangle$ of the Choi matrix of ϕ are null,

$$\omega\tau_\phi = \sum_{i,j=1}^{d^2-1} G_{ij} \frac{1}{d} \mathrm{tr}(F_i)\, \omega \left(\mathbb{1} \otimes F_j^\dagger\right) = 0\,,$$

and similarly for

$$\tau_\phi \omega = 0\,.$$

For the second and third terms of Eq. 3.4, it is easy to show that the corresponding operator is simply $\rho \mapsto -\kappa\rho - \rho\kappa^\dagger$, where we identify $|\Psi\rangle = (\mathbb{1} \otimes \kappa)|\Omega\rangle$.

Up to now we have shown that hermiticity preserving generators have the form

$$L[\rho] = \phi[\rho] - \kappa\rho - \rho\kappa^\dagger. \tag{3.6}$$

Using the condition $L^*[\mathbb{1}] = 0$, we have that

$$\kappa + \kappa^\dagger = \phi^*[\mathbb{1}],$$

i.e. the hermitian part of κ is given by $\frac{1}{2}\sum_{i,j=1}^{d^2-1} G_{ij} F_j^\dagger F_i$. Simply writing the anti-hermitian part as iH we end up with

$$\kappa = \mathrm{i}H + \frac{1}{2}\sum_{i,j=1}^{d^2-1} G_{ij} F_j^\dagger F_i.$$

Substituting this expression and eq. (3.5), in eq. (3.6), we arrive to the desired form, see 4.5. □

Notice that the operator ϕ is completely positive if and only if $G \geq 0$ [HZ12], thus, $G \geq 0 \Leftrightarrow \tau_\phi \geq 0$. In such case L has exactly a Lindblad form. This condition will be introduced later as *conditional complete positivity* [EL77, WECC08].

The following is a central and useful result for our work.

Proposition 2 (Conditional complete positivity)**.** *An hermiticity preserving linear operator $L : \mathscr{T}(\mathscr{H}) \to \mathscr{T}(\mathscr{H})$ fulfilling $\operatorname{tr}[L^*[\mathbb{1}]] = 0$, has Lindblad form if and only if*

$$\omega_\perp \tau_L \omega_\perp \geq 0.$$

Additionally choosing an arbitrary basis of the Hilbert space to write operators $\{F_i\}_{i=1}^{d^2}$, it is easy to prove that G and $\omega_\perp \tau_L \omega_\perp$ are related by an unitary conjugation [CDG19].

3.4 Qubit channels

We shall devote some time to the most simple but non-trivial quantum system, the qubit. This case turns to be rich enough to use and test the tools provided by the literature and the ones developed here, in the context of divisibility. We recall a particular representation and a couple of decomposition theorems for qubit channels.

3.4.1 Pauli representation and Ruskai's decomposition

In the case of qubit channels we can have at the same time an hermitian, traceless and unitary basis, it is the simple Pauli basis $\frac{1}{\sqrt{2}}\{\mathbf{1}, \sigma_x, \sigma_y, \sigma_z\}$. This induces a simple 4×4 representation with real entries given by

$$\hat{\mathscr{E}} = \begin{pmatrix} 1 & \vec{0}^T \\ \vec{t} & \Delta \end{pmatrix}, \tag{3.7}$$

where Δ is a 3×3 matrix with real entries and $\vec{t}$ a column vector. This describes the action of the channel in the Bloch sphere picture in which the points $\vec{r}$ are identified with density matrices $\rho_{\vec{r}} = \frac{1}{2}(\mathbb{1} + \vec{r} \cdot \vec{\sigma})$ [RSW02]. Therefore the action of the channel is described by $\mathscr{E}(\rho_{\vec{r}}) = \rho_{\Delta\vec{r}+\vec{t}}$.

In order to study qubit channels with simpler expressions, we will consider a decomposition in unitaries such that

$$\mathscr{E} = \mathscr{U}_1 \mathscr{D} \mathscr{U}_2. \tag{3.8}$$

This can be achieved using Ruskai's decomposition [RSW02], which can be performed by decomposing Δ in rotation matrices, i.e. $\Delta = R_1 D R_2$, where $D = \mathrm{diag}(\lambda_1, \lambda_2, \lambda_3)$ is diagonal and the rotations $R_{1,2} \in \mathrm{SO}(3)$ (of the Bloch sphere) correspond to the unitary channels $\mathscr{U}_{1,2}$. Notice that as D is not required to be positive-semidefinite, Ruskai's decomposition must not be confused with the singular value decomposition. The latter allows decompositions that include total reflections. Such operations do not correspond to unitaries over a qubit, in fact they are not CPTP. An example of this is the universal NOT gate defined by $\rho \mapsto \mathbb{1} - \rho$, it is PTP but not CPTP. The resulting form from Ruskai's decomposition is stated in the following theorem,

Theorem 9 (Special orthogonal normal form)**.** *For any qubit channel $\mathscr{E}$, there exist two unitary conjugations , $\mathscr{U}_1$ and $\mathscr{U}_2$, such that $\mathscr{E} = \mathscr{U}_1 \mathscr{D} \mathscr{U}_2$, where $\mathscr{D}$ has the following form in the Pauli basis,*

$$\hat{\mathscr{D}} = \begin{pmatrix} 1 & \vec{0}^T \\ \vec{\gamma} & D \end{pmatrix}, \tag{3.9}$$

and is called special orthogonal normal form of $\mathscr{E}$.

Here, $R_1^{\mathrm{T}} \Delta R_2^{\mathrm{T}} = D$ and $\vec{\gamma} = R_1^T \vec{t}$. The latter describes the shift of the center of the Bloch sphere under the action of $\mathscr{D}$. The parameters $\vec{\lambda}$ determine the length of semi-axes of the Bloch ellipsoid, being the deformation of Bloch sphere under the action of $\mathscr{E}$. In particular $\det \hat{\mathscr{D}} = \det \hat{\mathscr{E}} = \lambda_1 \lambda_2 \lambda_3$.

To develop geometric intuition in the space determined by the possible values of the three parameters of $\vec{\lambda}$, consider the Choi-Jamiołkowski representation of the special orthogonal normal form of an arbitrary channel in the basis that diagonalises D,

$$\tau_{\mathscr{D}} = \frac{1}{4} \begin{pmatrix} \gamma_3 + \lambda_3 + 1 & \gamma_1 - i\gamma_2 & 0 & \lambda_1 + \lambda_2 \\ \gamma_1 + i\gamma_2 & -\gamma_3 - \lambda_3 + 1 & \lambda_1 - \lambda_2 & 0 \\ 0 & \lambda_1 - \lambda_2 & \gamma_3 - \lambda_3 + 1 & \gamma_1 - i\gamma_2 \\ \lambda_1 + \lambda_2 & 0 & \gamma_1 + i\gamma_2 & -\gamma_3 + \lambda_3 + 1 \end{pmatrix}. \tag{3.10}$$

Complete positivity is determined by the non-negativity of its eigenvalues, given that it is hermitian, but it turns that for the general case they have complicated expressions. To overcome this problem we use the fact that if $\mathscr{D}$ is a channel, then

its *unital part*, defined by taking $\vec{\gamma} = \vec{0}$, is a channel too [Wol11]. Therefore the set of the possible values of $\vec{\lambda}$ for the general case is contained in the set arising from the unital case. The complete positivity conditions for the latter are

$$1 + \lambda_i \pm (\lambda_j + \lambda_k) \geq 0, \tag{3.11}$$

with i, j and k all different, this implies that the possible set of lambdas lives inside the tetrahedron with corners $(1,1,1)$, $(1,-1,-1)$, $(-1,1,-1)$ and $(-1,-1,1)$, see fig. 3.1. For unital channels, all points in the tetrahedron are allowed. The corner $\vec{\lambda} = (1,1,1)$ corresponds to the identity channel, $\vec{\lambda} = (1,-1,-1)$ to σ_x $\vec{\lambda} = (-1,1,-1)$ to σ_y and $\vec{\lambda} = (-1,-1,1)$ to σ_z (Kraus rank 1 operations). Points in the edges correspond to Kraus rank 2 operations, points in the faces to Kraus rank 3 operations and in the interior of the tetrahedron to Kraus rank 4 operations. In particular, this tetrahedron defines the set of *Pauli channels*, which are defined to have diagonal special orthogonal normal form.

Definition 9 (Pauli channels)**.** *A qubit channel $\mathscr{E}$ is a Pauli channel if*

$$\mathscr{E}[\rho] = \sum_{i=0}^{3} p_i \sigma_i \rho \sigma_i, \tag{3.12}$$

with $\sigma_0 := \mathbb{1}$, $p_i \geq 0$ and $\sum_{i=0}^{3} p_i = 1$.

For non-unital channels more restrictive conditions arise, an example will be given later.

3.4.2 1wSLOCC and singular value decomposition using the Lorentz metric

There is another parametrization for qubit channels called *Lorentz normal decomposition* [VDD01] which is specially useful to characterize infinitesimal divisibility $\mathsf{C}^{\mathrm{Inf}}$. To introduce it, let us resort to chapter 2 where we discussed local operations and classical communication. For the two-qubit case, the operations that Alice and Bob apply for their reduced states are

$$\begin{aligned} \rho_A &\mapsto X \rho_A X^\dagger \\ \rho_B &\mapsto Y \rho_B Y^\dagger, \end{aligned} \tag{3.13}$$

where we have shown that it is enough to consider $X, Y \in \mathrm{SL}(2,\mathbb{C})$ for X and Y invertible, see chapter 2 Now we are going to show that such operations can be

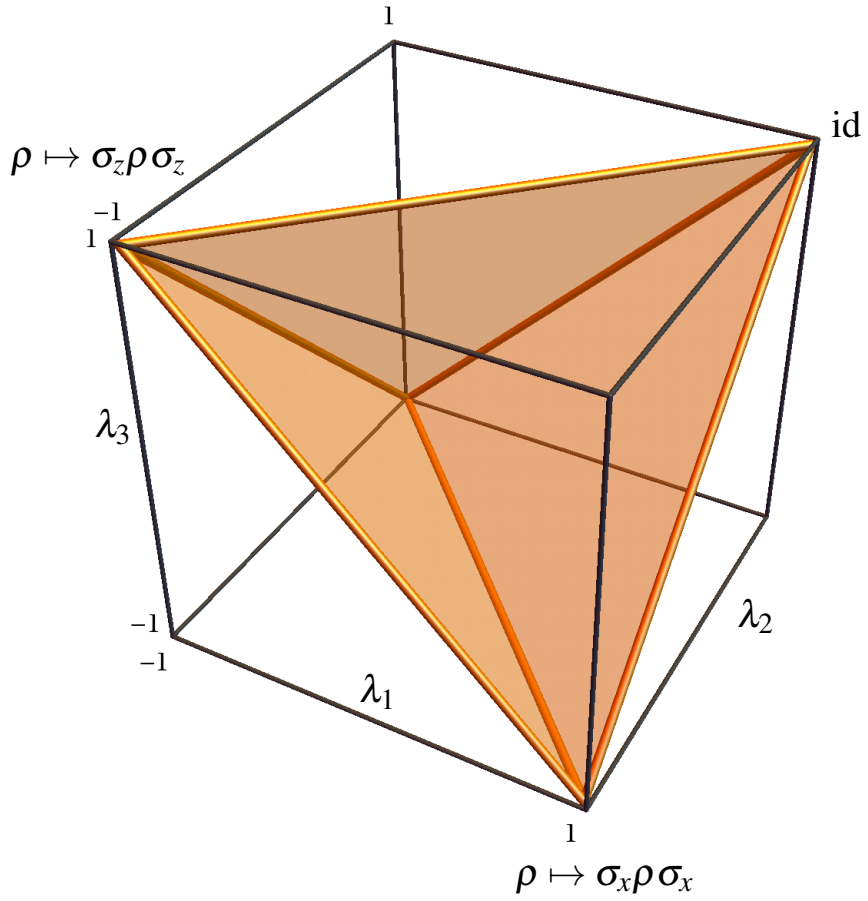

Figure 3.1: Set of the possible values of $\vec{\lambda}$. This set has the shape of a tetrahedron where the corners are the Pauli unitaries ($\mathbb{1}$, σ_x and σ_z are indicated in the figure, while σ_y lies behind). The rest of the body contains convex combinations of Pauli unitaries. Unital qubit channels can be obtained by concatenating Pauli channels with unitary conjugations, see theorem 9.

understood as proper orthochronous Lorentz transformations in the Pauli representation.

Consider an arbitrary hermitian operator Δ and its representation in the Pauli basis,

$$\Delta = (\mathbb{1}\,\mathrm{tr}\,\Delta + \vec{r}_\Delta \cdot \vec{\sigma})/2$$

with $\det\Delta = (\mathrm{tr}\,\Delta)^2 - |\vec{r}_\Delta|^2$. Now observe that $\det\Delta$ can be understood as the squared Lorentz norm of the four-vector $r_\Delta = (\mathrm{tr}\,\Delta, \vec{r}_\Delta)^{\mathrm{T}}$, lying in the Minkowski vector space, denoted as $(\mathbb{R}^4, \eta)$, where $\eta = \mathrm{diag}\,(1,-1,-1,-1)$ is the *Lorentz metric*. Therefore we have

$$\det\Delta = |r_\Delta|^2_{\mathrm{Lorentz}} = \langle r_\Delta, \eta\, r_\Delta\rangle, \tag{3.14}$$

with $\langle\cdot\rangle$ the standard inner product. Then $\mathrm{tr}\,\Delta$ is a time-like component and $\vec{r}_\Delta$ space-like components.

Given that operations shown in eq. (3.13) preserve the determinant, they are isometries in the Minkowski space. That is, they preserve the norm shown in eq. (3.14) for any vector r_Δ (with Δ hermitian). Additionally, due to linearity of eq. (3.13), these operations belong to $\mathrm{SO}(3,1)$ (the Lorentz group). In fact, due to the positivity of quantum operations, they do not change the sign of the trace (the time-like component); therefore the transformations are orthochronous. Also notice that $\mathrm{SL}(2,\mathbb{C})$ contains the identity transformation, therefore the set of one-way stochastic local operations and classical communication is identified with the proper orthochronous Lorentz group, $\mathrm{SO}^+(1,3)$ [Wol11, Tun85]. However, since $-X$ and X give the same result, see eq. (3.13), and both belong to $\mathrm{SL}(2,\mathbb{C})$, one says that the latter is a double cover of $\mathrm{SO}^+(1,3)$. This map is also called *spinor map*.

Given this map, it is expected that the operations mentioned in eq. (3.13) are explicitly Lorentz matrices, when writing them in the Pauli basis. Also notice that unitary conjugations are particular cases of them [RSW02], therefore one can think of a different decomposition using the Lorentz metric instead of the three dimensional Euclidean metric, used in Ruskai's decomposition.

The Lorentz normal form was introduced first for two-qubit states by writing them as

$$\tau = \frac{1}{4}\sum_{ij} R_{ij}\,\sigma_i \otimes \sigma_j, \tag{3.15}$$

where we have used the notation of Choi-Jamiołkowski states for convenience. This decomposition is derived from the theorem 3 of Ref. [VDD01], which essentially states that the matrix R can be decomposed as

$$R = L_1 \Sigma L_2^{\mathrm{T}}. \tag{3.16}$$

Here $L_{1,2}$ are proper orthochronous Lorentz transformations and Σ is either $\Sigma = \mathrm{diag}\,(s_0, s_1, s_2, s_3)$ with $s_0 \geq s_1 \geq s_2 \geq |s_3|$, or

$$\Sigma = \begin{pmatrix} a & 0 & 0 & b \\ 0 & d & 0 & 0 \\ 0 & 0 & -d & 0 \\ c & 0 & 0 & -b+c+a \end{pmatrix}. \tag{3.17}$$

Note that Σ corresponds to an unnormalized state, with trace $\mathrm{tr}\,\Sigma = a$. Thus, the normalization constant is $\alpha = a^{-1}$.

To introduce the Lorentz normal decomposition of qubit channels, let us first introduce the following. Let $\mathscr{E}$ a qubit channel and $\hat{\mathscr{E}}$ its matrix representation using the Pauli basis. The latter is related with the matrix R, which defines its Choi-Jamiołkowski state, see eq. (3.15),

$$\hat{\mathscr{E}}\Phi_{\mathrm{T}} = R, \tag{3.18}$$

where $\Phi_{\mathrm{T}} = \mathrm{diag}\,(1,1,-1,1)$. This can be shown by defining a generic Pauli channel, computing its Choi matrix and extracting R using the Hilbert-Schmidt inner product with the basis $\{\sigma_i \otimes \sigma_j\}_{i,j}$. Now, defining the decomposition for channels throughout decomposing the Choi-Jamiołkowski state, we can easily compute the corresponding Lorentz transformations using equations (3.18) and (3.16):

$$\begin{aligned} R\Phi_{\mathrm{T}} &= \alpha L_1 \Sigma L_2^{\mathrm{T}} \Phi_{\mathrm{T}} \\ \hat{\mathscr{E}} &= \alpha L_1 \Sigma L_2^{T} \Phi_{\mathrm{T}} && (3.19) \\ &= L_1 \left(\alpha \Sigma \Phi_{\mathrm{T}}\right) \Phi_{\mathrm{T}} L_2^{T} \Phi_{\mathrm{T}} && (3.20) \\ &= L_1 \hat{\tilde{\mathscr{E}}} \tilde{L}_2^{T}, && (3.21) \end{aligned}$$

where $\hat{\tilde{\mathscr{E}}} = \alpha \Sigma \Phi_{\mathrm{T}}$ is the Lorentz normal form of $\hat{\mathscr{E}}$. Also notice that $\tilde{L}_2^{\mathrm{T}} = \Phi_{\mathrm{T}} L_2^{\mathrm{T}} \Phi_{\mathrm{T}}$ is proper and orthochronous, given that its determinant is positive and Φ_{T} is proper. Therefore the possible Lorentz normal forms for channels are $\hat{\tilde{\mathscr{E}}} = \mathrm{diag}\,(s_0, s_1, -s_2, s_3)$ with $s_0 \geq s_1 \geq s_2 \geq |s_3|$, or

$$\Sigma = \begin{pmatrix} a & 0 & 0 & b \\ 0 & d & 0 & 0 \\ 0 & 0 & d & 0 \\ c & 0 & 0 & -b+c+a \end{pmatrix}. \tag{3.22}$$

Using this, the authors of Ref. [VV02] introduced a theorem (theorem 8 of the reference) defining the Lorentz normal form for channels by forcing $b = 0$, in order to have normal forms proportional to trace-preserving operations. The latter

is equivalent to say that the decomposition of Choi-Jamiołkowski states leads to states that are also Choi-Jamiołkowski. We didn't find a good argument to justify such assumption, and found a counterexample that shows that Lorentz normal forms with $b \neq 0$ exist (see appendix B). Therefore in general we can find a Σ with form of eq. (3.17) with $b \neq 0$. The consequence of this is that the theorem 8 of Ref. [VV02] is incomplete, but given that form of eq. (3.17) is Kraus rank deficient (it has rank three for $b \neq c$ and two for $b = c$), the full Kraus rank case is still useful. Thus, we propose a restricted version of their theorem:

Theorem 10 (Restricted Lorentz normal form for qubit quantum channels). *For any full Kraus rank qubit channel $\mathscr{E}$ there exist rank-one completely positive maps $\mathscr{T}_1, \mathscr{T}_2$ such that $\mathscr{T} = \mathscr{T}_1 \mathscr{E} \mathscr{T}_2$ is proportional to*

$$\begin{pmatrix} 1 & \vec{0}^T \\ \vec{0} & \Lambda \end{pmatrix}, \tag{3.23}$$

where $\Lambda = \mathrm{diag}(s_1, s_2, s_3)$ with $1 \geq s_1 \geq s_2 \geq |s_3|$.

The channel $\mathscr{T}$ is called the Lorentz normal form of the channel $\mathscr{E}$. For unital qubit channels D coincides with Λ.

3.5 Representation of Gaussian quantum channels

In this section we start from two ansätze, that put together with the Gaussian functional form considered in Ref. [MP12], lead to the complete set of functional forms in position state representation of one-mode Gaussian channels.

We will show that only two possible forms of δGQC hold according to *trace preserving* (TP) and *hermiticity preserving* (HP) conditions. The one corresponding to eq. (2.33) is one of these, as expected. Later on we will impose *complete positivity* in order to have valid GQC, i.e. *complete positive and trace preserving* (C) Gaussian operations.

Following definition 7, those channels can be characterized by how they act over Gaussian states. It is well known that the action of GQCs on Gaussian states is described by *affine transformations* [WPGP$^+$12]. Let $\mathscr{A}$ be a GQC defined by a tuple such that $\mathscr{A} = \mathscr{A}(\mathbf{T}, \mathbf{N}, \vec{\tau})$, where $\mathbf{T}$ and $\mathbf{N}$ are 2×2 real matrices with $\mathbf{N} = \mathbf{N}^{\mathrm{T}}$ [WPGP$^+$12]. The transformation acts on Gaussian states according to

$$\mathscr{A}(\mathbf{T}, \mathbf{N}, \vec{\tau}) \left[S\left(\sigma, \vec{d}\right) \right] = S\left(\mathbf{T}\sigma\mathbf{T}^{\mathrm{T}} + \mathbf{N}, \mathbf{T}\vec{d} + \vec{\tau} \right).$$

In the particular case of closed systems, where the system is governed by a Gaussian unitary, we have that $\mathbf{N} = \mathbf{0}$ and $\mathbf{T}$ is a symplectic matrix.

3.5.1 Possible functional forms of δGQC operations

Let us introduce the ansätze for the possible forms of GQC in the position representation, to perform the black-box characterization. Following eq. (2.29) and taking the continuous variable representation of difference and sum coordinates, the trace becomes an integral over position variables of the environment. Then we end up with a Fourier transform of a multivariate Gaussian. Since the Fourier transform of a Gaussian is again a Gaussian (unless there are singularities in the coefficients, as in the example of eq. (2.33)), the result of the Fourier transform for one mode can have the following structures: a Gaussian form [eq. (2.31)], a Gaussian form multiplied with one-dimensional delta or a Gaussian form multiplied by a two-dimensional delta. No more deltas are allowed given that there are only two integration variables when applying the channel, see eq. (2.30). Thus, in order to start with the black-box characterization, we shall propose the following general Gaussian operations with one and two deltas, respectively

$$J_{\mathrm{I}}(x_f, r_f; x_i, r_i) = \mathscr{N}_{\mathrm{I}}\delta(\vec{\alpha}^{\mathrm{T}}\vec{v}_f + \vec{\beta}^{\mathrm{T}}\vec{v}_i)e^{\Sigma(x_f,x_i;r_f,r_i)}, \tag{3.24}$$

$$J_{\mathrm{II}}(x_f, r_f; x_i, r_i) = \mathscr{N}_{\mathrm{II}}\delta(\mathbf{A}\vec{v}_f - \mathbf{B}\vec{v}_i)e^{\Sigma(x_f,x_i;r_f,r_i)}, \tag{3.25}$$

with $\vec{v}_{i,j} = (r_{i,j}, x_{i,j})$, and $\mathscr{N}_{\mathrm{I,II}}$ are normalization constants. Coefficient arrays $\mathbf{A}$, $\mathbf{B}$, $\vec{\alpha}$, and $\vec{\beta}$ have real entries since initial and final coordinates must be real. Finally, the exponent reads:

$$\begin{aligned}\Sigma(x_f, x_i; r_f, r_i) = \imath\Big(&b_1 x_f r_f + b_2 x_f r_i + b_3 x_i r_f + b_4 x_i r_i + c_1 x_f + c_2 x_i\Big) \\ &- a_1 x_f^2 - a_2 x_f x_i - a_3 x_i^2 - e_1 r_f^2 - e_2 r_f r_i - e_3 r_i^2 - d_1 r_f - d_2 r_i.\end{aligned}$$

They provide, together with eq. (2.31) all possible ansätze for GQC.

3.5.2 Hermiticity and trace preserving conditions

Before studying CPTP conditions it is useful to simplify expressions of equations (3.24) and (3.25). To do this we use the fact that linear CPTP operations preserve hermiticity and trace. For channels of continuous variable systems in the position

state representation, $J(q_f, q'_f; q_i, q'_i)$, HP condition is derived as follows,

$$\begin{aligned}\rho_f(q'_f, q_f)^* &= \int_{\mathbb{R}^2} dq_i dq'_i J(q'_f, q_f; q_i, q'_i)^* \rho_i(q_i, q'_i)^* \\ &= \int_{\mathbb{R}^2} dq_i dq'_i J(q'_f, q_f; q'_i, q_i)^* \rho_i(q_i, q'_i) \\ &= \rho_f(q_f, q'_f),\end{aligned} \tag{3.26}$$

where the last equality holds if

$$J(q_f, q'_f; q_i, q'_i) = J(q'_f, q_f; q'_i, q_i)^*.$$

Using sum and difference coordinates, HP becomes

$$J(-x_f, r_f; -x_i, r_i) = J(x_f, r_f; x_i, r_i)^*. \tag{3.27}$$

Following this equation and comparing exponents of the both sides of the last equations, it is easy to note that the coefficients a_n, b_n, c_n, e_n and d_n must be real. Concerning the delta factors, in eq. (3.27) we end up with expressions like

$$\delta\left(\alpha_1 x_f + \alpha_2 x_i + \beta_1 r_f + \beta_2 r_i\right) = \delta\left(-\alpha_1 x_f - \alpha_2 x_i + \beta_1 r_f + \beta_2 r_i\right)$$

for both cases. Therefore the equality holds for eq. (3.24) only for two possible combinations of variables: i) $\delta(\alpha x_f - \beta x_i)$ and ii) $\delta(\alpha r_f - \beta r_i)$. For the case of eq. (3.25), equality holds only for iii) $\delta(\gamma r_f - \eta r_i)\delta(\alpha x_f - \beta x_i)$. Let us now analyze the trace preserving condition (TP), since the trace of ρ_f in sum and difference coordinates is

$$\begin{aligned}\mathrm{tr}\,\rho_f &= \int_{\mathbb{R}} dr'_f \rho_f(x_f = 0, r'_f) \\ &= \int_{\mathbb{R}} dr'_f dr_i dx_i J(x_f = 0, r'_f; x_i, r_i)\rho_i(x_i, r_i) \\ &= \int_{\mathbb{R}} dr_i \rho_i(x_i = 0, r_i).\end{aligned}$$

To fulfill the last equality, the following must be accomplished

$$\int_{\mathbb{R}} dr'_f J(x_f = 0, r'_f; x_i, r_i) = \delta(x_i). \tag{3.28}$$

This condition immediately discards ii) from the above combinations of deltas, thus we end up with cases i) and iii). For case i) TP reads:

$$\mathscr{N}_1 \int dr_f \delta(-\beta x_i) e^{\Sigma} = \frac{\mathscr{N}_1}{|\beta|}\sqrt{\frac{\pi}{e_1}}\delta(x_i) e^{\left(\frac{e_2^2}{4e_1} - e_3\right) r_i^2}, \tag{3.29}$$

thus, the relation between the coefficients assumes the form

$$\frac{e_2^2}{4e_1} - e_3 = 0, d_1 = 0, d_2 = 0, \tag{3.30}$$

and the normalization constant $\mathscr{N}_{\mathrm{I}} = |\beta|\sqrt{\frac{e_1}{\pi}}$ with $\beta \neq 0$ and $e_1 > 0$. For case iii) the trace-preserving condition reads

$$\mathscr{N}_{\mathrm{II}} \int dr_f \delta(\gamma r_f - \eta r_i)\delta(-\beta x_i)e^{\Sigma} = \frac{\mathscr{N}_{\mathrm{II}}}{|\beta\gamma|}\delta(x_i)e^{-\left(e_1(\frac{\eta}{\gamma})^2 + e_2\frac{\eta}{\gamma} + e_3\right)r_i^2 - \left(d_1\frac{\eta}{\gamma} + d_2\right)r_i}.$$

Thus, the following relation between e_n and d_n coefficients must be fulfilled:

$$e_1\left(\frac{\eta}{\gamma}\right)^2 + e_2\frac{\eta}{\gamma} + e_3 = 0, \;\; d_1\frac{\eta}{\gamma} + d_2 = 0, \tag{3.31}$$

with $\gamma, \beta \neq 0$ and $\mathscr{N}_{\mathrm{II}} = |\beta\gamma|$. In the particular case of $\eta = 0$, eq. (3.31) is reduced to $e_3 = d_2 = 0$. As expected from the analysis of limits above, we showed that δGQC's admit quadratic terms in $r_{i,j}$.

3.5.3 Complete positivity conditions

Up to this point we have *hermitian and trace preserving Gaussian operations*; to derive the remaining CPTP conditions, it is useful to write its Wigner's function and Wigner's characteristic function. The representation of the Wigner's characteristic function reads

$$\begin{aligned}\chi(\vec{k}) &= \mathrm{tr}\left[\rho D(\vec{k})\right] \\ &= \exp\left[-\frac{1}{2}\vec{k}^{\mathrm{T}}\left(\Omega\sigma\Omega^{\mathrm{T}}\right)\vec{k} - \imath\left(\Omega\langle\hat{x}\rangle\right)^{\mathrm{T}}\vec{k}\right]\end{aligned} \tag{3.32}$$

and its relation with Wigner's function:

$$W(\mathbf{x}) = \int_{\mathbb{R}^2} d\vec{x} e^{-\imath\vec{x}^{\mathrm{T}}\Omega\vec{k}}\chi\left(\vec{k}\right) \tag{3.33}$$

$$= \int_{\mathbb{R}} e^{\imath px} dx \left\langle r - \frac{x}{2}\middle|\,\hat{\rho}\,\middle| r + \frac{x}{2}\right\rangle, \tag{3.34}$$

where $\vec{k} = (k_1, k_2)^{\mathrm{T}}$, $\vec{x} = (r, p)^{\mathrm{T}}$ and $\hbar = 1$ (we are using natural units). Using the previous equations to construct Wigner and Wigner's characteristic functions of the initial and final states, and substituting them in the equation 2.30, it is

straightforward to get the propagator in the Wigner's characteristic function representation:

$$\tilde{J}\left(\vec{k}_f,\vec{k}_i\right)=\int_{\mathbb{R}^6} d\Gamma K(\vec{l})J(\vec{v}_f,\vec{v}_i), \tag{3.35}$$

where the transformation kernel reads

$$K(\vec{l})=\frac{1}{(2\pi)^3}e^{\left[\imath\left(k_2^f r_f-k_1^f p_f-k_2^i r_i+k_1^i p_i-p_i x_i+p_f x_f\right)\right]},$$

with $d\Gamma = dp_f dp_i dx_f dx_i dr_f dr_i$ and $\vec{l}=(p_f,p_i,x_f,x_i,r_f,r_i)^{\mathrm{T}}$. By elementary integration of eq. (3.35) one can show that for both cases

$$\tilde{J}_{\mathrm{I,III}}\left(\vec{k}_f,\vec{k}_i\right)=\delta\left(k_1^i-\frac{\alpha}{\beta}k_1^f\right)\delta\left(k_2^i-\vec{\phi}_{\mathrm{I,III}}^{\mathrm{T}}\vec{k}_f\right)e^{P_{\mathrm{I,III}}(\vec{k}_f)}, \tag{3.36}$$

where $P_{\mathrm{I,III}}(\vec{k}_f)=\sum_{i,j=1}^{2}P_{ij}^{(\mathrm{I,III})}k_i^f k_j^f+\sum_{i=1}^{2}P_{0i}^{(\mathrm{I,III})}k_i^f$ with $P_{ij}^{(\mathrm{I,III})}=P_{ji}^{(\mathrm{I,III})}$. For case i) we obtain

$$\begin{aligned}
P_{11}^{(\mathrm{I})}&=-\left(\left(\frac{\alpha}{\beta}\right)^2\left(a_3+\frac{b_3^2}{4e_1}\right)+\frac{\alpha}{\beta}\left(a_2+\frac{1}{2}\frac{b_1b_3}{e_1}\right)+a_1+\frac{b_1^2}{4e_1}\right),\\
P_{12}^{(\mathrm{I})}&=-\left(\frac{\alpha}{\beta}\frac{b_3}{2e_1}+\frac{b_1}{2e_1}\right),\\
P_{22}^{(\mathrm{I})}&=-\frac{1}{4e_1}.
\end{aligned} \tag{3.37}$$

For case iii) we have

$$\begin{aligned}
P_{11}^{(\mathrm{III})}&=-\left(\left(\frac{\alpha}{\beta}\right)^2 a_3+\frac{\alpha}{\beta}a_2+a_1\right),\\
P_{12}^{(\mathrm{III})}&=P_{22}^{(\mathrm{III})}=0.
\end{aligned} \tag{3.38}$$

And for both cases we have $P_{01}^{(\mathrm{I,III})}=\imath\left(\frac{\alpha}{\beta}c_2+c_1\right)$ and $P_{02}^{(\mathrm{I,III})}=0$. Vectors $\vec{\phi}$ are given by

$$\begin{aligned}
\vec{\phi}_{\mathrm{I}}&=\left(\frac{\alpha}{\beta}\left(b_4-\frac{b_3e_2}{2e_1}\right)-\frac{b_1e_2}{2e_1}+b_2,-\frac{e_2}{2e_1}\right)^{\mathrm{T}},\\
\vec{\phi}_{\mathrm{III}}&=\left(\frac{\alpha}{\beta}\frac{\eta}{\gamma}b_3+\frac{\alpha}{\beta}b_4+\frac{\eta}{\gamma}b_1+b_2,\frac{\eta}{\gamma}\right)^{\mathrm{T}}.
\end{aligned} \tag{3.39}$$

We are now in position to write explicitly the conditions for complete positivity. Having a Gaussian operation characterized by $(\mathbf{T},\mathbf{N},\vec{\tau})$, the CP condition can be expressed in terms of the matrix

$$\mathbf{C} = \mathbf{N} + \imath\Omega - \imath\mathbf{T}\Omega\mathbf{T}^{\mathrm{T}}, \tag{3.40}$$

where $\Omega = \begin{pmatrix} 0 & 1 \\ -1 & 0 \end{pmatrix}$ is the symplectic matrix. An operation $\mathscr{A}(\mathbf{T},\mathbf{N},\vec{\tau})$ is CP if and only if $\mathbf{C} \geq 0$ [Lin00, WPGP$^+$12]. Applying the propagator on a test characteristic function, eq. (3.32), it is easy compute the corresponding tuples. For both cases we get:

$$\begin{aligned} \mathbf{N}_{\mathrm{I,III}} &= 2\begin{pmatrix} -P_{22} & P_{12} \\ P_{12} & -P_{11} \end{pmatrix}, \\ \vec{\tau}_{\mathrm{I,III}} &= \left(0, \imath P_{01}^{(\mathrm{I,III})}\right)^{\mathrm{T}}, \end{aligned} \tag{3.41}$$

while for case i) matrix $\mathbf{T}$ is given by

$$\mathbf{T}_{\mathrm{I}} = \begin{pmatrix} \frac{e_2}{2e_1} & 0 \\ \vec{\phi}_{\mathrm{I},1} & -\frac{\alpha}{\beta} \end{pmatrix}, \tag{3.42}$$

where $\vec{\phi}_{\mathrm{I},1}$ denotes the first component of vector $\vec{\phi}_{\mathrm{I}}$, see eq. (3.39). The complete positive condition is given by the inequalities raised from the eigenvalues of matrix eq. (3.40):

$$\pm\frac{\sqrt{\alpha^2 e_2^2 + 4\alpha\beta e_2 e_1 + 4\beta^2 e_1^2\left(4{P_{12}^{(\mathrm{I})}}^2 + \left(P_{11}^{(\mathrm{I})} - P_{22}^{(\mathrm{I})}\right)^2 + 1\right)}}{2\beta e_1} \geq P_{11}^{(\mathrm{I})} + P_{22}^{(\mathrm{I})}. \tag{3.43}$$

For case iii) matrix $\mathbf{T}$ is

$$\mathbf{T}_{\mathrm{III}} = \begin{pmatrix} -\frac{\eta}{\gamma} & 0 \\ \vec{\phi}_{\mathrm{III},1} & -\frac{\alpha}{\beta} \end{pmatrix}, \tag{3.44}$$

and complete positivity conditions read:

$$\pm\frac{\sqrt{(\beta\gamma - \alpha\eta)^2 + \beta^2\gamma^2{P_{11}^{(\mathrm{III})}}^2}}{\beta\gamma} - P_{11}^{(\mathrm{III})} \geq 0. \tag{3.45}$$

Note that in both cases the complete positivity conditions do not depend on $\vec{\phi}$.

Chapter 4

Divisibility of quantum channels and dynamical maps

Wine is sunlight, held together by water.
Galileo Galilei

In this chapter we introduce the formal definition of *divisibility of quantum channels*, inspired by questioning how can we implement a given quantum channel via the concatenation of simpler channels. Later on we define further types of divisibility by adding extra conditions, such as channels being infinitesimal divisible and channels belonging to one-parameter semigroups. These types are physically relevant since both lead to Markovian dynamical maps [ARHP14]. We additionally prove three theorems, which are the central contributions of this part of the work. Finally, a complete characterization of channels belonging to one-parameter semigroups that is given.

4.1 Divisibility of quantum maps

A quantum channel $\mathscr{E}$ is said to be divisible if it can be expressed as the concatenation of two non-trivial channels,

Definition 10 (Divisibility)**.** *A linear map $\mathscr{E} \in \mathsf{C}$ is divisible if there exists a decomposition,*

$$\mathscr{E} = \mathscr{E}_2 \mathscr{E}_1, \tag{4.1}$$

such that $\mathscr{E}_1$ and $\mathscr{E}_2$ are non-unitary channels, or $\mathscr{E}$ is unitary.

Notice that this definition ensures that unitary channels are divisible, and that non-unitary channels must be divisible in non-unitary channels. This prevents one to consider simple changes of basis as a "division" of a given quantum operation. This type of divisibility, which is the most general and less restrictive one, defines a set that will be denoted by C^{div}. The set of indivisible channels is the complement of C^{div} in C, therefore it will be denoted as $\overline{\mathsf{C}^{\text{div}}}$. Notice that this definition is different to the one given in Ref. [WC08] where unitary channels are excluded to be divisible.

The concept of indivisible channels resembles the concept of prime numbers, unitary channels play the role of unity (which are not indivisible/prime), i.e. a composition of indivisible and a unitary channel results in an indivisible channel.

We now introduce three results from Ref. [WC08] that shall be used later. We only give the proof for the second for the sake of brevity.

Theorem 11 (Full Kraus rank channels)**.** *Let $\mathscr{E}:\mathscr{T}(\mathscr{H})\to\mathscr{T}(\mathscr{H})$ be a quantum channel. If it has full Kraus Kraus rank, i.e. d^2 with $d=\dim(\mathscr{H})$, then it is divisible.*

An example of full Kraus rank channel is the total depolarizing channel $\rho\mapsto \mathbb{1}/\dim(\mathscr{H})$, which maps every state into the maximal mixed one.

Theorem 12 (Indivisible channels)**.** *Consider the set C_d of channels acting on the space of density matrices of $d\times d$, i.e. $\mathscr{E}:\mathscr{T}(\mathscr{H})\to\mathscr{T}(\mathscr{H})$ with $d=\dim(\mathscr{H})$. The channel with minimal determinant, $\mathscr{E}_0\in\mathsf{C}_\mathsf{d}$, is indivisible.*

Proof. To prove this we use the fact that channels with negative determinant exist [WC08] (two examples are given below), and the property of monotonicity of the determinant.

Let $\mathscr{E}\in\mathsf{C}$ with $\det\mathscr{E}<0$ and $\mathscr{E}=\mathscr{E}_2\mathscr{E}_1$ an arbitrary division of $\mathscr{E}$ with $\mathscr{E}_1,\mathscr{E}_2\in\mathsf{C}$. The monotonicity of the determinant implies the following,

$$|\det(\mathscr{E}_2\mathscr{E}_1)|=|\det\mathscr{E}_2||\det\mathscr{E}_1|\leq|\det\mathscr{E}_1|.$$

Assuming, without loss of generality that $\det\mathscr{E}_1<0$ and $\det\mathscr{E}_2>0$, we have that

$$\det\mathscr{E}_1\det\mathscr{E}_2\leq\det\mathscr{E}_1.$$

Multiplying both sides by -1 we arrive to

$$|\det\mathscr{E}_2||\det\mathscr{E}_1|\geq|\det\mathscr{E}_1|.$$

Therefore, by monotonicity of the determinant, we have

$$|\det \mathscr{E}_2||\det \mathscr{E}_1| = |\det \mathscr{E}_1|,$$

which implies that $\det \mathscr{E}_2 = 1$, i.e. $\mathscr{E}_2$ is an unitary conjugation [WC08] and $\mathscr{E}$ has minimum determinant. By definition 10 $\mathscr{E}$ is indivisible. □

Two examples for the qubit case are the approximate NOT and the approximate transposition maps:

$$\begin{aligned} \rho &\mapsto \frac{\mathrm{tr}(\rho)\mathbb{1} + \rho^{\mathrm{T}}}{3} \text{ (approximate transposition),} \\ \rho &\mapsto \frac{\mathrm{tr}(\rho)\mathbb{1} - \rho}{3} \text{ (approximate NOT gate),} \end{aligned} \tag{4.2}$$

both have minimal determinant corresponding to $-1/27$, which can be computed from their matrix representation.

Theorem 13 (Unital Kraus rank three channels)**.** *A unital qubit channel is indivisible if and only if it has Kraus rank equal to three.*

This is a restricted version of theorem 23 of Ref. [WECC08], where authors proved the theorem for any qubit channel instead of only unital ones. Since their proof rely on the validity of the Lorentz normal decomposition for channels, we have written here a restricted version, where Lorentz normal form is equivalent to the special orthogonal normal form (see theorem 10 and its discussion).

These results can be used immediately to identify the divisibility character of unital qubit channels, see fig. 4.5. The faces of the tetrahedron (without edges) correspond to indivisible channels, in particular the center of every face corresponds to channels with minimal determinant. The body (full Kraus rank channels) contain divisible channels.

4.1.1 Subclasses of divisible maps

Divisibility of quantum dynamical maps

We motivate the extra conditions to define new types of divisibility on the concept of Markovian process. In subsection 2.2.1 we have introduced the definition of Markovian process and its consequences at the level of propagators of one-point probabilities, see eq. (2.24). Based on this, we introduce the concept of

CP-divisibility of quantum dynamical maps, which is often used as definition of Markovianity in the quantum realm [ARHP14].

Definition 11 (CP-divisible quantum dynamical maps)**.** *Consider a quantum dynamical map $\mathscr{E}_{(t,0)} : \mathscr{T}(\mathscr{H}) \to \mathscr{T}(\mathscr{H})$ with $t \in \mathbb{R}^+$. It is CP-divisible in the interval $[0,t] \subset \mathbb{R}^+$ if for every decomposition of the form*

$$\mathscr{E}_{(t,0)} = \mathscr{E}_{(t,s)}\mathscr{E}_{(s,0)},$$

$\mathscr{E}_{(t,s)}$ is a quantum channel for every $s \in (0,t)$.

A remarkable theorem on CP-divisible maps is the following [Kos72b, Kos72a, Gor76, Lin76, ARHP14],

Theorem 14 (Gorini-Kossakowski-Susarshan-Lindblad)**.** *An operator L_t is the generator of a CP-divisible process if and only if it can be written in the following form:*

$$L_t[\rho] = -\mathrm{i}[H(t),\rho] + \sum_{i,j} G_{ij}(t)\left(F_i(t)\rho F_j^\dagger(t) - \frac{1}{2}\{F_j^\dagger(t)F_i(t),\rho\}\right), \qquad (4.3)$$

where G is hermitian and positive semidefinite, $H(t), F_k(t) \in \mathbb{C}^{d\times d}$ are time-dependent operators acting on $\mathscr{H}$, with $H(t)$ hermitian for every $t \in \mathbb{R}^+$, and $d = \dim(\mathscr{H})$.

In Ref. [RH12] a proof is given starting from the Kraus representation of quantum dynamical maps and the definition of CP-divisibility. Here we will give a simpler proof resorting to theorem 8.

Proof. Notice that for each time t we can define the "instant" map $\mathscr{E}_{(t+\varepsilon,t)}[\rho] = \rho + \varepsilon L_t[\rho] + \mathscr{O}(\varepsilon^2)$, with $\varepsilon > 0$, therefore the hermiticity preserving of L_t follows from the hermiticity preserving of $\mathscr{E}_{(t,0)}$. Also note that we can always choose the same traceless basis, $\{F_i\}_{i=0}^{d^2-1}$, to write eq. (4.3), such that the time dependence is dropped only in $G(t) \in \mathbb{C}^{d^2\times d^2}$ and $H(t)$. By theorem 8, L_t has the form stated in eq. (4.3), the only thing that remains to prove is that $G(t) \geq 0$ for every t. To do this we construct the Choi-Jamiołkowski matrix of the instant map, $\tau_{t,\varepsilon} = \omega + \varepsilon\,(\mathrm{id}_{d^2} \otimes L_t)\,[\omega] + \mathscr{O}(\varepsilon^2)$. We remind the reader that $\omega = |\Omega\rangle\langle\Omega|$, where $|\Omega\rangle$ is the Bell state between two copies of $\mathbb{C}^d$. Now we test positive-semidefinitiveness of $\tau_{t,\varepsilon}$,

$$\langle\varphi|\tau_{t,\varepsilon}|\varphi\rangle = \langle\varphi|\Omega\rangle\langle\Omega|\varphi\rangle + \varepsilon\langle\varphi|\,(\mathrm{id}_{d^2} \otimes L_t)\,[|\Omega\rangle\langle\Omega|]|\varphi\rangle + \mathscr{O}(\varepsilon^2) \geq 0,$$

$\forall|\varphi\rangle \in \mathbb{C}^{d^2}$. The inequality always holds for any $\langle\varphi|\Omega\rangle \neq 0$ and $\varepsilon > 0$. For $\langle\varphi|\Omega\rangle = 0$ we have that for $\varepsilon > 0$ the inequality $\langle\varphi|\left(\mathrm{id}_{d^2} \otimes L_t\right)[|\Omega\rangle\langle\Omega|]|\varphi\rangle \geq 0$ must be accomplished, i.e. $\omega_\perp \tau_L \omega_\perp \geq 0$ (conditional complete positivity). Therefore by proposition 2, one has that $G(t) \geq 0$. □

Analogously to CP-divisible processes, if we relax the condition of the intermediate maps to be PTP (and not necessarily CPTP), we arrive to the following definition:

Definition 12 (P-divisible quantum dynamical maps)**.** *Consider a quantum dynamical map $\mathscr{E}_{(t,0)} : \mathscr{T}(\mathscr{H}) \to \mathscr{T}(\mathscr{H})$ with $t \in \mathbb{R}^+$. It is P-divisible in the interval $[0,t] \subset \mathbb{R}^+$ if for every decomposition of the form*

$$\mathscr{E}_{(t,0)} = \mathscr{E}_{(t,s)}\mathscr{E}_{(s,0)},$$

$\mathscr{E}_{(t,s)}$ belongs to PTP for every $s \in (0,t)$.

Unfortunately, to the best of our knowledge, there doesn't exist a statement similar to theorem 14, nor a simple test of P-divisibility. But for certain types of generators of dynamical maps, conditions for P-divisibility were derived in Ref. [CDG19].

Divisibility of quantum channels

Let us discuss these two types of divisibility but now from a statical point of view. First notice that instant operations $\mathscr{E}_{(t+\varepsilon,t)}$ are arbitrarily close to the identity map as $\varepsilon \to 0^+$, for both P-divisible and CP-divisible processes. In other words, they are infinitesimal. Consider now the idea of quantum channels divisible in infinitesimal parts, i.e. what is given this time is a quantum channel instead of a dynamical map. This idea motivates the following definition [WC08],

Definition 13 (Infinitesimal divisible channels in CPTP)**.** *Let $\mathscr{L}_{CP}$ be the set containing operations $\mathscr{E} \in \mathsf{C}$ with the property that $\forall\varepsilon > 0$ there exist a finite number of channels $\mathscr{E}_i \in \mathsf{C}$ such that $|\mathscr{E}_i - id| < \varepsilon$ and $\mathscr{E} = \prod_i \mathscr{E}_i$, see fig. 4.1. It is said that a channel is infinitesimal divisible if it belongs to the closure of $\mathscr{L}_{CP}$. This set is denoted as C^{CP}.*

The necessity of the closure can be motivated using the following example. Consider the qubit channel defined as follows:

$$\mathscr{E}_\infty : \begin{pmatrix} \rho_{00} & \rho_{01} \\ \rho_{01}^* & \rho_{11} \end{pmatrix} \mapsto \begin{pmatrix} \rho_{00} & 0 \\ 0 & \rho_{11} \end{pmatrix}. \tag{4.4}$$

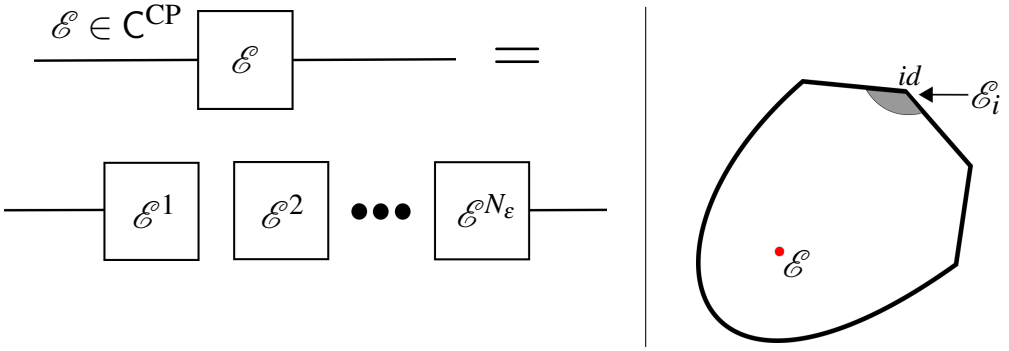

Figure 4.1: Diagrammatic decomposition of channels belonging to $\mathscr{L}_{\mathrm{CP}}$ whose closure is C^{CP}, see definition 13. We show the circuit representing the decomposition of $\mathscr{E}$ into channels (left) arbitrarily close to the identity map (right).

This channel is singular, i.e. does not belong to $\mathscr{L}_{\mathrm{CP}}$. Now observe that using the dynamical process, $\mathscr{E}_t$, given in example 1, one can get arbitrarily close to $\mathscr{E}_\infty$ when $t \to \infty$, i.e. $\mathscr{E}_\infty = \lim_{t\to\infty} \mathscr{E}_t$. Note that $\mathscr{E}_t \in \mathscr{L}_{\mathrm{CP}}$ for every $t \in \mathbb{R}^+$, see theorem 14, therefore $\mathscr{E}_\infty$ is an accumulation point of $\mathscr{L}_{\mathrm{CP}}$. Thus, the closure is taken to define infinitesimal divisible channels, to include channels such as $\mathscr{E}_\infty$.

Up to this point we have shown that CP-divisible processes are infinitesimal divisible, i.e. CP-divisible processes parametrize families of channels belonging to C^{CP}. In Ref. [WECC08], authors have shown that channels in C^{CP} can always be implemented with CP-divisible processes. This can be roughly shown as follows.

Since C is connected, we can understand infinitesimal channels as the ending point of an arbitrarily small curve parametrized by t, i.e. channels $\mathscr{E}_i$ in definition 13 can be written approximately as $\mathscr{E}_i \approx \mathrm{id} + L_i \approx \exp(L_i)$. We have shown that L_i has Lindblad form, see theorem 14. Therefore we have that if $\mathscr{E} \in \mathsf{C}^{\mathrm{CP}}$, it can be written as

$$\mathscr{E} = \prod_i e^{L_i}.$$

Therefore $\mathscr{E}$ can be implemented using a CP-divisible dynamical processes. Bounds of the convergence ratio using channels of the form $\exp(L_i)$ instead of general infinitesimal channels, are computed in Ref. [WECC08].

Analogous to infinitesimal divisible channels in C and its relation with CP-divisible processes, one can also define the following set involving PTP maps.

Definition 14 (Infinitesimal divisible channels in PTP)**.** *Let $\mathscr{L}_P$ be the set con-*

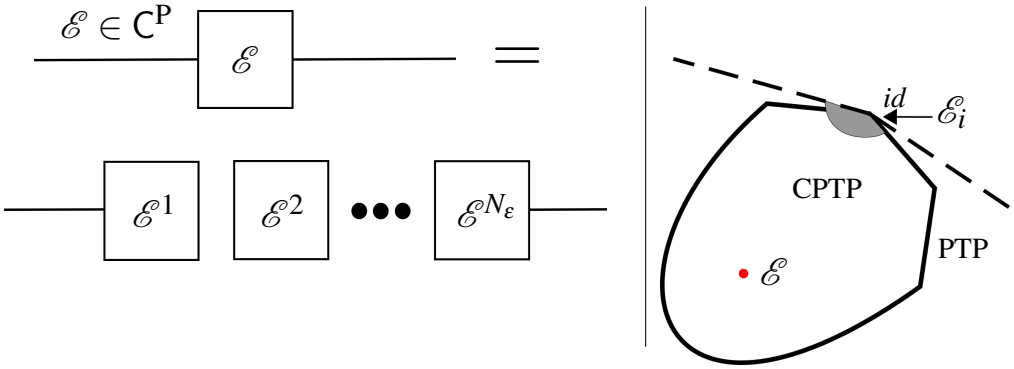

Figure 4.2: Diagramatic decomposition of channels belonging to $\mathscr{L}_{\mathrm{P}}$ which closure is C^{P}, see definition 14. At the left we show the circuit representing the decomposition of $\mathscr{E}$ into channels arbitrarily close to the identity map, see figure at the right. In contrast to figure 4.1, note that infinitesimal channels can be outside the set of CPTP maps, but inside PTP.

taining operations $\mathscr{E} \in \mathsf{C}$ with the property that $\forall \varepsilon > 0$ there exist a finite number of channels $\mathscr{E}_i \in$ PTP such that $|\mathscr{E}_i - id| < \varepsilon$ and $\mathscr{E} = \prod_i \mathscr{E}_i$, see fig. 4.2. It is said that a channel is infinitesimal divisible in PTP if it belongs to the closure of $\mathscr{L}_P$. This set is denoted as C^P.

Infinitesimal divisibility in PTP maps is interesting since this kind of maps can arise in settings where the system is initially correlated with its surroundings, or if the operation is correlated with the initial state [CTZ08].

Infinitesimal divisible (either in CPTP and PTP) channels have non-negative determinant due to its continuity [WECC08]. To see this note that channels arbitrarily close to the identity map have positive determinant; and by its multiplicative property, the channel resulting from the concatenation of infinitesimal channels has non-negative determinant.

Proposition 3 (Determinant of infinitesimal divisible channels)**.** *If a quantum map $\mathscr{E}$ belongs either to C^P or C^{CP}, then* $\det \mathscr{E} \geq 0$.

It turns out that a non-negative determinant is a sufficient condition for a channel to be infinitesimal divisible in PTP, see theorem 25 of Ref. [WECC08].

Other interesting type of divisibility that in turn forms a subset of C^{CP} is the following [WECC08, Den89].

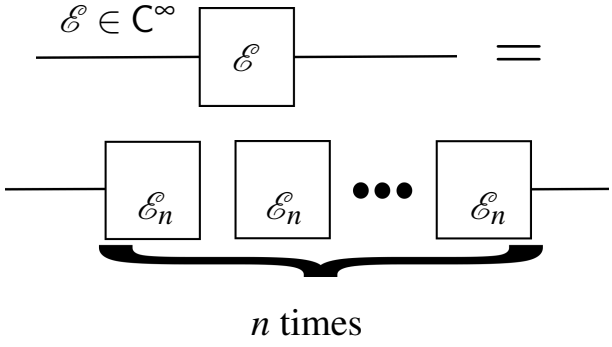

Figure 4.3: Diagrammatic decomposition of channels belonging to C^∞, see definition 15. This set contains channels for which every n-root exist and is a valid quantum channel, denoted in the circuit as $\mathscr{E}_n$.

Definition 15 (Infinitely divisible channels)**.** *A quantum channel $\mathscr{E}$ is infinitely divisible if $\forall n \in \mathbb{Z}^+ \ \exists \mathscr{E}_n \in \mathsf{C}$ such that $\mathscr{E} = (\mathscr{E}_n)^n$. This set is denoted as C^∞, see fig. 4.3.*

This set contains channels for which every n-root exists and is a valid quantum channel. Denisov has shown in [Den89] that infinitely divisible channels can be written as $\mathscr{E} = \mathscr{E}_0 \exp(L)$, with L a Lindblad generator, and an $\mathscr{E}_0$ idempotent operator that fulfills $\mathscr{E}_0 L \mathscr{E}_0 = \mathscr{E}_0 L$. In this work we will prove that every infinitely divisible Pauli channel has the simple form $\exp(L)$.

Let us now introduce the most restricted type of divisibility studied in this work,

Definition 16 (Channels belonging to one-parameter semigroups (L-divisibility))**.** *Let $\mathscr{L}_L$ be the set containing non-singular operations $\mathscr{E} \in \mathsf{C}$, such that there exist at least one logarithm, denoted as $L = \log \mathscr{E}$, such that*

$$L[\rho] = \mathrm{i}[\rho, H] + \sum_{i,j} G_{ij} \left(F_i \rho F_j^\dagger - \frac{1}{2} \{ F_j^\dagger F_i, \rho \} \right), \tag{4.5}$$

where H and G are hermitian with $G \geq 0$, and $\{F_i\}_i$ are bounded operators acting on $\mathscr{T}(\mathscr{H})$. It is said that a channel is L-divisible if it belongs to the closure of $\mathscr{L}_L$. This set is denoted as C^L.

Analogous to the relation of CP-divisible dynamical maps and its relations with C^{CP}, time-independent Markovian processes form families of L-divisible channels. The converse is true by definition. One of the principal objectives of this work is to construct a test to check whether a given channel belongs to C^{L} or not.

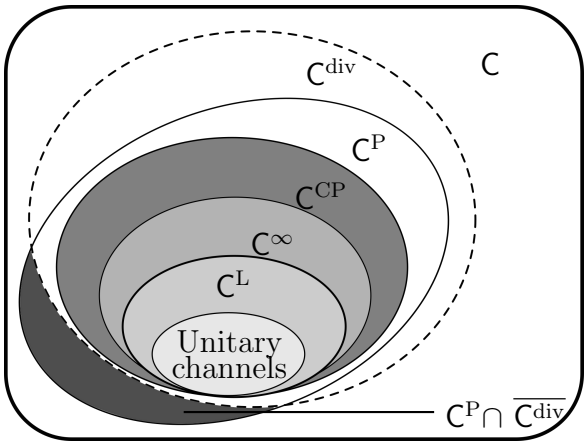

Figure 4.4: Scheme illustrating the different sets of quantum channels for a given dimension. In particular, the inclusion relations presented in eq. (4.6) are depicted.

4.1.2 Relation between channel divisibility classes

Let us summarize the introduced divisibility sets and the relations between them. Since channels belonging to C^{CP} can be implemented with time-dependent Lindblad master equations, and time-independent ones are a particular case of time dependent ones, we have $\mathsf{C}^{\mathrm{L}} \subset \mathsf{C}^{\mathrm{CP}}$. Now, since infinitely divisible channels have the form $\mathscr{E}_0 \exp(L)$, channels with form $\exp(L)$ are a particular case of C^{∞}, therefore $\mathsf{C}^{\mathrm{L}} \subseteq \mathsf{C}^{\infty}$. Also, given that CPTP maps are also PTP, then $\mathsf{C}^{\mathrm{CP}} \subset \mathsf{C}^{\mathrm{P}}$. Finally, every set except C^{P} is subset of $\mathsf{C}^{\mathrm{div}}$, given that an infinitesimal divisible channels in PTP is not necessarily divisible in CPTP channels. In summary we have [WC08],

$$\begin{array}{ccccc} \mathsf{C}^{\infty} & \subset & \mathsf{C}^{\mathrm{CP}} & \subset & \mathsf{C}^{\mathrm{div}} \\ \cup\mathrm{I} & & & & \\ \mathsf{C}^{\mathrm{L}} & \subset & \mathsf{C}^{\mathrm{CP}} & \subset & \mathsf{C}^{\mathrm{P}} \end{array} \quad . \tag{4.6}$$

The intersection of C^{P} and $\mathsf{C}^{\mathrm{div}}$ is not empty since $\mathsf{C}^{\mathrm{CP}} \subset \mathsf{C}^{\mathrm{div}}$ and $\mathsf{C}^{\mathrm{CP}} \subset \mathsf{C}^{\mathrm{P}}$, later on we will investigate if $\mathsf{C}^{\mathrm{P}} \subseteq \mathsf{C}^{\mathrm{div}}$ or not. A scheme of the inclusions is given in fig. 4.4.

4.2 Characterization of L-divisibility

Deciding L-divisibility is equivalent to proving the existence of a hermiticity preserving generator, which additionally fulfills the ccp condition, see proposition 2. To prove hermiticity preserving we recall that every HP operator has a real matrix representation when choosing an hermitian basis, see subsection 3.3.1. Since quantum channels preserve hermiticity, the problem is reduced to find a real logarithm $\log\hat{\mathscr{E}}$ given a real matrix $\hat{\mathscr{E}}$, where the hat means that $\mathscr{E}$ is written using an hermitian basis. This problem was already solved by Culver [Cul66] who characterized completely the existence of real logarithms of real matrices. In this work we restrict the analysis to diagonalizable channels. The results can be summarized as follows.

Theorem 15 (**Existence of hermiticity preserving generator**). *A non-singular matrix with real entries $\hat{\mathscr{E}}$ has a real generator (i.e. a $\log\hat{\mathscr{E}}$ with real entries) if and only if the spectrum fulfills the following conditions: i) negative eigenvalues are even-fold degenerate; ii) complex eigenvalues come in complex conjugate pairs.*

We now discuss the multiplicity of the solutions of $\log\hat{\mathscr{E}}$ and its parametrization, as finding an appropriate one is essential to test for the ccp condition. If $\hat{\mathscr{E}}$ has positive degenerate, negative, or complex eigenvalues, its real logarithms are not unique, and are spanned by *real logarithm branches* [Cul66]. The latter are defined using the real quaternion, which coincides with $\mathrm{i}\sigma_y$, using the fact that $\mathbb{1} = \exp(\mathrm{i}\sigma_y 2\pi k)$, with $k \in \mathbb{Z}$. In case of having negative eigenvalues, it turns out that real logarithms always have a continuous parametrization, in addition to real branches due to the freedom of the Jordan normal form transformation matrices [Cul66].

To compute the logarithm given a real representation of $\mathscr{E}$, i.e. $\hat{\mathscr{E}}$, we calculate its Jordan normal form, J, such that $\hat{\mathscr{E}} = wJw^{-1} = \tilde{w}J\tilde{w}^{-1}$, where $w = \tilde{w}K$ and K belongs to a continuum of matrices that commute with J [Cul66]. In the case of diagonalizable matrices, if there are no degeneracies, K commutes with $\log(J)$. In the case of having degeneracies, matrix K is responsible of the continuous parametrization of the logarithm. We compute explicitly the logarithms for the case of Pauli channels in section 4.3.4.

4.3 Divisibility of unital qubit channels

We will apply various of the results from the literature [WECC08] to decide if a given unital qubit channel belongs to C^{L}, C^{CP} and/or C^{P}. The non-unital case will be discussed later.

Before starting with the characterization let us point out the following. From the definition of divisibility, the concatenation of a given channel with unitary conjugations (which are infinitesimal divisible) do not change its divisibility character, except for L-divisibility. In addition to this, since unitary conjugations are infinitesimal divisible, they do not change the infinitesimal divisible character either. We can summarize this in the following,

Proposition 4 (Divisibility of special orthogonal normal forms). *Let $\mathscr{E}$ a qubit quantum channel and $\mathscr{D}$ its special orthogonal normal form, $\mathscr{E}$ belongs to C^X if and only if $\mathscr{D}$ does, where $X = \{$"Div", "P", "CP"$\}$.*

This proposition is in fact a consequence of theorem 17 of Ref. [WECC08]. Notice that this result does not apply for C^{L} since conjugating with unitaries breaks the implementability by means of time-independent Lindblad master equations. Thus, if a channel belongs to C^{L}, unitary conjugations can bring it to $\mathsf{C}^{\mathrm{Inf}} \setminus \mathsf{C}^{\mathrm{L}}$ and vice versa.

Therefore, by proposition 4 and the theorem 9, to study C^{P} and C^{CP} of unital qubit channels, it is enough to study Pauli channels.

4.3.1 Channels belonging to $\mathsf{C}^{\mathbf{div}}$

Divisibility in CPTP of unital qubit channels is completely characterized by means of theorem 13. Therefore the only indivisible channels lie in the faces of the tetrahedron (without the edges), see fig. 4.5.

4.3.2 Channels belonging to $\mathsf{C}^{\mathbf{P}}$

Recalling that all unital qubit channels belonging to C^{P} have non-negative determinant [WC08], and using special orthogonal normal forms, see theorem 9, the condition in terms of its parameters is given by

$$\lambda_1\lambda_2\lambda_3 \geq 0. \tag{4.7}$$

This set is the intersection of the tetrahedron with the octants where the product of all λs is positive. In fact, it consists of four triangular bipyramids starting in each vertex of the tetrahedron and meeting in its center, see fig. 4.5. Let us study the intersection of this set with the set of unital entanglement-breaking (EB) channels [ZB05], see definition 5. In the case of unital qubit channels, the set entanglement-breaking channels is an octahedron that lie inside the tetrahedron of unital qubit channels, see fig. 4.6. The inequalities that define such octahedron are the following,

$$\lambda_i \pm (\lambda_j + \lambda_k) \leq 1, \tag{4.8}$$

with i, j and k all different [ZB05], together eq. (3.11). It follows that unital qubit channels that are not achieved by P-divisible dynamical maps are necessarily entanglement-breaking (see fig. 4.6 and fig. 4.9). In fact this holds for general qubit channels, see section 4.4.

4.3.3 Channels belonging to $\mathsf{C}^{\mathbf{CP}}$

To characterize CP-divisible channels it is useful to consider the Lorentz normal form for channels, see theorem 10. A remarkable property of the Lorentz normal decomposition is that it preserves the infinitesimal divisible character of $\mathscr{E}$, see Corollary 13 of [WC08]. To use it, we resort to theorem 24 of Ref. [WC08]. Due to the mentioned drawback of Lorentz normal forms, see appendix B, we must modify such to theorem to a restricted class of channels.

Theorem 16 (Restricted characterization of channels belonging to C^{CP})**.** *A qubit channel $\mathscr{E}$ with diagonal Lorentz normal form belongs to C^{CP} if and only if*
i) the rank of the form is smaller than three or
ii) $s_{\min}^2 \geq s_1 s_2 s_3 > 0$, where $s_{\min}$ is the smallest of s_1, s_2 and s_3, see theorem 10.

For non-unital Kraus deficient channels, the pertinent theorems are based on non-diagonal Lorentz normal forms [VV02, WC08]. According to our appendix B such results should be reviewed and are out of the scope of this work.

Notice that the Lorentz normal form coincides with the special orthogonal normal form for unital qubit channels. Therefore, by theorem 16, unital channels belonging to C^{CP} are non-singular with

$$0 < \lambda_1 \lambda_2 \lambda_3 \leq \lambda_{\min}^2, \tag{4.9}$$

or singular with a matrix rank less than three. They determine a body that is symmetric with respect to permutation of Pauli unitary channels (i.e. in λ_j), hence,

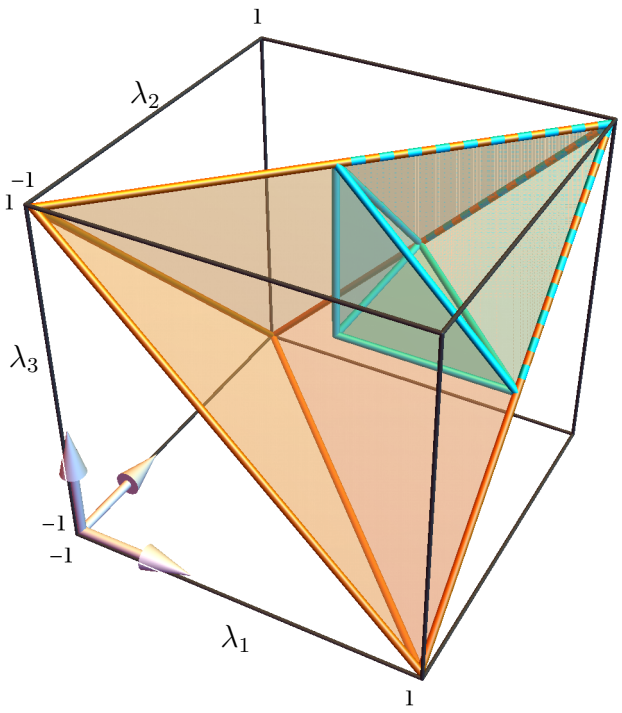

Figure 4.5: Tetrahedron of Pauli channels, see fig. 3.1. The bipyramid in blue correspond to channels with $\lambda_i > 0\ \forall i$, i.e. channels of the positive octant belonging to C^{P}. The whole set C^{P} includes other three bipyramids corresponding to the other vertexes of tetrahedron. This implies that C^{P} enjoys the symmetries of the tetrahedron, see eq. (4.7). The faces of the bipyramids matching the corners of the tetrahedron are subsets of the faces of the tetrahedron, i.e. contain Kraus rank three channels. Such channels are both C^{P} and $\overline{\mathsf{C}^{\mathrm{div}}}$, showing that the intersection shown in fig. 4.4 is not empty.

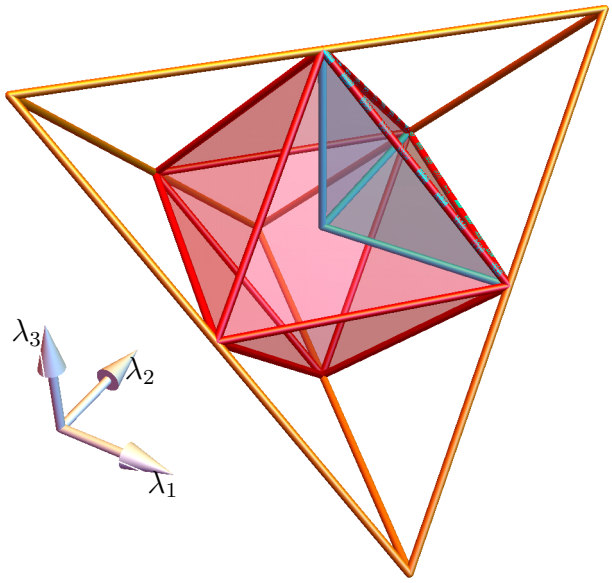

Figure 4.6: Tetrahedron of Pauli channels with the octahedron of entanglement breaking channels shown in red, see eq. (4.8). The blue pyramid inside the octahedron is the intersection of the bipyramid shown in 4.5, with the octahedron. The complement of the intersections of the four bipyramids forms the set of divisible but not infinitesimal divisible channels in PTP. Thus, a central feature of the figure is that the set $\mathsf{C}^{\mathrm{div}} \setminus \mathsf{C}^{\mathrm{P}}$ is always entanglement-breaking, but the converse is not true.

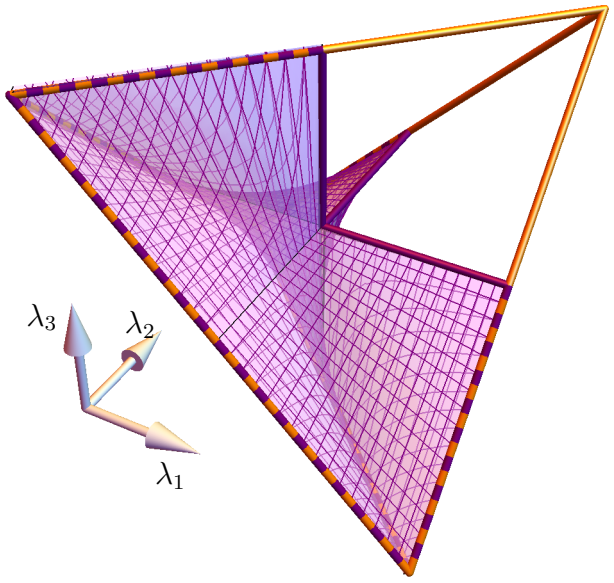

Figure 4.7: Tetrahedron of Pauli channels with part of the set of CP-divisible, see eq. (4.9), but not L-divisible channels ($\mathsf{C}^{\mathrm{CP}}\backslash\mathsf{C}^{\mathrm{L}}$) shown in purple. The whole set C^{CP} is obtained applying the symmetry transformations of the tetrahedron to the purple volume.

the set of C^{CP} of Pauli channels possesses the symmetries of the tetrahedron. The set $\mathsf{C}^{\mathrm{CP}}\backslash\mathsf{C}^{\mathrm{L}}$ is plotted in fig. 4.7.

4.3.4 L-divisible unital qubit channels

We restrict our analysis of L-divisibility for two particular sets of unital channels, Pauli channels and a family with complex eigenvalues that will be introduced later.

Pauli channels with non-degenerate positive eigenvalues

First let us now derive the conditions for L-divisibility of Pauli channels with positive eigenvalues $\lambda_1, \lambda_2, \lambda_3$ ($\lambda_0 = 1$). The logarithm of $\mathscr{D}$, induced by the principal logarithm of its eigenvalues is

$$L = K\mathrm{diag}(0, \log\lambda_1, \log\lambda_2, \log\lambda_3)K^{-1}, \tag{4.10}$$

which is real (hermiticity preserving). In case of no-degeneration the dependency on K vanishes and L is unique. In such case the ccp conditions, see theorem 2, read

$$\log\lambda_i - \log\lambda_j - \log\lambda_k \geq 0 \Rightarrow \frac{\lambda_i}{\lambda_j\lambda_k} \geq 1 \tag{4.11}$$

for all combinations of mutually different i, j, k. This set (channels belonging to C^{L} with positive eigenvalues) forms a three dimensional manifold, see fig. 4.8.

Pauli channels with degenerate positive eigenvalues

In case of degeneration, let us label the eigenvalues η, λ and λ. In this case, the real solution for L is not unique and is parametrized by real branches in the degenerate subspace and by the continuous parameters of K [Cul66]. Let us study the principal branch with $K = \mathbb{1}$. Eq. (4.11) is then reduced to

$$\lambda^2 \leq \eta \leq 1\,. \tag{4.12}$$

Therefore, if this inequalities are fulfilled, the generator has Lindblad form. If not, then *a priori* other branches can fulfill ccp condition and consequently have a Lindblad form. Thus, Eq. (4.12) provides a sufficient condition for the channel to be in C^{L}. We will prove it is also necessary.

The complete positivity condition requires $\eta, \lambda \leq 1$, thus, it remains to verify only the condition $\lambda^2 \leq \eta$. It holds trivially for the case $\lambda \leq \eta$. If $\eta \leq \lambda$, then this condition coincides with the CP-divisibility condition from eq. (4.9). Since C^{L} implies C^{CP} the proof is completed. In conclusion, the condition in eq. (4.11) is a necessary and sufficient for a given Pauli channel with positive eigenvalues to belong to C^{L}.

Let us stress that the obtained subset of L-divisible channels does not possess the tetrahedron symmetries. In fact, composing $\mathscr{D}$ with a σ_z rotation

$$\mathscr{U}_z = \mathrm{diag}(1,-1,-1,1)$$

results in the Pauli channel $\mathscr{D}' = \mathrm{diag}(1,-\lambda_1,-\lambda_2,\lambda_3)$. Clearly, if λ_j are positive ($\mathscr{D}$ is L-divisible), then $\mathscr{D}'$ has non-positive eigenvalues. Moreover, if all λ_j are different, then $\mathscr{D}'$ does not have any real logarithm, therefore, it cannot be L-divisible. In conclusion, the set of L-divisible unital qubit channel is not symmetric with respect to tetrahedron symmetries.

Pauli channels with negative eigenvalues

In what follows we will investigate the case of negative eigenvalues. Theorem 15 implies that that eigenvalues have the form (modulo permutations) $\eta, -\lambda, -\lambda$, where $\eta, \lambda > 0$. The corresponding Pauli channels are

$$\mathscr{D}_x = \mathrm{diag}(1, \eta, -\lambda, -\lambda), \;\; \mathscr{D}_y = \mathrm{diag}(1, -\lambda, \eta, -\lambda), \;\; \mathscr{D}_z = \mathrm{diag}(1, -\lambda, -\lambda, \eta),$$

thus forming three two-dimensional regions inside the tetrahedron. Take, for instance, $\mathscr{D}_z$ that specifies a plane (inside the tetrahedron) containing I, σ_z and completely depolarizing channel $\mathscr{N} = \mathrm{diag}(1,0,0,0)$. The real logarithms for this case are given by

$$L = K \begin{pmatrix} 0 & 0 & 0 & 0 \\ 0 & \log(\lambda) & (2k+1)\pi & 0 \\ 0 & -(2k+1)\pi & \log(\lambda) & 0 \\ 0 & 0 & 0 & \log(\eta) \end{pmatrix} K^{-1}, \tag{4.13}$$

where $k \in \mathbb{Z}$ and K, as mentioned above, belongs to a continuum of matrices that commute with $\mathscr{D}_z$. Note that L is always non-diagonal. For this case (similarly for $\mathscr{D}_x$ and $\mathscr{D}_y$) the ccp condition reduces again to conditions specified in Eq. (4.12). Using the same arguments one arrives to more general conclusion:

Theorem 17 (L-divisibility of Pauli channels)**.** *Let $\mathscr{E}$ be a non-singular Pauli channel. It belongs to C^L if and only if its non-trivial eigenvalues fulfill*

$$\frac{\lambda_i}{\lambda_j \lambda_k} \geq 0 \tag{4.14}$$

for i, j and k mutually different.

This is one of the central results of this work, and it implies that for testing L-divisibility of Pauli channels, it is enough to consider the principal real logarithm branch and $K = \mathbb{1}$. The singular cases are included in the closure of channels fulfilling eq. (4.14). The set of L-divisible Pauli channels is illustrated in fig. 4.8. To get a detailed picture of the position and inclusions of the divisibility sets, we illustrate in fig. 4.9 two slices of the tetrahedron where different types of divisibility are visualized. Notice the non-convexity of the considered divisibility sets.

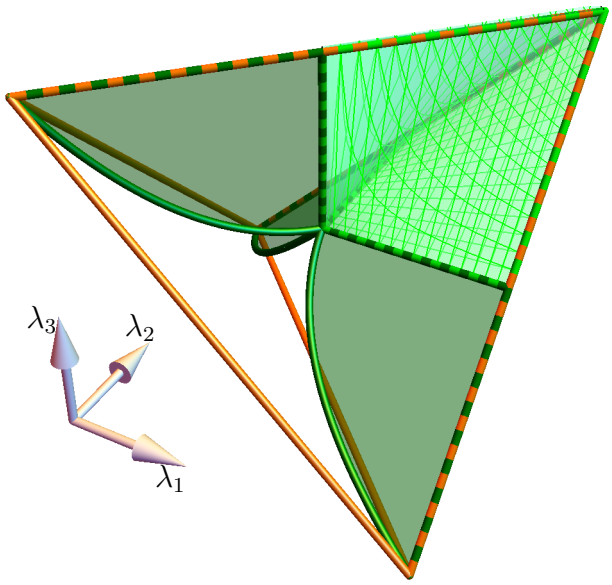

Figure 4.8: Tetrahedron of Pauli channels with the set of L-divisible channels (or equivalently infinitely divisible, see Theorem 19) shown in green, see equations (4.11) and (4.12). The solid set corresponds to channels with positive eigenvalues, and the 2D sets correspond to the negative eigenvalue case. The point where the four sets meet correspond to the *total depolarizing* channel. Notice that this set *does not* have the symmetries of the tetrahedron.

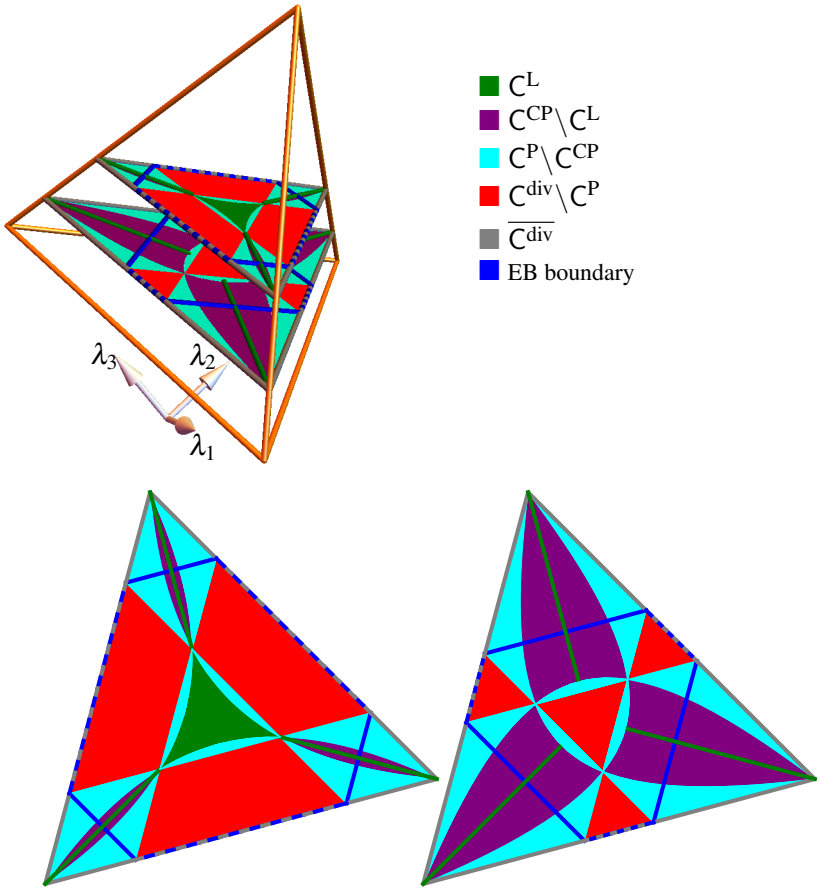

Figure 4.9: We show two slices of the unitary tetrahedron (figure in the left) determined by $\sum_i \lambda_i = 0.4$ (shown in the center) and $\sum_i \lambda_i = -0.4$ (shown in the right). The non-convexity of the divisibility sets can be seen, including the set of indivisible channels. The convexity of sets C and entanglement breaking channels can also be noticed in the slices. A central feature is that the set $\mathsf{C}^{\mathrm{div}} \setminus \mathsf{C}^{\mathrm{P}}$ is always inside the octahedron of entanglement breaking channels.

Family of unital channels with complex eigenvalues

To give an insight to the case of complex eigenvalues, consider the following family of channels with real logarithm, written in the Pauli basis,

$$\mathscr{E}_{\text{complex}} = \begin{pmatrix} 1 & 0 & 0 & 0 \\ 0 & c & 0 & 0 \\ 0 & 0 & a & -b \\ 0 & 0 & b & a \end{pmatrix}. \tag{4.15}$$

The latter has complex eigenvalues $a \pm ib$ and a real one $c > 0$, together with the trivial eigenvalue equal to 1. Its real logarithm is given by,

$$\begin{aligned} L &= K \log\left(\mathscr{E}_{\text{complex}}\right)_k K^{-1} \\ &= K \begin{pmatrix} 0 & 0 & 0 & 0 \\ 0 & \log(c) & 0 & 0 \\ 0 & 0 & \log(|z|) & \arg(z)+2\pi k \\ 0 & 0 & -\arg(z)-2\pi k & \log(|z|) \end{pmatrix} K^{-1} \end{aligned}$$

with $z = a + ib$. The non-diagonal block of the logarithm has the same structure of $\mathscr{E}_{\text{complex}}$, so K also commutes with $\log(\mathscr{E}_{\text{complex}})_k$, leading to a countable parametric space of hermitian preserving generators. The ccp condition, see proposition 2, is reduced to

$$a^2 + b^2 \leq c \leq 1. \tag{4.16}$$

Note that it does not depend on k and the second inequality is always fulfilled for CPTP channels. The set containing them is shown in fig. 4.10.

4.3.5 Relation of L-divisibility with other divisibility classes

Consider a Pauli channel with $0 < \lambda_{\min} = \lambda_1 \leq \lambda_2 \leq \lambda_3 < 1$, thus the condition $\lambda_1\lambda_2 \leq \lambda_3$ trivially holds. Since $\lambda_1\lambda_2 \leq \lambda_1\lambda_3 \leq \lambda_2\lambda_3 \leq \lambda_2$, it follows that $\lambda_1\lambda_3 \leq \lambda_2$, thus, two (out of three) L-divisibility conditions hold always for Pauli channels with positive eigenvalues. Moreover, one may observe that CP-divisibility condition eq. (4.9) reduces to one of L-divisibility conditions $\lambda_2\lambda_3 \leq \lambda_1$. In conclusion, the conditions of CP-divisibility and L-divisibility for Pauli channels with positive eigenvalues coincide, thus, in this case C^{CP} implies C^{L}.

Concatenating (positive-eigenvalues) L-divisible Pauli channels with $\mathscr{D}_{x,y,z}$, one can generate the whole set of C^{CP} Pauli channels. In other words, $\mathscr{D}_{x,y,z}$ brings the body (with vertex in id) shown in fig. 4.8 to the bodies shown in fig. 4.7 (with vertexes x, y, z). Therefore we can formulate the following theorem:

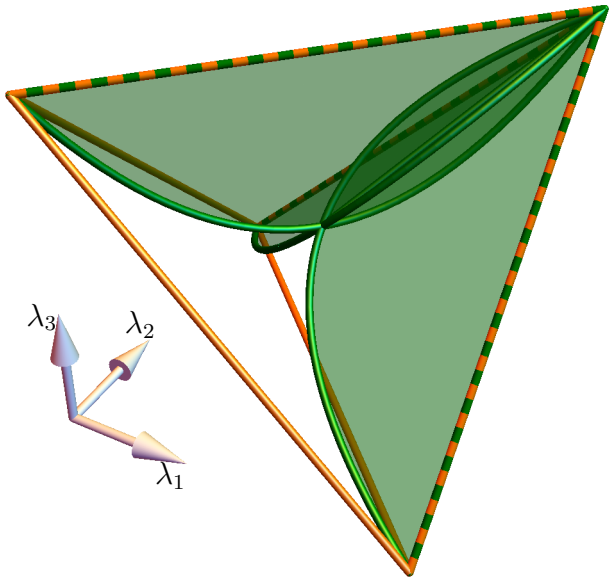

Figure 4.10: Tetrahedron of Pauli channels, with qubit unital L-divisible channels of the form $\hat{\mathscr{E}}_{\text{complex}}$ (see main text). Note that the set does not have the symmetries of the tetrahedron.

Theorem 18 (Infinitesimal divisible unital channels)**.** *Let $\mathscr{E}^{CP}_{unital}$ be an arbitrary infinitesimal divisible unital qubit channel. There exists at least one L-divisible Pauli channel $\tilde{\mathscr{E}}$, and two unitary conjugations $\mathscr{U}_1$ and $\mathscr{U}_2$, such that*

$$\mathscr{E}^{CP}_{unital} = \mathscr{U}_1 \tilde{\mathscr{E}} \mathscr{U}_2 \,.$$

Notice that if $\mathscr{E}^{CP}_{unital}$ is invertible, $\tilde{\mathscr{E}} = e^L$.

Let us continue with another equivalence relation valid for Pauli channels. In general, $\mathsf{C}^{\mathsf{L}} \subset \mathsf{C}^{\infty}$; however, for Pauli channels these two subsets coincide.

Theorem 19 (Infinitely divisible Pauli channels)**.** *The set of L-divisible Pauli channels is equivalent to the set of infinitely divisible Pauli channels.*

Proof. A channel is infinitely divisible if and only if it can be written as $\mathscr{E}_0 e^L$, where $\mathscr{E}_0$ is an idempotent channel satisfying $\mathscr{E}_0 L \mathscr{E}_0 = \mathscr{E}_0 L$ and L has Lindblad form, see definition 15. The only idempotent qubit channels are contractions of the Bloch sphere into single points, diagonalization channels $\mathscr{E}_{\text{diag}}$ transforming Bloch sphere into a line connecting a pair of basis states, and the identity channel. Among the single-point contractions, the only one that is a Pauli channel is the

contraction of the Bloch sphere into the complete mixture; let us call it $\mathscr{N}$. Notice that $\mathscr{E} = \mathscr{N}e^{L} = \mathscr{N}$ for all L. The channel $\mathscr{N}$ belongs to the closure of C^{L}, because a sequence of channels e^{L_n} with $\hat{L}_n = \mathrm{diag}\,(0,-n,-n,-n)$ converges to $\hat{\mathscr{N}}$ in the limit $n \to \infty$. For the case of $\mathscr{E}_0$ being the identity channel we have $\mathscr{E} = e^{L}$, thus, trivially such infinitely divisible channel $\mathscr{E}$ is in C^{L} too. It remains to analyze the case of diagonalization channels. First, let us note that the matrix of $e^{\hat{L}}$ is necessarily of full rank, since $\det\hat{\mathscr{E}} \neq 0$. It follows that the matrix $\hat{\mathscr{E}} = \hat{\mathscr{E}}_{\mathrm{diag}}e^{\hat{L}}$ has rank two as $\hat{\mathscr{E}}_{\mathrm{diag}}$ is a rank two matrix, thus, it takes one of the following forms $\hat{\mathscr{E}}_x^{\lambda} = \mathrm{diag}\,(1,\lambda,0,0)$, $\hat{\mathscr{E}}_y^{\lambda} = \mathrm{diag}\,(1,0,\lambda,0)$, $\hat{\mathscr{E}}_z^{\lambda} = \mathrm{diag}\,(1,0,0,\lambda)$. The infinitely divisibility implies $\lambda > 0$ in order to keep the roots of λ real. In what follows we will show that $\hat{\mathscr{E}}_z$ belongs to (the closure of) C^{L}. Let us define the channels $\hat{\mathscr{E}}_z^{\lambda,\varepsilon} = \mathrm{diag}\,(1,\varepsilon,\varepsilon,\lambda)$ with $\varepsilon > 0$. The complete positivity and ccp conditions translate into the inequalities $\varepsilon \leq \frac{1+\lambda}{2}$ and $\varepsilon^2 \leq \lambda$, respectively; therefore one can always find an $\varepsilon > 0$ such that $\hat{\mathscr{E}}_z^{\lambda,\varepsilon}$ is a L-divisible channel. If we choose $\varepsilon = \sqrt{\lambda}/n$ with $n \in \mathbb{Z}^{+}$, the channels $\hat{\mathscr{E}}_{z,n} = \mathrm{diag}\left(1,\sqrt{\lambda}/n,\sqrt{\lambda}/n,\lambda\right)$ form a sequence of L-divisible channels converging to $\hat{\mathscr{E}}_z^{\lambda}$ when $n \to \infty$. The analogous reasoning implies that $\hat{\mathscr{E}}_x^{\lambda}, \hat{\mathscr{E}}_y^{\lambda} \in \mathsf{C}^{\mathrm{L}}$ too. Let us note that one parameter family $\mathscr{E}_z$ are convex combinations of the complete diagonalization channel $\hat{\mathscr{E}}_z^{1} = \mathrm{diag}\,(1,0,0,1)$ and the complete mixture contraction $\hat{\mathscr{N}}$. This completes the proof. □

Finally, let us remark that using the theorem 13 we conclude that the intersection $\mathsf{C}^{\mathrm{P}} \cap \overline{\mathsf{C}^{\mathrm{div}}}$ depicted in fig. 4.4 is not empty. To show this, notice that there are channels with positive determinant inside the faces (i.e. C^{P} but not $\mathsf{C}^{\mathrm{div}}$), for example $\mathrm{diag}\left(1,\frac{4}{5},\frac{4}{5},\frac{3}{5}\right)$. Therefore we conclude that up to unitaries, $\mathsf{C}^{\mathrm{P}} \cap \overline{\mathsf{C}^{\mathrm{div}}}$ corresponds to the union of the four faces faces of the tetrahedron minus the faces of the octahedron that intersect with the faces of the tetrahedron, see fig. 4.6. We have to remove such intersection since it corresponds to channels with negative determinant, and thus not in C^{P}.

4.4 Non-unital qubit channels

Similar to unital channels, using theorem 4 we are able to characterize $\mathsf{C}^{\mathrm{div}}$, C^{P} and C^{CP} by studying special orthogonal normal forms. Such channels are characterized by $\vec{\lambda}$ and $\vec{\tau}$, see eq. (3.9). Thus, we can study if a channel is $\mathsf{C}^{\mathrm{div}}$ by computing the rank of its Choi matrix, see theorem 11. For this case algebraic equations are in general fourth order polynomials. In fact, in Ref. [RPZ18] a condition in terms of the eigenvalues and $\vec{\tau}$ is given. For special cases, however, we

can obtain compact expressions, see fig. 4.11. The characterization of C^{P} is given by again by the condition $\lambda_1\lambda_2\lambda_3 \geq 0$. C^{CP} is tested, for full Kraus rank non-unital channels, using theorem 16, the calculation of s_i's is done using the algorithm presented in Ref. [VDD01]. For the characterization of C^{L} we use theorem 15 and evaluate numerically the cpp condition.

We can plot illustrative pictures even though the whole space of qubit channels has 12 parameters. This can be done using special orthogonal normal forms and fixing $\vec{\tau}$, exactly in the same way as the unital case. Recall that unitaries only modify C^{L}, leaving the shape of other sets unchanged. CPTP channels are represented as a volume inside the tetrahedron presented in fig. 4.5, see fig. 4.11. In the later figure we show a slice corresponding to $\vec{\tau} = (1/2, 0, 0)^{\mathrm{T}}$. Indeed, it has the same structure of the slices for the unital case, but deformed, see fig. 4.9. A difference with respect to the unital case is that L-divisible channels with negative eigenvalues (up to unitaries) are not completely inside CP-divisible channels. A part of them are inside the C^{P} channels.

A central feature of Figs. 4.9 and 4.11 is that the set $\mathsf{C}^{\mathrm{div}} \setminus \mathsf{C}^{\mathrm{P}}$ is inside the convex slice of the set of entanglement breaking channels (deformed octahedron). Indeed, we can proof the following theorem.

Theorem 20 (Entanglement-breaking channels and divisibility)**.** *Consider a qubit channel $\mathscr{E}$. If $\det \hat{\mathscr{E}} < 0$, then $\mathscr{E}$ is entanglement-breaking, i.e. all qubit channels outside C^{P} are entanglement breaking.*

Before introducing the proof, let us first show that the proper orthochronous Lorentz transformations present in the Lorentz normal decomposition for channels, see sec. 3.4.2, correspond to 1wSLOCC at the level of their Choi-Jamiołkowski state. Consider a channel $\mathscr{E}$ and its Lorentz normal form $\tilde{\mathscr{E}}$ given by

$$\tilde{\mathscr{E}} = \alpha \mathscr{F}_2 \mathscr{E} \mathscr{F}_1, \tag{4.17}$$

where

$$\mathscr{F}_i : \rho \mapsto X_i \rho X_i^{\dagger}, \text{ with } X_i \in \mathrm{SL}(2,\mathbb{C}), \;\; i = 1, 2,$$

and α is a constant that must be included for $\tilde{\mathscr{E}}$ to be trace preserving, We showed already that $\mathrm{SL}(2,\mathbb{C})$ is a double cover of $\mathrm{SO}^{+}(3,1)$, i.e. $\mathscr{F}_i$'s correspond to the proper orthochronous Lorentz transformations of the decomposition.

Now let us compute the Choi-Jamiołkowski state of $\tilde{\mathscr{E}}$, $\tilde{\tau}$, using the Kraus decom-

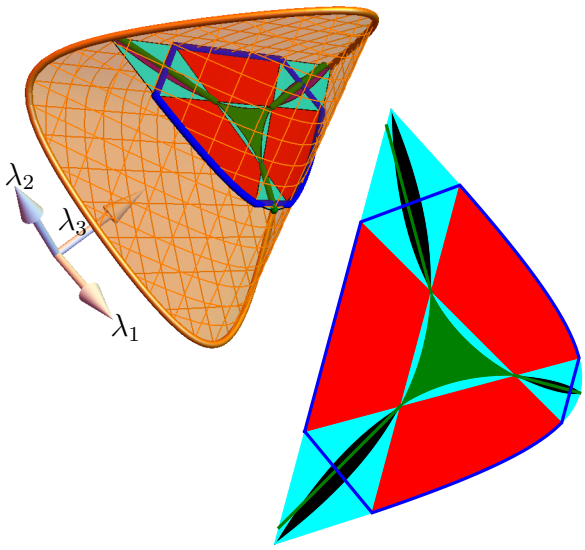

Figure 4.11: (left) Set of non-unital unital channels up to unitaries, defined by $\vec{\tau} = (1/2, 0, 0)$, see eq. (3.9). This set lies inside the tetrahedron. For this particular case the CP conditions reduce to the two inequalities $2 \pm 2\lambda_1 \geq \sqrt{1 + 4(\lambda_2 \pm \lambda_3)^2}$. A cut corresponding to $\sum_i \lambda_i = 0.3$ is presented inside and in the right, see fig. 4.9 for the color coding. The structure of divisibility sets presented here has basically the same structure as for the unital case except for C^{L}. A part of the channels with negative eigenvalues belonging to C^{L} lies outside $\mathsf{C}^{\mathrm{CP}} \setminus \mathsf{C}^{\mathrm{L}}$, see green lines. As for the unital case a central feature is that the channels in $\mathsf{C}^{\mathrm{div}} \setminus \mathsf{C}^{\mathrm{P}}$ are entanglement breaking channels. Channels in the boundary are not characterized due to the restricted character of Theorem 10.

position of $\mathscr{E}$ [Wol11],

$$\begin{aligned}\tilde{\tau} &= \alpha\,(\mathrm{id}_2 \otimes \mathscr{F}_2\mathscr{E}\mathscr{F}_1)\,[\omega] \\ &= \alpha \sum_i (\mathbb{1}\otimes X_2)\,(\mathbb{1}\otimes K_i)\,(\mathbb{1}\otimes X_1)\,|\Omega\rangle\langle\Omega|\left(\mathbb{1}\otimes X_1^\dagger\right)\left(\mathbb{1}\otimes K_i^\dagger\right)\left(\mathbb{1}\otimes X_2^\dagger\right) \\ &= \alpha \sum_i \left(X_1^{\mathrm{T}}\otimes X_2\right)\,(\mathbb{1}\otimes K_i)\,|\Omega\rangle\langle\Omega|)\left(\mathbb{1}\otimes K_i^\dagger\right)\left(\overline{X_1}\otimes X_2^\dagger\right) \\ &= \alpha(X_1^T\otimes X_2)\tau(X_1^T\otimes X_2)^\dagger, \end{aligned} \tag{4.18}$$

where $\{K_i\}_i$ are a choice of Kraus operators of $\mathscr{E}$ and

$$\tau = \sum_i (\mathbb{1}\otimes K_i)\,|\Omega\rangle\langle\Omega|\left(\mathbb{1}\otimes K_i^\dagger\right)$$

its Choi-Jamiołkowski matrix. Here, $|\Omega\rangle$ is the Bell state between two copies of the system, in this case a qubit, for which the identity $A\otimes\mathbb{1}|\Omega\rangle = \mathbb{1}\otimes A^{\mathrm{T}}|\Omega\rangle$ holds. It can be observed that eq. (4.18) has exactly the form of the normalized 1wSLOCC scheme, where α turns to be the normalization constant, see eq. (2.27), i.e. $\mathrm{tr}\,\tilde{\tau} = 1$. That's why we have introduced it at the first place. Now let us proceed with the proof of theorem 20,

Proof. Let $\mathscr{E}$ be a qubit channel with negative determinant and $\hat{\mathscr{E}}$ its matrix representation using the Pauli basis, see eq. (3.7). Recall that the matrix R defining the Choi-Jamiołkowski state of $\mathscr{E}$,

$$\tau_{\mathscr{E}} = \frac{1}{4}\sum_{jk}^{3} R_{jk}\,\sigma_j\otimes\sigma_k,$$

and $\hat{\mathscr{E}}$ are related by

$$R = \hat{\mathscr{E}}\Phi_{\mathrm{T}},$$

where $\Phi_{\mathrm{T}} = \mathrm{diag}\,(1,1,-1,1)$. It follows immediately that R has positive determinant,

$$\det R = -\det\hat{\mathscr{E}} > 0,$$

since $\det\Phi_{\mathrm{T}} = -1$. Using the aforementioned Lorentz normal decomposition for matrix R, we have

$$R = L_1^{\mathrm{T}}\tilde{R}L_2$$

where $\det L_{1,2} > 0$ and $\det\tilde{R} > 0$. Stressing that transformations $L_{1,2}$ correspond to 1wSLOCC (see eq. (4.18)), then $\tilde{R}$ parametrizes an unnormalized two-qubit state.

Let us first discuss the case when $\tilde{R}$ is diagonal. The channel corresponding to $\tilde{R}$ (in the Pauli basis) is

$$\hat{\mathscr{G}} = \tilde{R}\Phi_{\mathrm{T}}/\tilde{R}_{00},$$

where $R_{00} = \mathrm{tr}\tilde{R} = \mathrm{tr}\,\tau_{\mathscr{G}}$. Since $\tilde{R}$ is diagonal, then $\mathscr{G}$ is a Pauli channel with $\det\hat{\mathscr{G}} < 0$. A Pauli channel has a negative determinant, if either all λ_j are negative, or exactly one of them is negative. In Ref. [ZB05] it has been shown that the set of channels with $\lambda_j < 0 \quad \forall j$ are entanglement breaking channels. Now, using the symmetries of the tetrahedron, one can generate all channels with negative determinant by concatenating this set with the Pauli rotations. Therefore every Pauli channel with negative determinant is entanglement breaking, thus, $\tau_{\mathscr{G}}$ is separable. Given that LOCC operations can not create entanglement [HHHH09], we have that $\tau_{\mathscr{E}}$ is separable, therefore $\mathscr{E}$ is entanglement breaking.

The case when $\tilde{R}$ is non-diagonal corresponds to Kraus deficient channels (the matrix rank of 3.17 is at most 3). This case can be analyzed as follows. Since the neighborhood of any Kraus deficient channel with negative determinant contains full Kraus rank channels, by continuity of the determinant such channels have negative determinant too. The last ones are entanglement breaking since full Kraus rank channels have diagonal Lorentz normal form. Therefore, by continuity of the concurrence [ZB05], Kraus deficient channel with negative determinant are entanglement breaking. □

4.5 Divisibility transitions and examples with dynamical processes

The aim of this section is to use illustrative examples of quantum dynamical processes to show transitions between divisibility types of the instantaneous channels. From the slices shown above (see figures 4.9 and 4.11) it can be noticed that every transition between the studied divisibility types is permitted. This is due to the existence of common borders between all combinations of divisibility sets; we can think of any continuous line inside the tetrahedron [FPMZ17] as describing some quantum dynamical map.

We analyze two examples. The first is an implementation of the approximate NOT gate, $\mathscr{A}_{\mathrm{NOT}}$ throughout a specific collision model [RFZB12]. The second is the well known setting of a two-level atom interacting with a quantized mode of an optical cavity [HR06]. We define a simple function that assigns a particular value

to a channel $\mathscr{E}_t$ according to divisibility hierarchy, i.e.

$$\delta[\mathscr{E}] = \begin{cases} 1 & \text{if } \mathscr{E} \in \mathsf{C}^{\mathrm{L}}, \\ 2/3 & \text{if } \mathscr{E} \in \mathsf{C}^{\mathrm{CP}} \setminus \mathsf{C}^{\mathrm{L}}, \\ 1/3 & \text{if } \mathscr{E} \in \mathsf{C}^{\mathrm{P}} \setminus \mathsf{C}^{\mathrm{CP}}, \\ 0 & \text{if } \mathscr{E} \in \mathsf{C} \setminus \mathsf{C}^{\mathrm{P}}. \end{cases} \tag{4.19}$$

A similar function can be defined to study the transition to/from the set of entanglement-breaking channels, i.e.

$$\chi[\mathscr{E}] = \begin{cases} 1 & \text{if } \mathscr{E} \text{ is entanglement breaking}, \\ 0 & \text{if } \mathscr{E} \text{ if not.} \end{cases} \tag{4.20}$$

The quantum NOT gate is defined as $\mathrm{NOT} : \rho \mapsto \mathbb{1} - \rho$, i.e. it maps pure qubit states to its orthogonal state. Although this map transforms the Bloch sphere into itself it is not a CPTP map, and the closest CPTP map is $\mathscr{A}_{\mathrm{NOT}} : \rho \mapsto (\mathbb{1} - \rho)/3$. This is a rank-three qubit unital channel, thus, it is indivisible [WC08]. Moreover, $\det \mathscr{A}_{\mathrm{NOT}} = -1/27$ implies that this channel is not achievable by a P-divisible dynamical map. It is worth noting that $\mathscr{A}_{\mathrm{NOT}}$ belongs to $\overline{\mathsf{C}^{\mathrm{div}}}$.

A specific collision model was designed in Ref. [RFZB12] simulating stroboscopically a quantum dynamical map that implements the quantum NOT gate $\mathscr{A}_{\mathrm{NOT}}$ in finite time. The dynamical map is given by

$$\mathscr{E}_t(\rho) = \cos^2(t)\rho + \sin^2(t)\mathscr{A}_{\mathrm{NOT}}(\rho) + \frac{1}{2}\sin(2t)\mathscr{F}(\rho), \tag{4.21}$$

where $\mathscr{F}(\rho) = i\frac{1}{3}\sum_j [\sigma_j, \rho]$. It achieves the desired gate $\mathscr{A}_{\mathrm{NOT}}$ at $t = \pi/2$.

Let us stress that this dynamical map is unital, i.e. $\mathscr{E}_t(\mathbb{1}) = \mathbb{1}$ for all t, thus, its special orthogonal normal form can be illustrated inside the tetrahedron of Pauli channels, see fig. 4.12. In fig. 4.13 we plot $\delta[\mathscr{E}_t]$, $\chi[\mathscr{E}_t]$ and the value of the $\det \mathscr{E}_t$. We see the transitions $\mathsf{C}^{\mathrm{L}} \to \mathsf{C}^{\mathrm{P}} \setminus \mathsf{C}^{\mathrm{CP}} \to \mathsf{C}^{\mathrm{div}} \setminus \mathsf{C}^{\mathrm{P}} \to \overline{\mathsf{C}^{\mathrm{div}}}$ and back. Notice that in both plots the trajectory never goes through the $\mathsf{C}^{\mathrm{CP}} \setminus \mathsf{C}^{\mathrm{L}}$ region. This means that when the parametrized channels, up to rotations, belong to C^{L}, so do the original ones. The transition between P-divisible and divisible channels, i.e. $\mathsf{C}^{\mathrm{P}} \setminus \mathsf{C}^{\mathrm{CP}}$ and $\mathsf{C}^{\mathrm{div}} \setminus \mathsf{C}^{\mathrm{P}}$, occurs at the discontinuity in the yellow curve in fig. 4.12. Let us note that this discontinuity only occurs in the space of $\vec{\lambda}$; it is a consequence of the special orthogonal normal decomposition, see eq. (3.9). The complete channel is continuous in the full convex space of qubit CPTP maps. The transition from $\mathsf{C}^{\mathrm{P}} \setminus \mathsf{C}^{\mathrm{div}}$ and back occurs at times $\pi/3$ and $2\pi/3$. It can also be noted that the transition to entanglement breaking channels occurs shortly before the channel enters in the

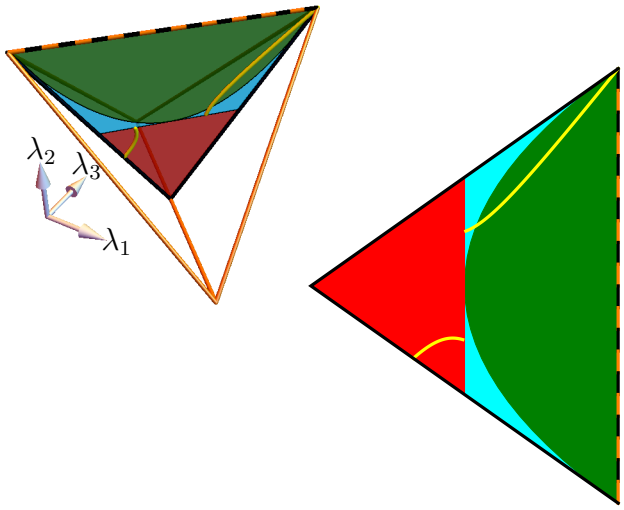

Figure 4.12: (top left) Tetrahedron of Pauli channels with the trajectory, up to rotations, of the quantum dynamical map eq. (4.21) leading to the $\mathscr{A}_{\text{NOT}}$ gate, as a yellow curve. (right) Cut along the plane that contains the trajectory; there one can see the different regions where the channel passes. For this case, the characterization of the C^{L} of the channels induced gives the same conclusions as for the corresponding Pauli channel, see eq. (3.9). The discontinuity in the trajectory is due to the reduced representation of the dynamical map, see eq. (4.21); the trajectory is continuous in the space of channels. See fig. 4.9 for the color coding.

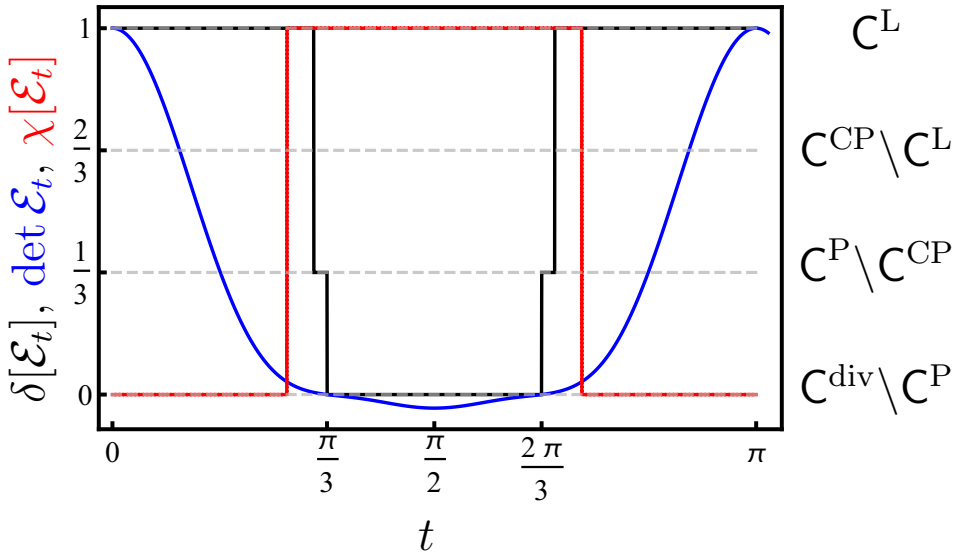

Figure 4.13: Evolution of divisibility, determinant, and entanglement breaking properties of the map induced by eq. (4.21), see eq. (4.19) and eq. (4.20). Notice that the channel $\mathscr{A}_{\mathrm{NOT}}$, implemented at $t = \pi/2$, has minimum determinant. The horizontal gray dashed lines show the image of the function δ, with the divisibility types in the right side. It can be seen that the dynamical map explores the divisibility sets as $\mathsf{C}^{\mathrm{L}} \to \mathsf{C}^{\mathrm{P}} \setminus \mathsf{C}^{\mathrm{CP}} \to \mathsf{C}^{\mathrm{div}} \setminus \mathsf{C}^{\mathrm{P}} \to \overline{\mathsf{C}^{\mathrm{div}}}$ and back. The channels are entanglement breaking in the expected region.

$\mathsf{C}^{\mathrm{div}} \setminus \mathsf{C}^{\mathrm{P}}$ region; likewise, the channel stops being entanglement breaking shortly after it leaves the $\mathsf{C}^{\mathrm{div}} \setminus \mathsf{C}^{\mathrm{P}}$ region, see theorem 20.

Consider now the dynamical map induced by a two-level atom interacting with a mode of a boson field. This model serves as a workhorse to explore a great variety of phenomena in quantum optics [GKL13]. Using the well known *rotating wave approximation* one arrives to the Jaynes-Cummings model [JC63], whose Hamiltonian is

$$H = \frac{\omega_a}{2}\sigma_z + \omega_f \left(a^\dagger a + \frac{1}{2}\right) + g\left(\sigma_- a^\dagger + \sigma_+ a\right). \tag{4.22}$$

By initializing the environment in a coherent state $|\alpha\rangle$, one gets the familiar *collapse and revival* setting. Considering a particular set of parameters shown in fig. 4.14, we constructed the channels parametrized by time numerically, and studied their divisibility and entanglement-breaking properties. In the same figure we plot functions $\delta[\mathscr{E}_t]$ and $\chi[\mathscr{E}_t]$, together with the probability of finding the atom in its excited state $p_e(t)$, to study and compare the divisibility properties with the features of the collapses and revivals. The probability $p_e(t)$ is calculated choosing the ground state of the free Hamiltonian $\omega_a/2\sigma_z$ of the qubit, and it is given by [KC09]:

$$p_e(t) = \frac{\langle \sigma_z(t)\rangle + 1}{2}, \tag{4.23}$$

where

$$\langle \sigma_z(t)\rangle = -\sum_{n=0}^{\infty} P_n \left(\frac{\Delta^2}{4\Omega_n^2} + \left(1 - \frac{\Delta^2}{4\Omega_n^2}\right)\cos\left(2\Omega_n t\right)\right),$$

with $P_n = e^{-|\alpha|^2}|\alpha|^{2n}/n!$, $\Omega_n = \sqrt{\Delta^2/4 + g^2 n}$ and $\Delta = \omega_f - \omega_a$ the detuning.

The divisibility indicator function δ exhibits an oscillating behavior, roughly at the same frequency of $p_e(t)$, see inset in fig. 4.14. The figure shows fast periodic transitions between $\mathsf{C}^{\mathrm{P}} \setminus \mathsf{C}^{\mathrm{CP}}$ and $\mathsf{C}^{\mathrm{CP}} \setminus \mathsf{C}^{\mathrm{L}}$ occurring in the region of revivals. There are also few transitions among $\mathsf{C}^{\mathrm{CP}} \setminus \mathsf{C}^{\mathrm{P}}$ and C^{L} in the second revival. Respect to the entanglement breaking and the function χ, there are no fast transitions in the former, and during revivals, channels are not entanglement breaking. We also observe that channels belonging to $\mathsf{C}^{\mathrm{div}} \setminus \mathsf{C}^{\mathrm{P}}$ are entanglement breaking, which agrees with theorem 20 for the non-unital case.

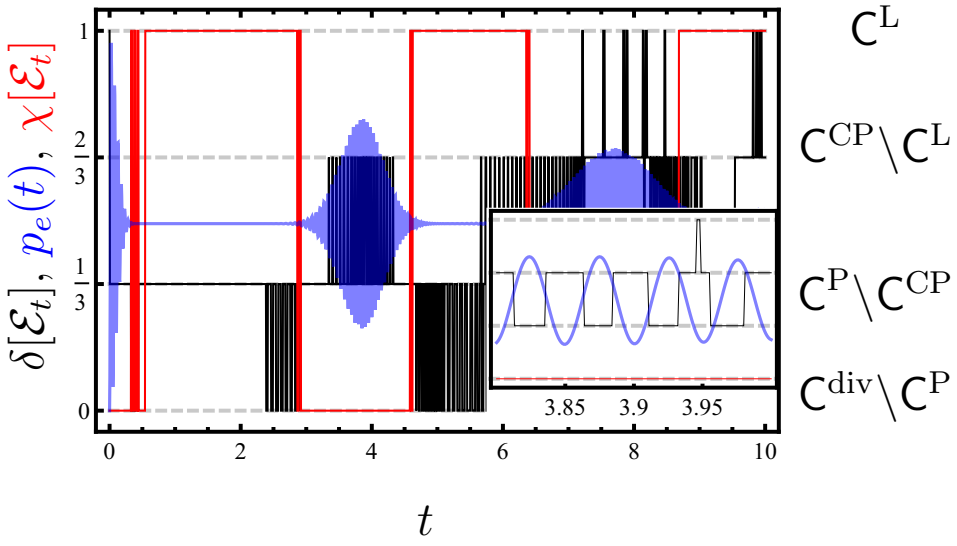

Figure 4.14: Black and red curves show functions δ and χ of the channels induced by the Jaynes-Cummings model over a two-level system, see eq. (4.22) with the environment initialized in a coherent state $|\alpha\rangle$. The blue curve shows the probability of finding the two-level atom in its excited state, $p_e(t)$. The figure shows that the fast oscillations in δ occur roughly at the same frequency as the ones of $p_e(t)$, see the inset. Notice that there are fast transitions between $\mathsf{C}^{\mathrm{P}} \setminus \mathsf{C}^{\mathrm{CP}}$ and $\mathsf{C}^{\mathrm{CP}} \setminus \mathsf{C}^{\mathrm{L}}$ occurring in the region of revivals, with a few transitions between $\mathsf{C}^{\mathrm{CP}} \setminus \mathsf{C}^{\mathrm{P}}$ and C^{L} in the second revival. The function χ shows that during revivals channels are not entanglement breaking, but we find that channels belonging to $\mathsf{C}^{\mathrm{div}} \setminus \mathsf{C}^{\mathrm{P}}$ are always entanglement breaking, in agreement with theorem 20. The particular chosen set of parameters are $\alpha = 6$, $g = 10$, $\omega_a = 5$, and $\omega_f = 20$.

Chapter 5

Singular Gaussian quantum channels

Self-education is, I firmly believe, the only kind of education there is.
Isaac Asimov

In this chapter we derive the conditions for δGQC to be singular, see sec. 3.5.1. In particular we will show that only the functional form involving one Dirac delta can be singular, together with the Gaussian form. Additionally we derive, for the non-singular cases, the conditions for the existence of master equations that parametrize channels that have always the same functional form. We do this by letting the channels parameters to depend on time.

5.1 Allowed singular forms

There are two classes of Gaussian singular channels. Since the inverse of a Gaussian channel $\mathscr{A}(\mathbf{T},\mathbf{N},\vec{\tau})$ is $\mathscr{A}\left(\mathbf{T}^{-1},-\mathbf{T}^{-1}\mathbf{N}\mathbf{T}^{-T},-\mathbf{T}^{-1}\vec{\tau}\right)$, its existence rests on the invertibility of $\mathbf{T}$. Therefore, studying the rank of the latter we are able to explore singular forms. We are going to use the classification of one-mode channels developed by Holevo [Hol07]. For singular channels there are two classes characterized by its *canonical form* [Hol08], i.e. any channel can be obtained by applying Gaussian unitaries before and after the canonical form. The class called "A_1" corresponds to singular channels with $\mathrm{Rank}(\mathbf{T}) = 0$ and coincide with the family of *total depolarizing channels*. The class "A_2" is characterized by $\mathrm{Rank}(\mathbf{T}) = 1$.

Both channels are entanglement-breaking [Hol08].

Before analyzing the functional forms constructed in this work, let us study channels with GF. The tuple of the affine transformation, corresponding to the propagator J_{G}, eq. (2.31), were introduced in Ref. [MP12] up to some typos. Our calculation for this tuple, following eq. (3.35), is:

$$\begin{aligned}
\mathbf{T}_{\mathrm{G}} &= \begin{pmatrix} -\frac{b_4}{b_3} & \frac{1}{b_3} \\ \frac{b_1 b_4}{b_3} - b_2 & -\frac{b_1}{b_3} \end{pmatrix}, \\
\mathbf{N}_{\mathrm{G}} &= \begin{pmatrix} \frac{2a_3}{b_3^2} & \frac{a_2}{b_3} - \frac{2a_3 b_1}{b_3^2} \\ \frac{a_2}{b_3} - \frac{2a_3 b_1}{b_3^2} & -2\left(-\frac{a_3 b_1^2}{b_3^2} + \frac{a_2 b_1}{b_3} - a_1\right) \end{pmatrix}, \\
\vec{\tau}_{\mathrm{G}} &= \left(-\frac{c_2}{b_3}, \frac{b_1 c_2}{b_3} - c_1\right)^{\mathrm{T}}.
\end{aligned} \tag{5.1}$$

It is straightforward to check that for $b_2 = 0$, $\mathbf{T}_{\mathrm{G}}$ is singular with $\mathrm{Rank}\,(\mathbf{T}_{\mathrm{G}}) = 1$, i.e. it belongs to class A_2. Due to the full support of Gaussian functions, it was surprising that Gaussian channels with GF have singular limit. In this case the singular behavior arises from the lack of a Fourier factor for $x_f r_i$, see eq. (2.31). This is the only singular case for GF.

Now we analyze functional forms derived in sec. 3.5.1. The complete positivity conditions of the form $\tilde{J}_{\mathrm{III}}$, presented in eq. (3.45), have no solution for $\alpha \to 0$ and/or $\gamma \to 0$, thus, this form cannot lead to singular channels. This is not the case for $\tilde{J}_{\mathrm{I}}$, eq. (3.36), which leads to singular operations belonging to class A_2 for

$$\alpha e_2 = 0, \tag{5.2}$$

and to class A_1 for

$$e_2 = \alpha = b_2 = 0. \tag{5.3}$$

For the latter, the complete positivity conditions, see eq. (3.40), read:

$$e_1 \leq a_1. \tag{5.4}$$

By using an initial state characterized by σ_i and $\vec{d}_i$ we can compute the explicit dependence of the final states on the initial parameters. The final states for channels of class A_2 with the functional form involving one delta, see eq. (3.25), and

with $e_2 = 0$, are

$$
\begin{aligned}
(\sigma_f)_{11} &= \frac{1}{2e_1}, \\
(\sigma_f)_{22} &= \left(\frac{\alpha}{\beta}\right)^2 \left(\frac{b_3^2}{2e_1} + 2a_3\right) + \frac{\alpha}{\beta}\left(2a_2 + \frac{b_1 b_3}{e_1}\right) + 2a_1 + \frac{b_1^2}{2e_1} + s_1, \\
(\sigma_f)_{12} &= -\frac{\alpha}{\beta}\frac{b_3}{2e_1} - \frac{b_1}{2e_1}, \\
\vec{d}_f(s_3) &= \left(0, -\frac{\alpha}{\beta}c_2 - c_1 + s_2\right)^{\mathrm{T}},
\end{aligned}
\tag{5.5}
$$

where

$$
\begin{aligned}
s_1 = &\left(b_2^2 + 2\frac{\alpha}{\beta}b_2 b_4 + \left(\frac{\alpha}{\beta}\right)^2 b_4^2\right)(\sigma_i)_{11} - 2\left(\frac{\alpha}{\beta}b_2 + \left(\frac{\alpha}{\beta}\right)^2 b_4\right)(\sigma_i)_{12} \\
&+ \left(\frac{\alpha}{\beta}\right)^2 (\sigma_i)_{22}, \\
s_2 = &\left(\frac{\alpha}{\beta}b_4 + b_2\right)(d_i)_1 - \frac{\alpha}{\beta}(d_i)_2.
\end{aligned}
\tag{5.6}
$$

For the same functional form but now with $\alpha = 0$, the final states are

$$
\begin{aligned}
(\sigma_f)_{11} &= \frac{e_2^2}{4e_1^2}(\sigma_i)_{11} + \frac{1}{2e_1}, \\
(\sigma_f)_{12} &= \left(\frac{b_2 e_2}{2e_1} - \frac{b_1 e_2^2}{4e_1^2}\right)(\sigma_i)_{11} - \frac{b_1}{2e_1}, \\
(\sigma_f)_{22} &= 2a_1 + \left(b_2 - \frac{b_1 e_2}{2e_1}\right)^2 (\sigma_i)_{11} + \frac{b_1^2}{2e_1},
\end{aligned}
\tag{5.7}
$$

and

$$
\vec{d}_f = \left(\frac{e_2}{2e_1}\left(\vec{d}_i\right)_1, \left(b_2 - \frac{b_1 e_2}{2e_1}\right)\left(\vec{d}_i\right)_1 - c_1\right)^{\mathrm{T}}. \tag{5.8}
$$

The explicit formulas of the final states for channels of class A_2 with Gaussian

form are

$$
\begin{aligned}
(\sigma_f)_{11}(s_1) &= \frac{2a_3}{b_3^2} + s_1, \\
(\sigma_f)_{12}(s_1) &= \frac{a_2}{b_3} - \frac{2a_3 b_1}{b_3^2} - b_1 s_1, \\
(\sigma_f)_{22}(s_1) &= \frac{b_1\left(b_3\left(b_1 b_3 s_1 - 2a_2\right) + 2a_3 b_1\right)}{b_3^2} + 2a_1, \\
\vec{d}_f(s_2) &= \left(s_2 - \frac{c_2}{b_3}, b_1\left(\frac{c_2}{b_3} - s_2\right) - c_1\right)^{\mathrm{T}},
\end{aligned}
\tag{5.9}
$$

where

$$
\begin{aligned}
s_1 &= \frac{b_4^2}{b_3^2}(\sigma_i)_{11} - \frac{2b_4}{b_3^2}(\sigma_i)_{12} + \frac{1}{b_3^2}(\sigma_i)_{22}, \\
s_2 &= \frac{1}{b_3}(d_i)_2 - \frac{b_4}{b_3}(d_i)_1 .
\end{aligned}
\tag{5.10}
$$

See fig. 5.1 for an schematic description of the final states. From such combinations it is obvious that we cannot solve for the initial state parameters given a final state as expected; this is because the parametric space dimension is reduced from 5 to at most 3. The channel belonging to A_1 [see eq. (3.42) with $e_2 = \alpha = b_2 = 0$ and eq. (5.4)] maps every initial state to a single one characterized by $\sigma_f = \mathbf{N}$ and $\vec{d}_f = (0, -c_1)^{\mathrm{T}}$, see fig. 5.2 for a schematic description.

According to our ansätze [see equations (3.24) and (3.25)], we conclude that one-mode SGQC can only have the functional forms given in eq. (2.31) and eq. (3.24). This is the central result of this chapter and can be stated as:

Theorem 21 (One-mode singular Gaussian channels)**.** *A one-mode Gaussian quantum channel is singular if and only if it has one of the following functional forms in the position space representation:*

1. $\frac{b_3}{2\pi}\exp\left[\imath\left(b_1 x_f r_f + b_3 x_i r_f + b_4 x_i r_i + c_1 x_f + c_2 x_i\right) - a_1 x_f^2 - a_2 x_f x_i - a_3 x_i^2\right]$,
2. $|\beta|\sqrt{e_1/\pi}\,\delta(\alpha x_f - \beta x_i)\exp\Big[-a_2 x_f x_i - a_1 x_f^2 - a_3 x_i^2$
   $+\imath\left(b_2 x_f r_i + b_3 r_f x_i + b_1 r_f x_f + b_4 r_i x_i + c_1 x_f + c_2 x_i\right) - e_1 r_f^2 - e_2 r_f r_i - \frac{e_2^2 r_i^2}{4e_1}\Big]$,
   with $e_2\alpha = 0$.

Corollary 1 (Singular classes)**.** *A one-mode singular Gaussian channel belongs to class A_1 if and only if its position representation has the following form:*

$$
\sqrt{e_1/\pi}\,\delta(x_i)\exp\left[-a_1 x_f^2 + \imath\left(b_2 x_f r_i + b_1 r_f x_f + c_1 x_f\right) - e_1 r_f^2\right].
$$

Otherwise the channel belongs to class A_2.

Since channels on each class are connected each other by unitary conjugations [Hol07], a consequence of the theorem and the subsequent corollary is that the set of allowed forms must remain invariant under unitary conjugations. To show this we must know the possible functional forms of Gaussian unitaries. They are given by the following lemma for one mode:

Lemma 1 (One-mode Gaussian unitaries)**.** *Gaussian unitaries can have only GF or the one given by eq. (3.25).*

Proof. Recalling that for a unitary GQC, $\mathbf{T}$ must be symplectic ($\mathbf{T}\Omega\mathbf{T}^{\mathrm{T}} = \Omega$) and $\mathbf{N} = \mathbf{0}$. However, an inspection to eq. (3.37) lead us to note that $\mathbf{N} \neq \mathbf{0}$ unless e_1 diverges. Thus, Gaussian unitaries cannot have the form J_{I} [see eq. (3.24)]. An inspection of matrices $\mathbf{T}$ and $\mathbf{N}$ of GQC with GF [see eq. (5.1)] and the ones for J_{II} [see equations (3.38) and (3.44)] lead us to note the following two observations: (i) in both cases we have $\mathbf{N} = 0$ for $a_n = 0 \ \ \forall n$; (ii) the matrix $\mathbf{T}$ is symplectic for GF when $b_2 = b_3$, and when $\alpha\eta = \beta\gamma$ for J_{II}. In particular the identity map has the last form. This completes the proof. □

One can now compute the concatenations of the SGQCs with Gaussian unitaries. This can be done straightforward using the well known formulas for Gaussian integrals and the Fourier transform of the Dirac delta. Given that the calculation is elementary, and for sake of brevity, we present only the resulting forms of each concatenation. To show this compactly we introduce the following abbreviations: Singular channels belonging to class A_2 with form J_{I} and with $\alpha = 0$, $e_2 = 0$ and $\alpha = e_2 = 0$, will be denoted as $\delta^{\alpha}_{\mathrm{A}_2}$, $\delta^{e_2}_{\mathrm{A}_2}$ and $\delta^{\alpha,e_2}_{\mathrm{A}_2}$, respectively; singular channels belonging to the same class but with GF will be denoted as $\mathscr{A}_{\mathrm{A}_2}$; channels belonging to class A_1 will be denoted as δ_{A_1}; finally Gaussian unitaries with GF will be denoted as $\mathscr{A}_{\mathscr{U}}$ and the ones with form J_{II} as $\delta_{\mathscr{U}}$. Writing the concatenation of two channels in the position representation as

$$J^{(\mathrm{f})}(x_f, r_f; x_i, r_i) = \int_{\mathbb{R}^2} dx' dr' J^{(1)}\left(x_f, r_f; x', r'\right) J^{(2)}\left(x', r'; x_i, r_i\right), \tag{5.11}$$

the resulting functional forms for $J^{(\mathrm{f})}$ are given in table 5.1. As expected, the table shows that the integral has only the forms stated by our theorem. Additionally it shows the cases when unitaries change the functional form of class A_2, while for class A_1 $J^{(\mathrm{f})}$ has always the unique form enunciated by the corollary.

$J^{(1)}$	$J^{(2)}$	$J^{(\mathrm{f})}$
$\delta^{\alpha}_{\mathrm{A}_2}$	$\mathscr{A}_{\mathscr{U}}$	$\mathscr{A}_{\mathrm{A}_2}$
$\mathscr{A}_{\mathscr{U}}$	$\delta^{\alpha}_{\mathrm{A}_2}$	$\delta^{\alpha}_{\mathrm{A}_2}$
$\delta^{\alpha}_{\mathrm{A}_2}$	$\delta_{\mathscr{U}}$	$\delta^{\alpha}_{\mathrm{A}_2}$
$\delta_{\mathscr{U}}$	$\delta^{\alpha}_{\mathrm{A}_2}$	$\delta^{\alpha}_{\mathrm{A}_2}$
$\delta^{e_2}_{\mathrm{A}_2}$	$\mathscr{A}_{\mathscr{U}}$	$\delta^{e_2}_{\mathrm{A}_2}$
$\mathscr{A}_{\mathscr{U}}$	$\delta^{e_2}_{\mathrm{A}_2}$	$\mathscr{A}_{\mathrm{A}_2}$
$\delta^{e_2}_{\mathrm{A}_2}$	$\delta_{\mathscr{U}}$	$\delta^{e_2}_{\mathrm{A}_2}$
$\delta_{\mathscr{U}}$	$\delta^{e_2}_{\mathrm{A}_2}$	$\delta^{e_2}_{\mathrm{A}_2}$
$\mathscr{A}_{\mathscr{U}},\delta_{\mathscr{U}}$	$\delta^{\alpha,e_2}_{\mathrm{A}_2}$	$\delta^{\alpha,e_2}_{\mathrm{A}_2}$
$\delta^{\alpha,e_2}_{\mathrm{A}_2}$	$\mathscr{A}_{\mathscr{U}},\delta_{\mathscr{U}}$	$\delta^{\alpha,e_2}_{\mathrm{A}_2}$
$\delta_{\mathscr{U}},\mathscr{A}_{\mathscr{U}}$	δ_{A_1}	δ_{A_1}
δ_{A_1}	$\delta_{\mathscr{U}},\mathscr{A}_{\mathscr{U}}$	δ_{A_1}

Table 5.1: The first and second columns show the functional forms of $J^{(1)}$ and $J^{(2)}$, respectively. The last column shows the resulting form of the concatenation of them, see eq. (5.11). See main text for symbol coding.

5.2 Existence of master equations

In this section we show the conditions under which master equations, associated with the channels derived in sec. 3.5.1, exist. To be more precise, we study if the functional forms derived above parametrize channels belonging to one-parameter differentiable families of GQCs. As a first step, we let the coefficients of forms presented in equations (3.24) and (3.25) to depend on time. Later we derive the conditions under which they bring any quantum state $\rho(x,r;t)$ to $\rho(x,r;t+\varepsilon)$ (with $\varepsilon > 0$ and $t \in [0,\infty)$) smoothly, while holding the specific functional form of the channel, i.e.

$$\rho(x,r;t+\varepsilon) = \rho(x,r;t) + \varepsilon \mathscr{L}_t[\rho(x,r;t)] + \mathscr{O}(\varepsilon^2), \tag{5.12}$$

where both $\rho(x,r;t)$ and $\rho(x,r;t+\varepsilon)$ are propagated from $t=0$ with channels either with the form J_{I} or J_{II}, and $\mathscr{L}_t$ is a bounded superoperator in the state subspace. This is basically the problem of *the existence of a master equation*

$$\partial_t \rho(x,r;t) = \mathscr{L}_t[\rho(x,r;t)], \tag{5.13}$$

for such functional forms. Thus, the problem is reduced to prove the existence of the linear generator $\mathscr{L}_t$, also known as *Liouvillian*.

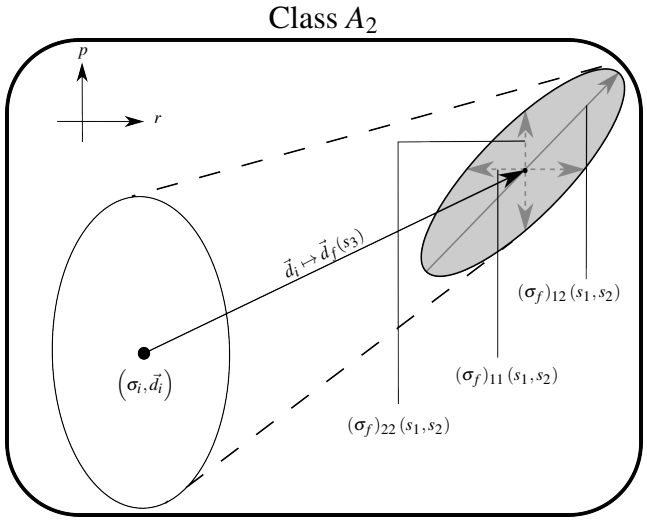

Figure 5.1: Schematic picture of the channels belonging to class A_2. The explicit dependence of the final state in terms of the combinations s_1, s_2 and s_3 are presented in the appendix. As well the formulas for s_i depending on the form of the channel.

To do this we use an ansatz proposed in Ref. [KG97] to investigate the existence and derive the master equation for GFs,

$$\mathscr{L} = \mathscr{L}_c(t) + (\partial_x, \partial_r)\mathbf{X}(t)\begin{pmatrix}\partial_x \\ \partial_r\end{pmatrix} + (x,r)\mathbf{Y}(t)\begin{pmatrix}\partial_x \\ \partial_r\end{pmatrix} + (x,r)\mathbf{Z}(t)\begin{pmatrix}x \\ r\end{pmatrix} \tag{5.14}$$

where $\mathscr{L}_c(t)$ is a complex function and

$$\mathbf{X}(t) = \begin{pmatrix}X_{xx}(t) & X_{xr}(t) \\ X_{rx}(t) & X_{rr}(t)\end{pmatrix} \tag{5.15}$$

is a complex matrix as well as $\mathbf{Y}(t)$ and $\mathbf{Z}(t)$, whose entries are defined in a similar way as in eq. (5.15). Note that $\mathbf{X}(t)$ and $\mathbf{Z}(t)$ can always be chosen symmetric, i.e. $X_{xr} = X_{rs}$ and $Z_{xr} = Z_{rx}$. Thus, we must determine 11 time-dependent functions from eq. (5.14). This ansatz is also appropriate to study the functional forms introduced in this work, given that the left hand side of eq. (5.13) only involves quadratic polynomials in x, r, $\partial/\partial x$ and $\partial/\partial r$, as in the GF case.

Notice that singular channels do not admit a master equation since its existence implies that channels with the functional form involved can be found arbitrarily

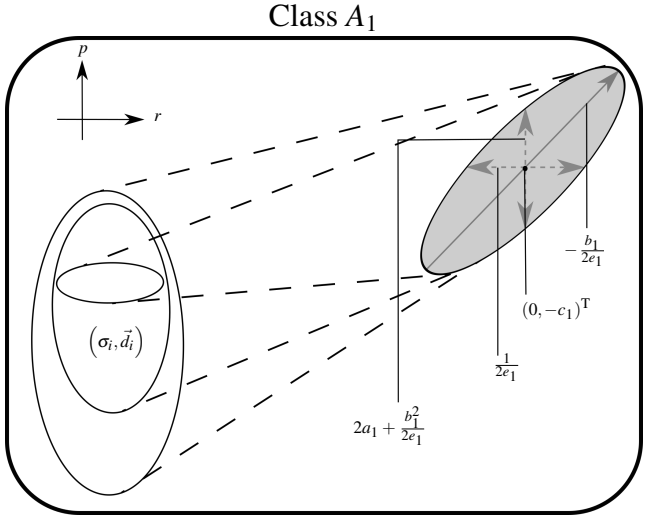

Figure 5.2: Schematic picture of the class A_1. Every channel of this class maps every initial quantum state, in particular GSs characterized by $\left(\sigma_i, \vec{d}_i\right)$, to a Gaussian state that depends only on the channel parameters. We indicate in the figure the values of the corresponding components of the first and second moments of the final Gaussian state.

close from the identity channel. This is not possible for singular channels due to the continuity of the determinant of the matrix $\mathbf{T}$.

For the non-singular cases presented in equations (3.24) and (3.25), the condition for the existence of a master equation is obtained as follows. (i) Substitute the ansatz of eq. (5.14) in the right hand side of the eq. (5.13). (ii) Define $\rho(x,r;t)$ using eq. (2.30), given an initial condition $\rho(x,r;0)$, for each functional form $J_{\mathrm{I,II}}$. (iii) Take $\rho_f(x_f,r_f) \to \rho(x,r;t)$ and $\rho_i(x_i,r_i) \to \rho(x,r;0)$. Finally, (iv) compare both sides of eq. (5.13). Defining $A(t) = \alpha(t)/\beta(t)$ and $B(t) = \gamma(t)/\eta(t)$, the conclusion is that for both J_{I} and J_{II}, a master equations exist if

$$c(t) \propto A(t) \tag{5.16}$$

holds, where $c(t) = c_1(t) + A(t)c_2(t)$. Additionally, for the form J_I the solutions for the matrices $\mathbf{X}(t)$, $\mathbf{Y}(t)$ and $\mathbf{Z}(t)$ are given by

$$\begin{aligned}
X_{xx} = X_{xr} = Y_{rx} = Z_{rr} &= 0,\\
Y_{xx} &= \frac{\dot{A}}{A},\\
\mathscr{L}_c = Y_{rr} &= \frac{\dot{e}_1}{e_1} - \frac{\dot{e}_2}{e_2},\\
X_{rr} &= \frac{\dot{e}_1}{4e_1^2} - \frac{\dot{e}_2}{2e_1e_2},\\
Y_{xr} &= \imath\left(\frac{\lambda_1\dot{e}_2}{e_1e_2} + \frac{\lambda_2\dot{A}}{e_2A} - \frac{\lambda_1\dot{e}_1}{2e_1^2} - \frac{\dot{\lambda}_2}{e_2}\right),\\
Z_{xx} &= \frac{\lambda_1^2}{2}\left(\frac{\dot{e}_2}{e_1e_2} - \frac{\dot{e}_1}{2e_1^2}\right) + \frac{\lambda_1}{e_2}\left(\frac{\lambda_2\dot{A}}{A} - \dot{\lambda}_2\right) + 2\lambda_3\frac{\dot{A}}{A} - \dot{\lambda}_3,\\
Z_{xr} &= \imath\left(\frac{\dot{A}}{A}\left(\frac{e_1\lambda_2}{e_2} - \frac{\lambda_1}{2}\right) + \frac{\dot{\lambda}_1}{2} - \frac{\dot{\lambda}_2e_1}{e_2} + \frac{\lambda_2}{2}\left(\frac{\dot{e}_2}{e_2} - \frac{\dot{e}_1}{e_1}\right)\right),
\end{aligned} \tag{5.17}$$

where we have defined the following coefficients: $\lambda_1 = b_1 + Ab_3$, $\lambda_2 = b_2 + Ab_4$ and $\lambda_3 = a_1 + Aa_2 + A^2a_3$.

For the form J_{II} the solutions are the following

$$\begin{gathered}
\mathscr{L}_c = X_{xx} = X_{xr} = X_{rr} = Z_{rr} = 0, \\
Y_{rx} = Y_{xr} = 0, \\
Y_{xx} = \frac{\dot{A}}{A}, Y_{rr} = \frac{\dot{B}}{B}. \\
Z_{xx} = a_2(t)\dot{A}(t) + \frac{2a_1(t)\dot{A}(t)}{A(t)} - A(t)^2 \\
-\dot{a}_3(t) - A(t)\dot{a}_2(t) - \dot{a}_1(t), \\
Z_{xr} = \imath\left(\frac{1}{2}\dot{\lambda} - \frac{\lambda}{2}\left(\frac{\dot{A}}{A} + \frac{\dot{B}}{B}\right)\right),
\end{gathered} \tag{5.18}$$

where $\lambda = b_1 + Ab_3 + B(b_2 + Ab_4)$.

Chapter 6

Summary and conclusions

Living is worthwhile if one can contribute in some small way to this endless chain of progress.
Paul A.M. Dirac

In this thesis we have introduced two works developed during my PhD. The first one was devoted to study quantum channels from the point of view of their divisibility properties. We made use of several results from the literature, specially from the seminal work by M. M. Wolf and J. I. Cirac [WECC08], and completed and fixed some results of Ref. [WC08]. This led to the construction of a tool to decide whether a quantum channel can be implemented using time-independent Markovian master equations or not, for the finite dimensional case. We additionally proved three theorems relating some of the studied divisibility types. Some of the tools introduced in chapter 3 are results from other paper developed during my PhD, where I am a secondary author, see Ref. [CDG19]. In the second work we have studied one-mode Gaussian channels without Gaussian functional form in the position state representation. We performed a characterization based on the universal properties that quantum channels must fulfill; in particular we studied the case of singular channels. We showed that the transition from unitarity to non-unitarity can correspond directly to a change in the functional form of the channel, in particular it turns out that functional form with one Dirac delta factor do not parametrize unitary channels. Additionally in this project we derived the conditions under which master equations for particular functional forms exist.

Let us summarize the results for the first project in more detail. We implemented the known conditions to decide the compatibility of channels with time-independent master equations (the so called L-divisibility) for the general diag-

onalizable case, and a discussion of the parametric space of Lindblad generators was given. We additionally clarified one of the results of the paper [WECC08]. There, the authors arrived to erroneous conclusions for the case of channels with negative eigenvalues. In our work we handled this case carefully. For unital qubit channels it was shown that every infinitesimal divisible map can be written as a concatenation of one L-divisible channel and two unitary conjugations. For the particular case of Pauli channels case, we have shown that the sets of infinitely divisible and L-divisible channels coincide. We made an interesting observation, connecting the concept of divisibility with the quantum information concept of entanglement-breaking channels: we found that divisible but not infinitesimal divisible qubit channels (in positive but not necessarily completely positive maps) are necessarily entanglement-breaking. We also noted that the intersection of indivisible and P-divisible channels is not empty. This allows us to implement indivisible channels with infinitesimal positive and trance preserving maps. Finally, we studied the possibility of dynamical transitions between different classes of divisibility channels. We argued that all the transitions are, in principle, possible, given that every divisibility set appears connected in our plots. We exploited two simple models of dynamical maps to demonstrate that these transitions exist. They clearly illustrate how the channels evolutions change from being implementable by Markovian dynamical maps (infinitesimal divisible in complete positive maps and/or L-divisible) to non-Markovian (divisible but not infinitesimal divisible or infinitesimal divisible in positive but not complete positive maps), and vice versa.

For the second project we have critically reviewed the deceptively natural idea that Gaussian quantum channels always admit a Gaussian functional form. To this end, we went beyond the pioneering characterization of Gaussian channels with Gaussian form presented in Ref. [MP12] in two new directions. First we have shown that, starting from their most general definition (a quantum ma that takes Gaussian states to Gaussian states), a more general parametrization of the coordinate representation of the one-mode case exists, that admits non-Gaussian functional forms. Second, we were able to provide a black-box characterization of such new forms by imposing complete positivity (not considered in Ref. [MP12]) and trace preserving conditions. While our parametrization connects with the analysis done by Holevo [Hol08] in the particular cases where besides having a non-Gaussian form the channel is also singular, it also allows the study of Gaussian unitaries, thus providing similar classification schemes. We completed the classification of the studied types of channels by deriving the form of the Liouvillian super operator that generates their time evolution in the form of a master equation. Surprisingly, Gaussian quantum channels without Gaussian form can be experimentally addressed by means of the celebrated Caldeira-Legget model for the quantum damped harmonic oscillator [GSI88], where the new types of

channels described here naturally appear in the sub-ohmic regime.

We are interested in several directions to continue the investigation. From the project of divisibility of quantum channels, an extension of this analysis to larger-dimensional systems could give a deeper sight to the structure of quantum channels. In particular we are interested on proving if the equivalence of infinitely divisible channels and L-divisible channels is present also in the general qubit case. Additionally a plethora of interesting questions are related to design of efficient verification procedures of the divisibility classes for channels and dynamical maps. For instance, *can we define an extension of the Lorentz normal decomposition to systems composed of many qubits?*, this would be useful to characterize infinitesimal divisibility of many particle systems; or *Is the non-countable parametrization of channels with negative eigenvalues relevant on deciding L-divisibility?*. Finally the area of channel divisibility contains several open structural questions, e.g. the existence of at most n-divisible channels. From the project concerning one-mode Gaussian channels, a natural direction to follow is to extend the analysis for other types of channels (or more modes) by following the classification introduced by Holevo, see Ref. [Hol07]. The latter is based on the form of a canonical form of one-mode Gaussian channels. Therefore a connection of this classification with ours could be useful to assess quantum information features, in particular for systems for which position state representation is advantageous.

Chapter 7

Appendices

Appendix A

Proof of theorem "Exact dynamics with Lindblad master equation"

The theorem announced in chapter 2 is,

Theorem 2 (Exact dynamics with Lindblad master equation) *Let $\mathscr{E}_t = e^{tL}$ a quantum process generated by a Lindblad operator L. The equation*

$$\mathscr{E}_t[\rho_S] = \mathrm{tr}_E\left[e^{-\mathrm{i}Ht}\left(\rho_S \otimes \rho_E\right) e^{\mathrm{i}Ht}\right],$$

where H has finite dimension, holds if and only if $\mathscr{E}_t$ is a unitary conjugation for every t.

Proof. To prove this theorem, we will compute $\rho_{\mathrm{S}}(t)$ to first order in t, see eq. (2.12). Following the master equation of eq. (2.10) and taking $t = \varepsilon \ll 1$, we have

$$\begin{aligned}\rho_{\mathrm{S}}(\varepsilon) &\approx \rho_{\mathrm{S}} + \mathrm{tr}_{\mathrm{E}} \int_0^{\varepsilon} dt \left\{\mathrm{i}\left[\rho_{\mathrm{S}} \otimes \rho_{\mathrm{E}}, H\right]\right\} \\ &= \rho_{\mathrm{S}} + \mathrm{tr}_{\mathrm{E}} \left\{\mathrm{i}\left[\rho_{\mathrm{S}} \otimes \rho_{\mathrm{E}}, H\right]\right\} \varepsilon \\ &= \rho_{\mathrm{S}} + L_{\mathrm{Exact}}[\rho_{\mathrm{S}}]\varepsilon.\end{aligned}$$

where $L_{\mathrm{Exact}} = \mathrm{tr}_{\mathrm{E}} \left\{\mathrm{i}\left[\rho_{\mathrm{S}} \otimes \rho_{\mathrm{E}}, H\right]\right\}$. Since $\mathscr{E}_t$ is generated by a Lindblad master equation, L_{Exact} must coincide with the Lindblad generator since the process is homogeneous in time, i.e. L_{Exact} is time-independent. Writing the global Hamiltonian as

$$H = \sum_{k,l=0} h_{kl} F_k^{(S)} \otimes F_l^{(E)},$$

where $h_{kl} \in \mathbb{R}$, and $\left\{F_k^{(S)}\right\}_k$ and $\left\{F_k^{(E)}\right\}_k$ are orthogonal hermitian bases of $\mathscr{B}\left(\mathscr{H}^{(S)}\right)$ and $\mathscr{B}\left(\mathscr{H}^{(E)}\right)$, respectively, with $\mathscr{H}^{(\mathrm{S})}$ and $\mathscr{H}^{(\mathrm{E})}$ are the Hilbert spaces of the central system S and the environment E. We have,

$$\begin{aligned} L_{\mathrm{Exact}}[\rho_{\mathrm{S}}] &= \mathrm{i}\,\mathrm{tr}_{\mathrm{E}}\left\{\sum_{k,l} h_{kl}[\rho_{\mathrm{S}}\otimes\rho_{\mathrm{E}}, F_k^{(S)}\otimes F_l^{(E)}]\right\} \\ &= \mathrm{i}\sum_{k,l} h_{kl}\left\{\rho_{\mathrm{S}}F_k^{(S)}\,\mathrm{tr}[\rho_{\mathrm{E}}F_l^{(E)}] - F_k^{(S)}\rho_{\mathrm{S}}\,\mathrm{tr}[F_l^{(E)}\rho_{\mathrm{E}}]\right\} \\ &= \mathrm{i}\sum_{k,l} h_{kl}\,\mathrm{tr}[F_l^{(\mathrm{E})}\rho_{\mathrm{E}}]\left\{\rho_{\mathrm{S}}F_k^{(\mathrm{S})} - F_k^{(\mathrm{S})}\rho_{\mathrm{S}}\right\} \\ &= \mathrm{i}[\rho_{\mathrm{S}}, \tilde{H}], \end{aligned}$$

where $\tilde{H} = \sum_{k,l} h_{kl}\,\mathrm{tr}[F_l^{(\mathrm{E})}\rho_{\mathrm{E}}]F_k^{(\mathrm{S})}$ is an hermitian operator. Therefore L_{Exact} is the generator of Hamiltonian dynamics with Hamiltonian $\tilde{H}$, thus $\mathscr{E}_t$ is unitary for all t. □

Appendix B

On Lorentz normal forms of Choi-Jamiolkowski state

In this appendix we compute the Lorentz normal decomposition of a channel for which one gets $b \neq 0$, supporting our observation that Lorentz normal decomposition does not take Choi-Jamiołkowski states to something proportional to a Choi-Jamiołkowski state. Consider the following Kraus rank three channel and its $R_{\mathscr{E}}$ matrix, both written in the Pauli basis:

$$\hat{\mathscr{E}} = \begin{pmatrix} 1 & 0 & 0 & 0 \\ 0 & -\frac{1}{3} & 0 & 0 \\ 0 & 0 & -\frac{1}{3} & 0 \\ \frac{2}{3} & 0 & 0 & \frac{1}{3} \end{pmatrix}, \tag{B.1}$$

and

$$R_{\mathscr{E}} = \begin{pmatrix} 1 & 0 & 0 & 0 \\ 0 & -\frac{1}{3} & 0 & 0 \\ 0 & 0 & \frac{1}{3} & 0 \\ \frac{2}{3} & 0 & 0 & \frac{1}{3} \end{pmatrix}. \tag{B.2}$$

Using the algorithm introduced in Ref. [VDD01] to calculate $R_{\mathscr{E}}$'s Lorentz decomposition into orthochronous proper Lorentz transformations we obtain

$$L_1 = \frac{1}{\gamma_1} \begin{pmatrix} 4 & 0 & 0 & 1 \\ 0 & -\gamma_1 & 0 & 0 \\ 0 & 0 & -\gamma_1 & 0 \\ 1 & 0 & 0 & 4 \end{pmatrix}, \tag{B.3}$$

$$L_2 = \frac{1}{\gamma_2}\begin{pmatrix} 89+9\sqrt{97} & 0 & 0 & -8 \\ 0 & -\gamma_2 & 0 & 0 \\ 0 & 0 & -\gamma_2 & 0 \\ -8 & 0 & 0 & 89+9\sqrt{97} \end{pmatrix},$$

and

$$\Sigma_{\mathscr{E}} = \frac{1}{\gamma_3}\begin{pmatrix} \sqrt{11+\frac{109}{\sqrt{97}}} & 0 & 0 & -\frac{\sqrt{97}+1}{\sqrt{89\sqrt{97}+873}} \\ 0 & -\frac{\gamma_3}{3} & 0 & 0 \\ 0 & 0 & \frac{\gamma_3}{3} & 0 \\ \sqrt{1+\frac{49}{\sqrt{97}}} & 0 & 0 & \sqrt{-1+\frac{49}{\sqrt{97}}} \end{pmatrix}$$

with $\gamma_1 = \sqrt{15}$, $\gamma_2 = 3\sqrt{178\sqrt{97}+1746}$, and $\gamma_3 = \sqrt{30}$. Although the central matrix $\Sigma_{\mathscr{E}}$ is not exactly of the form eq. (3.17), it is equivalent. To see this notice that the derivation of the theorem 2 in [VDD01] considers only decompositions into proper orthochronous Lorentz transformations. But to obtain the desired form, the authors change signs until they get eq. (3.17); this cannot be done without changing Lorentz transformations. If we relax the condition over $L_{1,2}$ of being proper and orthochronous, we can bring $\Sigma_{\mathscr{E}}$ to the desired form by conjugating $\Sigma_{\mathscr{E}}$ with $G = \operatorname{diag}(1,1,1,-1)$:

$$G^{-1}\Sigma_{\mathscr{E}}G = \frac{1}{\gamma_3}\begin{pmatrix} \sqrt{11+\frac{109}{\sqrt{97}}} & 0 & 0 & \frac{\sqrt{97}+1}{\sqrt{89\sqrt{97}+873}} \\ 0 & -\frac{\gamma_3}{3} & 0 & 0 \\ 0 & 0 & \frac{\gamma_3}{3} & 0 \\ -\sqrt{1+\frac{49}{\sqrt{97}}} & 0 & 0 & \sqrt{-1+\frac{49}{\sqrt{97}}} \end{pmatrix}.$$

In both cases (taking $\Sigma_{\mathscr{E}}$ or $G^{-1}\Sigma_{\mathscr{E}}G$ as the normal form of $R_{\mathscr{E}}$), the corresponding channel is not proportional to a trace-preserving one since $b \neq 0$, see eq. (3.17). This completes the counterexample.

Appendix C

Articles

C.1 Article: Divisibility of qubit channels and dynamical maps

Quantum 3, 144 (2019). Click to go to the webpage, Click to go to arXiv.

Divisibility of qubit channels and dynamical maps

David Davalos[1], Mario Ziman[2,3], and Carlos Pineda[1,4]

[1]Instituto de Física, Universidad Nacional Autónoma de México, México, D.F., México

[2]Institute of Physics, Slovak Academy of Sciences, Dúbravská cesta 9, Bratislava 84511, Slovakia

[3]Faculty of Informatics, Masaryk University, Botanická 68a, 60200 Brno, Czech Republic

[4]Faculty of Physics, University of Vienna, 1090 Vienna, Austria

May 7, 2019

The concept of divisibility of dynamical maps is used to introduce an analogous concept for quantum channels by analyzing the *simulability* of channels by means of dynamical maps. In particular, this is addressed for Lindblad divisible, completely positive divisible and positive divisible dynamical maps. The corresponding L-divisible, CP-divisible and P-divisible subsets of channels are characterized (exploiting the results by Wolf et al. [25]) and visualized for the case of qubit channels. We discuss the general inclusions among divisibility sets and show several equivalences for qubit channels. To this end we study the conditions of L-divisibility for finite dimensional channels, especially the cases with negative eigenvalues, extending and completing the results of Ref. [26]. Furthermore we show that transitions between every two of the defined divisibility sets are allowed. We explore particular examples of dynamical maps to compare these concepts. Finally, we show that every divisible but not infinitesimal divisible qubit channel (in positive maps) is entanglement-breaking, and open the question if something similar occurs for higher dimensions.

1 Introduction

The advent of quantum technologies opens questions aiming for deeper understanding of the fundamental physics beyond the idealized case of isolated quantum systems. Also the well established Born-Markov approximation used to describe open quantum systems (e.g. relaxation process such as spontaneous decay) is of limited use and a more general framework of open system dynamics is demanded. Recent efforts in this area have given rise to relatively novel research subjects - non-markovianity and divisibility.

Non-markovianity is a characteristic of continuous time evolutions of quantum systems (quantum dynamical maps), whereas divisibility refers to properties of system's transformations (discrete quantum processes) over a fixed time interval (quantum channels). The non-markovianity aims to capture and describe the back-action of the system's environment on the system's future time evolution. Such phenomena is identified as emergence of memory effects [1, 18, 22]. On the other side, the divisibility questions the possibility of splitting a given quantum channel into a concatenation of other quantum channels. In this work we will investigate the relation between these two notions.

David Davalos: davidphysdavalos@gmail.com

Our goal is to understand the possible forms of the dynamics standing behind the observed quantum channels, specially in regard to their divisibility properties which in turn determine their markovian or non-markovian nature. In particular, we provide characterization of the subsets of qubit channels depending on their divisibility properties and implementation by means of dynamical maps. An attempt to characterize the set of channels belonging to one-parameter semigroups induced by (time-independent) Lindblad master equations has been already done in Ref. [26]. However, it has drawbacks when dealing with channels with negative determinants. Using the results of Ref. [5] and Ref. [3], we will extend the analysis of [26] also for channels with negative eigenvalues.

The paper is organized as follows: In section 2 we give the formal definition of quantum channels and of quantum dynamical maps, and some of their properties. We discuss the meaning of divisibility for each object and discuss the known inclusions and equivalences between divisibility types. In section 3 we discuss properties and representations of qubit channels and their divisibility. We introduce a useful theorem to decide L-divisibility, which is in turn valid for any finite dimension. In section 4 we discuss the possible transition that can be occur between divisibility types, and show two examples of dynamical maps and their transitions. Finally in Section 5 we summarize our results and discuss open questions.

2 Basic definitions and divisibility

2.1 Channels and divisibility classes

We shall study transformations of a physical system associated with a complex Hilbert space $\mathcal{H}_d$ of dimension d. In particular, we consider linear maps on bounded operators, $\mathcal{B}(\mathcal{H}_d)$, that for the finite-dimensional case coincides with the set of trace-class operators that accommodate the subset of density operators representing the quantum states of the system. We say a linear map $\mathcal{E} : \mathcal{B}(\mathcal{H}_d) \to \mathcal{B}(\mathcal{H}_d)$ is *positive*, if it maps positive operators into positive operators, i.e. $X \geq 0$ implies $\mathcal{E}[X] \geq 0$. *Quantum channels* are associated with elements of the convex set C of *completely positive trace-preserving linear maps* (CPTP) transforming density matrices into density matrices, i.e. $\mathcal{E} : \mathcal{B}(\mathcal{H}) \to \mathcal{B}(\mathcal{H})$ such that $\mathrm{tr}(\mathcal{E}[X]) = \mathrm{tr}(X)$ for all $X \in \mathcal{B}(\mathcal{H})$, and all its extensions $\mathrm{id}_n \otimes \mathcal{E}$ are positive maps for all $n > 1$, where id_n is the identity channel on a n-dimensional quantum system. In general a channel has the form $\mathcal{E}[X] = \sum_i K_i X K_i^\dagger$. The minimum number of operators K_i required in the previous expression is called the *Kraus rank* of $\mathcal{E}$.

Let us introduce two subsets of channels. First, we say a channel is *unital* if it preserves the identity operator, i.e. $\mathcal{E}[\mathbb{1}] = \mathbb{1}$. Unital channels have a simple parametrization which will be useful for our purposes. Second, if $\mathcal{E}[X] = UXU^\dagger$ for some *unitary operator* U (meaning $UU^\dagger = U^\dagger U = \mathbb{1}$), we say the channel is *unitary*.

A quantum channel $\mathcal{E}$ is called *indivisible* if it cannot be written as a concatenation of two non-unitary channels, namely, if $\mathcal{E} = \mathcal{E}_1\mathcal{E}_2$ implies that either $\mathcal{E}_1$, or $\mathcal{E}_2$, exclusively, is a unitary channel. If the channel is not indivisible, it is said to be *divisible*. We denote the set of divisible channels by $\mathsf{C}^{\mathrm{div}}$ and that of indivisible channels by $\overline{\mathsf{C}^{\mathrm{div}}}$. Following this definition, unitary channels are divisible, because for them both (decomposing) channels $\mathcal{E}_{1,2}$ must be unitary. The concept of indivisible channels resembles the concept of prime numbers: unitary channels play the role of unity (which are not indivisible/prime), i.e. a composition of indivisible and a unitary channel results in an indivisible channel.

We now define the set of *infinitely divisible* channels (C^∞) and the set of *infinitesimal divisible* channels ($\mathsf{C}^{\mathrm{Inf}}$). Infinitely divisible channels, in some sense opposite to indivisible channels, are defined as channels $\mathcal{E}$ for which there exist for all $n = 1, 2, 3, \ldots$ a channel $\mathcal{A}_n$ such that $\mathcal{E} = (\mathcal{A}_n)^n$. Now, consider channels $\mathcal{E}$ that may be written as products of channels close to identity, i.e. such that for all $\epsilon > 0$ there exists a finite set of channels ε_j with $||\mathrm{id} - \varepsilon_j|| \leq \epsilon$ and $\mathcal{E} = \prod_j \varepsilon_j$. Its closure determines the set of infinitesimal divisible channels $\mathsf{C}^{\mathrm{Inf}}$.

2.2 Quantum dynamical maps and more divisibility classes

The next sets of channels are going to be defined using three types of dynamical maps. A *quantum dynamical map* is identified with a continuous parametrized curve drawn inside the set of channels starting at the identity channel, i.e. a one-parametric function $t \mapsto \mathcal{E}_t \in \mathsf{C}$ for all t belonging to an interval with minimum element 0 and satisfying the initial condition $\mathcal{E}_0 = \mathrm{id}$. Let $\mathcal{E}_{t,s} = \mathcal{E}_t^{-1}\mathcal{E}_s$ be the linear map describing the state transformations within the time interval $[t, s]$, whenever $\mathcal{E}_t^{-1}$ exists.

- A given quantum dynamical map is called *CP-divisible* if for all $t < s$ the map $\mathcal{E}_{t,s}$ is a channel.
- A given quantum dynamical map is called *P-divisible* [22] if $\mathcal{E}_{t,s}$ is a positive trace-preserving linear map for all $t < s$.
- A given quantum dynamical map is called *L-divisible* if it is induced by a time-independent Lindblad master equation [7, 14, 16], i.e. $\mathcal{E}_t = e^{tL}$ with

$$L(\rho) = i[\rho, H] + \sum_{\alpha,\beta} G_{\alpha\beta}\left(F_\alpha \rho F_\beta^\dagger - \frac{1}{2}\{F_\beta^\dagger F_\alpha, \rho\}\right),$$

  where $H = H^\dagger \in \mathcal{B}(\mathcal{H}_d)$ is known as Hamiltonian, $\{F_\alpha\}$ are hermitian and form an orthonormal basis of the operator space $\mathcal{B}(\mathcal{H}_d)$, and $G_{\alpha\beta}$ constitutes a hermitian positive semi-definite matrix.

If we allow the Lindblad generator L to depend on time, we recover the set of CP-divisible quantum dynamical maps as the resulting dynamical maps $\mathcal{E}_t = \hat{\mathrm{T}} e^{\int_0^t L(\tau)d\tau}$ ($\hat{\mathrm{T}}$ denotes the time-ordering operator) are compositions of infinitesimal completely-positive maps [1, 7, 14, 16]. Notice that there is a hierarchy for quantum dynamical maps: *L-divisible* quantum dynamical maps are *CP-divisible* which in turn are *P-divisible*.

Using the introduced families of quantum dynamical maps we can now classify quantum channels according to whether they can be implemented by the aforementioned kinds of quantum dynamical maps. We define subsets C^{L}, C^{CP}, and C^{P} of *L-divisible*, *CP-divisible* and *P-divisible* channels, respectively. In particular, we say $\mathcal{E} \in \mathsf{C}^{\mathrm{L}}$ if it belongs to the closure of a L-divisible quantum dynamical map. Let us stress that the requirement of the existence of Lindblad generator L such that $\mathcal{E} = e^L$ is not sufficient and closure is necessary. For example, the evolution governed by $L(\rho) = i[\rho, H] + \gamma[H, [H, \varrho]]$ results [27] in the diagonalization of states in the energy eigenbasis of H. Such transformation $\mathcal{E}_{\mathrm{diag}}$ is not invertible, thus (by definition) $L = \log \mathcal{E}_{\mathrm{diag}}$ does not exist (contains infinities). Analogously, we say $\mathcal{E} \in \mathsf{C}^{\mathrm{CP}}$ ($\mathcal{E} \in \mathsf{C}^{\mathrm{P}}$)

if there exists a CP-divisible (P-divisible) dynamical map $\mathcal{E}_t$ such that $\mathcal{E} = \mathcal{E}_t$ (with arbitrary precision) for some value of t (including $t = \infty$).

We now recall how to verify whether a channel is L-divisible since we will build upon the method for some of our results. Verifying whether $\mathcal{E} \in \mathsf{C}^{\mathrm{L}}$ [26] requires evaluation of the channel's logarithms, however, the matrix logarithm is defined only for invertible matrices and it is not unique. In fact, we need to check if at least one of its branches has the Lindblad form. It was shown in [5] that $\mathcal{E}$ is L-divisible if and only if there exists L such that: $\exp L = \mathcal{E}$, is hermitian preserving, trace-preserving and conditionally completely positive (ccp). Thus, we are looking for logarithm satisfying $L(X^\dagger) = L(X)^\dagger$ (hermiticity preserving), $L^*(\mathbb{1}) = 0$ (trace-preserving), and

$$(\mathbb{1} - \omega)(\mathrm{id} \otimes L)[\omega](\mathbb{1} - \omega) \geq 0 \tag{1}$$

(ccp condition), where $\omega = \frac{1}{d}\sum_{j,k=1}^{d} |j \otimes j\rangle\langle k \otimes k|$ is the projector onto a maximally entangled state. To the best of our knowledge, there is no general method to verify if a channel is P or CP divisible, with some exceptions [25].

2.3 Relation between channel divisibility classes

Due to the inclusion set relations between the three kinds of dynamical maps discussed in the previous sections, we can see that $\mathsf{C}^{\mathrm{L}} \subset \mathsf{C}^{\mathrm{CP}} \subset \mathsf{C}^{\mathrm{P}}$. Similarly, from the earlier definitions, one can easily argue that $\mathsf{C}^{\infty} \subset \mathsf{C}^{\mathrm{Inf}} \subset \mathsf{C}^{\mathrm{div}}$. By the definition of L-divisibility it is trivial to see that in general $\mathsf{C}^{\mathrm{L}} \subset \mathsf{C}^{\infty}$. Indeed Denisov has shown in [4] that infinitely divisible channels can be written as $\mathcal{E} = \mathcal{E}_0 e^{L}$, with L a Lindblad generator, and $\mathcal{E}_0$ idempotent operator such that $\mathcal{E}_0 L \mathcal{E}_0 = \mathcal{E}_0 L$. Further, it was shown in Ref. [25] that $\mathcal{E} \in \mathsf{C}^{\mathrm{inf}}$ implies $\det \mathcal{E} \geq 0$ and also that $\mathcal{E}$ can be approximated by $\prod_j e^{L_j}$, i.e. $\mathsf{C}^{\mathrm{CP}} = \mathsf{C}^{\mathrm{inf}}$. In other words, the positivity of determinant is necessary for the channel to be (in the closure of) channels attainable by CP-divisible dynamical maps. In summary, we have the following relations between sets (see also Fig. 1):

$$\begin{array}{ccccc} \mathsf{C}^{\infty} & \subset & \mathsf{C}^{\mathrm{Inf}} & \subset & \mathsf{C}^{\mathrm{div}} \\ \cup | & & \| & & \\ \mathsf{C}^{\mathrm{L}} & \subset & \mathsf{C}^{\mathrm{CP}} & \subset & \mathsf{C}^{\mathrm{P}} \end{array} . \tag{2}$$

The relation between C^{P} and $\mathsf{C}^{\mathrm{div}}$ is unknown, although it is clear that $\mathsf{C}^{\mathrm{div}} \subset \mathsf{C}^{\mathrm{P}}$ is not possible since channels in C^{P} are not necessarily divisible in CP maps. The intersection of C^{P} and $\mathsf{C}^{\mathrm{div}}$ is not empty since $\mathsf{C}^{\mathrm{CP}} \subseteq \mathsf{C}^{\mathrm{div}}$ and $\mathsf{C}^{\mathrm{CP}} \subseteq \mathsf{C}^{\mathrm{P}}$. Later on we will investigate if $\mathsf{C}^{\mathrm{P}} \subseteq \mathsf{C}^{\mathrm{div}}$ or not.

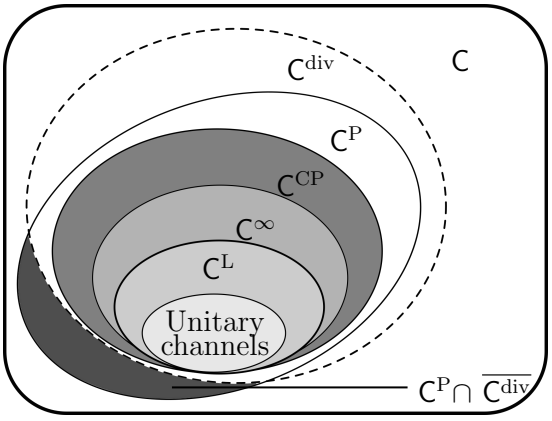

Figure 1: Scheme illustrating the different sets of quantum channels for a given dimension, discussed in sec. 2. In particular, the inclusion relations presented in Eq. (2) are depicted.

3 Qubit channels

3.1 Representations

Using the Pauli basis $\frac{1}{\sqrt{2}}\{\mathbf{1}, \sigma_x, \sigma_y, \sigma_z\}$, and the standard Hilbert-Schmidt inner product, the real representation for qubit channels is given by [10, 20]:

$$\hat{\mathcal{E}} = \begin{pmatrix} 1 & \vec{0}^T \\ \vec{t} & \Delta \end{pmatrix}. \tag{3}$$

This describes the action of the channel in the Bloch sphere picture in which the points $\vec{r}$ are identified with density operators $\varrho_{\vec{r}} = \frac{1}{2}(I + \vec{r} \cdot \vec{\sigma})$. We will write $\mathcal{E} = (\Delta, \vec{t})$ meaning that $\mathcal{E}(\rho_{\vec{r}}) = \rho_{\Delta\vec{r}+\vec{t}}$.

In order to study qubit channels with simpler expressions, we will consider a decomposition in unitaries such that

$$\mathcal{E} = \mathcal{U}_1 \mathcal{D} \mathcal{U}_2. \tag{4}$$

This can be performed by decomposing Δ in rotation matrices, i.e. $\Delta = R_1 D R_2$, where $D = \mathrm{diag}(\lambda_1, \lambda_2, \lambda_3)$ is diagonal and the rotations $R_{1,2} \in \mathrm{SO}(3)$ (of the Bloch sphere) correspond to the unitary channels $\mathcal{U}_{1,2}$. This decomposition should not be confused with the singular value decomposition. The latter allows decompositions that include, say, total reflections. Such operations do not correspond to unitaries over a qubit, in fact they are not CPTP. Therefore the channel $\mathcal{D}$, in the Pauli basis, is given by

$$\hat{\mathcal{D}} = \begin{pmatrix} 1 & \vec{0}^T \\ \vec{\tau} & D \end{pmatrix}, \tag{5}$$

where $\Delta = R_1 D R_2$ and $\vec{\tau} = R_1^T \vec{t}$. The latter describes the shift of the center of the Bloch sphere under the action of $\mathcal{D}$. The parameters $\vec{\lambda}$ determine the length of semi-axes of the Bloch ellipsoid, being the deformation of Bloch sphere under the action of $\mathcal{E}$. From

now we will call the form $\mathcal{D}$, *special orthogonal normal form*.

We shall develop a geometric intuition in the space determined by the possible values of these three parameters. For an arbitrary channel, complete positivity implies that the possible set of lambdas lives inside the tetrahedron with corners $(1,1,1)$, $(1,-1,-1)$, $(-1,1,-1)$ and $(-1,-1,1)$, see Fig. 2. For unital channels, all points in the tetrahedron are allowed, but for non-unital channels more restrictive conditions arise. In Fig. 8 we present a visualization of the permitted values of $\vec{\lambda}$ for a particular nontrivial value of $\vec{\tau}$, and in [2] the steps to study the general case from an algebraic point of view are presented. For the unital case, the corner $\vec{\lambda} = (1,1,1)$ corresponds to the identity channel, $\vec{\lambda} = (1,-1,-1)$ to σ_x $\vec{\lambda} = (-1,1,-1)$ to σ_y and $\vec{\lambda} = (-1,-1,1)$ to σ_z (Kraus rank 1 operations). Points in the edges correspond to Kraus rank 2 operations, points in the faces to Kraus rank 3 operations and in the interior of the tetrahedron to Kraus rank 4 operations.

In addition to this decomposition, following the definition of divisibility, concatenation with unitaries of a given quantum channel do not change the divisibility character of the latter. Thus orthogonal normal forms are useful to study divisibility since, following also the properties of C^{P} and C^{CP} introduced in sec. 3.1, immediately one has:

Theorem 1 (Divisibility of special orthogonal normal forms). *Let $\mathcal{E}$ a qubit quantum channel and $\mathcal{D}$ its special orthogonal normal form, $\mathcal{E}$ belongs to C^X if and only if $\mathcal{D}$ does, where $X = \{$"Div", "P", "CP"$\}$.*

There is another another parametrization for qubit channels called *Lorentz normal decomposition* [23, 24] which is specially useful to characterize infinitesimal divisibility $\mathsf{C}^{\mathrm{Inf}}$, and geometric aspects of entanglement [15]. This decomposition is derived from the theorem 3 of Ref. [24], which essentially states that for a qubit state $\rho = \frac{1}{4}\sum_{i,j=0}^{3} R_{ij}\sigma_i \otimes \sigma_j$ the matrix R can be decomposed as $R = L_1 \Sigma L_2^{\mathrm{T}}$. Here $L_{1,2}$ are proper orthochronous Lorentz transformations and Σ is either $\Sigma = \mathrm{diag}\,(s_0, s_1, s_2, s_3)$ with $s_0 \geq s_1 \geq s_2 \geq |s_3|$, or

$$\Sigma = \begin{pmatrix} a & 0 & 0 & b \\ 0 & d & 0 & 0 \\ 0 & 0 & -d & 0 \\ c & 0 & 0 & -b+c+a \end{pmatrix}. \qquad (6)$$

In theorem 8 of Ref. [23] the authors make a similar claim, exploiting the Choi-Jamiołkowski isomorphism. They forced $b = 0$ in order to have normal forms proportional to trace-preserving operations in the case of Kraus rank deficient ones, see Eq. (6). The latter is equivalent to saying that the decomposition of Choi-Jamiołkowski states leads to states that are proportional to Choi-Jamiołkowski states. We didn't find a good argument to justify such an assumption

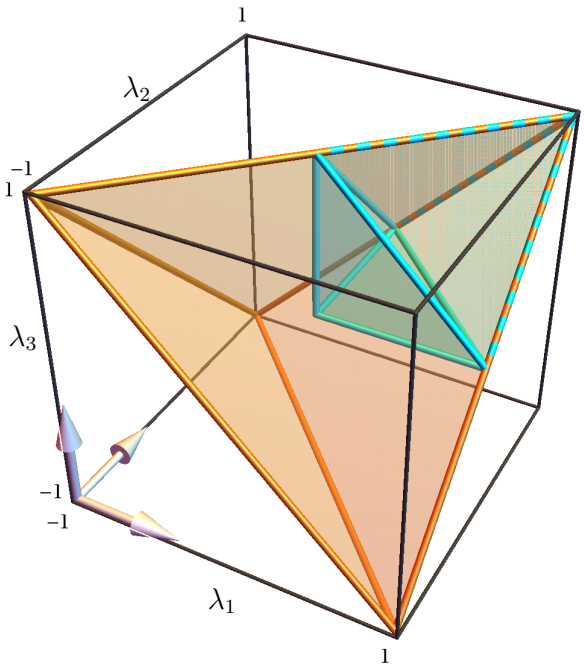

Figure 2: Tetrahedron of Pauli channels. The corners correspond to unitary Pauli operations ($\mathbb{1}$, $\sigma_{x,y,z}$) while the rest can be written as convex combinations of them. The bipyramid in blue corresponds to channels with $\lambda_i > 0 \forall i$, i.e. channels of the positive octant belonging to C^{P}. The whole set C^{P} includes three other bipyramids corresponding to the other vertexes of tetrahedron, i.e. C^{P} enjoys the symmetries of the tetrahedron, see Eq. (8). The faces of the bipyramids matching the corners of the tetrahedron are subsets of the faces of the tetrahedron, i.e. contain Kraus rank three channels. Such channels are then C^{P}but also $\overline{\mathsf{C}^{\mathrm{div}}}$, showing that the intersection shown in Fig. 1 is not empty.

and found a counterexample (see appendix A). Thus we propose a restricted version of their theorem:

Theorem 2 (**Restricted Lorentz normal form for qubit quantum channels**). *For any full Kraus rank qubit channel $\mathcal{E}$ there exists rank-one completely positive maps $\mathcal{T}_1, \mathcal{T}_2$ such that $\mathcal{T} = \mathcal{T}_1 \mathcal{E} \mathcal{T}_2$ is proportional to*

$$\begin{pmatrix} 1 & \vec{0}^T \\ \vec{0} & \Lambda \end{pmatrix}, \tag{7}$$

where $\Lambda = \mathrm{diag}(s_1, s_2, s_3)$ with $1 \geq s_1 \geq s_2 \geq |s_3|$.

The channel $\mathcal{T}$ is called the Lorentz normal form of the channel $\mathcal{E}$. For unital qubit channels D coincides with Λ, thus in such case the form of (7) holds for any Kraus rank.

3.2 Divisibility

In this subsection we will recall the criteria to decide if a qubit channel belongs to $\mathsf{C}^{\mathrm{div}}$, C^{P} and C^{CP} following [25]. We shall start with some general statements, and then focus on different types of channels (unital, diagonal non-unital and general ones). We will also discuss in detail the characterization of C^{L}, which entails a higher complexity.

It was shown ([25], Theorem 11) that full Kraus rank channels are divisible ($\mathsf{C}^{\mathrm{div}}$). This simply means that all points in the interior of the set of channels correspond to divisible channels. Moreover, according to Theorem 23 of the same reference, qubit channels are indivisible if and only if they have Kraus rank three and diagonal Lorentz normal form. Notice that since we dispute the theorem upon which such statement is based, the classification might be inaccurate, see the appendix. It follows from the definition that for qubit channels $\mathcal{E}$ is divisible if and only if $\mathcal{D}$ is divisible. To test if $\mathcal{D}$ is divisible, we check that all eigenvalues of its Choi matrix are different from zero.

A non-negative determinant of $\mathcal{E}$ is a necessary condition for a general channel to belong to C^{P} ([25], Proposition 15). For qubits, this is also sufficient ([25], Theorem 25), and given that $\det \mathcal{D} = \det \mathcal{E}$, the condition for qubit channels simply reads

$$\det \mathcal{E} = \lambda_1 \lambda_2 \lambda_3 \geq 0. \tag{8}$$

However, to our knowledge, a simple condition for arbitrary dimension is yet unknown.

With respect to testing for CP-divisibility we restrict the discussion to qubit channels. To characterize CP-divisible channels it is useful to consider the Lorentz normal form for channels. A full Kraus rank qubit channel $\mathcal{E}$ belongs to C^{CP} if and only if it has diagonal Lorentz normal form with

$$s_{\min}^2 \geq s_1 s_2 s_3 > 0 \tag{9}$$

where $s_{\min}$ is the smallest of s_1, s_2 and s_3, see theorem 2 and [26]. For Kraus deficient channels the pertinent theorems are based on Kraus deficient Lorentz normal forms that according to our appendix should be reviewed.

Deciding L-divisibility, as mentioned above, is equivalent to proving the existence of a hermiticity preserving generator which additionally fulfills the ccp condition.

To prove the former we recall that every hermiticity preserving operator has a real matrix representation when choosing a hermitian basis. Since quantum channels preserve hermiticity, the problem is reduced on finding a real logarithm $\log \hat{\mathcal{E}}$ given a real matrix $\hat{\mathcal{E}}$. This problem was already solved by Culver [3] who characterized completely the existence of real logarithms of real matrices. For diagonalizable matrices the results can be summarized as follows:

Theorem 3 (**Existence of hermiticity preserving generator**). *A non-singular matrix with real entries $\hat{\mathcal{E}}$ has a real generator (i.e. a $\log \hat{\mathcal{E}}$ has real entries) if and only if the spectrum fulfills the following conditions:*

(i) negative eigenvalues are even-fold degenerated;

(ii) complex eigenvalues come in complex conjugate pairs.

Let us examine this theorem for the particular case of qubits. In this case this theorem means that real logarithm(s) of $\hat{\mathcal{E}}$ exist if and only if $\mathcal{E}$ has either only positive eigenvalues, one positive and two complex, or one positive and two equal non-positive eigenvalues, apart from the trivial eigenvalue equal to one. Notice that quantum channels with complex eigenvalues will fulfill the last condition immediately since they preserve hermiticity.

We now continue discussing the multiplicity of the solutions of $\log \hat{\mathcal{E}}$, as finding an appropriate parametrization is essential to test for the ccp condition, see Eq. (1). If $\hat{\mathcal{E}}$ has positive degenerated, negative, or complex eigenvalues, its real logarithms are not unique, and are spanned by *real logarithm branches* [3]. In case of having negative eigenvalues, it turns out that real logarithms always have a non-continuous parametrization, in addition to real branches due to the freedom of the Jordan normal form transformation matrices. Given a real representation of $\mathcal{E}$, i.e. $\hat{\mathcal{E}}$, the Jordan form is given by $\hat{\mathcal{E}} = wJw^{-1} = \tilde{w}J\tilde{w}^{-1}$, where $w = \tilde{w}K$ with K belonging to a continuum of matrices that commutes with J [3]. In the case of diagonalizable matrices, if there are no degeneracies, K commutes with $\log(J)$.

Finally let us note that if a channel belongs to C^{L}, unitary conjugations can bring it to $\mathsf{C}^{\mathrm{Inf}} \setminus \mathsf{C}^{\mathrm{L}}$ and vice versa.

3.3 Unital channels

We shall start our study of unital qubit channels, by considering Pauli channels, defined as convex combi-

nations of the unitaries σ_i:

$$\mathcal{E}_{\text{Pauli}}[\rho] = \sum_{i=0}^{3} p_i \sigma_i \rho \sigma_i, \tag{10}$$

where $\sigma_0 = \mathbb{1}$ and $p_i \geq 0$ with $\sum_i p_i = 1$. The special orthogonal normal form of a Pauli channel [see Eqs. (4) and (5)] has $\mathcal{U}_1 = \mathcal{U}_2 = \text{id}$ and $\vec{\tau} = \vec{0}$. Thus Pauli channels are fully characterized only by $\vec{\lambda}$. Notice that every unital qubit channel can be written as

$$\mathcal{E}_{\text{unital}} = \mathcal{U}_1 \mathcal{E}_{\text{Pauli}} \mathcal{U}_2. \tag{11}$$

This implies that arbitrary unital qubit channels can be expressed as convex combinations of (at most) four unitary channels.

Following theorem 1 it is straightforward to note that by characterizing C^{div}, C^{P} and C^{CP} of Pauli channels, the same conclusions hold for general unital qubit channels having the same $\vec{\lambda}$. Additionally we can have a one-to-one geometrical view of the divisibility sets for Pauli channels given they have a one-to-one correspondence to the tetrahedron shown in Fig. 2, defined by the inequalities

$$1 + \lambda_i - \lambda_j - \lambda_k \geq 0 \tag{12}$$
$$1 + \lambda_1 + \lambda_2 + \lambda_3 \geq 0 \tag{13}$$

with i, j and k all different [28].

3.3.1 P-divisibility

Let us discuss the divisibility properties of Pauli channels. Divisibility in CPTP (C^{div}) is guaranteed for full Kraus rank channels, i.e. for the interior channels of the tetrahedron. For Pauli channels this is equivalent to taking only the inequality of equations (13). The characterization of C^{P} can be done directly using Eq. (8), as it depends only on $\vec{\lambda}$. This set is the intersection of the tetrahedron with the octants where the product of all λs is positive. In fact, it consists of four triangular bipyramids starting in each vertex of the tetrahedron and meeting in its center, see Fig. 2. Let us study the intersection of this set with the set of unital entanglement-breaking (EB) channels [28], forming an octahedron (being the intersection of the tetrahedron with its space inversion, see Fig. 3). It is defined by the inequalities

$$\begin{aligned} \lambda_1 + \lambda_2 + \lambda_3 &\leq 1 \\ \lambda_i - \lambda_j - \lambda_k &\leq 1, \end{aligned} \tag{14}$$

with i, j and k all different [28], together with Eq. (13). It follows that unital qubit channels that are not achieved by P-divisible dynamical maps are necessarily entanglement-breaking (see Fig. 3 and Fig. 7). In fact this holds for general qubit channels, see section 3.4.

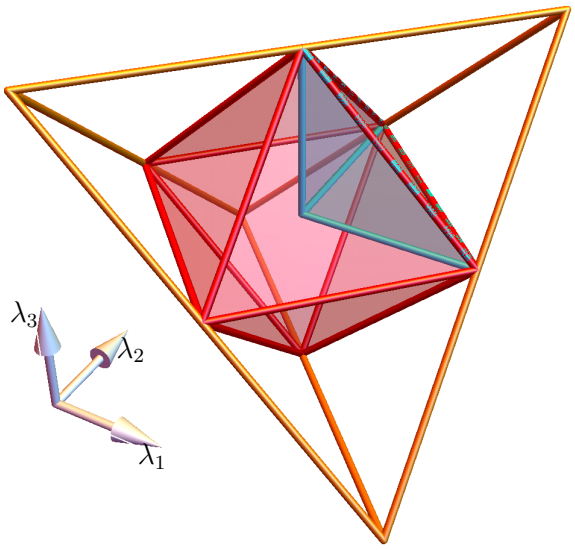

Figure 3: Tetrahedron of Pauli channels with the octahedron of entanglement breaking channels shown in red, see Eq. (14). The blue pyramid inside the octahedron is the intersection of the bipyramid shown in Fig. 2, with the octahedron. The complement of the intersections of the four bipyramids forms the set of divisible but not infinitesimal divisible channels in PTP. Thus, a central feature of the figure is that the set $\mathsf{C}^{\text{div}} \backslash \mathsf{C}^{\text{P}}$ is always entanglement-breaking, but the converse is not true.

3.3.2 CP-divisibility

The subset of CP-divisible Pauli channels, following Eq. (9) and theorem 2, is determined by the inequalities

$$0 < \lambda_1 \lambda_2 \lambda_3 \leq \lambda_{\text{min}}^2 \,. \tag{15}$$

They determine a body that is symmetric with respect to permutation of Pauli unitary channels (i.e. in λ_j), hence, the set of C^{CP} of Pauli channels possesses the symmetries of the tetrahedron. The set $\mathsf{C}^{\text{CP}} \backslash \mathsf{C}^{\text{L}}$ is plotted in Fig. 5. Notice that this set coincides with the set of unistochastic qubit channels, see Ref. [17].

3.3.3 L-divisibility

Let us now derive the conditions for L-divisibility of Pauli channels with positive eigenvalues $\lambda_1, \lambda_2, \lambda_3$ ($\lambda_0 = 1$). The logarithm of $\mathcal{D}$, induced by the principal logarithm of its eigenvalues, is thus

$$L = K \,\text{diag}(0, \log\lambda_1, \log\lambda_2, \log\lambda_3) K^{-1} \,, \tag{16}$$

which is real (hermiticity preserving). In case of no-degeneration the dependency on K vanishes and L is unique. In such case the ccp conditions $\log\lambda_j - \log\lambda_k - \log\lambda_l \geq 0$ imply

$$\lambda_j \lambda_k \leq \lambda_l \tag{17}$$

for all combinations of mutually different j, k, l. This set (channels belonging to C^{L} with positive eigenvalues) forms a three dimensional manifold, see Fig. 6.

In case of degeneration, let us label the eigenvalues η, λ and λ. In this case, the real solution for L is not unique and is parametrized by real branches in the degenerate subspace and by the continuous parameters of K [3]. Let us study the principal branch with $K = \mathbb{1}$. Eq. (17) is then reduced to

$$\lambda^2 \leq \eta \leq 1 \, . \tag{18}$$

Therefore, if these inequalities are fulfilled, the generator has Lindblad form. If not, then *a priori* other branches can fulfill the ccp condition and consequently have a Lindblad form. Thus, Eq. (18) provides a sufficient condition for the channel to be in C^{L}. We will see it is also necessary.

Indeed, the complete positivity condition requires $\eta, \lambda \leq 1$, thus, it remains to verify only the condition $\lambda^2 \leq \eta$. It holds for the case $\lambda \leq \eta$. If $\eta \leq \lambda$, then this condition coincides with the CP-divisibility condition from Eq. (15). Since C^{L} implies C^{CP} the proof is completed. In conclusion, the condition in Eq. (17) is a necessary and sufficient condition for a given Pauli channel with positive eigenvalues to belong to C^{L}.

Let us stress that the obtained subset of L-divisible channels does not possess the tetrahedron symmetries. In fact, composing $\mathcal{D}$ with a σ_z rotation $\mathcal{U}_z = \mathrm{diag}(1, -1, -1, 1)$ results in the Pauli channel $\mathcal{D}' = \mathrm{diag}(1, -\lambda_1, -\lambda_2, \lambda_3)$. Clearly, if λ_j are positive ($\mathcal{D}$ is L-divisible), then $\mathcal{D}'$ has non-positive eigenvalues. Moreover, if all λ_j are different, then $\mathcal{D}'$ does not have any real logarithm, therefore, it cannot be L-divisible. In conclusion, the set of L-divisible unital qubit channels is not symmetric with respect to tetrahedron symmetries.

In what follows we will investigate the case of non-positive eigenvalues. Theorem 3 implies that that eigenvalues have the form (modulo permutations) $\eta, -\lambda, -\lambda$, where $\eta, \lambda \geq 0$. The corresponding Pauli channels are $\mathcal{D}_x = \mathrm{diag}(1, \eta, -\lambda, -\lambda)$, $\mathcal{D}_y = \mathrm{diag}(1, -\lambda, \eta, -\lambda)$, $\mathcal{D}_z = \mathrm{diag}(1, -\lambda, -\lambda, \eta)$, thus forming three two-dimensional regions inside the tetrahedron. Take, for instance, $\mathcal{D}_z$ that specifies a plane (inside the tetrahedron) containing I, σ_z and completely depolarizing channel $\mathcal{N} = \mathrm{diag}(1, 0, 0, 0)$. The real logarithms for this case are given by

$$L = K \begin{pmatrix} 0 & 0 & 0 & 0 \\ 0 & \log(\lambda) & (2k+1)\pi & 0 \\ 0 & -(2k+1)\pi & \log(\lambda) & 0 \\ 0 & 0 & 0 & \log(\eta) \end{pmatrix} K^{-1}, \tag{19}$$

where $k \in \mathbb{Z}$ and K, as mentioned above, belongs to a continuum of matrices that commute with $\mathcal{D}_z$. Note that L is always non-diagonal. For this case (similarly for $\mathcal{D}_x$ and $\mathcal{D}_y$) the ccp condition reduces again to conditions specified in Eq. (18). Using the same arguments one arrives to a more general conclusion: Eq. (17) provides necessary and sufficient conditions for $L-$*divisibility* of a given Pauli channel, and if it is the case, the principal branch with $K = \mathbb{1}$ has Lindblad form. The set of L-divisible Pauli channels is illustrated in Fig. 6.

In order to decide L-divisibility of general unital channels it remains to analyze the case of complex eigenvalues. The logarithms are parametrized as follows

$$L_{k,K} = wK \log\left(J\right)_k K^{-1} w^{-1}, \tag{20}$$

where J is the *real Jordan form* of the (qubit) channel [3]:

$$J = \mathrm{diag}\left(1, c\right) \oplus \begin{pmatrix} a & -b \\ b & a \end{pmatrix} \tag{21}$$

with $a \pm ib$ being the complex eigenvalues and $c > 0$. Let us note that $K \log\left(J\right)_k K^{-1}$ is reduced to equations (16) and (19) in the case of real eigenvalues. In general, the generator is (up to diagonalization):

$$K \log\left(J\right)_k K^{-1} = K \mathrm{diag}\left(0, \log(c)\right) \oplus \begin{pmatrix} \log(|z|) & \arg(z) + 2\pi k \\ -\arg(z) - 2\pi k & \log(|z|) \end{pmatrix} K^{-1}.$$

with $z = a + ib$. The non-diagonal block of the logarithm has the same structure as the real Jordan form of the channel, so K also commutes with $\log(J)_k$, leading to a countable parametric space of hermitian preserving generators. In fact, generators of diagonalizable channels have continuous parametrizations if and only if they have degenerate eigenvalues; the non-diagonalizable case can be found elsewhere [3]. Since we are dealing with a diagonalization, the ccp condition can be very complicated and depends in general on k, see Eq. (1). But for the complex case we can simplify the condition for qubit channels which have exactly the form presented in Eq. (21), say $\hat{\mathcal{E}}_{\mathrm{complex}}$, i.e. $w = \mathbb{1}$. In such case the ccp condition is reduced to

$$a^2 + b^2 \leq c \leq 1. \tag{22}$$

Note that it does not depend on k and the second inequality is always fulfilled for CPTP channels.

We can present the conditions for L-divisibility for the case of complex eigenvalues. The orthogonal normal form of $\hat{\mathcal{E}}_{\mathrm{complex}}$ is $\hat{\mathcal{D}} = \mathrm{diag}\left(1, \eta, \lambda, \lambda\right)$ with $\eta = c$ and $\lambda = \mathrm{sign}(ab)\sqrt{a^2 + b^2}$. The ccp condition for degenerated eigenvalues, see Eq. (18), is reduced to Eq. (22) for this case. Therefore, the L-divisible channels with form $\hat{\mathcal{E}}_{\mathrm{complex}}$ are also L-divisible, up to unitaries. This also applies for channels arising from changing positions of the 1×1 block containing c and the 2×2 block containing a and b in $\hat{\mathcal{E}}_{\mathrm{complex}}$, with orthogonal normal forms $\mathrm{diag}\left(1, \lambda, \eta, \lambda\right)$ and $\mathrm{diag}\left(1, \lambda, \lambda, \eta\right)$. The set containing them is shown in Fig. 4.

3.3.4 Divisibility relations

Consider a Pauli channel with $0 < \lambda_{\min} = \lambda_1 \leq \lambda_2 \leq \lambda_3 < 1$, thus, the condition $\lambda_1\lambda_2 \leq \lambda_3$ trivially holds. Since $\lambda_1\lambda_2 \leq \lambda_1\lambda_3 \leq \lambda_2\lambda_3 \leq \lambda_2$, it

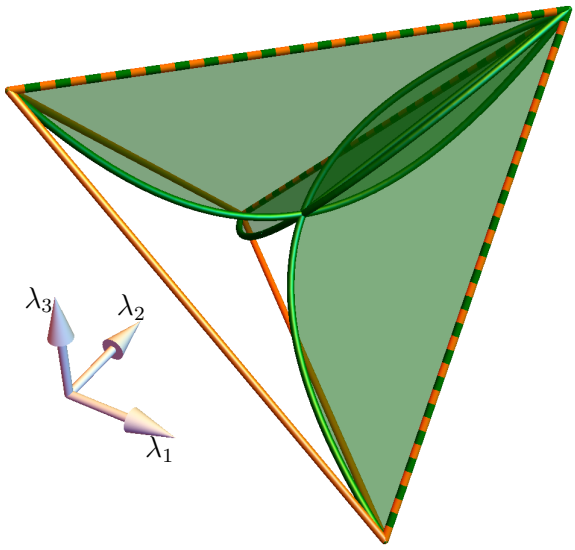

Figure 4: Tetrahedron of Pauli channels, with qubit unital L-divisible channels of the form $\hat{\mathcal{E}}_{\text{complex}}$ (see main text). Note that the set does not have the symmetries of the tetrahedron.

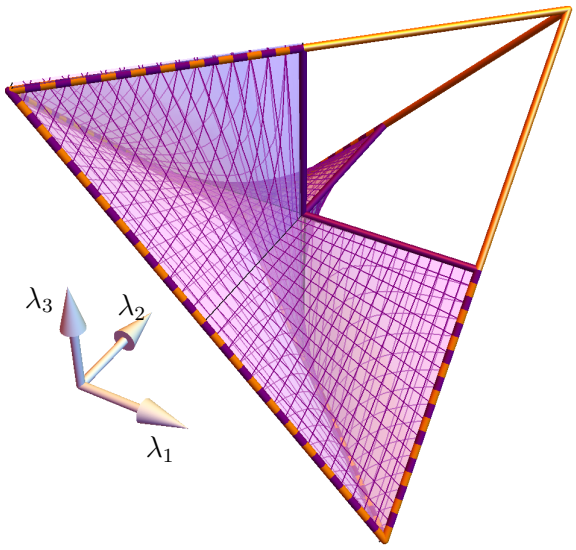

Figure 5: Tetrahedron of Pauli channels with part of the set of CP-divisible, see Eq. (15), but not L-divisible channels ($\mathsf{C}^{\mathrm{CP}}\backslash\mathsf{C}^{\mathrm{L}}$) shown in purple. The whole set C^{CP} is obtained applying the symmetry transformations of the tetrahedron to the purple volume.

follows that $\lambda_1\lambda_3 \leq \lambda_2$, thus, two (out of three) L-divisibility conditions hold always for Pauli channels with positive eigenvalues. Moreover, one may observe that CP-divisibility condition Eq. (15) reduces to one of L-divisibility conditions $\lambda_2\lambda_3 \leq \lambda_1$. In conclusion, the conditions of CP-divisibility and L-divisibility for Pauli channels with positive eigenvalues coincide, thus, in this case C^{CP} implies C^{L}.

Concatenating (positive-eigenvalues) Pauli channels with $\mathcal{D}_{x,y,z}$ one can generate the whole set of C^{CP} Pauli channels. Using the identity $\mathsf{C}^{\mathrm{CP}} = \mathsf{C}^{\mathrm{Inf}}$ and considering Eq. (11)we can formulate the following theorem:

Theorem 4 (Infinitesimal divisible unital channels)**.** *Let $\mathcal{E}^{CP}_{unital}$ be an arbitrary infinitesimal divisible unital qubit channel. There exists at least one L-divisible Pauli channel $\tilde{\mathcal{E}}$, and two unitary conjugations $\mathcal{U}_1$ and $\mathcal{U}_2$, such that*

$$\mathcal{E}^{CP}_{unital} = \mathcal{U}_1\tilde{\mathcal{E}}\mathcal{U}_2\,.$$

Notice that if $\mathcal{E}^{CP}_{unital}$ is invertible, $\tilde{\mathcal{E}} = e^L$.

Let us continue with another equivalence relation holding for Pauli channels. Regarding infinitely divisibility channels, we know that, in general, $\mathsf{C}^{\mathrm{L}} \subset \mathsf{C}^{\infty}$, however, for Pauli channels the corresponding subsets coincide.

Theorem 5 (Infinitely divisible Pauli channels)**.** *The set of L-divisible Pauli channels is equivalent to the set of infinitely divisible Pauli channels.*

Proof. A channel is infinitely divisible if and only if it can be written as $\mathcal{E}_0 e^L$, where $\mathcal{E}_0$ is an idempotent channel satisfying $\mathcal{E}_0 L \mathcal{E}_0 = \mathcal{E}_0 L$ and L has Lindblad form [4]. The only idempotent qubit channels are contractions of the Bloch sphere into single points, diagonalization channels $\mathcal{E}_{\text{diag}}$ transforming Bloch sphere into a line connecting a pair of basis states, and the identity channel. Among the single-point contractions, the only one that is a Pauli channel is the contraction of the Bloch sphere into the complete mixture. In particular, $\mathcal{E} = \mathcal{N}e^L = \mathcal{N}$ for all L. The channel $\mathcal{N}$ belongs to the closure of C^{L}, because a sequence of channels e^{L_n} with $\hat{L}_n = \mathrm{diag}\,(0, -n, -n, -n)$ converges to $\hat{\mathcal{N}}$ in the limit $n \to \infty$. For the case of $\mathcal{E}_0$ being the identity channel we have $\mathcal{E} = e^L$, thus, trivially such infinitely divisible channel $\mathcal{E}$ is in C^{L} too. It remains to analyze the case of diagonalization channels. First, let us note that the matrix of $e^{\hat{L}}$ is necessarily of full rank, since $\det\hat{\mathcal{E}} \neq 0$. It follows that the matrix $\hat{\mathcal{E}} = \hat{\mathcal{E}}_{\text{diag}}e^{\hat{L}}$ has rank two as $\hat{\mathcal{E}}_{\text{diag}}$ is a rank two matrix, thus, it takes one of the following forms $\hat{\mathcal{E}}^{\lambda}_x = \mathrm{diag}\,(1, \lambda, 0, 0)$, $\hat{\mathcal{E}}^{\lambda}_y = \mathrm{diag}\,(1, 0, \lambda, 0)$, $\hat{\mathcal{E}}^{\lambda}_z = \mathrm{diag}\,(1, 0, 0, \lambda)$. The infinitely divisibility implies $\lambda > 0$ in order to keep the roots of λ real. In what follows we will show that $\hat{\mathcal{E}}_z$ belongs to (the closure of) C^{L}. Let us define the channels $\hat{\mathcal{E}}^{\lambda,\epsilon}_z = \mathrm{diag}\,(1, \epsilon, \epsilon, \lambda)$ with $\epsilon > 0$. The complete positivity and ccp conditions translate into the inequalities $\epsilon \leq \frac{1+\lambda}{2}$ and $\epsilon^2 \leq \lambda$, respectively; therefore one can always find an $\epsilon > 0$ such that $\hat{\mathcal{E}}^{\lambda,\epsilon}_z$ is a L-divisible channel. If we choose $\epsilon = \sqrt{\lambda}/n$ with $n \in \mathbb{Z}^+$, the channels $\hat{\mathcal{E}}_{z,n} = \mathrm{diag}\left(1, \sqrt{\lambda}/n, \sqrt{\lambda}/n, \lambda\right)$ form a sequence of L-divisible channels converging to $\hat{\mathcal{E}}^{\lambda}_z$ when $n \to \infty$. The analogous reasoning implies that $\hat{\mathcal{E}}^{\lambda}_x, \hat{\mathcal{E}}^{\lambda}_y \in \mathsf{C}^{\mathrm{L}}$ too. Let us note that one parame-

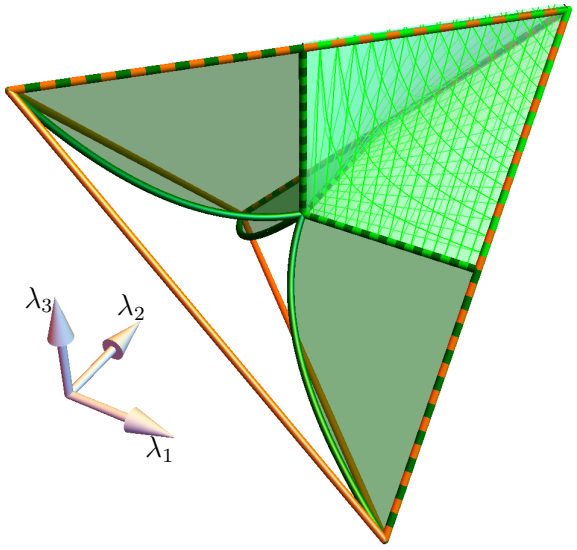

Figure 6: Tetrahedron of Pauli channels with the set of L-divisible channels (or equivalently infinitely divisible, see Theorem 5) shown in green, see equations (17) and (18). The solid set corresponds to channels with positive eigenvalues, and the 2D sets correspond to the negative eigenvalue case. The point where the four sets meet corresponds to the *total depolarizing* channel. Notice that this set *does not* have the symmetries of the tetrahedron.

ter family $\mathcal{E}_z$ are convex combinations of the complete diagonalization channel $\hat{\mathcal{E}}_z^1 = \mathrm{diag}\,(1,0,0,1)$ and the complete mixture contraction $\hat{\mathcal{N}}$. This completes the proof. □

Finally, let us remark that using theorem 23 of Ref. [25] we conclude that the intersection $\mathsf{C}^{\mathrm{P}} \cap \overline{\mathsf{C}^{\mathrm{div}}}$ depicted in Fig. 1 is not empty. To show this, notice that applying the mentioned theorem to Pauli channels we get that the faces of the tetrahedron are indivisible in CPTP channels. However, there are channels with positive determinant inside the faces, for example $\mathrm{diag}\left(1, \frac{4}{5}, \frac{4}{5}, \frac{3}{5}\right)$. Therefore we conclude that up to unitaries, $\mathsf{C}^{\mathrm{P}} \cap \overline{\mathsf{C}^{\mathrm{div}}}$ correspond to the union of the four faces faces of the tetrahedron minus the faces of the octahedron that intersects with the faces of the tetrahedron, see Fig. 3. We have to remove such intersection since it corresponds to channels with negative determinant, i.e. not in C^{P}.

To get a detailed picture of the position and inclusions of the divisibility sets, we illustrate in Fig. 7 two slices of the tetrahedron where different types of divisibility are visualized. Notice the non-convexity of the considered divisibility sets.

3.4 Non-unital qubit channels

Similar to unital channels, using theorem 1 we are able to characterize $\mathsf{C}^{\mathrm{div}}$, C^{P} and C^{CP} by studying special orthogonal normal forms of non-unital channels. They are characterized by $\vec{\lambda}$ and $\vec{\tau}$, see Eq. (5). Thus we can study if a channel is $\mathsf{C}^{\mathrm{div}}$ by computing the rank of its Choi matrix. For this case algebraic equations are in general fourth order polynomials. In fact, in Ref. [19] a condition in terms of the eigenvalues and $\vec{\tau}$ is given. For special cases, however, we can obtain compact expressions, see Fig. 8. The characterization of C^{P} is given by Eq. (8) (note that it only depends on $\vec{\lambda}$), and C^{CP} is tested, for full Kraus rank non-unital channels, using Eq. (9), see Ref. [24] for the calculation of the s_i's. For the characterization of C^{L} we use the results developed at the end of the last section, see Eqs. (18)-(22).

We can plot illustrative pictures even though the whole space of qubit channels has 12 parameters. This can be done using orthogonal normal forms and fixing $\vec{\tau}$, exactly in the same way as the unital case. Recall that unitaries only modify C^{L}, leaving the shape of other sets unchanged. CPTP channels are represented as a volume inside the tetrahedron presented in Fig. 2, see Fig. 8. In the later figure we show a slice corresponding to $\vec{\tau} = (1/2, 0, 0)^{\mathrm{T}}$. Indeed, it has the same structure of the slices for the unital case, but deformed, see Fig. 7. A difference with respect to the unital case is that L-divisible channels with negative eigenvalues (up to unitaries) are not completely inside CP-divisible channels. A part of them are inside the C^{P} channels.

A central feature of Figs. 7 and 8 is that the set $\mathsf{C}^{\mathrm{div}} \setminus \mathsf{C}^{\mathrm{P}}$ is inside the convex slice of the set of entanglement breaking channels (deformed octahedron). Indeed, we can proof the following theorem.

Theorem 6 (Entanglement-breaking channels and divisibility)**.** *Consider a qubit channel $\mathcal{E}$. If $\det \hat{\mathcal{E}} < 0$, then $\mathcal{E}$ is entanglement-breaking, i.e. all qubit channels outside C^{P} are entanglement breaking.*

Proof. Consider the Choi-Jamiołkowski state of a channel $\mathcal{E}$ written in the factorized Pauli operator basis [24] $\tau_{\mathcal{E}} = \frac{1}{4}\sum_{jk}^{3} R_{jk}\sigma_j \otimes \sigma_k$ and let $\hat{\mathcal{E}}$ be its representation in the Pauli operator basis. Then the matrix identity $R = \hat{\mathcal{E}}\Phi_{\mathrm{T}}$ with $\Phi_{\mathrm{T}} = \mathrm{diag}\,(1,1,-1,1)$ holds. Since $\det \hat{\mathcal{E}} < 0$ it follows that $\det R = -\det \hat{\mathcal{E}} > 0$. Using the aforementioned Lorentz normal decomposition $R = L_1^{\mathrm{T}} \tilde{R} L_2$ with $\det L_{1,2} > 0$ and $\tilde{R}$ diagonal, see Ref. [24]. The transformations $L_{1,2}$ correspond to one-way *stochastic local operations and classical communications* (SLOCC) of $\tau_{\mathcal{E}}$, thus, $\tilde{R}$ is an unnormalized two-qubit state with $\det \tilde{R} > 0$. The channel corresponding to $\tilde{R}$ (in the Pauli basis) is $\hat{\mathcal{G}} = \tilde{R}\Phi_{\mathrm{T}}/\tilde{R}_{00}$. Since the latter is diagonal, then $\mathcal{G}$ is a Pauli channel with $\det \hat{\mathcal{G}} < 0$. A Pauli channel has a negative determinant, if either all λ_j are negative, or exactly one of them is negative. In Ref. [28] it has been shown that the set of channels with $\lambda_j < 0 \ \ \forall j$ are entanglement breaking channels. Now, using the symmetries of the tetrahedron, one can generate all channels with negative determinant by concatenating this set with the Pauli rotations. Therefore every Pauli channel with

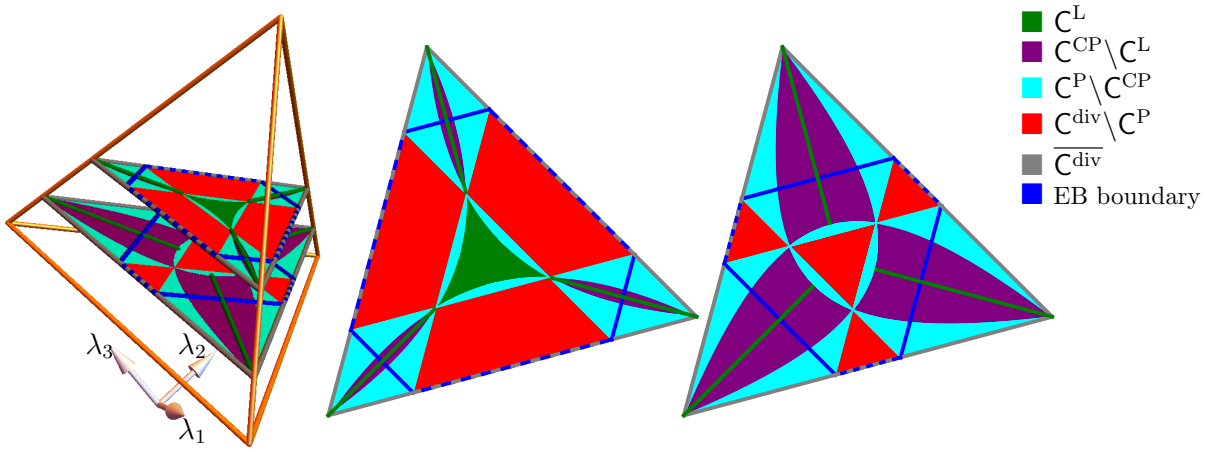

Figure 7: We show two slices of the unitary tetrahedron (figure in the left) determined by $\sum_i \lambda_i = 0.4$ (shown in the center) and $\sum_i \lambda_i = -0.4$ (shown in the right). The non-convexity of the divisibility sets can be seen, including the set of indivisible channels. The convexity of sets C and entanglement breaking channels can also be noticed in the slices. A central feature is that the set $\mathsf{C}^{\mathrm{div}} \setminus \mathsf{C}^{\mathrm{P}}$ is always inside the octahedron of entanglement breaking channels.

negative determinant is entanglement breaking, thus, $\tau_{\mathcal{G}}$ is separable and given that SLOCC operations can not create entanglement [11], we have that $\tau_{\mathcal{E}}$ is separable, too. This implies that if $\det \hat{\mathcal{E}} < 0$, then the qubit channel $\mathcal{E}$ is entanglement-breaking. □

4 Divisibility transitions and examples with dynamical process

The aim of this section is to use illustrative examples of quantum dynamical processes to show transitions between divisibility types of the instantaneous channels. From the slices shown above (see figures 7 and 8) it can be noticed that every transition between the studied divisibility types is permitted. This is due to the existence of common borders between all combinations of divisibility sets; we can think of any continuous line inside the tetrahedron [6] as describing some quantum dynamical map.

We analyze two examples, the first is an implementation of the approximate NOT gate, $\mathcal{A}_{\mathrm{NOT}}$ throughout a specific collision model [21]. The second is the well known setting of a two-level atom interacting with a quantized mode of an optical cavity [9]. We define a simple function that assigns a particular value to a channel $\mathcal{E}_t$ according to divisibility hierarchy, i.e.

$$\delta[\mathcal{E}] = \begin{cases} 1 & \text{if } \mathcal{E} \in \mathsf{C}^{\mathrm{L}}, \\ 2/3 & \text{if } \mathcal{E} \in \mathsf{C}^{\mathrm{CP}} \setminus \mathsf{C}^{\mathrm{L}}, \\ 1/3 & \text{if } \mathcal{E} \in \mathsf{C}^{\mathrm{P}} \setminus \mathsf{C}^{\mathrm{CP}}, \\ 0 & \text{if } \mathcal{E} \in \mathsf{C} \setminus \mathsf{C}^{\mathrm{P}}. \end{cases} \tag{23}$$

A similar function can be defined to study the transition to/from the set of entanglement-breaking chan-

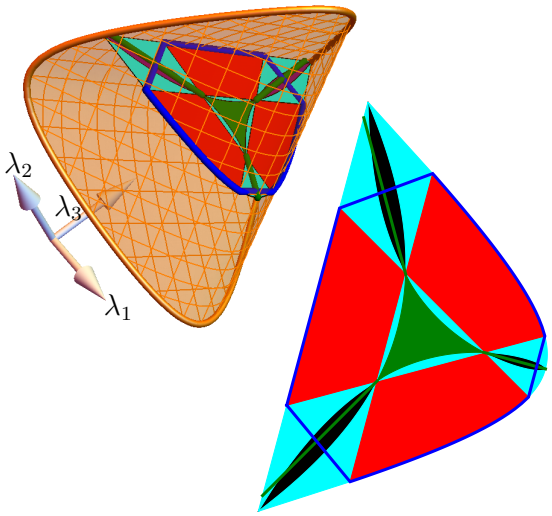

Figure 8: (left) Set of non-unital unital channels up to unitaries, defined by $\vec{\tau} = (1/2, 0, 0)$, see Eq. (5). This set lies inside the tetrahedron. For this particular case the CP conditions reduce to the two inequalities $2 \pm 2\lambda_1 \geq \sqrt{1 + 4(\lambda_2 \pm \lambda_3)^2}$. A cut corresponding to $\sum_i \lambda_i = 0.3$ is presented inside and in the right, see Fig. 7 for the color coding. The structure of divisibility sets presented here has basically the same structure as for the unital case except for C^{L}. A part of the channels with negative eigenvalues belonging to C^{L} lies outside $\mathsf{C}^{\mathrm{CP}} \setminus \mathsf{C}^{\mathrm{L}}$, see green lines. As for the unital case a central feature is that the channels in $\mathsf{C}^{\mathrm{div}} \setminus \mathsf{C}^{\mathrm{P}}$ are entanglement breaking channels. Channels in the boundary are not characterized due to the restricted character of Theorem 2.

nels, i.e.

$$\chi[\mathcal{E}] = \begin{cases} 1 & \text{if } \mathcal{E} \text{ is entanglement breaking}, \\ 0 & \text{if } \mathcal{E} \text{ if not.} \end{cases} \quad (24)$$

The quantum NOT gate is defined as NOT : $\rho \mapsto \mathbb{1} - \rho$, i.e. it maps pure qubit states to its orthogonal state. Although this map transforms the Bloch sphere into itself it is not a CPTP map, and the closest CPTP map is $\mathcal{A}_{\text{NOT}} : \rho \mapsto (\mathbb{1} - \rho)/3$. This is a rank-three qubit unital channel, thus, it is indivisible [25]. Moreover, $\det \mathcal{A}_{\text{NOT}} = -1/27$ implies that this channel is not achievable by a P-divisible dynamical map. It is worth noting that $\mathcal{A}_{\text{NOT}}$ belongs to $\overline{\mathsf{C}^{\text{div}}}$.

A specific collision model was designed in Ref. [21] simulating stroboscopically a quantum dynamical map that implements the quantum NOT gate $\mathcal{A}_{\text{NOT}}$ in finite time. The model reads

$$\mathcal{E}_t(\varrho) = \cos^2(t)\varrho + \sin^2(t)\mathcal{A}_{\text{NOT}}(\varrho) + \frac{1}{2}\sin(2t)\mathcal{F}(\varrho)\,, \quad (25)$$

where $\mathcal{F}(\varrho) = i\frac{1}{3}\sum_j [\sigma_j, \varrho]$. This quantum dynamical map achieves the desired gate $\mathcal{A}_{\text{NOT}}$ at $t = \pi/2$.

Let us stress that this dynamical map is unital, i.e. $\mathcal{E}_t(\mathbb{1}) = \mathbb{1}$ for all t, thus, its orthogonal normal form can be illustrated inside the tetrahedron of Pauli channels, see Fig. 9. In Fig. 10 we plot $\delta[\mathcal{E}_t]$, $\chi[\mathcal{E}_t]$ and the value of the $\det \mathcal{E}_t$. We see the transitions $\mathsf{C}^{\text{L}} \to \mathsf{C}^{\text{P}} \setminus \mathsf{C}^{\text{CP}} \to \mathsf{C}^{\text{div}} \setminus \mathsf{C}^{\text{P}} \to \overline{\mathsf{C}^{\text{div}}}$ and back. Notice that in both plots the trajectory never goes through the $\mathsf{C}^{\text{CP}} \setminus \mathsf{C}^{\text{L}}$ region. This means that when the parametrized channels up to rotations belong to C^{L}, so do the original ones. The transition between P-divisible and divisible channels, i.e. $\mathsf{C}^{\text{P}} \setminus \mathsf{C}^{\text{CP}}$ and $\mathsf{C}^{\text{div}} \setminus \mathsf{C}^{\text{P}}$, occurs at the discontinuity in the yellow curve in Fig. 9. Let us note that this discontinuity only occurs in the space of $\vec{\lambda}$; it is a consequence of the orthogonal normal decomposition, see Eq. (5). The complete channel is continuous in the full convex space of qubit CPTP maps. The transition from $\mathsf{C}^{\text{P}} \setminus \mathsf{C}^{\text{div}}$ and back occurs at times $\pi/3$ and $2\pi/3$. It can also be noted that the transition to entanglement breaking channels occurs shortly before the channel enters in the $\mathsf{C}^{\text{div}} \setminus \mathsf{C}^{\text{P}}$ region; likewise, the channel stops being entanglement breaking shortly after it leaves the $\mathsf{C}^{\text{div}} \setminus \mathsf{C}^{\text{P}}$ region.

Consider now the dynamical map induced by a two-level atom interacting with a mode of a boson field. This model serves as a workhorse to explore a great variety of phenomena in quantum optics [8]. Using the well known *rotating wave approximation* one arrives to the Jaynes-Cummings model [12], whose Hamiltonian is

$$H = \frac{\omega_a}{2}\sigma_z + \omega_f\left(a^\dagger a + \frac{1}{2}\right) + g\left(\sigma_- a^\dagger + \sigma_+ a\right). \quad (26)$$

By initializing the environment in a coherent state $|\alpha\rangle$, one gets the familiar *collapse and revival* setting. Considering a particular set of parameters shown

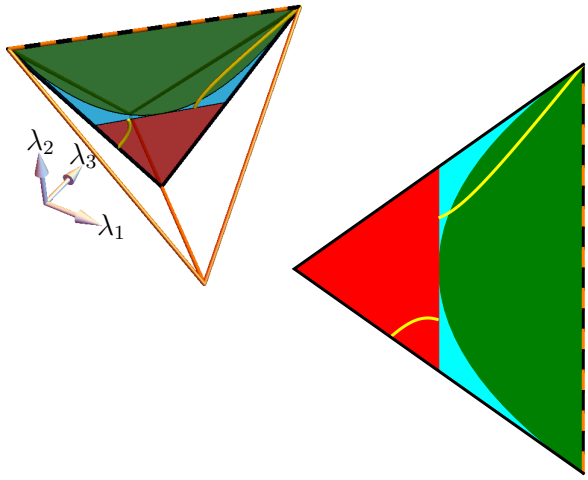

Figure 9: (top left) Tetrahedron of Pauli channels with the trajectory, up to rotations, of the quantum dynamical map Eq. (25) leading to the $\mathcal{A}_{\text{NOT}}$ gate, as a yellow curve. (right) Cut along the plane that contains the trajectory; there one can see the different regions where the channel passes. For this case, the characterization of the C^{L} of the channels induced gives the same conclusions as for the corresponding Pauli channel, see Eq. (5). The discontinuity in the trajectory is due to the reduced representation of the dynamical map, see Eq. (25); the trajectory is continuous in the space of channels. See Fig. 7 for the color coding.

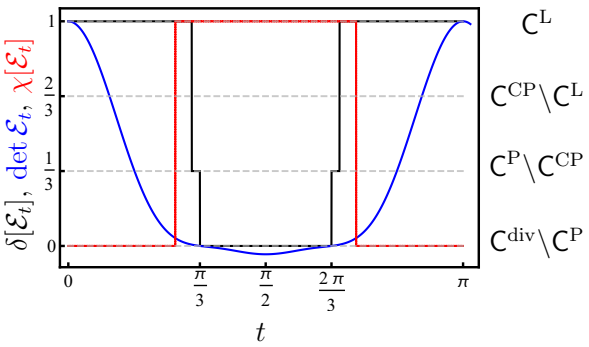

Figure 10: Evolution of divisibility, determinant, and entanglement breaking properties of the map induced by Eq. (25), see Eq. (23) and Eq. (24). Notice that the channel $\mathcal{A}_{\text{NOT}}$, implemented at $t = \pi/2$, has minimum determinant. The horizontal gray dashed lines show the image of the function δ, with the divisibility types in the right side. It can be seen that the dynamical map explores the divisibility sets as $\mathsf{C}^{\text{L}} \to \mathsf{C}^{\text{P}} \setminus \mathsf{C}^{\text{CP}} \to \mathsf{C}^{\text{div}} \setminus \mathsf{C}^{\text{P}} \to \overline{\mathsf{C}^{\text{div}}}$ and back. The channels are entanglement breaking in the expected region.

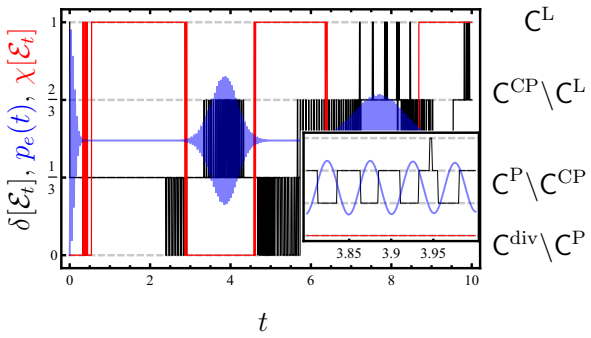

Figure 11: Black and red curves show functions δ and χ of the channels induced by the Jaynes-Cummings model over a two-level system, see Eq. (26) with the environment initialized in a coherent state $|\alpha\rangle$. The blue curve shows the probability of finding the two-level atom in its excited state, $p_e(t)$. The figure shows that the fast oscillations in δ occur roughly at the same frequency as the ones of $p_e(t)$, see the inset. Notice that there are fast transitions between $\mathsf{C}^{\mathrm{P}} \setminus \mathsf{C}^{\mathrm{CP}}$ and $\mathsf{C}^{\mathrm{CP}} \setminus \mathsf{C}^{\mathrm{L}}$ occurring in the region of revivals, with a few transitions between $\mathsf{C}^{\mathrm{CP}} \setminus \mathsf{C}^{\mathrm{P}}$ and C^{L} in the second revival. The function χ shows that during revivals channels are not entanglement breaking, but we find that channels belonging to $\mathsf{C}^{\mathrm{div}} \setminus \mathsf{C}^{\mathrm{P}}$ are always entanglement breaking, in agreement with theorem 6. The particular chosen set of parameters are $\alpha = 6$, $g = 10$, $\omega_a = 5$, and $\omega_f = 20$.

in Fig. 11, we constructed the channels parametrized by time numerically, and studied their divisibility and entanglement-breaking properties. In the same figure we plot functions $\delta[\mathcal{E}_t]$ and $\chi[\mathcal{E}_t]$, together with the probability of finding the atom in its excited state $p_e(t)$, to study and compare the divisibility properties with the features of the collapses and revivals. The probability $p_e(t)$ is calculated choosing the ground state of the free Hamiltonian $\omega_a/2\sigma_z$ of the qubit, and it is given by [13]:

$$p_e(t) = \frac{\langle \sigma_z(t) \rangle + 1}{2}, \tag{27}$$

where

$$\langle \sigma_z(t) \rangle = -\sum_{n=0}^{\infty} P_n \left(\frac{\Delta^2}{4\Omega_n^2} + \left(1 - \frac{\Delta^2}{4\Omega_n^2}\right) \cos\left(2\Omega_n t\right) \right),$$

with $P_n = e^{-|\alpha|^2}|\alpha|^{2n}/n!$, $\Omega_n = \sqrt{\Delta^2/4 + g^2 n}$ and $\Delta = \omega_f - \omega_a$ the detuning.

The divisibility indicator function δ exhibits an oscillating behavior, roughly at the same frequency of $p_e(t)$, see inset in Fig. 11. The figure shows fast periodic transitions between $\mathsf{C}^{\mathrm{P}} \setminus \mathsf{C}^{\mathrm{CP}}$ and $\mathsf{C}^{\mathrm{CP}} \setminus \mathsf{C}^{\mathrm{L}}$ occurring in the region of revivals. There are also few transitions among $\mathsf{C}^{\mathrm{CP}} \setminus \mathsf{C}^{\mathrm{P}}$ and C^{L} in the second revival. Respect to the entanglement breaking and the function χ, there are no fast transitions in the former, and during revivals, channels are not entanglement breaking. We also observe that channels belonging to $\mathsf{C}^{\mathrm{div}} \setminus \mathsf{C}^{\mathrm{P}}$ are entanglement breaking, supporting theorem 6 for the non-unital case.

5 Conclusions

We studied the relations between different types of divisibility of time-discrete and time-continuous quantum processes, i.e. channels and dynamical maps, respectively. In particular, we investigated classes of channels by means of their achievability by dynamical maps of different divisibility types, and also the divisibility of channels occurring during the time evolutions. Apart from investigating the relations between these concepts in general, we provided a detailed analysis for the case of qubit channels.

We implemented the known conditions to decide C^{L} for the general diagonalizable case, and a discussion of the parametric space of Lindblad generators was given (clarifying one of the results of the paper [26]). For unital qubit channels it was shown that every infinitesimal divisible map can be written as a concatenation of one C^{L} channel and two unitary conjugations. For the particular case of Pauli channels case, we have shown that the sets of infinitely divisible and L-divisible channels coincide. We made an interesting observation, connecting the concept of divisibility with the quantum information paradigm of entanglement-breaking channels. We found that divisible but not infinitesimal divisible qubit channels, in PTP maps, are necessarily entanglement-breaking. We also noted that the intersection of indivisible and P-divisible channels is not empty. This allows us to implement indivisible channels with infinitesimal PTP maps. Finally, we questioned the existence of dynamical transitions between different classes of divisibility channels. We argued that all the transitions are, in principle, possible, and exploited two simple models of dynamical maps to demonstrate these transitions. They clearly illustrate how the channels evolutions change from being implementable by markovian dynamical maps to non-markovian, and vice versa.

There are several directions how to proceed further in investigation of divisibility of channels and dynamical maps. Apart from extension of this analysis to larger-dimensional systems, a plethora of interesting questions are related to design of efficient verification procedures of the divisibility classes for channels and dynamical maps. In this paper we question the divisibility features of snapshots of the evolution, however, it might be of interest to understand when the time intervals of dynamical maps implemented by non-markovian evolutions, can be simulated by markovian dynamical maps. Also the area of channel divisibility contains several open structural questions, e.g. the existence of at most n-divisible channels.

Acknowledgements

We acknowledge Thomas Gorin and Tomáš Rybár for useful discussions, as well PAEP and RedTC for financial support. Support by projects CONACyT 285754,

UNAM-PAPIIT IG100518, IN-107414, APVV-14-0878 (QETWORK) is acknowledged. CP acknowledges support by PASPA program from DGAPA-UNAM. MZ acknowledges the support of VEGA 2/0173/17 (MAXAP) and GAČR project no. GA16-22211S.

A On Lorentz normal forms of Choi-Jamiolkowski state

In this appendix we compute the Lorentz normal decomposition of a channel for which one gets $b \neq 0$, supporting our observation that Lorentz normal decomposition does not take Choi-Jamiołkowski states to something proportional to a Choi-Jamiołkowski state. Consider the following Kraus rank three channel and its $R_{\mathcal{E}}$ matrix, both written in the Pauli basis:

$$\hat{\mathcal{E}} = \begin{pmatrix} 1 & 0 & 0 & 0 \\ 0 & -\frac{1}{3} & 0 & 0 \\ 0 & 0 & -\frac{1}{3} & 0 \\ \frac{2}{3} & 0 & 0 & \frac{1}{3} \end{pmatrix}, \tag{28}$$

and

$$R_{\mathcal{E}} = \begin{pmatrix} 1 & 0 & 0 & 0 \\ 0 & -\frac{1}{3} & 0 & 0 \\ 0 & 0 & \frac{1}{3} & 0 \\ \frac{2}{3} & 0 & 0 & \frac{1}{3} \end{pmatrix}. \tag{29}$$

Using the algorithm introduced in Ref. [24] to calculate $R_{\mathcal{E}}$'s Lorentz decomposition into orthochronous proper Lorentz transformations we obtain

$$L_1 = \frac{1}{\gamma_1} \begin{pmatrix} 4 & 0 & 0 & 1 \\ 0 & -\gamma_1 & 0 & 0 \\ 0 & 0 & -\gamma_1 & 0 \\ 1 & 0 & 0 & 4 \end{pmatrix}, \tag{30}$$

$$L_2 = \frac{1}{\gamma_2} \begin{pmatrix} 89+9\sqrt{97} & 0 & 0 & -8 \\ 0 & -\gamma_2 & 0 & 0 \\ 0 & 0 & -\gamma_2 & 0 \\ -8 & 0 & 0 & 89+9\sqrt{97} \end{pmatrix},$$

and

$$\Sigma_{\mathcal{E}} = \frac{1}{\gamma_3} \begin{pmatrix} \sqrt{11+\frac{109}{\sqrt{97}}} & 0 & 0 & -\frac{\sqrt{97}+1}{\sqrt{89\sqrt{97}+873}} \\ 0 & -\frac{\gamma_3}{3} & 0 & 0 \\ 0 & 0 & \frac{\gamma_3}{3} & 0 \\ \sqrt{1+\frac{49}{\sqrt{97}}} & 0 & 0 & \sqrt{-1+\frac{49}{\sqrt{97}}} \end{pmatrix}$$

with $\gamma_1 = \sqrt{15}$, $\gamma_2 = 3\sqrt{178\sqrt{97}+1746}$, and $\gamma_3 = \sqrt{30}$. Although the central matrix $\Sigma_{\mathcal{E}}$ is not exactly of the form Eq. (6), it is equivalent. To see this notice that the derivation of the theorem 2 in [24] considers only decompositions into proper orthochronous Lorentz transformations. But to obtain the desired form, the authors change signs until they get Eq. (6); this cannot be done without changing Lorentz transformations. If we relax the condition over $L_{1,2}$ of being proper and orthochronous, we can bring $\Sigma_{\mathcal{E}}$ to the desired form by conjugating $\Sigma_{\mathcal{E}}$ with $G = \mathrm{diag}\,(1,1,1,-1)$:

$$G^{-1}\Sigma_{\mathcal{E}}G = \frac{1}{\gamma_3} \begin{pmatrix} \sqrt{11+\frac{109}{\sqrt{97}}} & 0 & 0 & \frac{\sqrt{97}+1}{\sqrt{89\sqrt{97}+873}} \\ 0 & -\frac{\gamma_3}{3} & 0 & 0 \\ 0 & 0 & \frac{\gamma_3}{3} & 0 \\ -\sqrt{1+\frac{49}{\sqrt{97}}} & 0 & 0 & \sqrt{-1+\frac{49}{\sqrt{97}}} \end{pmatrix}.$$

In both cases (taking $\Sigma_{\mathcal{E}}$ or $G^{-1}\Sigma_{\mathcal{E}}G$ as the normal form of $R_{\mathcal{E}}$), the corresponding channel is not proportional to a trace-preserving one since $b \neq 0$, see Eq. (6). This completes the counterexample.

References

[1] Ángel Rivas, Susana F Huelga, and Martin B Plenio. Quantum non-markovianity: characterization, quantification and detection. *Rep. Prog. Phys.*, 77(9):094001, 2014. DOI: 10.1088/0034-4885/77/9/094001.

[2] I. Bengtsson and K. Życzkowski. *Geometry of Quantum States: An Introduction to Quantum Entanglement*. Cambridge University Press, 2017. ISBN 9781107026254. URL https://books.google.com.mx/books?id=sYswDwAAQBAJ.

[3] W. J Culver. On the Existence and Uniqueness of the Real Logarithm of a Matrix. *Proceedings of the American Mathematical Society*, 17 (5):1146–1151, 1966. DOI: 10.1090/S0002-9939-1966-0202740-6.

[4] L. V. Denisov. Infinitely Divisible Markov Mappings in Quantum Probability Theory. *Theory Prob. Appl.*, 33(2):392–395, 1989. DOI: 10.1137/1133064.

[5] D. E. Evans and J. T. Lewis. *Dilations of Irreversible Evolutions in Algebraic Quantum Theory*, volume 24 of *Communications of the Dublin Institute for Advanced Studies: Theoretical physics*. Dublin Institute for Advanced Studies, 1977. URL http://orca.cf.ac.uk/34031/.

[6] S. N. Filippov, J. Piilo, S. Maniscalco, and M. Ziman. Divisibility of quantum dynamical maps and collision models. *Phys. Rev. A*, 96(3):032111, 2017. DOI: 10.1103/PhysRevA.96.032111.

[7] V. Gorini, A. Kossakowski, and E. C. G. Sudarshan. Completely positive dynamical semigroups of N-level systems. *J. Math. Phys.*, 17(5):821, 1976. DOI: 10.1063/1.522979.

[8] A. D. Greentree, J. Koch, and J. Larson. Fifty years of Jaynes–Cummings physics. *J. Phy. B*, 46(22):220201, 2013. DOI: 10.1088/0953-4075/46/22/220201.

[9] S. Haroche and J.-M. Raimond. *Exploring the Quantum: Atoms, Cavities, and Photons*. Oxford University Press, USA, 2006. URL http://www.worldcat.org/isbn/0198509146.

[10] T. Heinosaari and M. Ziman. *The Mathematical Language of Quantum Theory: From Uncertainty to Entanglement*. Cambridge University Press, 2012. DOI: 10.1017/CBO9781139031103.

[11] R. Horodecki, P. Horodecki, M. Horodecki, and K. Horodecki. Quantum entanglement. *Rev. Mod. Phys.*, 81(2):865–942, 2009. DOI: 10.1103/RevModPhys.81.865.

[12] E. T. Jaynes and F. W. Cummings. Comparison of quantum and semiclassical radiation theories with application to the beam maser. *Proc. IEEE*, 51:89, 1963. DOI: 10.1109/PROC.1963.1664.

[13] A. B. Klimov and S. M. Chumakov. *A Group-Theoretical Approach to Quantum Optics: Models of Atom-Field Interactions*. Wiley-VCH, 2009. DOI: 10.1002/9783527624003.

[14] A. Kossakowski. On quantum statistical mechanics of non-hamiltonian systems. *Rep. Math. Phys.*, 3(4):247 – 274, 1972. DOI: 10.1016/0034-4877(72)90010-9.

[15] J. M. Leinaas, J. Myrheim, and E. Ovrum. Geometrical aspects of entanglement. *Phys. Rev. A*, 74:012313, Jul 2006. DOI: 10.1103/PhysRevA.74.012313.

[16] G. Lindblad. On the generators of quantum dynamical semigroups. *Comm. Math. Phys.*, 48(2): 119–130, 1976. DOI: 10.1007/BF01608499.

[17] M. Musz, M. Kuś, and K. Życzkowski. Unitary quantum gates, perfect entanglers, and unistochastic maps. *Phys. Rev. A*, 87:022111, Feb 2013. DOI: 10.1103/PhysRevA.87.022111.

[18] C. Pineda, T. Gorin, D. Davalos, D. A. Wisniacki, and I. García-Mata. Measuring and using non-Markovianity. *Phys. Rev. A*, 93:022117, 2016. DOI: 10.1103/PhysRevA.93.022117.

[19] Ł. Rudnicki, Z. Puchała, and K. Zyczkowski. Gauge invariant information concerning quantum channels. *Quantum*, 2:60, April 2018. ISSN 2521-327X. DOI: 10.22331/q-2018-04-11-60.

[20] M. B. Ruskai, S. Szarek, and E. Werner. An analysis of completely-positive trace-preserving maps on M_2. *Lin. Alg. Appl.*, 347(1):159 – 187, 2002. DOI: 10.1016/S0024-3795(01)00547-X.

[21] T. Rybár, S. N. Filippov, M. Ziman, and V. Bužek. Simulation of indivisible qubit channels in collision models. *J. Phys. B*, 45(15):154006, 2012. DOI: 10.1088/0953-4075/45/15/154006.

[22] B. Vacchini, A. Smirne, E.-M. Laine, J. Piilo, and H.-P. Breuer. Markovianity and non-markovianity in quantum and classical systems. *New J. Phys.*, 13(9):093004, 2011. DOI: 10.1088/1367-2630/13/9/093004.

[23] F. Verstraete and H. Verschelde. On quantum channels. *Unpublished*, 2002. URL http://arxiv.org/abs/quant-ph/0202124.

[24] F. Verstraete, J. Dehaene, and B. DeMoor. Local filtering operations on two qubits. *Phys. Rev. A*, 64(1):010101, 2001. DOI: 10.1103/PhysRevA.64.010101.

[25] M. M. Wolf and J. I. Cirac. Dividing quantum channels. *Comm. Math. Phys.*, 279(1):147–168, 2008. DOI: 10.1007/s00220-008-0411-y.

[26] M. M. Wolf, J. Eisert, T. S. Cubitt, and J. I. Cirac. Assessing non-Markovian quantum dynamics. *Phys. Rev. Lett.*, 101(15):150402, 2008. DOI: 10.1103/PhysRevLett.101.150402.

[27] M. Ziman and V. Bužek. All (qubit) decoherences: Complete characterization and physical implementation. *Phys. Rev. A*, 72:022110, Aug 2005. DOI: 10.1103/PhysRevA.72.022110.

[28] M. Ziman and V. Bužek. Concurrence versus purity: Influence of local channels on Bell states of two qubits. *Phys. Rev. A*, 72(5):052325, 2005. DOI: 10.1103/PhysRevA.72.052325.

C.2 Article: Gaussian quantum channels beyond the Gaussian functional form: full characterization of the one-mode case

The following article was sent to Physical Review A. Click to go to arXiv.

Gaussian quantum channels beyond the Gaussian functional form: full characterization of the one-mode case

David Davalos,[1] Camilo Moreno,[2] Juan-Diego Urbina,[2] and Carlos Pineda[1]

[1] *Instituto de Física, Universidad Nacional Autónoma de México, México*[*]

[2] *Institut für Theoretische Physik, Universität Regensburg, D-93040 Regensburg, Germany*

We study one-mode Gaussian quantum channels in continuous-variable systems by performing a *black-box* characterization using complete positivity and trace preserving conditions, and report the existence of two subsets that do not have a functional Gaussian form. Our study covers as particular limit the case of singular channels, thus connecting our results with their known classification scheme based on canonical forms. Our full characterization of Gaussian channels without Gaussian functional form is completed by showing how Gaussian states are transformed under these operations, and by deriving the conditions for the existence of master equations for the non-singular cases.

PACS numbers: 03.65.Yz, 03.65.Ta, 05.45.Mt

I. INTRODUCTION

Within the theory of continuous-variable quantum systems (a central topic of study given their role in the description of physical systems like the electromagnetic field [1], solids and nano-mechanical systems [2] and atomic ensembles [3]) the simplest states, both from a theoretical an experimental point of view, are the so-called Gaussian states. An operation that transforms such family of states into itself is called a Gaussian quantum channel (GQC). Even though Gaussian states and channels form small subsets among general states and channels, they have proven to be useful in a variate of tasks such as quantum communication [4], quantum computation [5] and the study of quantum entanglement in simple [6] and complicated scenarios [7].

Writing Gaussian channels in the *position state representation* is often of theoretical convenience, for instance for the calculation of position correlation functions. Thus an obvious way to proceed is to characterize the possible functional forms of GQC in such representation. First attempts in this direction were given in Ref. [8], but their *ansatz* is limited to only Gaussian functional forms (denoted simply by *Gaussian forms* or GF). Going beyond such restrictive assumption, in the present work we characterize another two possible forms that can arise directly from the definition of Gaussian channel in the one-mode case. We thus give a complete characterization of GQC in position state representation, and study the special case of *singular Gaussian quantum channels* (SGQC), i.e. the operations for which the inverse operation doesn't exist.

The paper is organized as follows. In section II we discuss the definition of GQC and introduce functional forms beyond the GF that emerge from singularities in the coefficients that define a GQC with GF. In section III we give a *black-box* characterization of such channels, using complete positivity and trace preserving conditions. In section IV we study functional forms that lead to SGQC and derive their explicit form. Finally in section V we derive conditions of existence of master equations and their explicit forms. We conclude in section VI.

II. GAUSSIAN QUANTUM CHANNELS

Gaussian states are characterized completely by first (mean) and second (correlations) moments encoded in the *mean vector* $\vec{d}$ and the *covariance matrix* σ. Therefore, a Gaussian state S can be denoted as $S = S\left(\sigma, \vec{d}\right)$, where for the one-mode case we have

$$\sigma = \begin{pmatrix} \langle \hat{q}^2 \rangle - \langle \hat{q} \rangle^2 & \frac{1}{2}\langle \hat{q}\hat{p} + \hat{p}\hat{q} \rangle - \langle \hat{q} \rangle \langle \hat{p} \rangle \\ \frac{1}{2}\langle \hat{q}\hat{p} + \hat{p}\hat{q} \rangle - \langle \hat{q} \rangle \langle \hat{p} \rangle & \langle \hat{p}^2 \rangle - \langle \hat{p} \rangle^2 \end{pmatrix},$$

and

$$\vec{d} = \left(\langle \hat{q} \rangle, \langle \hat{p} \rangle\right)^{\mathrm{T}}$$

with $\hat{q}$ and $\hat{p}$ denoting the standard position and momentum (quadrature) operators [9].

To start with, we recall the following definition [10]:

Definition 1 (Gaussian quantum channels)**.** *A quantum channel is Gaussian (GQC) if and only if it transforms Gaussian states into Gaussian states.*

This definition is strictly equivalent to the statement that any GQC, say $\mathcal{G}$, can be written as

$$\mathcal{G}[\rho] = \mathrm{tr}_{\mathrm{E}}\left[U\left(\rho \otimes \rho_{\mathrm{E}}\right) U^{\dagger}\right] \tag{1}$$

where U is a unitary transformation, acting on a combined global state obtained from enlarging the system with an environment E, that is generated by a quadratic bosonic Hamiltonian (i.e. U is a *Gaussian unitary*) [10]. The environmental initial state ρ_E is a Gaussian state and the trace is taken over the environmental degrees of freedom.

Following definition 1, a GQC is fully characterized by its action over Gaussian states, and this action is in

[*] davidphysdavalos@gmail.com

turn defined by *affine transformations* [10]. Specifically, $\mathcal{G} = \mathcal{G}(\mathbf{T}, \mathbf{N}, \vec{\tau})$ is given by a tuple $(\mathbf{T}, \mathbf{N}, \vec{\tau})$ where $\mathbf{T}$ and $\mathbf{N}$ are 2×2 real matrices with $\mathbf{N} = \mathbf{N}^{\mathrm{T}}$ [10] acting on Gaussian states according to $\mathcal{G}(\mathbf{T}, \mathbf{N}, \vec{\tau})\left[S\left(\sigma, \vec{d}\right)\right] = S\left(\mathbf{T}\sigma\mathbf{T}^{\mathrm{T}} + \mathbf{N}, \mathbf{T}\vec{d} + \vec{\tau}\right)$. In the particular case of closed systems we have $\mathbf{N} = \mathbf{0}$ and $\mathbf{T}$ is a symplectic matrix.

Let us note that although channels with Gaussian form trivially transform Gaussian states into Gaussian states, the definition goes beyond GF. Introducing *difference* and *sum* coordinates, $x = q_2 - q_1$ and $r = (q_1 + q_2)/2$, and $\rho(x, r) = \left\langle r - \frac{x}{2} \middle| \hat{\rho} \middle| r + \frac{x}{2} \right\rangle$, a quantum channel

$$\rho_f(x_f, r_f) = \int_{\mathbb{R}^2} dx_i dr_i J(x_f, x_i; r_f, r_i) \rho_i(r_i, x_i), \quad (2)$$

maps an initial $\hat{\rho}_i$ into a final $\hat{\rho}_f$ state linearly through the kernel $J(x_f, x_i; r_f, r_i)$. In order to see how a channel without GF can be constructed as a limiting case of a quantum channel with GF, consider the general parametrization of the later as given in [12]

$$J_{\mathrm{G}}(x_f, x_i; r_f, r_i) = \frac{b_3}{2\pi} \exp\Big[\imath\Big(b_1 x_f r_f + b_2 x_f r_i + b_3 x_i r_f + b_4 x_i r_i + c_1 x_f + c_2 x_i\Big) - a_1 x_f^2 - a_2 x_f x_i - a_3 x_i^2\Big], \quad (3)$$

where all coefficients are real and no quadratic terms in $r_{i,f}$ are allowed. Now it is easy to see that if the coefficients of the quadratic form in the exponent of J in eq. (3) depend on a parameter ϵ such that for $\epsilon \to 0$ they scale as $a_n \propto \epsilon^{-1}$ and $b_n \propto \epsilon^{-1/2}$, then

$$\lim_{\epsilon \to 0} J_{\mathrm{G}}(x_f, x_i; r_f, r_i) = \mathcal{N}\delta(\alpha x_f - \beta x_i) e^{\Sigma'(x_f, x_i; r_f, r_i)}, \quad (4)$$

where $\alpha, \beta \in \mathbb{R}$ and $\Sigma'(x_f, x_i; r_f, r_i)$ is a quadratic form that now admits quadratic terms in $r_{i,f}$. This is the first example of a δGQC, namely a Gaussian quantum channel that contains Dirac-delta functions in its coordinate representation. This particular example is not only of academic interest. Physically, it can be implemented by means of the ubiquitous quantum Brownian motion model for harmonic systems (damped harmonic oscillator) [13]. In such system δGQC occur at isolated points of time, defined in the limit of the *antisymmetric position autocorrelation function* tending to zero.

Since the form of eq. (4) admits quadratic terms in $r_{i,f}$, it suggest that a form with two deltas can exist and can be defined with an appropriate limit. In order to avoid working with such limits, in this work we provide a *black-box* characterization of general GQCs without Gaussian form. In particular we study channels that can arise when singularities on the coefficients of Gaussian forms GF occur, that lead immediately to singular Gaussian operations. We characterize which forms in δGQC lead to valid quantum channels, and under which conditions singular operations lead to valid *singular quantum channels* (SGQC). We will show that only two possible forms of δGQC hold according to *trace preserving* (TP) and *hermiticity preserving* (HP) conditions. The channel of eq. (4) is one of these forms, as expected. Later on we will impose *complete positivity* in order to have valid GQC, i.e. *complete positive and trace preserving* (CPTP) Gaussian operations, going beyond previous characterizations of GQC [12].

III. COMPLETE POSITIVE AND TRACE-PRESERVING δ–GAUSSIAN OPERATIONS

Let us introduce the ansätze for the possible forms of GQC in the position representation, to perform the black-box characterization. Following eq. (1) and taking the continuous variable representation of difference and sum coordinates, the trace becomes an integral over position variables of the environment. Then we end up with a Fourier transform of a multivariate Gaussian, having for one mode the following structures: a Gaussian form eq. (3), a Gaussian form multiplied with one-dimensional delta or a Gaussian form multiplied by a two-dimensional delta. Thus, in order to start with the black-box characterization, we shall propose the following general Gaussian operations with one and two deltas, respectively

$$J_{\mathrm{I}}(x_f, r_f; x_i, r_i) = \mathcal{N}_{\mathrm{I}}\delta(\vec{\alpha}^{\mathrm{T}}\vec{v}_f + \vec{\beta}^{\mathrm{T}}\vec{v}_i) e^{\Sigma(x_f, x_i; r_f, r_i)}, \quad (5)$$

$$J_{\mathrm{II}}(x_f, r_f; x_i, r_i) = \mathcal{N}_{\mathrm{II}}\delta(\mathbf{A}\vec{v}_f - \mathbf{B}\vec{v}_i) e^{\Sigma(x_f, x_i; r_f, r_i)}, \quad (6)$$

where the exponent reads

$$\Sigma(x_f, x_i; r_f, r_i) = \imath\Big(b_1 x_f r_f + b_2 x_f r_i + b_3 x_i r_f + b_4 x_i r_i + c_1 x_f + c_2 x_i + d_1 r_f + d_2 r_i\Big) - a_1 x_f^2 - a_2 x_f x_i - a_3 x_i^2 - e_1 r_f^2 - e_2 r_f r_i - e_3 r_i^2, \quad (7)$$

$\vec{v}_{i,j} = (r_{i,j}, x_{i,j})$ and $\mathcal{N}_{\mathrm{I,II}}$ are normalization constants. They provide, together with eq. (3) all possible ansätze for GQC. Note that the coefficients in the exponential of every form must be finite, otherwise the functional form can be modified.

Let us study now CPTP conditions, since *complete positivity* implies *positivity* and in turn it implies *hermiticity preserving* (HP). For sum and difference coordinates HP reads

$$J(-x_f, r_f; -x_i, r_i) = J(x_f, r_f; x_i, r_i)^*. \quad (8)$$

Following this equation, it is easy to note that the coefficients a_n, b_n, c_n, e_n must be real with $d_n = 0$, as well the entries of matrices (and vectors) $\mathbf{A}$, $\mathbf{B}$, $\vec{\alpha}$, $\vec{\beta}$. The factor concerning the delta function of eq. (5), is reduced into two possible combinations variables: i) $\delta(\alpha x_f - \beta x_i)$ and ii) $\delta(\alpha r_f - \beta r_i)$. For the case of eq. (6), the prefactor concerning the two-dimensional delta is reduced to iii) $\delta(\gamma r_f - \eta r_i)\delta(\alpha x_f - \beta x_i)$. Let us now analyze the trace preserving condition (TP), which for continuous variable systems reads

$$\int_{\mathbb{R}} dr_f J(x_f = 0, r_f; x_i, r_i) = \delta(x_i). \quad (9)$$

This condition immediately discards ii) from the above combinations of deltas, thus we end up with cases i) and iii). For case i) TP reads

$$\mathcal{N}_{\rm I}\int dr_f\delta(-\beta x_i)e^{\Sigma}=\frac{\mathcal{N}_{\rm I}}{|\beta|}\sqrt{\frac{\pi}{e_1}}\delta(x_i)e^{\frac{e_2^2r_i^2}{4e_1}}e^{-e_3r_i^2}, \quad (10)$$

thus the relation between the coefficients assumes the form

$$\frac{e_2^2}{4e_1}-e_3=0, \quad (11)$$

and the normalization constant $\mathcal{N}_{\rm I}=|\beta|\sqrt{\frac{e_1}{\pi}}$ with $\beta\neq 0$ and $e_1>0$. For case iii) the trace-preserving condition reads

$$\mathcal{N}_{\rm II}\int dr_f\delta(\gamma r_f-\eta r_i)\delta(-\beta x_i)e^{\Sigma} = \frac{\mathcal{N}_{\rm II}}{|\beta\gamma|}\delta(x_i)e^{-e_1(\frac{\eta}{\gamma})^2r_i^2-e_2\frac{\eta}{\gamma}r_i^2-e_3r_i^2}.$$

Thus the following relation between e_n coefficients must be fulfilled

$$e_1\left(\frac{\eta}{\gamma}\right)^2+e_2\frac{\eta}{\gamma}+e_3=0, \quad (12)$$

with $\gamma,\beta\neq 0$ and $\mathcal{N}_{\rm II}=|\beta\gamma|$. In the particular case of $\eta=0$, eq. (12) is reduced to $e_3=0$. As expected from the analysis of limits above, we showed that δGQC admit quadratic terms in $r_{i,j}$.

Up to this point we have *hermitian and trace preserving Gaussian operations*; to derive the remaining CPTP conditions, it is useful to write Wigner's function and Wigner's characteristic function, which we now derive. The representation of the Wigner's characteristic function reads

$$\chi(\vec{k})=\mathrm{tr}\left[\rho D(\vec{k})\right] = \exp\left[-\frac{1}{2}\vec{k}^{\rm T}\left(\Omega\sigma\Omega^{\rm T}\right)\vec{k}-\imath\left(\Omega\langle\hat{x}\rangle\right)^{\rm T}\vec{k}\right] \quad (13)$$

and its relation with Wigner's function

$$W(\mathbf{x})=\int_{\mathbb{R}^2}d\vec{x}e^{-\imath\vec{x}^{\rm T}\Omega\vec{k}}\chi\left(\vec{k}\right) \quad (14)$$

$$=\int_{\mathbb{R}}e^{\imath px}dx\left\langle r-\frac{x}{2}\right|\hat{\rho}\left|r+\frac{x}{2}\right\rangle. \quad (15)$$

where $\vec{k}=(k_1,k_2)^{\rm T}$, $\vec{x}=(r,p)^{\rm T}$ and $\hbar=1$ (we are using natural units). Using the previous equations to construct Wigner and Wigner's characteristic functions of the initial and final states, and substituting them in eq. (2), it is straightforward to get the propagator in the Wigner's characteristic function representation

$$\tilde{J}\left(\vec{k}_f,\vec{k}_i\right)=\int_{\mathbb{R}^6}d\Gamma K(\vec{l})J(\vec{v}_f,\vec{v}_i), \quad (16)$$

where the transformation kernel reads

$$K(\vec{l})=\frac{1}{(2\pi)^3}e^{\left[\imath\left(k_2^fr_f-k_1^fp_f-k_2^ir_i+k_1^ip_i-p_ix_i+p_fx_f\right)\right]},$$

with

$$d\Gamma=dp_fdp_idx_fdx_idr_fdr_i \text{ and}$$
$$\vec{l}=(p_f,p_i,x_f,x_i,r_f,r_i)^{\rm T}.$$

By elementary integration of eq. (16) one can show that for both cases

$$\tilde{J}_{\rm I,III}\left(\vec{k}_f,\vec{k}_i\right)=\delta\left(k_1^i-\frac{\alpha}{\beta}k_1^f\right)\delta\left(k_2^i-\vec{\phi}_{\rm I,III}^{\rm T}\vec{k}_f\right)e^{P_{\rm I,III}(\vec{k}_f)}, \quad (17)$$

where $P_{\rm I,III}(\vec{k}_f)=\sum_{i,j=1}^2P_{ij}^{\rm (I,III)}k_i^fk_j^f+\sum_{i=1}^2P_{0i}^{\rm (I,III)}k_i^f$ with $P_{ij}^{\rm (I,III)}=P_{ji}^{\rm (I,III)}$. For case i) we obtain

$$P_{11}^{\rm (I)}=-\left(\left(\frac{\alpha}{\beta}\right)^2\left(a_3+\frac{b_3^2}{4e_1}\right)+\frac{\alpha}{\beta}\left(a_2+\frac{1}{2}\frac{b_1b_3}{e_1}\right)+a_1+\frac{b_1^2}{4e_1}\right),$$
$$P_{12}^{\rm (I)}=-\left(\frac{\alpha}{\beta}\frac{b_3}{2e_1}+\frac{b_1}{2e_1}\right),$$
$$P_{22}^{\rm (I)}=-\frac{1}{4e_1}. \quad (18)$$

For case iii) we have

$$P_{11}^{\rm (III)}=-\left(\left(\frac{\alpha}{\beta}\right)^2a_3+\frac{\alpha}{\beta}a_2+a_1\right),$$
$$P_{12}^{\rm (III)}=P_{22}^{\rm (III)}=0, \quad (19)$$

And for both cases we have $P_{01}^{\rm (I,III)}=\imath\left(\frac{\alpha}{\beta}c_2+c_1\right)$ and $P_{02}^{\rm (I,III)}=0$. Vectors $\vec{\phi}$ are given by

$$\vec{\phi}_{\rm I}=\left(\frac{\alpha}{\beta}\left(b_4-\frac{b_3e_2}{2e_1}\right)-\frac{b_1e_2}{2e_1}+b_2,-\frac{e_2}{2e_1}\right)^{\rm T},$$
$$\vec{\phi}_{\rm III}=\left(\frac{\alpha}{\beta}\frac{\eta}{\gamma}b_3+\frac{\alpha}{\beta}b_4+\frac{\eta}{\gamma}b_1+b_2,\frac{\eta}{\gamma}\right)^{\rm T}. \quad (20)$$

We are now in position to write explicitly the conditions for complete positivity. Having a Gaussian operation characterized by $(\mathbf{T},\mathbf{N},\vec{\tau})$, the CP condition can be expressed in terms of the matrix

$$\mathbf{C}=\mathbf{N}+\imath\Omega-\imath\mathbf{T}\Omega\mathbf{T}^{\rm T}, \quad (21)$$

where $\Omega=\begin{pmatrix}0&1\\-1&0\end{pmatrix}$ is the symplectic matrix. An operation $\mathcal{G}(\mathbf{T},\mathbf{N},\vec{\tau})$ is CP if and only if $\mathbf{C}\geq 0$ [10, 14]. Applying the propagator on a test characteristic function, eq. (13), it is easy to compute the corresponding tuples. For both cases we get $(\mathbf{T}_{\rm I,III},\mathbf{N}_{\rm I,III},\vec{\tau}_{\rm I,III})$:

$$\mathbf{N}_{\rm I,III}=2\begin{pmatrix}-P_{22}&P_{12}\\P_{12}&-P_{11}\end{pmatrix},$$
$$\vec{\tau}_{\rm I,III}=\left(0,\imath P_{01}^{\rm (I,III)}\right)^{\rm T}, \quad (22)$$

while for case i) matrix $\mathbf{T}$ is given by

$$\mathbf{T}_{\rm I} = \begin{pmatrix} \frac{e_2}{2e_1} & 0 \\ \vec{\phi}_{\rm I,1} & -\frac{\alpha}{\beta} \end{pmatrix}, \tag{23}$$

where $\vec{\phi}_{\rm I,1}$ denotes the first component of vector $\vec{\phi}_{\rm I}$, see eq. (20). The complete positive condition is given by the inequalities raised from the eigenvalues of matrix eq. (21)

$$\pm\frac{\sqrt{\alpha^2 e_2^2 + 4\alpha\beta e_2 e_1 + 4\beta^2 e_1^2\left(4{P_{12}^{(\rm I)}}^2 + \left(P_{11}^{(\rm I)} - P_{22}^{(\rm I)}\right)^2 + 1\right)}}{2\beta e_1} - \left(P_{11}^{(\rm I)} + P_{22}^{(\rm I)}\right) \geq 0. \tag{24}$$

For case iii) matrix $\mathbf{T}$ is

$$\mathbf{T}_{\rm III} = \begin{pmatrix} -\frac{\eta}{\gamma} & 0 \\ \vec{\phi}_{\rm III,1} & -\frac{\alpha}{\beta} \end{pmatrix}, \tag{25}$$

and complete positivity conditions read

$$\pm\frac{\sqrt{(\beta\gamma - \alpha\eta)^2 + \beta^2\gamma^2 {P_{11}^{(\rm III)}}^2}}{\beta\gamma} - P_{11}^{(\rm III)} \geq 0. \tag{26}$$

Note that in both cases complete positivity conditions do not depend on $\vec{\phi}$.

IV. ALLOWED SINGULAR FORMS

There are two classes of Gaussian singular channels. Since the inverse of a Gaussian channel $\mathcal{G}(\mathbf{T}, \mathbf{N}, \vec{\tau})$ is $\mathcal{G}\left(\mathbf{T}^{-1}, -\mathbf{T}^{-1}\mathbf{N}\mathbf{T}^{-T}, -\mathbf{T}^{-1}\vec{\tau}\right)$, its existence rests on the invertibility of $\mathbf{T}$. Thus studying the rank of the latter we are able to explore singular forms. We are going to use the classification of one-mode channels developed by Holevo [15].

For singular channels there are two classes characterized by its *canonical form* [16], i.e. any channel can be obtained by applying Gaussian unitaries before and after the canonical form. The class called "A_1" correspond to singular channels with $\mathrm{Rank}(\mathbf{T}) = 0$ and coincide with the family of *total depolarizing channels*. The class "A_2" is characterized by $\mathrm{Rank}(\mathbf{T}) = 1$. Both channels are entanglement-breaking [16].

Before analyzing the functional forms constructed in this work, let us study channels with GF. The tuple of the affine transformation, corresponding to the propagator $J_{\rm G}$, eq. (3), were introduced in Ref. [12] up to some typos. Our calculation for this tuple is

$$\begin{aligned}
\mathbf{T}_{\rm G} &= \begin{pmatrix} -\frac{b_4}{b_3} & \frac{1}{b_3} \\ \frac{b_1 b_4}{b_3} - b_2 & -\frac{b_1}{b_3} \end{pmatrix}, \\
\mathbf{N}_{\rm G} &= \begin{pmatrix} \frac{2a_3}{b_3^2} & \frac{a_2}{b_3} - \frac{2a_3 b_1}{b_3^2} \\ \frac{a_2}{b_3} - \frac{2a_3 b_1}{b_3^2} & -2\left(-\frac{a_3 b_1^2}{b_3^2} + \frac{a_2 b_1}{b_3} - a_1\right) \end{pmatrix}, \\
\vec{\tau}_{\rm G} &= \left(-\frac{c_2}{b_3}, \frac{b_1 c_2}{b_3} - c_1\right)^{\rm T}.
\end{aligned} \tag{27}$$

It is straightforward to check that for $b_2 = 0$, $\mathbf{T}_{\rm G}$ is singular with $\mathrm{Rank}(\mathbf{T}_{\rm G}) = 1$, i.e. it belongs to class A_2. Due to the full support of Gaussian functions, it was surprising that Gaussian channels with GF have singular limit. In this case the singular behavior arises from the lack of a Fourier factor for $x_f r_i$. This is the only singular case for GF.

Now we analyze functional forms derived in sec. III. The complete positivity conditions of the form $\tilde{J}_{\rm III}$, presented in eq. (26), have no solution for $\alpha \to 0$ and/or $\gamma \to 0$, thus this form cannot lead to singular channels. This is not the case for $\tilde{J}_{\rm I}$, eq. (17), which leads to singular operations belonging to class A_2 for

$$\alpha e_2 = 0, \tag{28}$$

and to class A_1 for

$$e_2 = \alpha = b_2 = 0. \tag{29}$$

For the latter, the complete positivity conditions read

$$e_1 \leq a_1. \tag{30}$$

By using an initial state characterized by σ_i and $\vec{d}_i$ we can compute the explicit dependence of the final states on the initial parameters. For channels belonging to class A_2 [see eq. (27) with $b_2 = 0$ and eq. (23) with $e_2\alpha = 0$] the final state only depends one combination of the components of σ_i, and in one combination of the components of $\vec{d}_i$, i.e. $\sum_{mn} l_{mn} (\sigma_i)_{mn}$ and $\sum_m n_m \left(\vec{d}_i\right)_m$, respectively, where l_{mn} and n_m depend on the channel parameters. See the appendix for the explicit formulas and fig. 1 for an schematic description of the final states. From such combinations it is obvious that we cannot solve for the initial state parameters given a final state as expected; this is because the parametric space dimension is reduced from 5 to 2. The channel belonging to A_1 [see eq. (23) with $e_2 = \alpha = b_2 = 0$ and eq. (30)] maps every initial state to a single one characterized by $\sigma_f = \mathbf{N}$ and $\vec{d}_f = (0, -c_1)^{\rm T}$, see fig. 2 for a schematic description.

According to our ansätze [see equations (5) and 6)], we conclude that one-mode SGQC can only have the functional forms given in eq. (3) and eq. (5). This is the central result our work and can be stated as:

Theorem 1 (One-mode singular Gaussian channels)**.** *A one-mode Gaussian quantum channel is singular if and only if it has one of the following functional forms in the position space representation*

1. $\frac{b_3}{2\pi}\exp\Big[\imath\Big(b_1 x_f r_f + b_3 x_i r_f + b_4 x_i r_i + c_1 x_f + c_2 x_i\Big) - a_1 x_f^2 - a_2 x_f x_i - a_3 x_i^2\Big]$,
2. $|\beta|\sqrt{e_1/\pi}\,\delta(\alpha x_f - \beta x_i) \times \exp\Big[-a_2 x_f x_i - a_1 x_f^2 - a_3 x_i^2 + \imath\Big(b_2 x_f r_i + b_3 r_f x_i + b_1 r_f x_f + b_4 r_i x_i + c_1 x_f + c_2 x_i\Big) - e_1 r_f^2 - e_2 r_f r_i - \frac{e_2^2 r_i^2}{4e_1}\Big]$, *with* $e_2\alpha = 0$.

Corollary 1 (Singular classes)**.** *A one-mode singular Gaussian channel belongs to class A_1 if and only if its position representation has the following form:*

$$\sqrt{e_1/\pi}\delta(x_i)\exp\Big[-a_1x_f^2+\imath\Big(b_2x_fr_i+b_1r_fx_f+c_1x_f\Big)-e_1r_f^2\Big].$$

Otherwise the channel belongs to class A_2.

Since channels on each class are connected each other by unitary conjugations [15], a consequence of the theorem and the subsequent corollary is that the set of allowed forms must remain invariant under unitary conjugations. To show this we must know the possible functional forms of Gaussian unitaries. They are given by following lemma for one mode

Lemma 1 (One-mode Gaussian unitaries)**.** *Gaussian unitaries can have only GF or the one given by eq. (6).*

Proof. Recalling that for a unitary GQC, $\mathbf{T}$ must be symplectic ($\mathbf{T}\Omega\mathbf{T}^{\mathrm{T}}=\Omega$) and $\mathbf{N}=\mathbf{0}$. However, an inspection to eq. (18) lead us to note that $\mathbf{N}\neq\mathbf{0}$ unless e_1 diverges. Thus Gaussian unitaries cannot have the form J_{I} [see eq. (5)]. An inspection of matrices $\mathbf{T}$ and $\mathbf{N}$ of GQC with GF [see eq. (27)] and the ones for J_{II} [see equations (19) and (25)] lead us to note the following two observations: (i) in both cases we have $\mathbf{N}=0$ for $a_n=0\quad\forall n$; (ii) the matrix $\mathbf{T}$ is symplectic for GF when $b_2=b_3$, and when $\alpha\eta=\beta\gamma$ for J_{II}. In particular the identity map has the last form. This completes the proof. □

One can now compute the concatenations of the SGQCs with Gaussian unitaries. This can be done straightforward using the well known formulas for Gaussian integrals and the Fourier transform of the Dirac delta. Given that the calculation is elementary, and for sake of brevity, we present only the resulting forms of each concatenation. To show this compactly we introduce the following abbreviations: Singular channels belonging to class A_2 with form J_{I} and with $\alpha=0$, $e_2=0$ and $\alpha=e_2=0$, will be denoted as $\delta^{\alpha}_{\mathrm{A}_2}$, $\delta^{e_2}_{\mathrm{A}_2}$ and $\delta^{\alpha,e_2}_{\mathrm{A}_2}$, respectively; singular channels belonging to the same class but with GF will be denoted as $\mathcal{G}_{\mathrm{A}_2}$; channels belonging to class A_1 will be denoted as δ_{A_1}; finally Gaussian unitaries with GF will be denoted as $\mathcal{G}_{\mathcal{U}}$ and the ones with form J_{II} as $\delta_{\mathcal{U}}$. Writing the concatenation of two channels in the position representation as

$$J^{(\mathrm{f})}(x_f,r_f;x_i,r_i)=\int_{\mathbb{R}^2}dx'dr'J^{(1)}(x_f,r_f;x',r')\,J^{(2)}(x',r';x_i,r_i),\quad(31)$$

the resulting functional forms for $J^{(\mathrm{f})}$ are given in table I. As expected, the table shows that the integral has only the forms stated by our theorem. Additionally it shows the cases when unitaries change the functional form of class A_2, while for class A_1 $J^{(\mathrm{f})}$ has always the unique form enunciated by the corollary.

$J^{(1)}$	$J^{(2)}$	$J^{(\mathrm{f})}$
$\delta^{\alpha}_{\mathrm{A}_2}$	$\mathcal{G}_{\mathcal{U}}$	$\mathcal{G}_{\mathrm{A}_2}$
$\mathcal{G}_{\mathcal{U}}$	$\delta^{\alpha}_{\mathrm{A}_2}$	$\delta^{\alpha}_{\mathrm{A}_2}$
$\delta^{\alpha}_{\mathrm{A}_2}$	$\delta_{\mathcal{U}}$	$\delta^{\alpha}_{\mathrm{A}_2}$
$\delta_{\mathcal{U}}$	$\delta^{\alpha}_{\mathrm{A}_2}$	$\delta^{\alpha}_{\mathrm{A}_2}$
$\delta^{e_2}_{\mathrm{A}_2}$	$\mathcal{G}_{\mathcal{U}}$	$\delta^{e_2}_{\mathrm{A}_2}$
$\mathcal{G}_{\mathcal{U}}$	$\delta^{e_2}_{\mathrm{A}_2}$	$\mathcal{G}_{\mathrm{A}_2}$
$\delta^{e_2}_{\mathrm{A}_2}$	$\delta_{\mathcal{U}}$	$\delta^{e_2}_{\mathrm{A}_2}$
$\delta_{\mathcal{U}}$	$\delta^{e_2}_{\mathrm{A}_2}$	$\delta^{e_2}_{\mathrm{A}_2}$
$\mathcal{G}_{\mathcal{U}}$,	$\delta^{\alpha,e_2}_{\mathrm{A}_2}$	$\delta^{\alpha,e_2}_{\mathrm{A}_2}$
$\delta^{\alpha,e_2}_{\mathrm{A}_2}$	$\mathcal{G}_{\mathcal{U}}$	$\mathcal{G}_{\mathrm{A}_2}$
$\delta_{\mathcal{U}}$,	$\delta^{\alpha,e_2}_{\mathrm{A}_2}$	$\delta^{\alpha,e_2}_{\mathrm{A}_2}$
$\delta^{\alpha,e_2}_{\mathrm{A}_2}$	$\delta_{\mathcal{U}}$	$\delta^{\alpha,e_2}_{\mathrm{A}_2}$
$\delta_{\mathcal{U}}$,$\mathcal{G}_{\mathcal{U}}$	δ_{A_1}	δ_{A_1}
δ_{A_1}	$\delta_{\mathcal{U}}$,$\mathcal{G}_{\mathcal{U}}$	δ_{A_1}

TABLE I. The first and second columns show the functional forms of $J^{(1)}$ and $J^{(2)}$, respectively. The last column shows the resulting form of the concatenation of them [see eq. (31)]. See main text for symbol coding.

V. EXISTENCE OF MASTER EQUATIONS

In this section we show the conditions under which master equations, associated with the channels derived in sec. III, exist. To be more precise, we study if the functional forms derived above parametrize channels belonging to one-parameter differentiable families of GQCs. As a first step, we let the coefficients of forms presented in equations (5) and (6) to depend on time. Later we derive the conditions under which they bring any quantum state $\rho(x,r;t)$ to $\rho(x,r;t+\epsilon)$ (with $\epsilon>0$ and $t\in[0,\infty)$) smoothly, while holding the specific functional form of the channel, i.e.

$$\rho(x,r;t+\epsilon)=\rho(x,r;t)+\epsilon\mathcal{L}_t\left[\rho(x,r;t)\right]+\mathcal{O}(\epsilon^2),\quad(32)$$

where both $\rho(x,r;t)$ and $\rho(x,r;t+\epsilon)$ are propagated from $t=0$ with channels either with the form J_{I} or J_{II}, and $\mathcal{L}_t$ is a bounded superoperator in the state subspace. This is basically the problem of *the existence of a master equation*

$$\partial_t\rho(x,r;t)=\mathcal{L}_t\left[\rho(x,r;t)\right],\quad(33)$$

for such functional forms. Thus the problem is reduced to prove the existence of the linear generator $\mathcal{L}_t$, also known as *Liouvillian*.

To do this we use an ansatz proposed in Ref. [17] to investigate the existence and derive the master equation

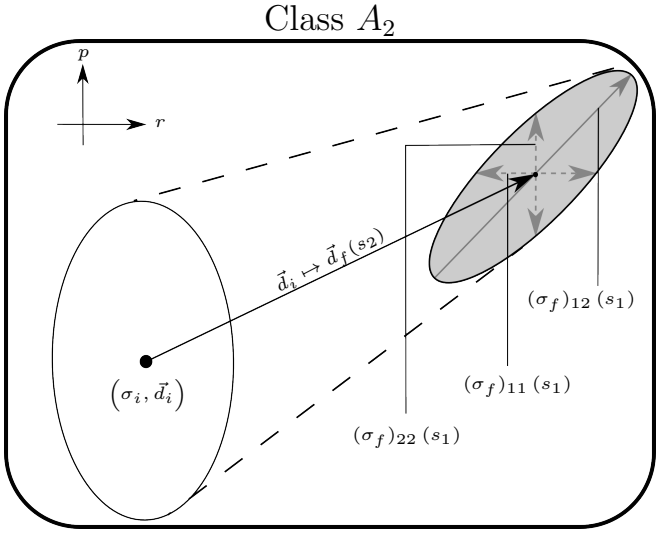

FIG. 1. Schematic picture of the channels belonging to class A_2, acting on Wigner functions of Gaussian states. The explicit dependence of the final state in terms of the combinations s_1 and s_2 are presented in the appendix. As well the formulas for s_i depending on the form of the channel. The pictured coordinate system corresponds to the position variable r and its conjugate momentum.

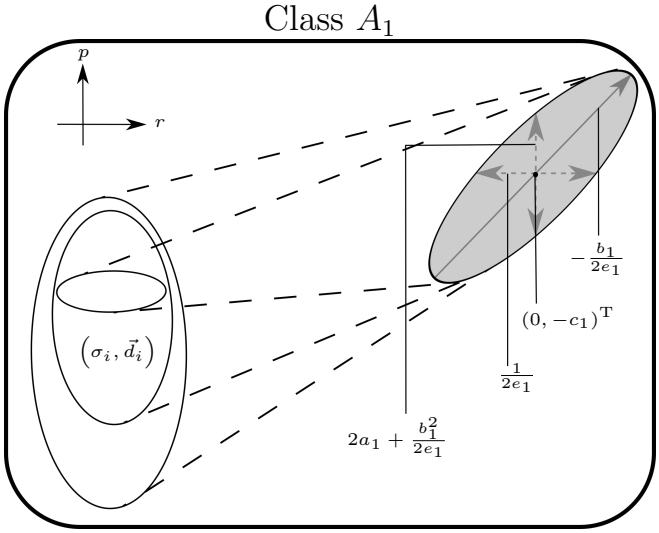

FIG. 2. Schematic picture of the channels belonging to class A_1, acting on Wigner functions of Gaussian states. Every channel of this class maps every initial quantum state, in particular GSs characterized by $(\sigma_i, \vec{d}_i)$, to a Gaussian state that depends only on the channel parameters. We indicate in the figure the values of the corresponding components of the first and second moments of the final Gaussian state. The pictured coordinate system corresponds to the position variable r and its conjugate momentum.

for GFs,

$$\mathcal{L} = \mathcal{L}_c(t) + (\partial_x, \partial_r)\mathbf{X}(t)\begin{pmatrix}\partial_x \\ \partial_r\end{pmatrix} + (x, r)\mathbf{Y}(t)\begin{pmatrix}\partial_x \\ \partial_r\end{pmatrix} + (x, r)\mathbf{Z}(t)\begin{pmatrix}x \\ r\end{pmatrix} \quad (34)$$

where $\mathcal{L}_c(t)$ is a complex function and

$$\mathbf{X}(t) = \begin{pmatrix}X_{xx}(t) & X_{xr}(t) \\ X_{rx}(t) & X_{rr}(t)\end{pmatrix} \quad (35)$$

is a complex matrix as well as $\mathbf{Y}(t)$ and $\mathbf{Z}(t)$, whose entries are defined in a similar way as in eq. (35). Note that $\mathbf{X}(t)$ and $\mathbf{Z}(t)$ can always be chosen symmetric, i.e. $X_{xr} = X_{rs}$ and $Z_{xr} = Z_{rx}$. Thus we must determine 11 time-dependent functions from eq. (34). This ansatz is also appropriate to study the functional forms introduced in this work, given that the left hand side of eq. (33) only involves quadratic polynomials in x, r, $\partial/\partial x$ and $\partial/\partial r$, as in the GF case.

Notice that singular channels do not admit a master equation since its existence implies that channels with the functional form involved can be found arbitrarily close from the identity channel. This is not possible for singular channels due to the continuity of the determinant of the matrix $\mathbf{T}$. This fact can be also shown using the ansatz of eq. (34), one finds infinitely Liuville operators, thus the master equation is not well defined.

For the non-singular cases presented in equations (5) and (6), the condition for the existence of a master equation is obtained as follows. (i) Substitute the ansatz of eq. (34) in the right hand side of the eq. (33). (ii) Define $\rho(x, r; t)$ using eq. (2), given an initial condition $\rho(x, r; 0)$, for each functional form $J_{\mathrm{I,II}}$. (iii) Take $\rho_f(x_f, r_f) \to \rho(x, r; t)$ and $\rho_i(x_i, r_i) \to \rho(x, r; 0)$. Finally, (iv) compare both sides of eq. (33). Defining $A(t) = \alpha(t)/\beta(t)$ and $B(t) = \gamma(t)/\eta(t)$, the conclusion is that for both J_{I} and J_{II}, a master equations exist if

$$c(t) \propto A(t) \quad (36)$$

holds, where $c(t) = c_1(t) + A(t)c_2(t)$. Additionally, for the form J_I the solutions for the matrices $\mathbf{X}(t)$, $\mathbf{Y}(t)$

and $\mathbf{Z}(t)$ are given by

$$\begin{aligned}
X_{xx} = X_{xr} = Y_{rx} = Z_{rr} = 0,\\
Y_{xx} = \frac{\dot{A}}{A},\\
\mathcal{L}_c = Y_{rr} = \frac{\dot{e}_1}{e_1} - \frac{\dot{e}_2}{e_2},\\
X_{rr} = \frac{\dot{e}_1}{4e_1^2} - \frac{\dot{e}_2}{2e_1e_2},\\
Y_{xr} = \imath\left(\frac{\lambda_1\dot{e}_2}{e_1e_2} + \frac{\lambda_2\dot{A}}{e_2A} - \frac{\lambda_1\dot{e}_1}{2e_1^2} - \frac{\dot{\lambda}_2}{e_2}\right),\\
Z_{xx} = \frac{\lambda_1^2}{2}\left(\frac{\dot{e}_2}{e_1e_2} - \frac{\dot{e}_1}{2e_1^2}\right) + \frac{\lambda_1}{e_2}\left(\frac{\lambda_2\dot{A}}{A} - \dot{\lambda}_2\right) + 2\lambda_3\frac{\dot{A}}{A} - \dot{\lambda}_3,\\
Z_{xr} = \imath\left(\frac{\dot{A}}{A}\left(\frac{e_1\lambda_2}{e_2} - \frac{\lambda_1}{2}\right) + \frac{\dot{\lambda}_1}{2} - \frac{\dot{\lambda}_2e_1}{e_2} + \frac{\lambda_2}{2}\left(\frac{\dot{e}_2}{e_2} - \frac{\dot{e}_1}{e_1}\right)\right),
\end{aligned} \tag{37}$$

where we have defined the following coefficients: $\lambda_1 = b_1 + Ab_3$, $\lambda_2 = b_2 + Ab_4$ and $\lambda_3 = a_1 + Aa_2 + A^2a_3$.

For the form J_{II} the solutions are the following

$$\begin{aligned}
\mathcal{L}_c = X_{xx} = X_{xr} = X_{rr} = Z_{rr} = 0,\\
Y_{rx} = Y_{xr} = 0,\\
Y_{xx} = \frac{\dot{A}}{A},\ Y_{rr} = \frac{\dot{B}}{B}.\\
Z_{xx} = a_2(t)\dot{A}(t) + \frac{2a_1(t)\dot{A}(t)}{A(t)} - A(t)^2\\
-\dot{a}_3(t) - A(t)\dot{a}_2(t) - \dot{a}_1(t),\\
Z_{xr} = \imath\left(\frac{1}{2}\dot{\lambda} - \frac{\lambda}{2}\left(\frac{\dot{A}}{A} + \frac{\dot{B}}{B}\right)\right),
\end{aligned} \tag{38}$$

where $\lambda = b_1 + Ab_3 + B(b_2 + Ab_4)$.

VI. CONCLUSIONS

In this work we have critically reviewed the deceptively natural idea that Gaussian quantum channels always admit a Gaussian functional form. To this end, we went beyond the pioneering characterization of Gaussian channels with Gaussian form presented in Ref. [12] in two new directions. First we have shown that, starting from their most general definition as mapping Gaussian states into Gaussian states, a more general parametrization of the coordinate representation of the one-mode case exists, that admits non-Gaussian functional forms. Second, we were able to provide a black-box characterization of such new forms by imposing complete positivity (not considered in Ref. [12]) and trace preserving conditions. While our parametrization connects with the analysis done by Holevo [16] in the particular cases where besides having a non-Gaussian form the channel is also singular, it also allows the study of Gaussian unitaries, thus providing similar classification schemes. We completed the classification of the new types of channels by deriving the form of the Liouvillian super operator that generates their time evolution in the form of a master equation. Surprisingly, Gaussian quantum channels without Gaussian form can be experimentally addressed by means of the celebrated Caldeira-Legget model for the quantum damped harmonic oscillator, where the new types of channels described here naturally appear in the subohmic regime.

ACKNOWLEDGEMENTS

We acknowledge PAEP and RedTC for financial support. Support by projects CONACyT 285754, UNAM-PAPIIT IG100518 is acknowledged. CP acknowledges support by PASPA program from DGAPA-UNAM. CAM and JDU acknowledge financial support from the German Academic Exchange Service (DAAD). We are thankful to the University of Vienna where part of this project was done.

Appendix A: Explicit formulas for class $\mathbf{A_2}$

The explicit formulas of the final states for channels of class A_2 with the form presented in eq. (6) with $e_2 = 0$ are

$$\begin{aligned}
(\sigma_f)_{11} &= \frac{1}{2e_1},\\
(\sigma_f)_{22} &= \left(\frac{\alpha}{\beta}\right)^2\left(\frac{b_3^2}{2e_1} + 2a_3\right) + \frac{\alpha}{\beta}\left(2a_2 + \frac{b_1b_3}{e_1}\right) +\\
&\quad 2a_1 + \frac{b_1^2}{2e_1} + s_1,\\
(\sigma_f)_{12} &= -\frac{\alpha}{\beta}\frac{b_3}{2e_1} - \frac{b_1}{2e_1},\\
\vec{d}_f\,(s_3) &= \left(0, -\frac{\alpha}{\beta}c_2 - c_1 + s_2\right)^{\mathrm{T}},
\end{aligned} \tag{A1}$$

where

$$\begin{aligned}
s_1 &= \left(b_2^2 + 2\frac{\alpha}{\beta}b_2b_4 + \left(\frac{\alpha}{\beta}\right)^2 b_4^2\right)(\sigma_i)_{11}\\
&\quad - 2\left(\frac{\alpha}{\beta}b_2 + \left(\frac{\alpha}{\beta}\right)^2 b_4\right)(\sigma_i)_{12} + \left(\frac{\alpha}{\beta}\right)^2(\sigma_i)_{22},\\
s_2 &= \left(\frac{\alpha}{\beta}b_4 + b_2\right)(d_i)_1 - \frac{\alpha}{\beta}(d_i)_2.
\end{aligned} \tag{A2}$$

The explicit formulas of the final states for channels of class A_2 with the form presented in eq. (6) with $\alpha = 0$ are

$$\begin{aligned}
(\sigma_f)_{11} &= \frac{e_2^2}{4e_1^2}(\sigma_i)_{11} + \frac{1}{2e_1},\\
(\sigma_f)_{12} &= \left(\frac{b_2 e_2}{2e_1} - \frac{b_1 e_2^2}{4e_1^2}\right)(\sigma_i)_{11} - \frac{b_1}{2e_1},\\
(\sigma_f)_{22} &= 2a_1 + \left(b_2 - \frac{b_1 e_2}{2e_1}\right)^2 (\sigma_i)_{11} + \frac{b_1^2}{2e_1},
\end{aligned} \tag{A3}$$

and

$$\vec{d}_f = \left(\frac{e_2}{2e_1}\left(\vec{d}_i\right)_1, \left(b_2 - \frac{b_1 e_2}{2e_1}\right)\left(\vec{d}_i\right)_1 - c_1\right)^{\mathrm{T}}. \tag{A4}$$

The explicit formulas of the final states for channels of class A_2 with Gaussian form are

$$\begin{aligned}
(\sigma_f)_{11}(s_1) &= \frac{2a_3}{b_3^2} + s_1,\\
(\sigma_f)_{12}(s_1) &= \frac{a_2}{b_3} - \frac{2a_3 b_1}{b_3^2} - b_1 s_1,\\
(\sigma_f)_{22}(s_1) &= \frac{b_1\left(b_3\left(b_1 b_3 s_1 - 2a_2\right) + 2a_3 b_1\right)}{b_3^2} + 2a_1,\\
\vec{d}_f(s_2) &= \left(s_2 - \frac{c_2}{b_3}, b_1\left(\frac{c_2}{b_3} - s_2\right) - c_1\right)^{\mathrm{T}},
\end{aligned} \tag{A5}$$

where

$$\begin{aligned}
s_1 &= \frac{b_4^2}{b_3^2}(\sigma_i)_{11} - \frac{2b_4}{b_3^2}(\sigma_i)_{12} + \frac{1}{b_3^2}(\sigma_i)_{22},\\
s_2 &= \frac{1}{b_3}(d_i)_2 - \frac{b_4}{b_3}(d_i)_1.
\end{aligned} \tag{A6}$$

[1] N. J. Cerf, G. Leuchs, and E. S. Polzik, *Quantum Information with Continuous Variables of Atoms and Light* (Imperial College Press, 2007) https://www.worldscientific.com/doi/pdf/10.1142/p489.

[2] M. Aspelmeyer, T. J. Kippenberg, and F. Marquardt, Rev. Mod. Phys. **86**, 1391 (2014).

[3] K. Hammerer, A. S. Sørensen, and E. S. Polzik, Rev. Mod. Phys. **82**, 1041 (2010).

[4] F. Grosshans, G. Van Assche, J. Wenger, R. Brouri, N. J. Cerf, and P. Grangier, Nature **421**, 238 (2003).

[5] S. Lloyd and S. L. Braunstein, Phys. Rev. Lett. **82**, 1784 (1999).

[6] S. L. Braunstein and P. van Loock, Rev. Mod. Phys. **77**, 513 (2005).

[7] L. Lami, B. Regula, X. Wang, R. Nichols, A. Winter, and G. Adesso, Phys. Rev. A **98**, 022335 (2018).

[8] E. A. Martinez and J. P. Paz, Phys. Rev. Lett. **110**, 130406 (2013).

[9] J. Eisert and M. M. Wolf, in *Quantum Information with Continuous Variables of Atoms and Light* (Imperial College Press, 2007) pp. 23–42.

[10] C. Weedbrook, S. Pirandola, R. García-Patrón, N. J. Cerf, T. C. Ralph, J. H. Shapiro, and S. Lloyd, Reviews of Modern Physics **84**, 621 (2012).

[11] A. Holevo and R. Werner, Physical Review A **63**, 032312 (2001).

[12] E. A. Martinez and J. P. Paz, (2012).

[13] H. Grabert, P. Schramm, and G.-L. Ingold, Physics Reports **168**, 115 (1988).

[14] G. Lindblad, Journal of Physics A: Mathematical and General **33**, 5059 (2000).

[15] A. S. Holevo, Problems of Information Transmission **43**, 1 (2007), arXiv:quant-ph/0607051 [quant-ph].

[16] A. S. Holevo, Problems of Information Transmission **44**, 171 (2008), arXiv:arXiv:0802.0235v1.

[17] R. Karrlein and H. Grabert, Physical Review E **55**, 153 (1997), arXiv:9610001 [physics].

C.3 Article: Positivity and Complete positivity of differentiable quantum processes

Physics Letters A 383, 23 (2019). Click to go to the webpage, Click to go to arXiv.

Physics Letters A ••• (••••) •••–•••

Contents lists available at ScienceDirect

Physics Letters A

www.elsevier.com/locate/pla

Positivity and complete positivity of differentiable quantum processes

Gustavo Montes Cabrera [a], David Davalos [b], Thomas Gorin [a,*]

[a] Departamento de Física, Universidad de Guadalajara, Guadalajara, Jalisco, Mexico
[b] Instituto de Física, Universidad Nacional Autónoma de México, Ciudad de México, Mexico

ARTICLE INFO

Article history:
Received 7 February 2019
Received in revised form 27 May 2019
Accepted 28 May 2019
Available online xxxx
Communicated by M.G.A. Paris

Keywords:
Quantum process
Divisibility
Quantum non-Markovianity

ABSTRACT

We study quantum processes, as one parameter families of differentiable completely positive and trace preserving (CPTP) maps. Using different representations of the generator, and the Sylvester criterion for positive semi-definite matrices, we obtain conditions for the divisibility of the process into completely positive (CP-divisibility) and positive (P-divisibility) infinitesimal maps. Both concepts are directly related to the definition of quantum non-Markovianity. For the single qubit case we show that CP- and P-divisibility only depend on the dissipation matrix in the master equation form of the generator. We then discuss three classes of processes where the criteria for the different types of divisibility result in simple geometric inequalities, among these the class of non-unital anisotropic Pauli channels.

1. Introduction

Non-Markovianity of quantum processes has been a topic of increasing interest during approximately the last ten years [1–3]. Starting with the papers by Breuer et al. [4] and Rivas et al. [5], a definition of quantum Markovianity has been reduced to the question whether all intermediate quantum maps are physically realizable; this induces a characterization that is more closely related to the Chapman-Kolmogorov condition than to the full definition of classical Markovianity [6]. For differentiable quantum processes, the question of divisibility into physically realizable quantum maps can be further reduced to the analysis of the time dependent generator of the process. This is the approach taken for this work.

The concept of divisibility has been introduced in Refs. [7,8]. In its original form, it refers to the condition that all intermediate maps are completely positive (CP-divisibility). However, one may as well consider P-divisibility, where it is sufficient that the intermediate maps are positive [9,10]. Note that it has been shown in Ref. [11] that P-divisibility provides a direct connection to classical Markovianity. If an intermediate map is positive but not completely positive, one may observe information backflow for entangled states between system and some ancillary system, but not in the system alone [5,12].

In this work, we derive general criteria for the positivity and the complete positivity (of the local infinitessimal intermediate map). In particular, for single qubit processes we show that both, CP-divisibility and P-divisibility conditions, only depend on the dissipation matrix of the master equation. We identify three different classes of single qubit processes, where the criteria for CP- and P-divisibility are reduced to simple explicit geometric inequalities. One of these classes consists of processes where the Choi-matrix has the shape of an X (*i.e.* all non-zero elements are located on the diagonal or the anti-diagonal). Many examples considered in the literature of quantum non-Markovianity are of this type. A second class consists of those processes, where the Choi-matrix has the shape of an O. The third class is that of the non-unital anisotropic Pauli channels. While criteria applicable to the generators have been studied in the context of CP-divisibility, see for instance Ref. [13,29], this has rarely been done for P-divisibility. The complete positivity of non-unital anisotropic Pauli channels, as such, has been considered in Refs. [30] and [31].

Explicit analytical criteria are valuable for the construction of Markovian approximations to a non-Markovian process as proposed in Ref. [8] and more specifically in Ref. [5]. Another area of applications is that of quantum process tomography [14–16], where it is important to identify the independent parameters which are to be determined. Finally, it may be of interest to identify quantum channels, which are P-divisible but not CP-divisible as processes where non-Markovianity may be identified as a genuine quantum effect [17].

Our work relies on a few general results which have been derived previously: (i) The Kossakowski theorem, which establishes the equivalence between positivity and contractivity (for the domain of Helstrom matrices), see Ref. [12] (and references therein), (ii) necessary and sufficient criteria which can be applied directly to the time dependent generator of the quantum process, see Ref. [9] for positivity and Ref. [8] for complete positivity, (iii)

* Corresponding author.
E-mail address: thomas.gorin@cucei.udg.mx (T. Gorin).

https://doi.org/10.1016/j.physleta.2019.05.049
0375-9601/

Sylvester's criterion for definite and semi-definite positivity [18, 19].

The paper is organized as follows: In Sec. 2 we discuss the description of quantum processes in terms of their generators and the general conditions for CP- and P-divisibility in terms of the generator. In Sec. 3 we analyze these conditions for general single qubit processes. In Sec. 4 we present classes of single qubit processes, where the conditions for P- and CP-divisibility can be solved analytically. In Sec. 5 we present our conclusions.

2. Differentiable quantum processes

In this section we introduce differentiable quantum processes and the definitions of P-divisibility and CP-divisibility. For both properties, we present criteria which can be applied directly to the generator of the quantum process in question.

2.1. Processes and generators

Let us denote a quantum process Λ_t, $(\forall t \in \mathbb{R}_0^+)$, as a one-parameter family of differentiable (with respect to t) completely positive and trace preserving linear maps (CPTP-maps), with $\Lambda_0 = \mathbb{1}$, the identity. For simplicity, we assume that the corresponding Hilbert space is of finite dimension, $\dim(\mathcal{H}) = d < \infty$. The quantum process Λ_t can be defined equivalently by the generator $\mathcal{L}_t$, such that

$$\frac{\mathrm{d}}{\mathrm{d}t}\Lambda_t = \mathcal{L}_t\,\Lambda_t\,, \qquad \Lambda_0 = \mathbb{1}\,. \tag{1}$$

One natural question to ask would be the following: What properties must be fulfilled by $\mathcal{L}_t$ in order to produce a valid quantum process of CPTP maps? Very recently this question has been addressed in Ref. [20]. In the present work, our objective is different. Assuming that $\mathcal{L}_t$ generates a valid quantum process, we ask whether that process is CP-divisible and/or P-divisible.

Note that for a given quantum process Λ_t, we can compute its generator as

$$\mathcal{L}_t = \frac{\mathrm{d}\Lambda_t}{\mathrm{d}t}\,\Lambda_t^{-1}\,. \tag{2}$$

In what follows we will assume that Λ_t is invertible. Where this is not the case (if at all, this typically happens at isolated points in time), one has to proceed with care [21]. In order to derive P-divisibility and CP-divisibility criteria in terms of the generator, we need to relate $\mathcal{L}_t$ to the intermediate quantum map,

$$\Lambda_{t+\delta,t} = \Lambda_{t+\delta}\,\Lambda_t^{-1}\,, \qquad \delta > 0\,. \tag{3}$$

This can be achieved by considering an infinitesimal intermediate quantum map, such that

$$\mathcal{L}_t = \lim_{\delta\to 0}\delta^{-1}\left(\Lambda_{t+\delta,t} - \mathbb{1}\right). \tag{4}$$

Choi-matrix representation. A direct method to represent linear quantum maps (this includes generators such as $\mathcal{L}_t$) consists in embedding the state space into the vector space $\mathcal{M}^{d\times d}$ of complex quadratic matrices of dimension d. In that case, the elements $\{|i\rangle\langle j|\}_{1\le i,j\le d}$ form an orthonormal basis with respect to the Hilbert-Schmidt scalar product $\langle A, B\rangle = \mathrm{tr}(A^\dagger B)$, and their images under the quantum map uniquely define that map. Arranging these images in a $d\times d$ block-matrix results in the Choi matrix representation. Formally, the Choi-matrix representation [22] of a linear map Λ in $\mathcal{M}^{d\times d}$ can be defined as

$$C_\Lambda = \sum_{i,j}|i\rangle\langle j|\otimes\Lambda[\,|i\rangle\langle j|\,]\,. \tag{5}$$

It has the following remarkable properties: (i) $C_\Lambda = C_\Lambda^\dagger$ iff $\Lambda[\Delta^\dagger] = \Lambda[\Delta]$ for every bounded operator Δ, (ii) $C_\Lambda \ge 0$ iff Λ is complete positive, (iii) $\mathrm{tr}\,(C_\Lambda) = d$ if Λ preserves the trace [22,23].

Master equation. The generator obtained in Eq. (4) preserves Hermiticity by construction, thus we can bring it to the following standard form [8,24] (see Appendix E for a detailed derivation):

$$\frac{\mathrm{d}}{\mathrm{d}t}\varrho = \mathcal{L}_t[\varrho]\,, \tag{6}$$

$$\mathcal{L}_t[\varrho] = -\mathrm{i}\,[H,\varrho] + \sum_{i,j=1}^{d^2-1} D_{ij}\left(F_i\,\varrho\,F_j^\dagger - \frac{1}{2}\left\{F_j^\dagger F_i\,,\,\varrho\right\}\right).$$

In this expression, Planck's constant $\hbar$ has been absorbed into the Hamiltonian H. The matrix D is Hermitian, and the set $\{F_i\}_{1\le i\le d^2}$ forms an orthonormal basis in the space of operators, such that $\mathrm{tr}(F_i^\dagger F_j) = \delta_{ij}$. In addition, the operators are chosen such that $\mathrm{tr}(F_i) = 0$, except for the last element, which is given by $F_{d^2} = \mathbb{1}/\sqrt{d}$.

In this work, we will use Eq. (6) as one possible representation of the generator $\mathcal{L}_t$, at some arbitrary, fixed time t. We call this representation the "master equation representation" of $\mathcal{L}_t$, and D the "dissipation matrix". Note that an intermediate quantum process $\Lambda_{t+\delta,t} \approx \mathbb{1} + \delta\mathcal{L}_t$, as defined in Eq. (3), is CPTP if and only if D is positive semidefinite [2,13]. In this case, Λ_t becomes a valid CPTP map [11]. Finally, if the generator is time-independent, Λ_t becomes a one-parameter semigroup in the space of CPTP maps [25–27].

2.2. Markovianity: P-divisibility vs. CP-divisibility

In this subsection we present the definitions for the P-divisibility and the CP-divisibility of quantum processes. We use the term "Markovianity" in cases, where we want to refer to both properties, indistinctively.

CP-divisibility. A process Λ_t is called CP-divisible if and only if the intermediate map $\Lambda_{t+\delta,t}$ as defined in Eq. (3) is CPTP for all $t, \delta \in \mathbb{R}_0^+$. Complete positivity of a quantum map Λ is conveniently verified using the Choi matrix representation, introduced in Eq. (5).

P-divisibility. A process Λ_t is called P-divisible if and only if the intermediate map $\Lambda_{t+\delta,t}$ as defined in Eq. (3) is PTP (positivity and trace preserving) for all $t, \delta \in \mathbb{R}_0^+$.

Positivity of a Hermiticity and trace preserving quantum map Λ is more complicated to verify. In that case, one has to show that $\Lambda[\varrho] \ge 0$ for all density matrices ϱ. In practice, it is sufficient to check the condition for all density matrices representing pure states.

Local complete positivity. Following Refs. [8], and [28], let $C_\mathcal{L}$ be the Choi-matrix representation of the generator $\mathcal{L}_t$, and let $C_\perp$ be a matrix representation of $C_\mathcal{L}$ in the subspace orthogonal to the Bell state

$$|\Phi_\mathrm{B}\rangle = \frac{1}{\sqrt{d}}\sum_i |ii\rangle\,, \tag{7}$$

where d is the dimension of the Hilbert space. Then, the quantum process Λ_t is locally CP at time t, if and only if

$$C_\perp \ge 0\,. \tag{8}$$

Please cite this article in press as: G. Montes Cabrera et al., Positivity and complete positivity of differentiable quantum processes, Phys. Lett. A (2019), https://doi.org/10.1016/j.physleta.2019.05.049

Therefore the process Λ_t is CP-divisible, if and only if it is locally CP for all $t \in \mathbb{R}_0^+$. Note that in Ref. [28], it has been shown that $C_\perp$ is unitarily equivalent to the dissipation matrix D (see Appendix E for a detailed derivation).

Local positivity. A quantum process is locally positive at time t, if and only if for all orthogonal states $|\psi\rangle, |\phi\rangle \in \mathcal{H}$ it holds that

$$\langle\psi|\,\mathcal{L}_t[\,|\phi\rangle\langle\phi|\,]\,\psi\rangle \geq 0\,. \tag{9}$$

Similar to the CP case, it holds that a quantum process Λ_t is P-divisible if and only if it is locally positive for all $t \in \mathbb{R}_0^+$ [9]. The equivalence between local positivity and P-divisibility follows from Eq. (4):

$$\begin{aligned} &\langle\psi|\,\Lambda_{t+\delta,t}[\,|\phi\rangle\langle\phi|\,]\,|\psi\rangle \geq 0 \\ \Leftrightarrow\quad &\delta\,\langle\psi|\,\mathcal{L}_t[\,|\phi\rangle\langle\phi|\,]\,|\psi\rangle + \langle\psi|\phi\rangle\,\langle\phi|\psi\rangle \geq 0\,. \end{aligned} \tag{10}$$

In the limit $\delta \to 0$, this can only happen if ψ and ϕ are orthogonal, $\langle\psi|\phi\rangle = 0$. In fact, if $|\langle\psi|\phi\rangle|^2 > 0$, it might very well be that $\langle\psi|\,\mathcal{L}_t[\,|\phi\rangle\langle\phi|\,]\,|\psi\rangle < 0$ even if the process is P-divisible in the neighborhood of that point.

To summarize, we may express both properties CP-divisibility and P-divisibility in terms of local conditions which have to be fulfilled by the generator $\mathcal{L}_t$. In what follows, we analyze these in more detail. To avoid overly cumbersome terminology, we denote generators which fulfill Eq. (9) and/or Eq. (8) simply as "positive" and/or "completely positive generators".

3. Single qubit processes

In the case of single qubit processes, the Bloch vector representation is yet another method to represent quantum channels and their generators. In Sec. 3.1 we discuss the following three representations: (i) the master equation, (ii) the Choi-matrix, and (iii) the Bloch vector representation and how they are related one-to-another. In Sec. 3.2, we derive explicit criteria for local positivity and local complete positivity in terms of the dissipation matrix D.

3.1. Equivalent representations

Choi matrix representation. For our purposes, the Choi matrix representation will be the most useful. A CPTP-map Λ, which belongs to a quantum process, may be parametrized as

$$\begin{aligned} C_\Lambda &= \begin{pmatrix} \Lambda[\,|0\rangle\langle 0|\,] & \Lambda[\,|0\rangle\langle 1|\,] \\ \Lambda[\,|1\rangle\langle 0|\,] & \Lambda[\,|1\rangle\langle 1|\,] \end{pmatrix} \\ &= \begin{pmatrix} 1-r_1 & y_1^* & x^* & 1-z_1^* \\ y_1 & r_1 & z_2 & -x^* \\ x & z_2^* & r_2 & y_2^* \\ 1-z_1 & -x & y_2 & 1-r_2 \end{pmatrix}. \end{aligned} \tag{11}$$

The structure of C_Λ is due to the fact that Λ must preserve Hermiticity and the trace. We have chosen the parametrization in such a way that the parameters $r_1, r_2,\ y_1, y_2, x,\ z_1, z_2$ as functions of time are all zero at $t = 0$.

Note that any intermediate map $\Lambda_{t+\delta,t}$ is at least Hermiticity and trace preserving. Therefore, Eq. (4) implies that the Choi-matrix representation of the generator $\mathcal{L}_t$ must be Hermitian, and in all blocks, the partial trace must be equal to zero. That leaves us with the following parametrization:

$$C_\mathcal{L} = \begin{pmatrix} -q_1 & Y_1^* & X^* & -Z_1^* \\ Y_1 & q_1 & Z_2 & -X^* \\ X & Z_2^* & q_2 & Y_2^* \\ -Z_1 & -X & Y_2 & -q_2 \end{pmatrix}. \tag{12}$$

In general, there is no simple relation between the parametrization used here, and that of Eq. (11). This is because the expression for the generator $\mathcal{L}_t$ includes the inverse of Λ_t.

Master equation representation. Note that every generator $\mathcal{L}_t$ of a Hermiticity and trace preserving quantum process, can be written in the form of Eq. (6), with Hermitian matrices H and D. Therefore, we may calculate the Choi-representation of the generator, by inserting $\varrho = |i\rangle\langle j|$ into the RHS of Eq. (6), and compare the result to the general form in Eq. (12). For the calculation, we choose the following orthonormal operator basis $\{F_i\}_{1\leq i\leq d^2}$:

$$\begin{aligned} F_1 &= \frac{1}{\sqrt{2}}\big(|0\rangle\langle 0| - |1\rangle\langle 1|\big)\,, & F_2 &= |0\rangle\langle 1|\,, \\ F_3 &= |1\rangle\langle 0|\,, \quad \text{and} & F_4 &= \mathbb{1}/\sqrt{2}\,. \end{aligned} \tag{13}$$

As a result, we obtain a linear one-to-one correspondence between the parameters used in the master equation representation and those, used in the Choi representation:

$$\begin{aligned} \begin{pmatrix} q_1 \\ q_2 \\ \mathrm{Re}\,Z_1 \end{pmatrix} &= \begin{pmatrix} 0 & 0 & 1 \\ 0 & 1 & 0 \\ 1 & 1/2 & 1/2 \end{pmatrix} \begin{pmatrix} D_{11} \\ D_{22} \\ D_{33} \end{pmatrix}, \\ \mathrm{Im}\,Z_1 &= H_{22} - H_{11}\,, \\ Z_2 &= D_{32}\,, \\ \begin{pmatrix} Y_1 \\ Y_2 \\ X^* \end{pmatrix} &= \begin{pmatrix} -\sqrt{2}/4 & \sqrt{18}/4 & -\mathrm{i} \\ -\sqrt{18}/4 & \sqrt{2}/4 & \mathrm{i} \\ \sqrt{2}/4 & \sqrt{2}/4 & \mathrm{i} \end{pmatrix} \begin{pmatrix} D_{12} \\ D_{31} \\ H_{21} \end{pmatrix}. \end{aligned} \tag{14}$$

As one might have expected, the quantity $H_{11} + H_{22}$ is irrelevant for the representation of the generator, and may be set equal to zero without loss of generality. Then, Eq. (14) is clearly an invertible linear system of equations.

Bloch vector representation. Any qubit density matrix can be written in terms of the Pauli matrices and the identity matrix $\mathbb{1}$ as follows:

$$\varrho = \frac{1}{2}\left(v_0\,\mathbb{1} + \sum_{j=1}^{3} v_j\,\sigma_j\right), \tag{15}$$

where $v_0 = 1$ and $\vec{v} = (v_1, v_2, v_3)$ is a vector in $\mathbb{R}^3$ of norm $\|\vec{v}\| \leq 1$. Any Hermiticity and trace preserving quantum map Λ can then be written as an affine transformation [32]

$$\Lambda\ :\ \vec{v} \to \vec{v}' = R\,\vec{v} + \vec{t}\,, \tag{16}$$

where R is a real not necessarily symmetric square matrix and $\vec{t}$ is a real three-dimensional vector. The coefficients of R and $\vec{t}$ are given by

$$t_j = \frac{1}{2}\,\mathrm{tr}\big(\sigma_j\,\mathcal{L}_t[\,\mathbb{1}\,]\big)\,, \quad R_{jk} = \frac{1}{2}\,\mathrm{tr}\big(\sigma_j\,\mathcal{L}_t[\,\sigma_k\,]\big)\,. \tag{17}$$

For the generator with the Choi-matrix representation given in Eq. (12), we find

$$\begin{aligned} R &= \begin{pmatrix} \mathrm{Re}(Z_2 - Z_1) & \mathrm{Im}(Z_1 + Z_2) & \mathrm{Re}(Y_1 - Y_2) \\ \mathrm{Im}(Z_2 - Z_1) & -\mathrm{Re}(Z_1 + Z_2) & \mathrm{Im}(Y_1 - Y_2) \\ 2\,\mathrm{Re}(X) & -2\,\mathrm{Im}(X) & -q_1 - q_2 \end{pmatrix}, \\ \vec{t} &= \begin{pmatrix} \mathrm{Re}(Y_1 + Y_2) \\ \mathrm{Im}(Y_1 + Y_2) \\ q_2 - q_1 \end{pmatrix}. \end{aligned} \tag{18}$$

Again, it is easy to verify that the relation between this Bloch vector representation and the Choi representation is invertible.

Please cite this article in press as: G. Montes Cabrera et al., Positivity and complete positivity of differentiable quantum processes, Phys. Lett. A (2019), https://doi.org/10.1016/j.physleta.2019.05.049

3.2. Criteria for positivity and complete positivity

Local complete positivity. In order to verify if the Choi-matrix (as a linear transformation) projected onto the orthogonal subspace of $|\phi_B\rangle\langle\phi_B|$, is positive, we choose the orthonormal states

$$|\psi_1\rangle = \frac{1}{\sqrt{2}}\begin{bmatrix}1\\0\\0\\-1\end{bmatrix}, \quad |\psi_2\rangle = \begin{bmatrix}0\\0\\1\\0\end{bmatrix}, \quad |\psi_3\rangle = \begin{bmatrix}0\\1\\0\\0\end{bmatrix}, \tag{19}$$

to span that subspace. Then we obtain for the matrix representation of the Choi matrix of $\mathcal{L}_t$, projected on that subspace:

$$C_\perp = \begin{pmatrix} \mathrm{Re}(Z_1) - \frac{q_1+q_2}{2} & \frac{X^*-Y_2}{\sqrt{2}} & \frac{X+Y_1^*}{\sqrt{2}} \\ \frac{X-Y_2^*}{\sqrt{2}} & q_2 & Z_2^* \\ \frac{X^*+Y_1}{\sqrt{2}} & Z_2 & q_1 \end{pmatrix} = \begin{pmatrix} D_{11} & D_{12} & D_{13} \\ D_{21} & D_{22} & D_{23} \\ D_{31} & D_{32} & D_{33} \end{pmatrix}. \tag{20}$$

The second equality is obtained by solving Eq. (14) for the matrix elements D_{ij}. It simply means that $C_\perp = D$.

We may now use the Sylvester criterion to check whether $D \geq 0$ or not. A general discussion of that criterion can be found in the text book [18]; the present positive semidefinite case has been treated in Ref. [19]. In that case, the statement is the following: A Hermitian matrix is positive semidefinite if and only if all principal minors are larger or equal to zero. Hence, for $D \geq 0$, it must hold:

$$\begin{aligned} &D_{11}, D_{22}, D_{33} \geq 0\,, \quad D_{11}D_{33} - |D_{31}|^2 \geq 0\,, \\ &D_{11}D_{22} - |D_{21}|^2 \geq 0\,, \quad D_{33}D_{22} - |D_{32}|^2 \geq 0\,, \\ &D_{11}D_{22}D_{33} + 2\,\mathrm{Re}(D_{12}D_{23}D_{31}) \geq \\ &\qquad D_{11}|D_{32}|^2 + D_{22}|D_{31}|^2 + D_{33}|D_{21}|^2\,. \end{aligned} \tag{21}$$

Local positivity. According to the criterion in Eq. (9), we need to verify that $\langle\psi|\,\mathcal{L}[\,|\phi\rangle\langle\phi|\,]\,|\psi\rangle \geq 0$ for all $|\psi\rangle \perp |\phi\rangle$. Such general orthonormal states may be written as the column vectors of a unitary matrix, taken from the group $SU(2)$. Removing an ineffective global phase we find:

$$|\psi\rangle = \begin{pmatrix}\cos(\theta/2)\\ \mathrm{e}^{\mathrm{i}\beta}\sin(\theta/2)\end{pmatrix}, \qquad |\phi\rangle = \begin{pmatrix}-\sin(\theta/2)\\ \mathrm{e}^{\mathrm{i}\beta}\cos(\theta/2)\end{pmatrix}.$$

Hence, we consider $p(\theta,\beta) = \langle\psi|\,\mathcal{L}[\,|\phi\rangle\langle\phi|\,]\,|\psi\rangle$ as a function of θ and β. Therefore, we may say that the $\mathcal{L}_t$ is positive at time t, if and only if $p(\theta,\beta) \geq 0$ for all θ and β. Using the parametrization of Eq. (12), $p(\theta,\beta)$ may be written as

$$\begin{aligned} p(\theta,\beta) = {} & \frac{q_1+q_2}{2}\cos^2\theta + \frac{q_2-q_1}{2}\cos\theta + \frac{A}{2}\sin^2\theta \\ & + \frac{\mathrm{Re}\big[\,(Y_1+Y_2)\,\mathrm{e}^{-\mathrm{i}\beta}\,\big]}{2}\sin\theta \\ & + \frac{\mathrm{Re}\big[\,(Y_2-Y_1)\,\mathrm{e}^{-\mathrm{i}\beta} - 2X\,\mathrm{e}^{\mathrm{i}\beta}\,\big]}{2}\sin\theta\,\cos\theta\,, \end{aligned} \tag{22}$$

where $A = \mathrm{Re}[Z_1 - Z_2\,\mathrm{e}^{-2\mathrm{i}\beta}]$. In terms of the master equation parameters, we find

$$\begin{aligned} &R = D_{22} + D_{33}\,, \quad Y_1 + Y_2 = \sqrt{2}\,(D_{21} - D_{13})\,, \\ &S = D_{33} - D_{22}\,, \quad A_1 = D_{11} - \frac{D_{33}+D_{22}}{2} - \mathrm{Re}\,D_{23}\,, \\ &Y_2 - Y_1 - 2\,X^* = -\sqrt{2}\,(D_{21} + D_{13})\,, \end{aligned} \tag{23}$$

such that

$$\begin{aligned} 2\,p(\theta,\beta) = {} & R + S\,\cos\theta + \Big(D_{11} - \frac{R}{2}\Big)\,\sin^2\theta \\ & + \mathrm{Re}\big[\,-D_{23}\,\mathrm{e}^{-2\mathrm{i}\beta}\,\sin\theta + \sqrt{2}\,(D_{21} - D_{13})\,\mathrm{e}^{-\mathrm{i}\beta} \\ & - \sqrt{2}\,(D_{21} + D_{13})\,\mathrm{e}^{-\mathrm{i}\beta}\,\cos\theta\,\big]\,\sin\theta\,. \end{aligned} \tag{24}$$

This shows that positivity, just as complete positivity, only depends on the dissipation matrix D.

In general, one should try to find all minima of this function and verify that those are non-negative. Since the domain of $p(\theta,\beta)$ is a torus without boundaries, it is sufficient to find the critical points where the partial derivatives $\partial p/\partial\theta$ and $\partial p/\partial\beta$ are both equal to zero. The corresponding equations may be reduced to a root-finding problem for 4'th order polynomials. Thus analytical expressions may be obtained in principle, even so they are probably not very useful. Still, numerical evaluations are pretty straight forward to implement. In Sec. 4 we will discuss different classes of generators, where particularly simple analytical solutions can be found.

4. Examples

In this section, we consider three different classes of generators. For each class, the set of positive (completely positive) generators is interpreted as a region in a certain parameter space (a subspace of the 9-dimensional vector space of dissipation matrices). In general, these regions must be convex, since the respective criteria involve expectation values of some linear matrix which represents the generator. Hence, if we consider the expectation value of any convex combination of two generators, it immediately decomposes into the corresponding convex combination of expectation values. Unless stated otherwise, we analyze the criteria for positivity and complete positivity in terms of the dissipation matrix D.

4.1. X-shaped quantum channels and generators

The term "X-shape" refers to the case, where the non-zero elements in the Choi matrix appear to form the letter "X", that means that $Y_1 = Y_2 = X = 0$ in Eq. (12). Hence,

$$C_\mathcal{L} = \begin{pmatrix} -q_1 & 0 & 0 & -Z_1^* \\ 0 & q_1 & Z_2 & 0 \\ 0 & Z_2^* & q_2 & 0 \\ -Z_1 & 0 & 0 & -q_2 \end{pmatrix}. \tag{25}$$

In this case, the X-shape of the generator implies the X-shape of the quantum channel, and vice versa. Many important models lead to quantum channels of that type [2,4]. In terms of the Bloch vector representation, the X-shape implies that the dynamics along the z-axis is independent from that in the (x,y)-plane [13].

According to Eq. (14) the X-shape of the Choi matrix $C_\mathcal{L}$ implies for H and D from the master equation representation in Eq. (6): $H_{12} = 0$, $D_{13} = D_{12} = 0$ as well as

$$\begin{aligned} &q_1 = D_{22}\,, \qquad q_2 = D_{33}\,, \qquad Z_2 = D_{23} \\ &\text{and} \quad Z_1 = \mathrm{i}\,(H_{22} - H_{11}) + D_{11} + \frac{D_{33}+D_{22}}{2}\,. \end{aligned} \tag{26}$$

For the matrix $C_\perp$ we thus obtain:

$$C_\perp = \begin{pmatrix} D_{11} & 0 & 0 \\ 0 & D_{22} & D_{23} \\ 0 & D_{32} & D_{33} \end{pmatrix}. \tag{27}$$

Complete positivity. Considering all principal minors of the dissipation matrix in Eq. (27), we find

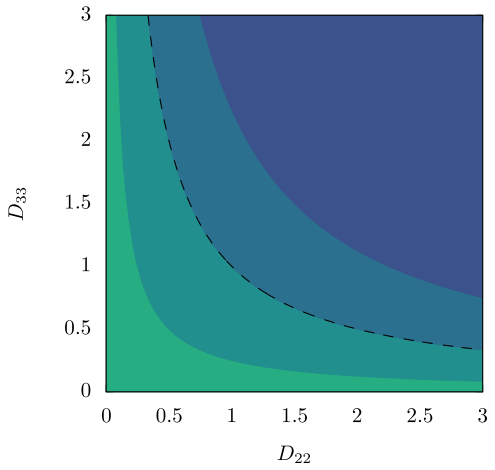

Fig. 1. The parameter space $D_{22}, D_{33} \geq 0$ for visualizing the regions of positivity and complete positivity for the X-shaped generator, for $|D_{32}| = 1$. For complete positivity, the point (D_{22}, D_{33}) must lie above the black dashed line, while $D_{11} \geq 0$ is required. For positivity, the allowed region for (D_{22}, D_{33}) depends on D_{11}: For $D_{11} \geq 1$, it is the whole quadrant; for $D_{11} = 1/2$ the allowed region consists of the dark green and blue areas; for $D_{11} = 0$ it consists of the blue areas above the black dashed line; and for $D_{11} = -1/2$ it consists of the dark blue area alone. (For interpretation of the colors in the figure(s), the reader is referred to the web version of this article.)

$$D_{11}, D_{22}, D_{33} \geq 0\,, \qquad D_{22}\,D_{33} - |D_{23}|^2 \geq 0\,,$$
$$D_{11}\,D_{22} \geq 0\,, \qquad D_{11}\left[\,D_{22}\,D_{33} - |D_{23}|^2\,\right] \geq 0\,. \tag{28}$$

Removing redundant inequalities, we are left with

$$D_{11}, D_{22}, D_{33} \geq 0\,, \quad D_{22}\,D_{33} \geq |D_{23}|^2\,. \tag{29}$$

Positivity. From Eq. (24) we find:

$$2p(\theta,\beta) = R + S\,\cos\theta + A\,\sin^2\theta \geq 0\,, \tag{30}$$
$$\text{where} \quad A = D_{11} - \frac{R}{2} - \mathrm{Re}\big[\,D_{23}\,\mathrm{e}^{-2\mathrm{i}\beta}\,\big]\,,$$

$R = D_{22} + D_{33}$, and $S = D_{33} - D_{22}$. This inequality must hold for all values of θ and β, parametrizing the quantum state to which the generator is applied. Thus, we only need to verify if the minimum of this expression is larger than zero. As far as β is concerned, this means that we may replace A by its minimum (as a function of β), which is given by $A_{\min} = D_{11} - R/2 - |D_{23}|$. We are then left with the condition

$$\forall\,\theta \;:\; R + S\,\cos\theta + A_{\min}\,\sin^2\theta \geq 0\,. \tag{31}$$

This condition is further evaluated in Appendix A. As a result, we find that the conditions for positivity become

$$D_{22}, D_{33} \geq 0\,, \tag{32}$$

and if $D_{11} < |D_{23}|$, in addition

$$\big|\,|D_{23}| - D_{11}\big| \leq \sqrt{D_{22}\,D_{33}}\,. \tag{33}$$

In Fig. 1, we show the parameter space $D_{22}, D_{33} \geq 0$ for visualizing the regions of positivity and complete positivity for the X-shaped generator. For complete positivity, the inequalities to fulfill are given in Eq. (29), which states independent conditions on D_{11} on the one hand and $D_{22}, D_{33}, |D_{23}|^2$ on the other. For positivity, by contrast, the conditions on D_{22} and D_{33} depend on D_{11}. Here, we observe an interesting behavior: As D_{11} approaches zero from above, the region of positivity becomes more and more similar to the region of complete positivity, until they coincide for $D_{11} = 0$. When D_{11} becomes negative, complete positivity is violated while positivity is still maintained sufficiently far away from the black dashed line.

4.2. O-shaped quantum channels

Here, we consider another subset of single qubit generators, which also allow for an analytic solution. These are in some sense complementary to the X-shaped channels, These are obtained from the general case by setting $q_1 = q_2 = q$, $Y_1 = -Y_2 = Y$, and $Z_2 = 0$. The Choi matrix, representing the generator resembles an O, instead of an X, that is why we call them O-shaped channels.

$$C_{\mathcal{L}} = \begin{bmatrix} -q & Y^* & X^* & -Z_1^* \\ Y & q & 0 & -X^* \\ X & 0 & q & -Y^* \\ -Z_1 & -X & -Y & -q \end{bmatrix} \tag{34}$$

According to Eq. (14), this implies for the matrix elements of H and D from the master equation (6):

$$q = D_{33}\,, \qquad Z_1 = \mathrm{i}\,(H_{22} - H_{11}) + D_{11} + D_{33}\,,$$
$$Y = -\mathrm{i}\,H_{21} + \frac{D_{13}}{\sqrt{2}}\,, \quad X^* = \mathrm{i}\,H_{21} + \frac{D_{13}}{\sqrt{2}}\,, \tag{35}$$

with $D_{22} = D_{33}$, $D_{21} = D_{13}$, and $D_{23} = 0$. The matrix for verifying complete positivity reads

$$C_{\perp} = \begin{pmatrix} D_{11} & D_{31} & D_{13} \\ D_{13} & D_{22} & 0 \\ D_{31} & 0 & D_{22} \end{pmatrix}\,, \tag{36}$$

Complete positivity. Expressed in terms of the dissipation matrix, considering all principal minors.

$$D_{11}, D_{22} \geq 0\,, \quad D_{11}D_{22} - |D_{13}|^2 \geq 0\,,$$
$$D_{11}\,D_{22}^2 - D_{13}D_{31}D_{22} - D_{31}D_{22}D_{13} \geq 0 \tag{37}$$

This can be reduced to

$$D_{11}, D_{22} \geq 0\,, \quad D_{11}D_{22} \geq 2\,|D_{13}|^2\,. \tag{38}$$

Positivity. Under the conditions mentioned above, the function $2\,p(\theta,\beta)$ from Eq. (24) becomes (in terms of the master equation parameters)

$$2p(\theta,\beta) = 2\,D_{22} + (D_{11} - D_{22})\,\sin^2\theta$$
$$- 2\sqrt{2}\,\mathrm{Re}\big[D_{13}\,\mathrm{e}^{-\mathrm{i}\beta}\big]\,\sin\theta\cos\theta \geq 0\,. \tag{39}$$

Again, it is possible to derive the conditions for positivity, which do no longer involve the angles θ and β. The respective calculation is outlined in Appendix B, with the result [see Eq. (B.4)]

$$3\,D_{22} + D_{11} \geq 0\,, \quad D_{22}\,(D_{11} + D_{22}) \geq |D_{13}|^2\,. \tag{40}$$

In Fig. 2, we show the different regions of positivity and complete positivity in the parameter space of D_{22}, D_{11}. We distinguish two qualitatively different cases, $|D_{13}| = 0$ and $|D_{13}| = 1$. In both cases, the region of positivity is considerably larger than the region for complete positivity.

Please cite this article in press as: G. Montes Cabrera et al., Positivity and complete positivity of differentiable quantum processes, Phys. Lett. A (2019), https://doi.org/10.1016/j.physleta.2019.05.049

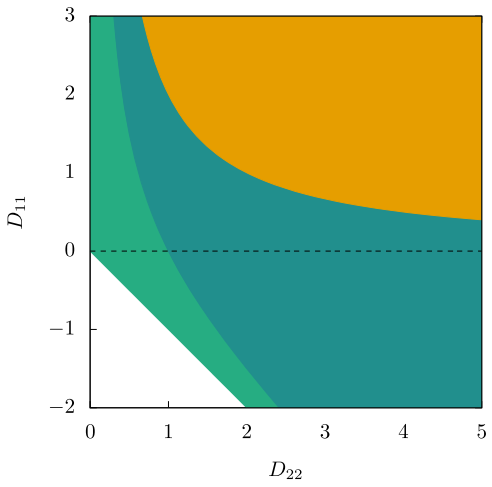

Fig. 2. The parameter space D_{22}, D_{11} for visualizing the regions of positivity [Eq. (40)] and complete positivity [Eq. (38)] for the O-shaped generator. For $|D_{13}| = 0$, the region of complete positivity is simply the positive quadrant $D_{22}, D_{11} \geq 0$, while the region for positivity is the whole colored region. For $|D_{13}| = 1$, the region of complete positivity is colored in orange, the region of positivity is dark green and orange.

4.3. Non-unital anisotropic Pauli channels

Here, Λ_t is given as an affine transformation of state vectors in the Bloch sphere [32] (see the corresponding paragraph in Sec. 3.1):

$$\Lambda_t \ : \ \vec{v} \to \vec{v}' = R\,\vec{v} + \vec{s}\,, \tag{41}$$

where R is a real diagonal matrix and $\vec{s}$ a real vector.

$$R = \begin{pmatrix} R_{11} & 0 & 0 \\ 0 & R_{22} & 0 \\ 0 & 0 & R_{33} \end{pmatrix}\,, \qquad \vec{s} = \begin{pmatrix} s_1 \\ s_2 \\ s_3 \end{pmatrix}\,. \tag{42}$$

Using the general formula, Eq. (2), for constructing the generator, we find

$$\mathcal{L}_{\rm P} \ : \ \vec{v} \to \vec{v}' = \frac{\mathrm{d}R}{\mathrm{d}t}\left[\,R^{-1}\,(\vec{v} - \vec{s})\,\right] + \frac{\mathrm{d}\vec{s}}{\mathrm{d}t}\,. \tag{43}$$

Hence, the generator for this Pauli channel is given by the affine transformation $\vec{v} \to \vec{v}' = R_{\mathcal{L}\rm P}\,\vec{v} + \vec{t}_{\mathcal{L}\rm P}$, with

$$R_{\mathcal{L}\rm P} = \begin{pmatrix} -\gamma_1 & 0 & 0 \\ 0 & -\gamma_2 & 0 \\ 0 & 0 & -\gamma_3 \end{pmatrix}\,, \quad t_{\mathcal{L}\rm P} = \begin{pmatrix} \tau_1 \\ \tau_2 \\ \tau_3 \end{pmatrix}\,,$$

$$\text{where} \quad \gamma_j = \frac{-1}{R_{jj}}\frac{\mathrm{d}R_{jj}}{\mathrm{d}t}\,, \qquad \tau_j = \frac{\mathrm{d}s_j}{\mathrm{d}t} + \gamma_j\,s_j\,. \tag{44}$$

The Choi matrix representation of $\mathcal{L}_{\rm P}$ is obtained by inverting Eq. (18), with the result

$$C_{\mathcal{L}\rm P} = \frac{1}{2}\begin{pmatrix} -\gamma_3 + \tau_3 & \tau_1 - \mathrm{i}\tau_2 & 0 & -\gamma_1 - \gamma_2 \\ \tau_1 + \mathrm{i}\tau_2 & \gamma_3 - \tau_3 & \gamma_2 - \gamma_1 & 0 \\ 0 & \gamma_2 - \gamma_1 & \gamma_3 + \tau_3 & \tau_1 - \mathrm{i}\tau_2 \\ -\gamma_1 - \gamma_2 & 0 & \tau_1 + \mathrm{i}\tau_2 & -\gamma_3 - \tau_3 \end{pmatrix}\,. \tag{45}$$

In what follows, we compute the positivity and the complete positivity condition in terms of the parameters γ_j and τ_j, since this allows for relatively simple geometric interpretations. In the case of complete positivity, this has been worked out previously, in Ref. [29]. For the parametrization in terms of the master equation (6), we obtain from Eq. (12) and (14):

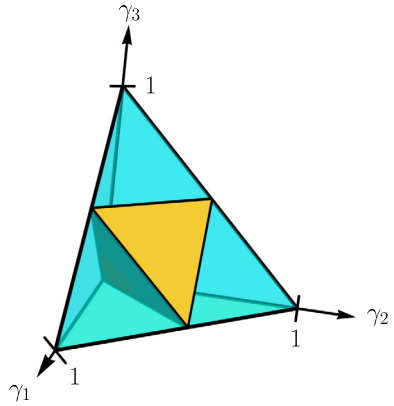

Fig. 3. Parameter space of γ_1, γ_2 and γ_3. For the generator $\mathcal{L}_{\rm P}$ in Eq. (43) to be positive, all elements γ_j must be positive (blue transparent color). For $\mathcal{L}_{\rm P}$ to be completely positive, the elements γ_j must fulfill the conditions in Eq. (48). The corresponding region is colored in orange. Note that we show a cut through the regions of positivity and complete positivity which really extend towards arbitrary large positive values.

$$\begin{aligned} D_{22} &= \frac{\gamma_3 - \tau_3}{2}\,, & D_{33} &= \frac{\gamma_3 + \tau_3}{2}\,, & H_{22} &= H_{11}\,, \\ D_{11} &= \frac{\gamma_1 + \gamma_2 - \gamma_3}{2}\,, & D_{23} &= \frac{\gamma_2 - \gamma_1}{2}\,, & H_{12} &= 0\,, \\ D_{21} &= \frac{\tau_1 + \mathrm{i}\tau_2}{2\sqrt{2}} = -D_{13}\,. \end{aligned} \tag{46}$$

This yields

$$C_\perp = \frac{1}{2}\begin{pmatrix} \gamma_1 + \gamma_2 - \gamma_3 & w^* & -w \\ w & \gamma_3 - \tau_3 & \gamma_2 - \gamma_1 \\ -w^* & \gamma_2 - \gamma_1 & \gamma_3 + \tau_3 \end{pmatrix}\,, \tag{47}$$

with $w = (\tau_1 + \mathrm{i}\tau_2)/\sqrt{2}$.

Complete positivity. The complete derivation can be found in Appendix C. It yields separate conditions for the diagonal elements γ_j and the vector $\vec{\tau}$. For the diagonal elements γ_j we find:

$$\forall\, i \neq j \neq k \neq i \ : \ |\gamma_i - \gamma_j| \leq \gamma_k \leq \gamma_i + \gamma_j\,. \tag{48}$$

The corresponding region in the parameter space of the elements γ_j is depicted as a orange region in Fig. 3. Assuming these conditions are fulfilled, the vector $\vec{\tau}$ must lie inside the following ellipsoid:

$$\begin{aligned} &\frac{\tau_1^2}{a_1^2} + \frac{\tau_2^2}{a_2^2} + \frac{\tau_3^2}{a_3^2} \leq 1\,, \qquad a_1 = \gamma_1^2 - (\gamma_2 - \gamma_3)^2\,, \\ &a_2 = \gamma_2^2 - (\gamma_1 - \gamma_3)^2\,, \quad a_3 = \gamma_3^2 - (\gamma_1 - \gamma_2)^2\,. \end{aligned} \tag{49}$$

The regions of $\vec{\tau}$ where the generator $\mathcal{L}_{\rm P}$ fulfills the conditions of complete positivity are shown in Fig. 4 in orange. Note that in this figure, we consider two particular cases, where $\gamma_1 = \gamma_2$ such that the resulting ellipsoid as defined above is symmetric with respect to the τ_3 axis.

Positivity. In the general expression for $p(\theta, \beta)$ in Eq. (24), we replace the parameters with those from the Pauli channel, given in Eq. (46). This yields

$$\begin{aligned} 2\,p(\theta,\beta) = {} & \gamma_3\,\cos^2\theta + \left[\,\gamma_1\,\cos^2\beta + \gamma_2\,\sin^2\beta\,\right]\sin^2\theta \\ & + \tau_3\,\cos\theta + \left(\,\tau_1\,\cos\beta + \tau_2\,\sin\beta\,\right)\sin\theta\,. \end{aligned} \tag{50}$$

We can express the general inequality $2\,p(\theta, \beta) \geq 0$ in a geometric form:

Please cite this article in press as: G. Montes Cabrera et al., Positivity and complete positivity of differentiable quantum processes, Phys. Lett. A (2019), https://doi.org/10.1016/j.physleta.2019.05.049

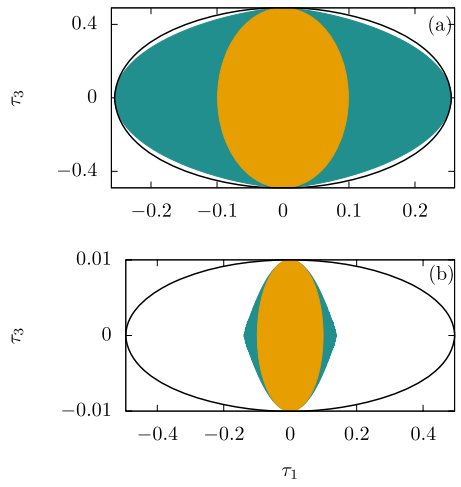

Fig. 4. Comparison of the region of positivity and complete positivity in the parameter space of $\vec{\tau}$ for $\gamma_1 = \gamma_2$. The black solid line shows the ellipsoid $\vec{\tau} = \underline{\gamma}\,\vec{e}_r$, the orange region shows the region of complete positivity, the green region (including orange) the region of positivity. In panel (a), $\gamma_1 = 0.255, \gamma_3 = 0.49$ which amounts to an ellipsoid of the shape of a rugby ball, in panel (b) $\gamma_1 = 0.495, \gamma_3 = 0.01$ where the ellipsoid looks more like a pancake.

$$\vec{e}_r = \begin{pmatrix} \sin\theta\,\cos\beta \\ \sin\theta\,\sin\beta \\ \cos\theta \end{pmatrix} \quad : \quad \vec{e}_r \cdot \left(\underline{\gamma}\,\vec{e}_r + \vec{\tau}\right) \geq 0\,, \tag{51}$$

where $\underline{\gamma}$ is the diagonal matrix with elements γ_j.

The interpretation of this result is easy: $-\underline{\gamma}\,\vec{e}_r + \vec{\tau}$ is the image of $\vec{e}_r$ under the generator $\mathcal{L}_P$. Thus an infinitesimal intermediate map would yield

$$\Lambda_{t,t+\delta} \;:\; \vec{e}_r \to \vec{e}_r{}' = \vec{e}_r + \delta\,\mathcal{L}_P[\vec{e}_r]\,.$$

In order to have $\|\vec{e}_r{}'\| \leq 1$, the image under the generator must be pointing towards the center of the Bloch sphere, i.e. the scalar product between $-\underline{\gamma}\,\vec{e}_r + \vec{\tau}$ and $\vec{e}_r$ must be negative. Multiplying the resulting inequality by minus one, we find

$$\forall \vec{e}_r \;:\; \vec{e}_r \cdot \left(\underline{\gamma}\,\vec{e}_r - \vec{\tau}\right) \geq 0\,.$$

This relation is equivalent to the inequality in Eq. (51), as can be seen by replacing $\vec{e}_r$ by $-\vec{e}_r$.

As shown in Appendix D, the set of $\vec{\tau}$ for which the Pauli generator $\mathcal{L}_P$ is positive, i.e. the inequality in Eq. (51) holds, is the convex region, which contains the origin and is limited by the surface [see Eq. (D.2)]

$$\mathcal{T} = \{\vec{\tau}(\theta,\beta) = (\vec{e}_r \cdot \underline{\gamma}\,\vec{e}_r)\,\vec{e}_r - 2\,\underline{\gamma}\vec{e}_r\}\,. \tag{52}$$

In Fig. 4, we show the region in $\vec{\tau}$-space which corresponds to positivity and complete positivity of the Pauli channel generator $\mathcal{L}_P$. We consider two cases: $\gamma_1 = \gamma_2 = 0.255$, $\gamma_3 = 0.49$ in panel (a), and $\gamma_1 = \gamma_2 = 0.495$, $\gamma_3 = 0.01$ in panel (b). In the yellow triangle shown in Fig. 3, these points are located near the upper horizontal line (a) and near the lower corner (b), respectively. Choosing $\gamma_1 = \gamma_2$ leads to regions of (complete) positivity, which are symmetric with respect to the τ_3-axis, which allows us to show two-dimensional projections. We find that the regions of positivity and complete positivity are always contained in ellipsoid with the parametrization $\vec{\tau}(\theta,\beta) = \underline{\gamma}\,\vec{e}_r$. As required, the region of complete positivity (orange) is fully contained in the region of positivity (olive green). In panel (a), we show a case where the ellipsoid $\underline{\gamma}\,\vec{e}_r$ resemble roughly a rugby ball. In that case, the are only rather thin stripes near the border of the ellipsoid, where the generator is not positive any more. In panel (b), the ellipsoid has the shape of a flat pancake, and the region of positivity in the center is much smaller.

5. Conclusions

In order to determine whether a given differentiable quantum process is CP-divisible and/or P-divisible, we derive criteria to be applied to the generator of the process. For the single qubit case, we discuss three common representations of the generator and work out the one-to-one mappings between them. We find criteria for CP- and P-divisibility, which can be expressed as inequalities in terms of the elements of the dissipation matrix. In the CP case, we avoid solving an eigenvalue problem by using the principal minor test for semidefinite matrices. In the P case, the corresponding inequality must be fulfilled for a whole two-parameter family of functions, which leads to an optimization problem without explicit general solution.

We then discuss three different classes of generators, where our criteria do yield explicit results: the familiar X-shaped channels where the elements of the Choi matrix are non-zero in the diagonal and the anti-diagonal, only; the so called O-shaped channels, where $C_{23} = 0$, $C_{11} = C_{44}$ and $C_{12} = -C_{34}$; and most importantly the non-unital Pauli channels.

Besides its general value, as for instance the positivity criteria for the Pauli channel, we expect our results to prove useful in the area of quantum process tomography and the construction of optimal P-divisible or CP-divisible approximations to non-Markovian quantum processes. In particular there, the renouncement on the calculation of higher order roots may help to find analytical or semi-analytical solutions.

Acknowledgements

We gratefully acknowledge Sergey Filippov for useful discussions, as well as Carlos Pineda for valuable comments on the manuscript.

Appendix A. Positivity of X-shaped generators

The condition in Eq. (31) can be expressed equivalently in terms of the variable $x = \cos\theta$ as follows:

$$\forall\, x \in [-1,1] \;:$$

$$f(x) = (R - A_{\min})\,x^2 + S\,x + A_{\min} \geq 0\,. \tag{A.1}$$

First note the following obviously necessary conditions

$$f(0) \;:\; A_{\min} \geq 0 \quad \text{and}$$

$$f(\pm 1) \;:\; R \pm S \geq 0 \quad \Leftrightarrow \quad 0 \leq |S| \leq R\,. \tag{A.2}$$

To find the necessary and sufficient conditions, we will divide the problem in two cases: (i) $\Delta = R - A_{\min} \leq 0$ and (ii) $\Delta > 0$.

In case (i) the conditions in Eq. (A.2) are also sufficient as can be seen as follows: $f(x)$ is convex, such that for any x_1, x_2 and $0 < \lambda < 1$:

$$f(\lambda\,x_1 + (1-\lambda)\,x_2) \geq \lambda\,f(x_1) + (1-\lambda)\,f(x_2)\,.$$

Choosing $x_1 = -1$ and $x_2 = 1$, we find

$$f(1 - 2\lambda) \geq \lambda\,f(-1) + (1-\lambda)\,f(1)\,,$$

which implies that $f(x) \geq 0$ in the interval $(-1,1)$.

In case (ii) $\Delta > 0$, the conditions in Eq. (A.2) are not sufficient. In this case, positivity requires that either $f(x)$ has no zeros, or its zeros

$$x_{1,2} = -\frac{S}{2\Delta} \pm \sqrt{\frac{S^2}{\Delta^2} - \frac{4\,A_{\min}}{\Delta}}\,,$$

are lying both to the left or both to the right of the interval (-1.1). This can be expressed as

$$|S| \leq 2\sqrt{A_{\min}\,\Delta} \quad \text{or} \quad |S| \geq 2\Delta + \sqrt{S^2 - 4A_{\min}\,\Delta}\,.$$

Please cite this article in press as: G. Montes Cabrera et al., Positivity and complete positivity of differentiable quantum processes, Phys. Lett. A (2019), https://doi.org/10.1016/j.physleta.2019.05.049

The inequality to the right is equivalent to

$$|S| \geq 2\Delta \quad \text{and} \quad (|S| - 2\Delta)^2 \geq S^2 - 4A_{\min}\Delta\,,$$

which is equivalent to

$$|S| \geq 2\Delta \quad \text{and} \quad |S| \leq R\,,$$

where $|S| \leq R$ had already been identified as a necessary condition, previously. Therefore, in case (ii) the necessary and sufficient conditions for positivity are $A_{\min} \geq 0\,, \quad 0 \leq |S| \leq R$ and

$$|S| \leq 2\sqrt{A_{\min}\Delta} \quad \text{or} \quad |S| \geq 2\Delta\,.$$

It turns out that for $\Delta \leq A_{\min}$ it holds that $2\sqrt{A_{\min}\Delta} < 2\Delta$ such that the two conditions cancel each other, i.e. one of the two conditions is always fulfilled. For $\Delta > A_{\min}$ which is equivalent to $2\Delta > R$, by contrast, implies that $|S| \geq 2\Delta$ cannot hold, such that $|S| \leq 2\sqrt{A_{\min}\Delta}$ must be fulfilled. To summarize, the necessary and sufficient conditions for positivity are as follows:

- $A_{\min} = \mathrm{Re}\, Z_1 - |Z_2| \geq 0\,, \quad 0 \leq |S| \leq R.$
- In addition, if $R > 2A_{\min}$:

$$|S| \leq 2\sqrt{A_{\min}(R - A_{\min})}\,.$$

For the parametrization in terms of the master equation, we find that positivity only depends on the dissipation matrix D. Since

$$R = D_{33} + D_{22}\,, \quad S = D_{22} - D_{33}\,, \tag{A.3}$$

the condition $0 \leq |S| \leq R$ implies that both D_{22} and D_{33} must be larger than or equal to zero. Furthermore, with

$$A_{\min} = D_{11} + \frac{D_{33} + D_{22}}{2} - |D_{32}|\,, \tag{A.4}$$

the condition $R > 2\,A_{\min}$ implies that $|D_{32}| > D_{11}$. Finally,

$$\begin{aligned} A_{\min}(R - A_{\min}) &= \Big[\frac{D_{33} + D_{22}}{2} - \big(|D_{32}| - D_{11}\big)\Big] \times \\ &\quad \Big[\frac{D_{33} + D_{22}}{2} + \big(|D_{32}| - D_{11}\big)\Big] \\ &= \frac{(D_{33} + D_{22})^2}{4} - \big(|D_{32}| - D_{11}\big)^2\,, \end{aligned} \tag{A.5}$$

such that $|S| \leq 2\sqrt{A_{\min}(R - A_{\min})}$ is equivalent to

$$\begin{aligned} &|D_{22} - D_{33}|^2 \leq (D_{33} + D_{22})^2 - 4\big(|D_{32}| - D_{11}\big)^2 \\ \Leftrightarrow \quad &\big(|D_{32}| - D_{11}\big)^2 \leq D_{33}\,D_{22}\,. \end{aligned} \tag{A.6}$$

To summarize, in this parametrization, the conditions for positivity read

$$D_{22}, D_{33} \geq 0\,, \quad D_{11} - |D_{32}| + \frac{D_{33} + D_{22}}{2} \geq 0 \tag{A.7}$$

and if $D_{11} < |D_{32}|$, in addition

$$\big|\,|D_{32}| - D_{11}\big| \leq \sqrt{D_{33}\,D_{22}}\,. \tag{A.8}$$

Note that this last inequality implies the second inequality of Eq. (A.7), which can therefore be ignored.

Appendix B. Positivity of *O*-shaped generators

We start from the condition for positivity in Eq. (39). Using the trigonometric identities $2\sin^2\theta = 1 - \cos 2\theta$ and $\sin 2\theta = 2\sin\theta\cos\theta$, Eq. (39) becomes

$$\begin{aligned} 2p(\theta,\beta) = \frac{3D_{22} + D_{11}}{2} + \frac{D_{22} - D_{11}}{2}\,\cos 2\theta \\ - \sqrt{2}\,\mathrm{Re}\big(D_{12}\,\mathrm{e}^{-\mathrm{i}\beta}\big)\,\sin 2\theta \geq 0\,. \end{aligned} \tag{B.1}$$

This expression is minimized with respect to β, simply by making sure that $\mathrm{Re}(D_{12}\,\mathrm{e}^{-\mathrm{i}\beta}) = \pm|D_{12}|$. In other words: $2p(\theta,\beta) \geq 0$ for all β and θ is equivalent to

$$\frac{3D_{22} + D_{11}}{2} + \frac{D_{22} - D_{11}}{2}\,\cos 2\theta \pm \sqrt{2}\,|D_{12}|\,\sin 2\theta \geq 0\,. \tag{B.2}$$

This condition is equivalent to

$$\begin{aligned} &\frac{3D_{22} + D_{11}}{2} \geq 0 \quad \text{and} \\ &\frac{(3D_{22} + D_{11})^2}{4} \geq \frac{(D_{22} - D_{11})^2}{4} + 2|D_{12}|^2 \end{aligned} \tag{B.3}$$

These two inequalities are equivalent to

$$3D_{22} + D_{11} \geq 0 \quad \text{and} \quad D_{22}\,(D_{22} + D_{11}) \geq |D_{12}|^2 \tag{B.4}$$

Appendix C. Complete positivity of the non-unital anisotropic Pauli channel

For the generator $\mathcal{L}_{\mathrm{P}}$ to be completely positive, the matrix $C_\perp$ given in Eq. (47) must fulfill the inequalities in Eq. (21). In the present case, this yields three sets of inequalities:

$$\begin{aligned} &\gamma_1 + \gamma_2 - \gamma_3 \geq 0\,, \quad \gamma_3 - \tau_3 \geq 0\,, \quad \gamma_3 + \tau_3 \geq 0\,, \\ &(\gamma_3 - \tau_3)(\gamma_3 + \tau_3) - (\gamma_2 - \gamma_1)^2 \geq 0\,, \end{aligned} \tag{C.1}$$

$$\begin{aligned} &(\gamma_1 + \gamma_2 - \gamma_3)(\gamma_3 - \tau_3) - |w|^2 \geq 0\,, \\ &(\gamma_1 + \gamma_2 - \gamma_3)(\gamma_3 + \tau_3) - |w|^2 \geq 0\,, \end{aligned} \tag{C.2}$$

and

$$\begin{aligned} &(\gamma_1 + \gamma_2 - \gamma_3)\left[(\gamma_3 - \tau_3)(\gamma_3 + \tau_3) - (\gamma_2 - \gamma_1)^2\right] \\ &\quad - w\,\left[w^*(\gamma_3 + \tau_3) + w(\gamma_2 - \gamma_1)\right] \\ &\quad - w^*\left[w^*(\gamma_2 - \gamma_1) + w(\gamma_3 - \tau_3)\right] \geq 0\,, \end{aligned} \tag{C.3}$$

where $w = (\tau_1 + \mathrm{i}\,\tau_2)/\sqrt{2}$. From Eq. (C.1), we find

$$\gamma_3 \geq |\tau_3| \geq 0\,, \quad \gamma_1 + \gamma_2 \geq \gamma_3\,, \quad (\gamma_2 - \gamma_1)^2 \leq \gamma_3^2 - \tau_3^2\,,$$

which yields the following conditions as necessary conditions (since we set $\tau_3 = 0$ to arrive there):

$$\gamma_1, \gamma_2, \gamma_3 \geq 0\,, \quad |\gamma_2 - \gamma_1| \leq \gamma_3 \leq \gamma_1 + \gamma_2\,. \tag{C.4}$$

It is easy to verify that these inequalities are invariant under any permutation of indices; see Fig. 3. The remaining conditions, may be interpreted as conditions for the vector $\vec{\tau}$. These consist of the inequalities in Eq. (C.2) together with

$$|\tau_3| \leq \sqrt{\gamma_3^2 - (\gamma_2 - \gamma_1)^2}\,, \quad \text{and} \tag{C.5}$$

$$\begin{aligned} &(\gamma_1 + \gamma_2 - \gamma_3)\,(\gamma_2 + \gamma_3 - \gamma_1)\,(\gamma_3 + \gamma_1 - \gamma_2) \geq \\ &(\gamma_1 + \gamma_2 - \gamma_3)\,\tau_3^2 + (\gamma_2 + \gamma_3 - \gamma_1)\,\tau_1^2 + (\gamma_3 + \gamma_1 - \gamma_2)\,\tau_2^2\,. \end{aligned} \tag{C.6}$$

In Appendix C.1 we demonstrate that condition (C.6) implies all other conditions for the vector τ, which can therefore be omitted. Reorganizing the terms in Eq. (C.6), we arrive at

$$\begin{aligned} &\frac{\tau_1^2}{a_1^2} + \frac{\tau_2^2}{a_2^2} + \frac{\tau_3^2}{a_3^2} \leq 1\,, \qquad a_1 = \gamma_1^2 - (\gamma_2 - \gamma_3)^2\,, \\ &a_2 = \gamma_2^2 - (\gamma_1 - \gamma_3)^2\,, \quad a_3 = \gamma_3^2 - (\gamma_1 - \gamma_2)^2\,. \end{aligned} \tag{C.7}$$

Please cite this article in press as: G. Montes Cabrera et al., Positivity and complete positivity of differentiable quantum processes, Phys. Lett. A (2019), https://doi.org/10.1016/j.physleta.2019.05.049

Appendix C.1. Omissible inequalities for $\vec{\tau}$

In what follows, we demonstrate that Eq. (C.5) as well as Eq. (C.2) follow from Eq. (C.7) such that we may consider Eq. (C.7) as the only condition on $\vec{\tau}$. To that end note first that setting $\tau_1 = \tau_2 = 0$ we can make the LHS of Eq. (C.7) only smaller which hence implies

$$\tau_3^2 \leq a_3^2 = \gamma_3^2 - (\gamma_1 - \gamma_2)^2 \,,$$

which is exactly Eq. (C.5). To show that Eq. (C.7) also implies Eq. (C.2), it is convenient to express $\vec{\tau}$ in elliptical coordinates,

$$\vec{\tau} = \lambda \begin{pmatrix} a_1 \sin\theta \cos\varphi \\ a_2 \sin\theta \sin\varphi \\ a_3 \cos\theta \end{pmatrix} ,$$

such that Eq. (C.7) allows arbitrary values for the angles θ, φ and limits λ to the range $0 \leq \lambda \leq 1$.

The two inequalities in Eq. (C.2) may be combined, and then read

$$\gamma_3 \pm \lambda a_3 \cos\theta \geq \frac{\lambda^2 \sin^2\theta \,(a_1^2 \cos^2\varphi + a_2^2 \sin^2\varphi)}{2\,(\gamma_1 + \gamma_2 - \gamma_3)} \,.$$

Since a_1^2 and a_2^2 have the common factor $(\gamma_1 + \gamma_2 - \gamma_3)$ this inequality simplifies to

$$\begin{aligned}(\gamma_3 \pm \lambda a_3 \cos\theta) &\geq \frac{\lambda^2 \sin^2\theta}{2} \big[(\gamma_3 + \gamma_1 - \gamma_2)\cos^2\varphi \\ &\qquad + (\gamma_3 - \gamma_1 + \gamma_2)\sin^2\varphi\big] \\ &= \frac{\lambda^2 \sin^2\theta}{2} \big[\gamma_3 + (\gamma_1 - \gamma_2)\cos(2\varphi)\big] \qquad \text{(C.8)}\end{aligned}$$

Due to the conditions in Eq. (C.7), we may assume that $\gamma_3 \geq a_3$ and $\gamma_3 \geq |\gamma_1 - \gamma_2|$. Therefore, in order to show that Eq. (C.2) holds, it is sufficient to prove that

$$\gamma_3 \pm \lambda a_3 \cos\theta \geq \frac{\lambda^2 \sin^2\theta}{2} \big[\gamma_3 + |\gamma_1 - \gamma_2|\big] \,.$$

For that purpose, we substitute $x = \cos\theta$ to obtain a quadratic expression:

$$A\,x^2 \pm \lambda a_3\, x + \gamma_3 - A \geq 0 \,, \quad A = \frac{\lambda^2}{2}\big[\gamma_3 + |\gamma_1 - \gamma_2|\big] \,.$$

The LHS describes a parabola. Therefore, the inequality holds, if we can prove that the equation $A\,x^2 \pm \lambda a_3\, x + \gamma_3 - A = 0$ has no solution or at most one solution. For that purpose we consider the discriminant and show that it is less or equal to zero. For later convenience, we define $g_\pm = \lambda_3 \pm |\gamma_1 - \gamma_2|$. Then we may write:

$$\begin{aligned} & \lambda^2 a_3^2 - 4A\,(\gamma_3 - A) \leq 0 \\ \Leftarrow \quad & a_3^2 - g_+\,(2\gamma_3 - \lambda^2 g_+) \leq 0 \,, \quad A = \frac{\lambda^2 g_+}{2} \\ \Leftarrow \quad & g_+ g_- - 2g_+\gamma_3 + \lambda^2 g_+^2 \leq 0 \,, \quad a_3^2 = g_+ g_- \\ \Leftarrow \quad & g_- - 2\gamma_3 + \lambda^2 g_+ \leq 0 \\ \Leftarrow \quad & -g_+(1 - \lambda^2) \leq 0 \,, \quad g_- - 2\lambda_3 = -g_+ \,. \end{aligned}$$

This completes the proof. The discriminant is negative semidefinite. Therefore the two inequalities in Eq. (C.2) are always fulfilled and can be omitted.

Appendix D. Positivity of the non-unital anisotropic Pauli channel

We start from the condition, given in Eq. (51),

$$\vec{e}_r \cdot (\underline{\gamma}\,\vec{e}_r + \vec{\tau}\,) \geq 0 \,,$$

where $\vec{e}_r$ is a unit vector in spherical coordinates, parametrized by the angles θ, β. We aim at constructing the surface $\mathcal{T}$ which forms the outer boundary of the region of points $\vec{\tau}$, where the above inequality holds (note that this region contains the origin $\vec{\tau} = \vec{o}$, and that it must be convex[1]). The condition for $\vec{\tau} \in \mathcal{T}$ can be cast into the following set of equations:

$$\begin{aligned} & \vec{e}_r \cdot (\underline{\gamma}\,\vec{e}_r + \vec{\tau}\,) = 0 \\ & \frac{\partial}{\partial\theta}\,\vec{e}_r \cdot (\underline{\gamma}\,\vec{e}_r + \vec{\tau}\,) = 0 \\ & \frac{\partial}{\partial\beta}\,\vec{e}_r \cdot (\underline{\gamma}\,\vec{e}_r + \vec{\tau}\,) = 0 \,. \end{aligned} \qquad \text{(D.1)}$$

The argument is as follows: Consider the LHS of the first equation as a function $f(\vec{\tau}, \theta, \beta)$, then we may compute

$$f_{\max}(\vec{\tau}) = \max_{\theta,\beta} f(\vec{\tau}, \theta, \beta) \,,$$

by finding the critical points (there may be more than one) (θ_i, β_i), where the last two equalities of Eq. (D.1) hold. Typically, for some fixed but arbitrary point $\vec{\tau}$, some of the values of $\{f(\vec{\tau}, \theta_i, \beta_i)\}$ may be positive and others negative; some may correspond to local maxima, others to local minima, and still others may correspond neither to one nor to the other group. However, the global maximum will always be among these points.

The calculation of the partial derivatives is simplified by the fact that

$$\begin{aligned} \frac{\partial\,\vec{e}_r}{\partial\theta} &= \begin{pmatrix} \cos\theta\cos\beta \\ \cos\theta\sin\beta \\ -\sin\theta \end{pmatrix} = \vec{e}_\theta \,, \\ \frac{\partial\,\vec{e}_r}{\partial\beta} &= \begin{pmatrix} -\sin\theta\sin\beta \\ \sin\theta\cos\beta \\ 0 \end{pmatrix} = \sin\theta\,\vec{e}_\beta \,, \end{aligned}$$

such that $\{\vec{e}_r, \vec{e}_\theta, \vec{e}_\beta\}$ form a system of orthonormal vectors. Therefore the system of equations in Eq. (D.1) becomes

$$\begin{aligned} \vec{e}_r \cdot (\underline{\gamma}\,\vec{e}_r + \vec{\tau}\,) &= 0 \\ \vec{e}_\theta \cdot (\underline{\gamma}\,\vec{e}_r + \vec{\tau}\,) + \vec{e}_r \cdot \underline{\gamma}\,\vec{e}_\theta &= 0 \\ \vec{e}_\beta \cdot (\underline{\gamma}\,\vec{e}_r + \vec{\tau}\,) + \vec{e}_r \cdot \underline{\gamma}\,\vec{e}_\beta &= 0 \,, \end{aligned}$$

which is equivalent to

$$\begin{aligned} \vec{e}_r \cdot (\underline{\gamma}\,\vec{e}_r + \vec{\tau}\,) &= 0 \\ \vec{e}_\theta \cdot (2\,\underline{\gamma}\,\vec{e}_r + \vec{\tau}\,) &= 0 \\ \sin\theta\,\vec{e}_\beta \cdot (2\,\underline{\gamma}\,\vec{e}_r + \vec{\tau}\,) &= 0 \,. \end{aligned}$$

We started by asking for which points $\vec{\tau}$, there exist a critical point (θ_i, β_i) corresponding to a global maximum such that this set of equations is fulfilled. That point would then fore sure belong to the desired surface $\mathcal{T}$. However, starting from this relation, we may say that it assigns to any pair of angles (θ, β), a unique $\vec{\tau}$, such that that pair of angles is a critical point (of any nature), while

[1] For fixed R, two different quantum generators $\mathcal{L}_1, \mathcal{L}_2$ are given by $\vec{\tau}_1$ and $\vec{\tau}_2$, and any intermediate generator $\lambda\,\mathcal{L}_1 + (1-\lambda)\,\mathcal{L}_2$ is given by $\lambda\,\vec{\tau}_1 + (1-\lambda)\,\vec{\tau}_2$.

Please cite this article in press as: G. Montes Cabrera et al., Positivity and complete positivity of differentiable quantum processes, Phys. Lett. A (2019), https://doi.org/10.1016/j.physleta.2019.05.049

$f(\vec{\tau},\theta,\beta)=0$. That means that for $\vec{\tau}\in\mathcal{T}$, it is a necessary but not sufficient condition that it satisfies this equation for some pair of angles (θ,β). Therefore, the surface $\mathcal{T}$ must be a subset of the set of solutions $\vec{\tau}$ to this equation.

The last to equalities imply that $2\underline{\gamma}\,\vec{e}_r+\vec{\tau}=\alpha\,\vec{e}_r$ for some unknown real parameter α. Inserting this into the first equality, we obtain

$$\vec{e}_r\cdot(\alpha\,\vec{e}_r-\underline{\gamma}\,\vec{e}_r)=0 \quad\Rightarrow\quad \alpha=\vec{e}_r\cdot\underline{\gamma}\,\vec{e}_r\,,$$

and finally

$$\vec{\tau}=(\vec{e}_r\cdot\underline{\gamma}\,\vec{e}_r)\,\vec{e}_r-2\,\underline{\gamma}\,\vec{e}_r\,. \tag{D.2}$$

Appendix E. Canonical form of quantum process generators

Here, we prove that the dissipation matrix D, introduced in Eq. (6) is unitarily equivalent to $C_\perp$, defined in Sec. 2.2. For that purpose, we start from the master equation representation of the generator $\mathcal{L}$ of a quantum process, compute its Choi-matrix representation $C_\mathcal{L}$. Finally, we compute $C_\perp$, the projection of $C_\mathcal{L}$ onto the subspace orthogonal to the Bell state, given in Eq. (7).

We start by rewriting Eq. (6) as

$$\mathcal{L}[\varrho]=\phi[\varrho]-\kappa\,\varrho-\varrho\,\kappa^\dagger\,,\quad\text{where} \tag{E.1}$$

$$\phi[\varrho]=\sum_{i,j=1}^{d^2-1}D_{ij}\,F_i\,\varrho\,F_j^\dagger\,,\quad \kappa=\mathrm{i}\,H+\frac{1}{2}\sum_{i,j=1}^{d^2-1}D_{ij}\,F_j^\dagger F_i\,.$$

To shorten the notation, we introduce the projector on the Bell state, as $\omega=|\Phi_\mathrm{B}\rangle\langle\Phi_\mathrm{B}|$ and the projector on the complementary subspace as $\omega_\perp=\mathbb{1}-\omega$. We find,

$$d\,(\mathrm{id}\otimes\mathcal{L})[w]=d\,(\mathrm{id}\otimes\phi)[w]-\mathrm{id}\otimes\kappa\,w-w\,\mathrm{id}\otimes\kappa^\dagger\,,$$

and therefore

$$\omega_\perp\,C_\mathcal{L}\,\omega_\perp=d\,\omega_\perp\,(\mathrm{id}\otimes\phi)[w]\,\omega_\perp=C_\phi\,, \tag{E.2}$$

the Choi-matrix representation of the map $\phi[\varrho]$. The latter equality means that C_ϕ already is orthogonal to w. This can be seen from

$$\begin{aligned}\omega\,(\mathrm{id}\otimes\phi)[\omega]&=\sum_{i,j=1}^{d^2-1}D_{ij}\,\omega\,(\mathbb{1}\otimes F_i)\,\omega\,(\mathbb{1}\otimes F_j^\dagger)\\&=\sum_{i,j=1}^{d^2-1}D_{ij}\,\mathrm{tr}(F_i)\,\omega\,(\mathbb{1}\otimes F_j^\dagger)=\mathbf{0}\,,\end{aligned} \tag{E.3}$$

and similarly $(\mathrm{id}\otimes\phi)[\omega]\,\omega=\mathbf{0}$, also.

Finally, we consider the matrix representation $C_\perp$ of C_ϕ, with respect to a basis $\{|\phi_i\rangle\}_{i=1}^{d^2-1}$ orthogonal to $|\Phi_\mathrm{B}\rangle$. Then, we prove that $C_\perp$ is related to D by an unitary transformation. For that purpose, consider the matrix elements of $C_\perp$, given by

$$\begin{aligned}(C_\perp)_{nm}&=\langle\phi_n|C_\perp|\phi_m\rangle=d\,\langle\phi_n|\,(\mathrm{id}\otimes\phi[\omega])\,|\phi_m\rangle\\&=d\sum_{i,j=1}^{d^2-1}D_{ij}\,a_i a_j\,\langle\phi_n|\Phi^{(i)}\rangle\langle\Phi^{(j)}|\phi_m\rangle,\end{aligned} \tag{E.4}$$

with $\sqrt{a_i}\,|\Phi^{(i)}\rangle=\mathbb{1}\otimes F_i\,|\Phi_\mathrm{B}\rangle$ and $a_i=\|(\mathbb{1}\otimes F_i)\,\Phi_\mathrm{B}\|^2$. Now observe that

$$\langle\Phi^{(i)}|\Phi^{(j)}\rangle=\langle\Phi_\mathrm{B}|\mathbb{1}\otimes F_i^\dagger F_j|\Phi_\mathrm{B}\rangle=\frac{1}{d}\mathrm{tr}\left(F_i^\dagger F_j\right)=\frac{1}{d}\delta_{ij}\,,$$

thus $a_i=\frac{1}{d}$, independent of i. Defining $V_{ni}=\langle\phi_n|\Phi^{(i)}\rangle$ and substituting the value of a_i in Eq. (E.4) we end up with

$$C_\perp=V\,D\,V^\dagger\,,$$

with V unitary, given that $|\phi_n\rangle$ and $|\Phi^{(i)}\rangle$ are properly normalized quantum states.

References

[1] H.-P. Breuer, Foundations and measures of quantum non-Markovianity, J. Phys. B, At. Mol. Opt. Phys. 45 (2012) 154001.
[2] Á. Rivas, S.F. Huelga, M.B. Plenio, Quantum non-Markovianity: characterization, quantification and detection, Rep. Prog. Phys. 77 (2014) 094001.
[3] L. Li, M.J. Hall, H.M. Wiseman, Concepts of quantum non-Markovianity: a hierarchy, Phys. Rep. 759 (2018) 1–51.
[4] H.-P. Breuer, E.-M. Laine, J. Piilo, Measure for the degree of non-Markovian behavior of quantum processes in open systems, Phys. Rev. Lett. 103 (2009) 210401.
[5] A. Rivas, S.F. Huelga, M.B. Plenio, Entanglement and non-Markovianity of quantum evolutions, Phys. Rev. Lett. 105 (2010) 050403.
[6] H.-P. Breuer, F. Petruccione, The Theory of Open Quantum Systems, Oxford University Press, New York, 2002.
[7] M. Wolf, J. Cirac, Dividing quantum channels, Commun. Math. Phys. 279 (2008) 147–168.
[8] M.M. Wolf, J. Eisert, T.S. Cubitt, J.I. Cirac, Assessing non-Markovian quantum dynamics, Phys. Rev. Lett. 101 (2008) 150402.
[9] F. Benatti, R. Floreanini, M. Piani, Quantum dynamical semigroups and non-decomposable positive maps, Phys. Lett. A 326 (2004) 187–198.
[10] D. Chruściński, S. Maniscalco, Degree of non-markovianity of quantum evolution, Phys. Rev. Lett. 112 (2014) 120404.
[11] S. Wißmann, H.-P. Breuer, B. Vacchini, Generalized trace-distance measure connecting quantum and classical non-Markovianity, Phys. Rev. A 92 (2015) 042108.
[12] D. Chruściński, A. Kossakowski, A. Rivas, Measures of non-markovianity: divisibility versus backflow of information, Phys. Rev. A 83 (2011) 052128.
[13] M.J.W. Hall, Complete positivity for time-dependent qubit master equations, J. Phys. A, Math. Theor. 41 (2008) 205302.
[14] M.A. Nielsen, I.L. Chuang, Quantum Computation and Quantum Information, Cambridge University Press, Cambridge, 2000.
[15] N. Boulant, T.F. Havel, M.A. Pravia, D.G. Cory, Robust method for estimating the Lindblad operators of a dissipative quantum process from measurements of the density operator at multiple time points, Phys. Rev. A 67 (2003) 042322.
[16] J.M. Dominy, L.C. Venuti, A. Shabani, D.A. Lidar, Evolution prediction from tomography, Quantum Inf. Process. 16 (2017) 78.
[17] D. Chruściński, S. Pascazio, A brief history of the GKLS equation, Open Syst. Inf. Dyn. 24 (2017) 1740001.
[18] C.D. Meyer, Matrix Analysis and Applied Linear Algebra, SIAM, Philadelphia, 2000.
[19] J.E. Prussing, The principal minor test for semidefinite matrices, J. Guid. Control Dyn. 9 (1986) 121–122.
[20] J. Kołodyński, J.B. Brask, M. Perarnau-Llobet, B. Bylicka, Adding dynamical generators in quantum master equations, Phys. Rev. A 97 (2018) 062124.
[21] D. Chruściński, A. Rivas, E. Størmer, Divisibility and information flow notions of quantum Markovianity for noninvertible dynamical maps, Phys. Rev. Lett. 121 (2018) 080407.
[22] M.-D. Choi, Completely positive linear maps on complex matrices, Linear Algebra Appl. 10 (1975) 285–290.
[23] T. Heinosaari, M. Ziman, The Mathematical Language of Quantum Theory: From Uncertainty to Entanglement, Cambridge University Press, New York, 2011.
[24] D.E. Evans, J.T. Lewis, Dilations of Irreversible Evolutions in Algebraic Quantum Theory, Dublin Institute for Advanced Studies, Dublin, 1977.
[25] E.C.G. Sudarshan, P.M. Mathews, J. Rau, Stochastic dynamics of quantum-mechanical systems, Phys. Rev. 121 (1961) 920–924.
[26] V. Gorini, A. Kossakowski, E.C.G. Sudarshan, Completely positive dynamical semigroups of n-level systems, J. Math. Phys. 17 (1976) 821–825.
[27] G. Lindblad, On the generators of quantum dynamical semigroups, Commun. Math. Phys. 48 (1976) 119–130.
[28] M.J.W. Hall, J.D. Cresser, L. Li, E. Andersson, Canonical form of master equations and characterization of non-Markovianity, Phys. Rev. A 89 (2014) 042120.
[29] M. Žnidarič, Geometry of local quantum dissipation and fundamental limits to local cooling, Phys. Rev. A 91 (2015) 052107.
[30] M.B. Ruskai, S. Szarek, E. Werner, An analysis of completely-positive trace-preserving maps on $\mathcal{M}_2$, Linear Algebra Appl. 347 (2002) 159.
[31] D. Braun, O. Giraud, I. Nechita, C. Pellegrini, M. Žnidarič, A universal set of qubit quantum channels, J. Phys. A, Math. Theor. 47 (2014) 135302.
[32] I. Bengtsson, K. Zyczkowski, Geometry of Quantum States: An Introduction to Quantum Entanglement, Cambridge University Press, New York, 2006.

Please cite this article in press as: G. Montes Cabrera et al., Positivity and complete positivity of differentiable quantum processes, Phys. Lett. A (2019), https://doi.org/10.1016/j.physleta.2019.05.049

C.4 Article: Positivity and Complete positivity of differentiable quantum processes

Physical Review A 96, 062127 (2017). Click to go to the webpage, Click to go to arXiv.

Quantum non-Markovianity and localization

David Davalos[1] and Carlos Pineda[1,2]
[1]*Instituto de Física, Universidad Nacional Autónoma de México, México D. F. 01000, México*
[2]*University of Vienna, Faculty of Physics, Boltzmanngasse 5, 1090 Wien, Austria*
(Received 22 August 2017; published 21 December 2017)

We study the behavior of non-Markovianity with respect to the localization of the initial environmental state. The "amount" of non-Markovianity is measured using divisibility and distinguishability as indicators, employing several schemes to construct the measures. The system used is a qubit coupled to an environment modeled by an Ising spin chain kicked by ultrashort pulses of a magnetic field. In the integrable regime, non-Markovianity and localization do not have a simple relation, but as the chaotic regime is approached, simple relations emerge, which we explore in detail. We also study the non-Markovianity measures in the space of the parameters of the spin coherent states and point out that the pattern that appears is robust under the choice of the interaction Hamiltonian but does not have a classical-like phase-space structure.

DOI: 10.1103/PhysRevA.96.062127

I. INTRODUCTION

Open quantum systems were recognized as an important subfield of quantum mechanics early in their history [1], because understanding them allows one to explain ubiquitous phenomena, such as spontaneous decay [2]. Later, the Lindblad equation was proposed to describe the evolution of the reduced density matrix of a quantum system weakly coupled to a memoryless environment [3–5]. Environments that lie outside that approximation (Lindblad equation) have attracted the attention of the community in later years. This is, arguably, because we now have such delicate control of quantum systems that memory effects become experimentally relevant [6] and environment engineering is possible [7,8] to mitigate or even use such effects [6,9,10]. A whole community is now dedicated to the study of such systems, known as *non-Markovian* environments. Numerous efforts have been made to define non-Markovianity (NM) in a precise manner, to measure it, and to take advantage of it (see the previous review papers and Refs. [11,12]). Many systems have been studied under this program, both theoretically and experimentally [6].

Currently, there are many examples of non-Markovian environments that produce a variety of effects. However, not much is known regarding what the key properties that might boost the non-Markovianity of an environment are. Some properties, such as the structure of the phase space of the classical counterpart of the environment, have proven to be crucial; however, what happens when we do not find such a classical analog? In this paper, we focus on two questions. First, is the value of the several measures of non-Markovianity for long times only dependent on the effective dimension of the Hilbert space? Second, is there a hidden underlying classical structure in the environment that we can unveil with the help of these measures?

To study these questions, we consider a qubit coupled to a kicked spin chain, which has integrable, mixed, and chaotic dynamical regimes [13,14], but, as far as we know, no semiclassical analog. The interaction between qubit and environment is set up so as to have dephasing, so all the decoherence effects on the qubit are contained in a suitably defined fidelity of the environment. To quantify NM, we use two commonly used measures [15,16] and a third that was recently introduced and which has a direct relation with a physical task [11].

We find complex relations between NM and the localization of initial environmental states in the integrable and mixed regimes, which depend on the peculiarities of each NM measure. In fact, in Ref. [17] a relation between localization, induced by disordered, and a particular non-Markovianity measure was explored for an environment consisting of an array of cavities. In the case of the recently introduced measures [11], the effective dimension of the Hilbert space of the environmental states has an important role which leads to more complex behavior. In the chaotic regime, due to the ergodic properties of the Hamiltonian, the relation is simpler and almost homogeneous. Regarding the search for underlying classical structure, we focus our attention on the features that emerge in the space of the parameters of the initial states (spin coherent states) when the NM and the inverse participation ratio (IPR) [18] are calculated. We searched for the characteristic finely granulated fractal structure predicted by the Kolmogorov–Arnold–Moser (KAM) theorem but found only a coarse nonfractal one.

The paper is organized as follows. In Sec. II, we give a brief introduction to the measures used for non-Markovianity and for localization of quantum states. In Sec. III, we present the general scheme of dephasing dynamics and the details of the dynamics. In Sec. IV, we present and discuss the results. We finish by summarizing the results in Sec. V.

II. TOOLS

A. Identifying non-Markovianity

Many measures of non-Markovianity have been proposed: The two most widespread are the BLP (introduced by Breuer, Laine and Piilo in [15]) and RHP (introduced by Rivas, Huelga and Plenio in [16]) measures. The first is based on the violation of the contraction property of Markovian systems, i.e., decreasing distinguishability between initial quantum states. The second is based on the violation of a well-known mathematical property of Markovian process, divisibility of the quantum map. Both criteria come from the classical theory of Markovian stochastic process. A whole new set of measures

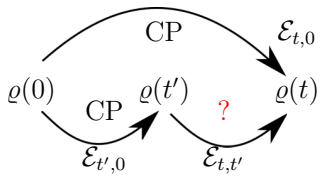

FIG. 1. Illustration of the concept of CP divisibility. The process $\mathcal{E}$ is CP divisible if all existing intermediate maps $\mathcal{E}_{(t,t')}$ are complete positive and trace preserving.

have been proposed [10]. One of these [11], proposed by the authors of this paper, is based on quantifying the probability of successfully performing a certain task.

It is hard to strictly verify if a stochastic system fulfills the classical definition of Markovianity [19], since it depends on the whole history of the stochastic process. An additional caveat for quantum systems is the fact that in order to observe intermediate states of the system, one would have to measure, thus collapsing the wave function and thus also the probability distributions. This leads, among other problems, to violation of Kolmogorov consistency conditions even for closed quantum systems [10].

One can, however, check the necessary conditions for Markovianity that can be easily interpreted from a physical point of view. For example, notice that a classical stochastic process (not necessarily Markovian) can be described by a time-dependent right stochastic matrix $A(t)$ that maps the initial probability distribution $\vec{p}(t=0)$ to $A(t)\vec{p}(0)=\vec{p}(t)$. Matrices describing the intermediate process, say the map from time t' to $t \geqslant t' \geqslant 0$, described by $A_{t,t'} \equiv A_{t,0}A_{t',0}^{-1}$, will also be right stochastic matrices for Markovian processes. We argue that the intermediate process is a valid one, and if $A_{t,t'}$ is right stochastic for all $t \geqslant t' \geqslant 0$, the process is said to be divisible. This construction can extended to the quantum case, replacing the divisibility concept with the *completely positive* map (CP map), which characterizes a valid quantum channel. Given a quantum process $\mathcal{E}_{t,0}$, we shall say that it is CP divisible if the intermediate dynamics

$$\mathcal{E}_{t,t'} \equiv \mathcal{E}_{t,0}\mathcal{E}_{t',0}^{-1}, \quad t \geqslant t' \geqslant 0 \tag{1}$$

are CP maps. Figure 1 illustrates the general idea for divisibility and CP divisibility. A general property of a CP-divisible process is that given any Hermitian operator Δ the trace norm decreases under the action of the map [9] $||\mathcal{E}(\Delta)||_1 \leqslant ||\Delta||_1$, where $||\cdot||_1$ is the *trace norm*. In particular, choosing $\Delta = 1/2(\varrho_1 - \varrho_2)$ we have

$$D(\mathcal{E}(\varrho_1),\mathcal{E}(\varrho_2)) \leqslant D(\varrho_1,\varrho_2), \tag{2}$$

where $D(\varrho_1,\varrho_2) = 1/2||\varrho_1 - \varrho_2||_1$ is the *trace distance*. This property shows the contraction of the state space under a Markovian process. This in turn shows how two initial conditions are increasingly forgotten and are more difficult to distinguish as the trace norm is directly related with the two state discrimination problem. Some authors *define* Markovianity with this property: If there exists a pair of quantum states such that the last equation does not hold, in Ref. [15] the process is said to be non-Markovian.

B. Quantifying non-Markovianity

Two well-known measures of non-Markovianity can be constructed, based on violations of either Eqs. (1) or (2). In particular, the authors of both measures constructed them adding up the local contributions of the chosen criterion.

For the case of the RHP measure (based on divisibility), the authors define

$$g(t) = \lim_{\epsilon \to 0^+} \frac{||\mathcal{J}[\mathcal{E}_{(t+\epsilon,t)}]||_1 - 1}{\epsilon}, \tag{3}$$

where $\mathcal{J}[\mathcal{E}_{(t+\epsilon,t)}]$ is the Jamiołkowski isomorphism [20] that relates quantum channels and density matrices. In particular, it takes CP maps to positive operators with unit trace. Thus, if $\mathcal{E}_{(t+\epsilon,t)}$ is a CP map, the eigenvalues of the $\mathcal{J}[\mathcal{E}_{(t+\epsilon,t)}]$ will all be positive and add up to one. Otherwise, they will still add up to one, but with negative contributions. Thus, $g(t)$ is greater than zero if at time t the dynamics are not divisible; otherwise, $g(t) = 0$. The measure proposed in Ref. [16] is obtained by integrating the contributions of the non-CP-divisible behavior throughout the entire evolution:

$$\mathcal{N}_{\mathrm{RHP}}[\mathcal{E}] = \int_0^\infty g(t)dt. \tag{4}$$

The brackets here indicate functional dependency.

In a similar spirit, we can integrate the deviations from the contractive behavior, expected for Markovian evolution. Considering the derivative of the trace distance

$$\sigma(t,\varrho_{1,2}(0)) = \frac{dD(\varrho_1(t),\varrho_2(t))}{dt}. \tag{5}$$

According to Eq. (2), $\sigma \leqslant 0$ for Markovian dynamics. We can integrate this deviation to obtain the measure proposed in Ref. [15], where a maximization over all states is taken. Thus,

$$\mathcal{N}_{\mathrm{BLP}}[\mathcal{E}] = \max_{\varrho_1,\varrho_2} \int_{\sigma>0} \sigma(t,\varrho_1(0),\varrho_2(0))dt. \tag{6}$$

These two measures have some serious drawbacks. In particular, they are not continuous in the spaces of functions, and small fluctuations can change the value of the measure by an arbitrarily large amount. Notice that these issues arise always with a finite Hilbert-size environment and also in finite number statistics. One has the option to cut the integration interval to a finite time or smooth out the fluctuations by windowing the data. One can also consider other proposals [11] which not only remove that problem but also provide a physical interpretation for the number obtained. The proposals are

$$\mathcal{N}_{\mathcal{K}}^{\max}[\Lambda_t] = \max_{t_f,\tau \leqslant t_f} [K(t_f) - K(\tau)] \tag{7}$$

and

$$\mathcal{N}_{\mathcal{K}}^{\langle\cdot\rangle}[\Lambda_t] = \max\{0, \max_{t_f}[K(t_f) - \langle K(\tau)\rangle_{\tau<t_f}]\}. \tag{8}$$

In this case, K is a quantity associated with the channel and/or its derivative. This can be, say, the quantum capacity, the trace distance with respect to some fixed states, or even $K(t) = g(t)$ as defined in Eq. (3).

C. Fidelity and localization

A very simple model of an open quantum system is one in which the dynamics of both the system of interest (central system) and environment are considered and taken to be unitary. If the interaction between them commutes with the Hamiltonian governing the system, one has dephasing dynamics. This kind of dynamics is the simplest decoherence type and is the one considered in this article. If the central system is a qubit, one can write the evolution operator as

$$U = |0\rangle\langle 0| \otimes U_0 + |1\rangle\langle 1| \otimes U_\delta \tag{9}$$

with U_0 and U_δ acting on the environment and $|i\rangle\langle i|$ $(i = 0,1)$ appropriate projectors on the qubit. Given that the initial state of the whole system is the separable state $|\psi_{\rm sys}\rangle \otimes |\psi_{\rm env}\rangle$, the dynamics on the qubit only depend on the *fidelity amplitude* [21], defined as

$$f(t) = \langle\psi_{\rm env}|U_\delta^\dagger(t)U_0(t)|\psi_{\rm env}\rangle, \tag{10}$$

and the expectation value of the echo operator $M(t) = U_\delta^\dagger(t)U_0(t)$ with respect to the state $|\psi_{\rm env}\rangle$. In particular, the unitary dynamics of the qubit are going to be encoded in the phase of f; other quantities, such as purity, that are invariant under unitary transformations depend only on the fidelity

$$\mathcal{F}(t) = |f(t)|^2. \tag{11}$$

It follows that in the dephasing scenario, the study of non-Markovianity reduces to the study of the fidelity amplitude in the environment.

If we consider long discrete times, and under ergodic conditions, one can assume that the sequence of states $M(t)|\psi_{\rm env}\rangle$ is random with respect to $|\psi_{\rm env}\rangle$; by that we mean that $\langle\psi_{\rm env}|M(t)|\psi_{\rm env}\rangle$ is a sequence of random Gaussian numbers. In this model, the fidelities are uncorrelated Gaussian random numbers with zero mean and standard deviation inversely proportional to the square root of the dimension of the Hilbert space in which $|\psi_{\rm env}\rangle$ lives. However, systems that are not ergodic, from a classical point of view, do not explore the whole phase space. The simplest correction to the model proposed leads to the concept of *effective Hilbert space*. The dynamics, for a fixed initial state, can often be described with smaller subset of states sharing a quantum number with the initial state. Say, if the initial state of a semiclassical integrable system lives in a torus, we can describe the evolution with the eigenstates belonging to that same torus. Thus, the dynamics are taking place in an effective Hilbert space of dimension roughly equal to the number of coherent states that cover that torus. In a purely quantum scenario, such a situation arises naturally when one has "good" quantum numbers. A reasonable way to quantify to what extent one can describe states in terms of a small number of states of an orthonormal basis is using the inverse participation ratio (IPR). This quantity is defined for a normalized state $|\psi\rangle$ with respect to the orthonormal basis $\{|n\rangle\}$ as

$$\mathrm{P}^{-1}(|\psi\rangle) = \sum_n^{\dim\mathcal{H}} |\langle n|\psi\rangle|^4. \tag{12}$$

The lower bound for the IPR is $1/\dim\mathcal{H}$ and is attained when we have equal weights of $|n\rangle$ on the state $|\psi\rangle$; we say that $|\psi\rangle$ is a fully delocalized state. The upper bound of 1 is obtained by states of the base $\{|n\rangle\}$; we say that $|\psi\rangle$ is localized. Typically the basis $\{|n\rangle\}$ is chosen as the normal eigenbasis of some operator, typically the Hamiltonian prior to a perturbation. It should be noted that such an operator can not have degenerate spectra in order to avoid ambiguities in the basis and get well-defined IPRs.

D. Putting together the tools

At this point, we wish to connect the three quantities discussed: non-Markovianity measures, fidelity, and IPR. Non-Markovianity measures are determined, for dephasing channels, by the fidelity of an environment. In particular, as can be seen from Eqs. (4) and (6), they are determined by the fluctuations of fidelity. In turn, under an ergodic hypothesis, the IPR can tell us how asymptotic fidelity behaves, with an effective dimension yet to be determined. In this paper, we want to study under which circumstances we can reduce the study of non-Markovianity to the study of an effective dimension of a quantum system.

III. MODEL

In this section, we start with a generic Hamiltonian that induces dephasing dynamics. We then specify the particular model to be used as environment, namely, a kicked chain of spin-1/2 particles and the initial states of the environment. We complete our model specifying the interactions considered in this work.

A. Dephasing dynamics

The Hamiltonian of a qubit under dephasing dynamics is, up to rotations in the qubit,

$$H = \frac{\Delta}{2}\sigma_z \otimes \mathbb{1} + \mathbb{1} \otimes H_{\rm env} + \epsilon\sigma_z \otimes V \tag{13}$$

[as in Eq. (9), when writing tensor products, the first term acts on the qubit and the second, on the environment]. The first term is the free Hamiltonian of the qubit and Δ is the transition energy between the two levels; $H_{\rm env}$ is the environmental Hamiltonian; finally, ϵ modulates the coupling strength of the qubit-environment system, provided by the last term. Since the internal Hamiltonian of the qubit commutes with the interaction Hamiltonian we can ignore the latter; it contributes with a unitary transformation in the qubit that does not affect the non-Markovianity measures. The total Hamiltonian can thus be written as

$$H = |0\rangle\langle 0| \otimes H^{(+)} + |1\rangle\langle 1| \otimes H^{(-)}, \tag{14}$$

where $H^{(\pm)} = H_{\rm env} \pm \epsilon V$; its associate unitary operator takes the form Eq. (9). If we write the channel in the Pauli basis $1/\sqrt{2}\{\mathbb{1},\sigma_x,\sigma_y,\sigma_z\}$, its matrix elements are given by $\mathcal{E}_{jk} = (1/2)\mathrm{tr}[\sigma_j U(t)\sigma_k \otimes \varrho_{\rm env}U^\dagger(t)]$, where $|\psi_{\rm env}\rangle\langle\psi_{\rm env}|$ is the initial state of the environment and $\sigma_0 \equiv \mathbb{1}$. We arrive to the expression

$$\mathcal{E} = \begin{pmatrix} 1 & 0 & 0 & 0 \\ 0 & \mathrm{Re}[f(t)] & \mathrm{Im}[f(t)] & 0 \\ 0 & \mathrm{Im}[f(t)] & \mathrm{Re}[f(t)] & 0 \\ 0 & 0 & 0 & 1 \end{pmatrix} \tag{15}$$

with f the fidelity of $|\psi_{\text{env}}\rangle$ with respect to the unitary operators $U^+(t) = \exp(-itH^+)$ and $U^-(t) = \exp(-itH^-)$.

For this channel, all measures of non-Markovianity given in the last section can be easily computed and depend only on $F(t) = \sqrt{\mathcal{F}(t)}$. For example,

$$\mathcal{N}_{\text{RHP}}[\mathcal{E}] = \int_{\dot{F}>0} \frac{\dot{F}(t)}{F(t)} dt = \sum_i [\ln(F(b_i)) - \ln(F(a_i))], \tag{16}$$

with b_i and a_i the times of the ith maximum and minimum of $F(t)$ respectively. For the computation of the BLP measure, the states that maximize Eq. (6) are those lying on the equator of the Bloch sphere in antipodal positions. The trace distance is the Loschmidt echo, $D(\varrho_1(t),\varrho_2(t)) = F(t)$. From Eq. (6), the measure is

$$\mathcal{N}_{\text{BLP}}[\mathcal{E}] = \int_{\dot{F}>0} \frac{dF(t)}{dt} dt = \sum_i [F(b_i) - F(a_i)]. \tag{17}$$

This shows a direct relation with both revivals and fluctuations of the Loschmidt echo of the environmental dynamics. Finally, measures $\mathcal{N}_{\mathcal{K}}^{\max}[\Lambda_t]$ and $\mathcal{N}_{\mathcal{K}}^{\langle\cdot\rangle}[\Lambda_t]$, as long as they are invariant with respect to unitary operations in the qubit, will depend only on F in the same way that the particular $\mathcal{K}$ chosen depends on F.

B. The environment

The system used as environment is the homogeneous Ising spin-1/2 chain kicked by short pulses of magnetic field. This system was proposed by Prosen to study the relation between ergodicity and fidelity [13,14]. The Hamiltonian reads

$$H_{\text{env}} = \sum_{i=0}^{N-1} \sigma_i^z \sigma_{i+1}^z + \hat{\delta}(t) \sum_{i=0}^{N-1} b^{\perp} \sigma_i^x + b^{\parallel} \sigma_i^z, \tag{18}$$

where $\hat{\delta}(t) = \sum_{n=-\infty}^{\infty} \delta(t-n)$ and $\vec{\sigma}_N \equiv \vec{\sigma}_0$. The first term corresponds to a homogeneous Ising interaction strength; $b^{\perp}$ and $b^{\parallel}$ are the perpendicular and parallel components of the magnetic field with respect to the direction of the Ising interaction; finally, $\hat{\delta}(t)$ is a train of Dirac δs with period 1. This system has three well-known dynamical regimes. For both $b^{\perp} = 0$ or $b^{\parallel} = 0$ the chain is integrable [13]. For $b^{\parallel} = b^{\perp} \approx \sqrt{2}$, the dynamics is chaotic in the sense of random matrix theory [22]. It follows that the nearest neighbor spacing distribution $P(s)$ of the quasienergies resembles the one of the circular orthogonal ensemble; see the appendix. The third regime is an intermediate one where there is level repulsion but the system is not fully chaotic. The Floquet operator is

$$U = \exp\left(-i \sum_{i=0}^{N-1} b^{\perp} \sigma_i^x + b^{\parallel} \sigma_i^z\right) \exp\left(-i \sum_{i=0}^{N-1} \sigma_i^z \sigma_{i+1}^z\right), \tag{19}$$

and the evolution operator for longer times is simply $U(n) = U^n$. This model has the advantage that it can be split in one- and two-qubit operations, as the terms in each of the exponentials commute with one another, and one can thus express the exponential as a multiplication of exponentials each with only one or two particles involved.

In order to map local features of the non-Markovianity and have initially null correlations in any part of the complete system, we use the spin coherent states as initial states of the environment. They are invariant under permutations and can be regarded as a macroscopic state.

Coherent states are defined as a coherent displacement of the fiducial state $|J = j; m_z = j\rangle$:

$$|\vartheta,\varphi\rangle = e^{-i\varphi S_z} e^{-i\vartheta S_y} |j;j\rangle = \mathcal{D}^{(j)}_{\vartheta,\varphi} |j;j\rangle, \tag{20}$$

where the total spin is given by $j = N/2$, $\mathcal{D}^{(j)}_{\vartheta,\varphi}$ is the rotation matrix in the subspace of spin j. These states form a complete basis in the symmetric subspace. In fact, one can parametrize these states in a Poincaré sphere, and rewrite

$$|\vartheta,\varphi\rangle = \left(\cos\frac{\vartheta}{2}|0\rangle + \sin\frac{\vartheta}{2} e^{i\varphi}|1\rangle\right)^{\otimes N}. \tag{21}$$

The environmental Hamiltonian is invariant under external rotations: The translation operator, which takes state $\otimes_i |\psi_i\rangle$ to state $\otimes_i |\psi_{i+1}\rangle$, commutes with Eq. (19). This symmetry foliates the Hilbert space in quasimomentum k subspaces [22]. As the translation symmetry leaves Eq. (20) invariant, such states live in the $k = 0$ subspaces, and as the evolution respects the symmetry, it will remain in such subspace. The calculation of the IPR is thus simply

$$\text{P}^{-1}_{\vartheta,\varphi} = \sum_{i=1}^{\dim \mathcal{H}_{k=0}} \left|\langle \phi_i^{(k=0)} | \vartheta,\varphi\rangle\right|^4. \tag{22}$$

C. Interaction operator

We shall study three kinds of couplings (local, global, and generic) and look for common trends and differences. Local and generic couplings will break the symmetry of the environment, whereas the global one is chosen to maintain it. We continue by presenting the local perturbations.

As mentioned above, the interaction was chosen to induce a dephasing channel, for sake of simplicity. The operator V appearing in Eq. (13) can be seen as a perturbation operator of the environment dynamics [see Eq. (14)]. For the case of global perturbations, we probed altering either the magnetic field or the Ising interaction between neighbors, which correspond to choosing V as

$$V_b \equiv \delta_1(t) \sum_{i=0}^{N-1} \sigma_i^x, \quad V_J \equiv \sum_{i=0}^{N-1} \sigma_i^z \sigma_{i+1}^z. \tag{23}$$

Analogously, for the local interaction of the qubit with the environment, we chose the coupling as

$$V_{0,1} \equiv \sigma_0^z \sigma_1^z, \quad V_0 \equiv \delta_1(t) \sigma_0^x, \tag{24}$$

where only two and one qubits of the environment, respectively, interact directly with the central qubit. Finally, to study the generic case, we consider the simplest choice, inspired in ergodicity arguments of quantum chaos [23]. We select V from one of the classical ensembles, namely the Gaussian unitary ensemble (GUE). We shall denote that case as V_{GUE}, and it corresponds to a global and structureless perturbation.

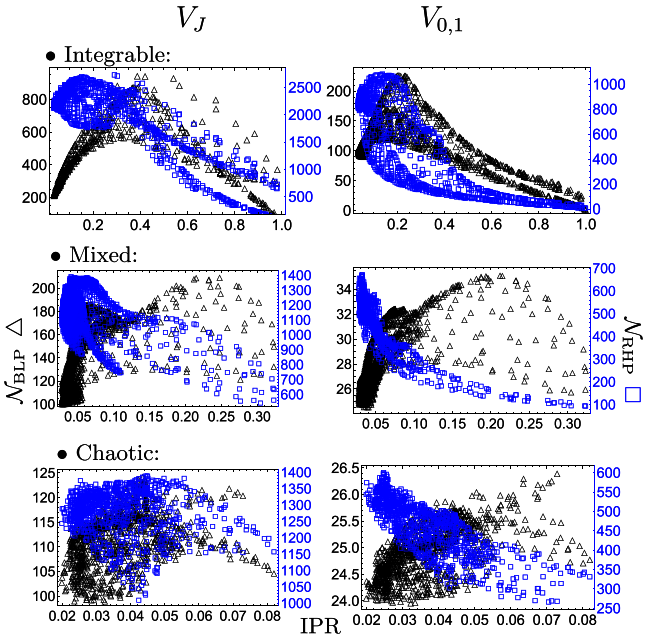

FIG. 2. BLP (black triangles, left axis) and RHP (blue squares, right axis) measures as a function of the IPR for initial coherent states of the environment, Eq. (20), distributed uniformly on the Poincaré sphere. Each column corresponds to a different kind of coupling of the qubit to the environment [see Eqs. (23) and (24)], whereas different rows correspond to different dynamical regimes of the environment. The parameters used for this and the rest of the figures are indicated at the beginning of Sec. IV. The results for the global and local field perturbation, V_b and V_0, respectively, are very similar to their global and local Ising counterparts.

IV. RESULTS

The unitary dynamics in qubit plus environment [defined by Eqs. (13) and (18) and the interactions discussed in Sec. III C] induce a specific dephasing channel, Eq. (15), once the initial state of the environment is specified. In our case, such state is a coherent state, Eq. (20), specified by the parameters ϑ and φ. The environment, a spin chain, will be used in integrable, mixed, and chaotic regimes, varying $b^{\perp} = 0.1$, 1, and 1.4 respectively while fixing $b^{\parallel} = 1.4$. We use $b^{\perp} = 0.1$ instead of 0 for integrable dynamics, in order to avoid degeneracies in the spectrum and have a well-defined IPR. Corresponding spectral statistics are presented in the appendix. For all calculations, we chose the coupling parameter $\epsilon = 0.1$.

We performed numerical calculations of the measures of NM using time cutoffs of $t_{\rm cut} = 10\,000$ and a mesh in coherent-state parameters (ϑ,φ) of $\Delta\vartheta = \Delta\varphi = 0.1$; the two measures Eqs. (4) and (6) were slightly modified to accommodate to the intrinsic discrete time structure of Eq. (18). We also considered a time cutoff in the integrals of the measures, as the fluctuations caused by a finite-dimensional environment would send the aforementioned measures to infinity. The IPR of the initial environmental states were calculated with respect to the eigenbasis of U^{+} for simplicity. Since we are taking a small ϵ, the IPR does not vary considerably if instead of U^{+}, we consider U^{-} or a Floquet operator with an intermediate ϵ.

We discuss first the relation of the different measures of NM with respect to the IPR. Next we study the dependence of these quantities with respect to the choice of the state of the environment; that is, we study the structure of the environment that can be seen, studying the decoherence of the qubit. The section is closed with some comments on the generality of the results when one varies the dimension of the environment and the total evolution time considered.

A. Dependence of non-Markovianity on the state localization

We study the behavior of NM, using $\mathcal{N}_{\rm RHP}$ and $\mathcal{N}_{\rm BLP}$ in Sec. IV A 1 and then using $\mathcal{N}_{\mathcal{K}}^{\max}$ and $\mathcal{N}_{\mathcal{K}}^{(\cdot)}$ in Sec. IV A 2, with $\mathcal{K}$ being $\mathcal{D}$ or $\mathcal{G}$. In the first section, we focus in the cases which the coupling is via global and local nearest neighbor Ising interaction, V_J and $V_{0,1}$, respectively, and a global $V_{\rm GUE}$ operator. In the second section, we focus only on global V_J and $V_{\rm GUE}$. These interactions represent well what happens for the other cases for each study.

1. Using BLP and RHP measures

In Fig. 2, we show, for different initial conditions of the environment and a coupling of the type V_J, the value of NM using BLP and RHP measures as a function of the IPR.

In the integrable regime, the two measures have different behaviors; $\mathcal{N}_{\rm BLP}$ grows for increasing IPR until it reaches a maximum around $\mathrm{P}^{-1} \sim 0.4$, where it starts to decrease. $\mathcal{N}_{\rm RHP}$ has an approximate monotonic decreasing behavior, showing a change of slope around $\mathrm{P}^{-1} \sim 0.4$ and another close to $\mathrm{P}^{-1} \sim 0.6$. A local coupling, namely $V_{0,1}$, yields similar results; however, the peak in the BLP measure is sharper and the decay of RHP measure is faster (Fig. 2 second column). The behavior of $\mathcal{N}_{\rm BLP}$ can be explained qualitatively by studying the fidelity which, for the dephasing case, is related to the distinguishability via the equation $\mathcal{D}(t) = |f(t)|^2$. In Fig. 3,

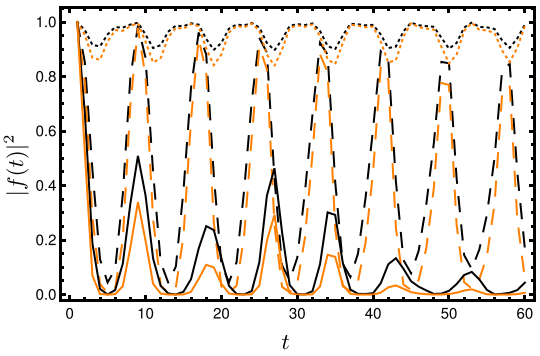

FIG. 3. Typical behavior of the fidelities of the environment, Eq. (18), in the integrable regime with a global Ising perturbation V_J, for several coherent states, Eq. (20). We consider 10 and 16 qubits, shown in black and orange curves, respectively. The figure shows the fidelity for the state $|\vartheta = 2.8, \varphi = 4.8\rangle$ (with IPR equal to 0.457 and 0.375 for 10 and 16 qubits, respectively), which is among the states that yield larger values for measures based on $\mathcal{D}(t)$ (dashed curves). Fidelities for the states that give low values of the BLP measure are the dotted and solid curves, obtained from the states $|\vartheta = 3.0, \varphi = 2.2\rangle$ (IPR equal to 0.994, 0.984) and $|\vartheta = 1.5, \varphi = 3.5\rangle$ (IPR equal to 0.046, 0.010), respectively, which are high and low localized states.

we show its evolution in the integrable regime, for three initial conditions and two different environment sizes. For high and low values of localization, oscillations of $\mathcal{D}(t)$ are constrained around high and low values of asymptotic fidelity, respectively. Therefore, the relatively low values of non-Markovianity belong to the high and low values of localization. There are also states with high IPR that lead to distinguishabilities that oscillate with large amplitude but at a low frequency; those states have low asymptotic fidelity. The maximum value of NM is achieved at ∼0.4, where fidelity can oscillate with a large amplitude. One can understand the behavior of $\mathcal{N}_{\mathrm{RHP}}$ with similar arguments [see Eq. (16)] but this time taking into account the role of the logarithm. For high localized states, the typical values of the minimums and maximums of $\mathcal{D}(t)$ are very close to one or with lower frequency, yielding very small values of the logarithm and thus low values of the RHP measure. As the IPR decreases, the minimums in $\mathcal{D}(t)$ diminishes faster than the maximums, and one reaches quickly the regime in which $-\ln(F(a_i))\sim\mathcal{O}(1)$, causing an increasing of the measure until IPR ∼ 0.4. For small values of the localization, the typical minimum is very close to zero, for which the logarithm is large, in absolute value. One can approximate $\mathcal{N}_{\mathrm{RHP}} \approx \sum_i \ln(F(b_i)) + n\ln(F(\tilde{a}^{-1}))$, where n is the number of minimums included in the interval of the computation of the measure and $F(\tilde{a})$ is its typical value. The value of the measure is now seen to be directly related with the localization, giving again a monotonic behavior with different slope. For both measures, low localized states tend to cluster. These states are localized in the equator of the Poincaré sphere (see Fig. 9). This explains the two leaflike structures connected by a stem in the integrable regime.

In the mixed and chaotic regimes, fidelities begin with a fast decay, after which they fluctuate around the inverse of the effective dimension of the state (Fig. 4). Since the asymptotic fidelity is inversely proportional to the effective dimension of Hilbert space, the scale of the NM is lower in these regimes with respect to the integrable. The IPR is also small due to

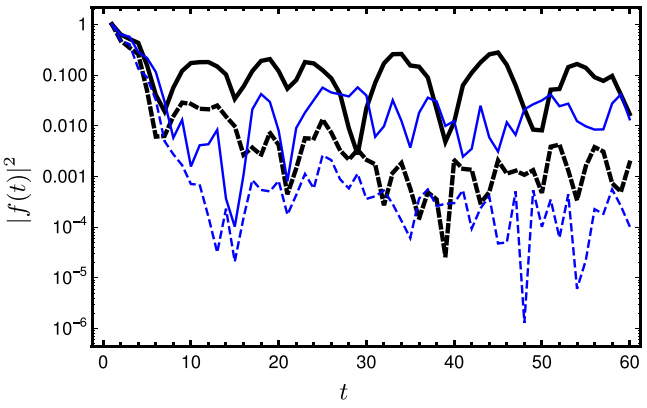

FIG. 4. Typical behavior of the fidelities of the environment in the chaotic (blue curves) and mixed (black thick curves) regimes for 10 (solid curves) and 16 (dashed curves) qubits, with the coupling $V = V_J$; the initial state is a coherent state characterized by $|\vartheta = 0.7, \varphi = 0.8\rangle$; see Eq. (20). A fast decay and fluctuations around a value determined by the effective dimension of the Hilbert spaces explains the values of the different measures of non-Markovianity.

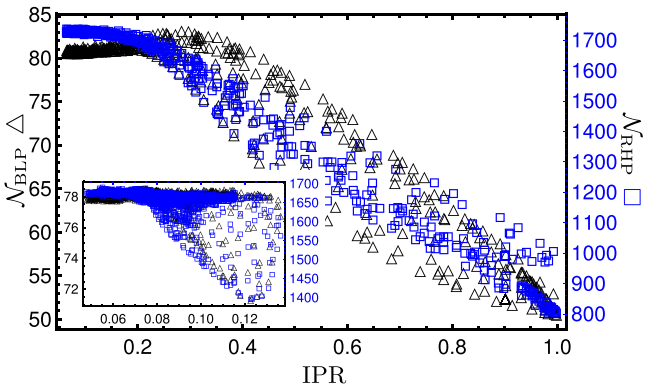

FIG. 5. RHP and BLP measures of the spin chain using a random coupling, chosen from the GUE, in the integrable regime (main panel) and the chaotic regime (inset). We observe a monotonic decreasing behavior for both measures in all regimes, with a short growth for BLP measure in the integrable regime.

ergodic properties of the Hamiltonian. In the mixed regime, the slope of the data using V_J and $V_{0,1}$ is positive for BLP measure, while for RHP it is clearly decreasing for both perturbations, mimicking the integrable cases. Thus, both measures behave differently also in the mixed regime. In the chaotic regime, we expect full ergodic properties, and consequently, a reasoning similar to that of the mixed case will follow, however, with smaller IPR. Indeed, all initial conditions cluster around a smaller region but a slope, consistent with the mixed cases, is observed.

Finally, we show the results when a random potential provides the coupling in Eq. (13); namely, when we take $V = V_{\mathrm{GUE}}$. The dependence of NM on the IPR is shown in Fig. 5 for both the integrable and the chaotic cases. Its behavior is qualitatively similar to the one observed for the other couplings, when comparing among integrable cases, mixed and chaotic. However, there are some quantitative differences. For example, the BLP measure still has an initial growth but is very short compared with the case of $V = V_J$. The same arguments as before can be stated to explain the general features of the behavior.

2. *Using measure schemes $\mathcal{N}_{\mathcal{K}}^{\max}$ and $\mathcal{N}_{\mathcal{K}}^{(\cdot)}$*

In the previous section, we considered measures BLP and RHP, which are based on the nonmonotonicity of distinguishability, as measured by $\mathcal{D}(t)$, and of divisibility, as measured by $\mathcal{G}(t) = \int_0^t g(\tau)d\tau$. In this section, we use measures based on the same quantities, but use Eqs. (7) and (8) to obtain a quantity that can be directly related to a physical process [11] and contrast its behavior with measures BLP and RHP.

For the integrable case, we observe that there are two distinct behaviors, for both measures $\mathcal{N}_{\mathcal{K}}^{\max}$ and $\mathcal{N}_{\mathcal{K}}^{(\cdot)}$, regardless of whether they are based on $\mathcal{D}$ or $\mathcal{G}(t)$. In Fig. 6, we show the results for the case in which the coupling is V_J. These two different behaviors are associated with the two hemispheres of the Poincaré sphere, and its details can be understood by studying the evolution of fidelity. In particular, for $\mathcal{N}_{\mathcal{D}}^{\max}$, one of the branches displays a maximum (IPR ∼ 0.4), then it decays linearly. The other branch, corresponding to the

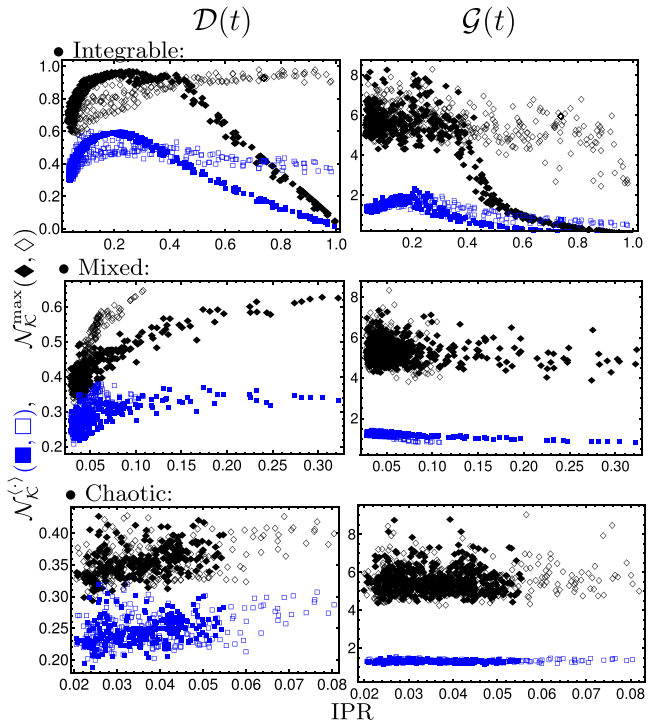

FIG. 6. Measures $\mathcal{N}_{\mathcal{K}}^{(\cdot)}$ (blue) and $\mathcal{N}_{\mathcal{K}}^{\max}$ (black) with $\mathcal{D}(t)$ [left column] and $\mathcal{G}(t)$ [right column], for the spin chain using global Ising perturbation V_J, as a function of the initial IPR of the environment; see Fig. 2. The initial states of the environment are coherent states uniformly chosen from the northern or southern hemispheres of the Poincaré sphere and indicated by the hollow and filled markers, respectively. In the integrable regime (and in the mixed for $\mathcal{N}_{\mathcal{D}}^{\max}$), we see two different behaviors, coming from the two hemispheres of the Poincaré sphere. The results for local Ising interaction, $V_{0,1}$, are very similar to the presented here. Results for global and local field perturbations, V_b and V_0 respectively, presented only the behavior plotted by filled markers.

southern hemisphere ($\pi/2 < \vartheta \leqslant \pi$), has a slight increase with IPR. The behavior of $\mathcal{N}_{\mathcal{D}}^{(\cdot)}$ is similar; however, it is scaled down, and instead of a slight increase, the southern hemisphere displays a small increase with IPR. A quantitatively similar behavior is seen when we base our measures in $\mathcal{G}(t)$, with the bending point being again at IPR ~ 0.4, for $\mathcal{N}_{\mathcal{G}}^{\max}$. $\mathcal{N}_{\mathcal{G}}^{(\cdot)}$ is also a scaled down and slightly deformed version of $\mathcal{N}_{\mathcal{D}}^{(\cdot)}$. For low localized states, the explanation of the aforementioned behavior is similar to the one given for BLP and RHP measures. Since the size of the fluctuations of the fidelity depend on the effective dimension of the state, $\mathcal{N}_{\mathcal{K}}^{(\cdot)}$ and $\mathcal{N}_{\mathcal{K}}^{\max}$ increase as we take more localized initial environmental states. For highly localized states in the integrable regime, there are two families of states. One, with asymptotic fidelity greater than $1/2$ and whose fidelity has a high frequency but small amplitude, and other with asymptotic fidelity smaller than $1/2$ but with a fidelity that has smaller frequency and a larger oscillation amplitude. Since the schemes under discussion depend mainly in the amplitude of the oscillations, they are critically sensitive to the asymptotic fidelity of the environmental states. This

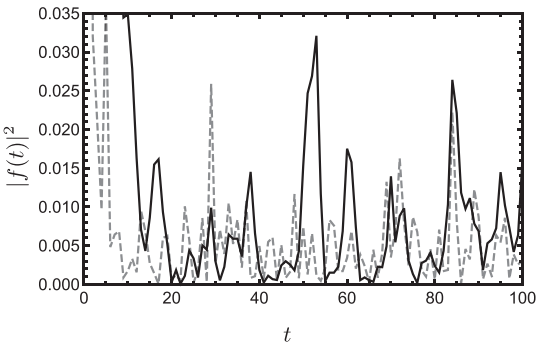

FIG. 7. Typical behavior of the fidelities in the integrable regime for $V = V_{\mathrm{GUE}}$. In solid black we plot the fidelity of the state $|\vartheta = 3.2, \varphi = 1.1\rangle$ as a representative state of highly localized states, and $|\vartheta = 2.2, \varphi = 2.4\rangle$ in dashed gray as a representative of low localized states. High localized states lead to a low frequency of occurrence of pairs of local minima and maxima, while for localized states such frequency is increased. This explains the different behaviors among BLP and $\mathcal{N}_{\mathcal{D}}^{\max,(\cdot)}$.

feature is a significant difference between the newly proposed schemes [11] and the more often used BLP and RHP.

In the mixed and chaotic regimes, the behavior of the measures is monotonically increasing. Since all coherent states have a small IPR, the same arguments given before for low localized states in the integrable regime hold to explain such monotonicity. For the chaotic regime, the measures also tend

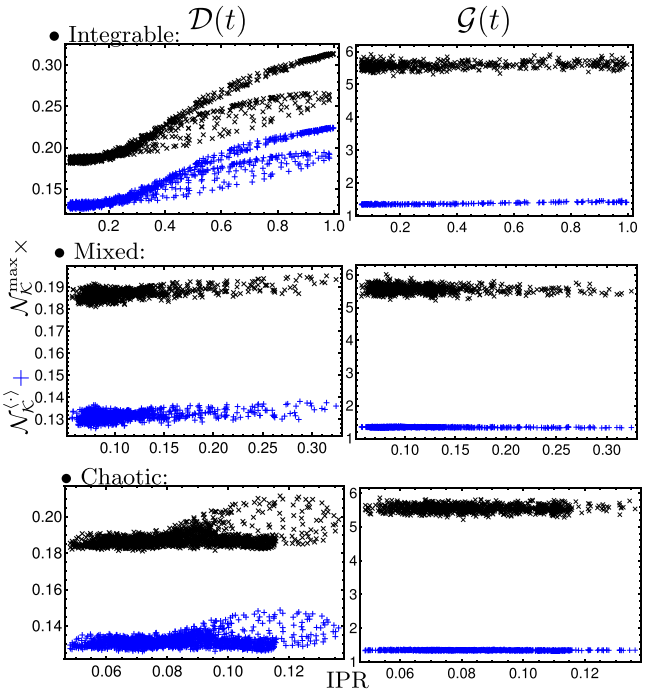

FIG. 8. Relation between $\mathcal{N}_{\mathcal{K}}^{(\cdot)}$ and $\mathcal{N}_{\mathcal{K}}^{\max}$ with IPR, using a global random perturbation. We consider the two measures, based on both $\mathcal{D}(t)$ and $\mathcal{G}(t)$ and a spin chain of eight spins for an ensemble of 40 matrices. Measures based on $\mathcal{G}$ are almost constant in all regimes. For $\mathcal{N}_{\mathcal{D}}^{\max,(\cdot)}$ in the integrable regime, we observe different behaviors for each hemisphere of the Poincaré sphere.

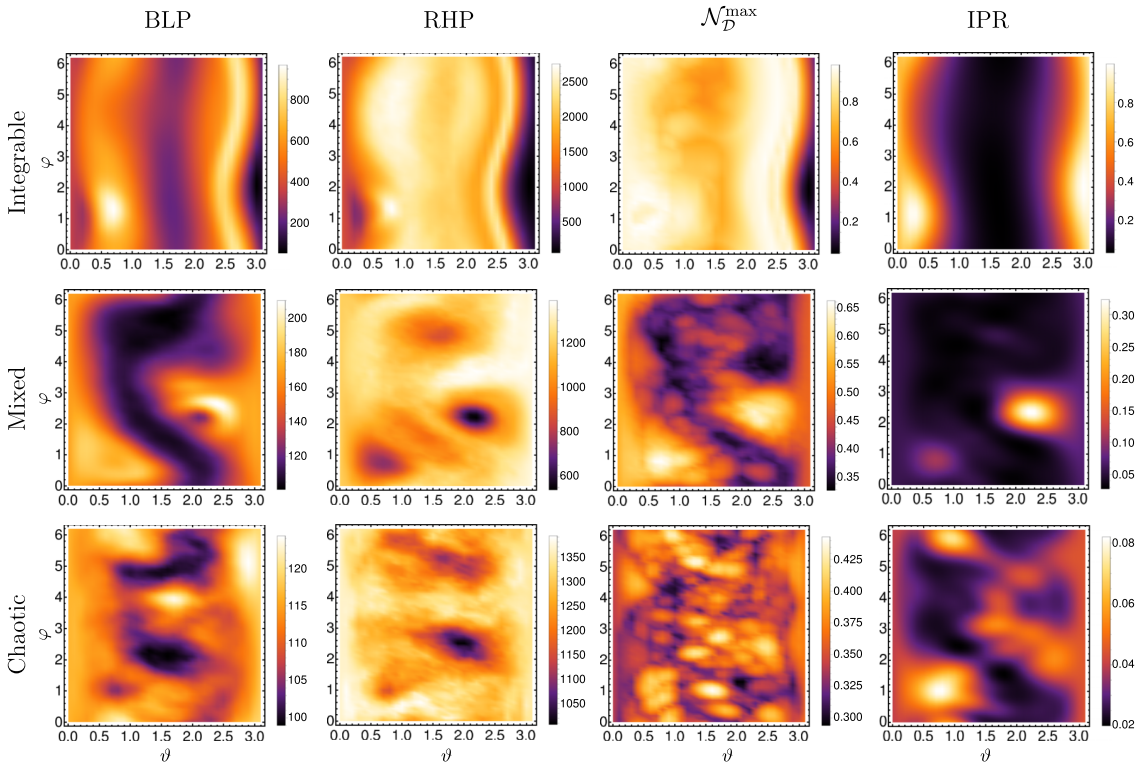

FIG. 9. The different columns correspond to density plots of several measures of non-Markovianity and the IPR, for a chain with 10 qubits using the homogeneous perturbation V_J. For $\mathcal{N}_{\mathcal{D}}^{\max}$ some smaller structures appear as we go into the chaotic regime. We can also observe a relation in the integrable and mixed regimes between IPR and all non-Markovianity measures. The results for local Ising interaction, $V_{0,1}$, are very similar, just with more extended depressions. The results for the global and local field perturbations, V_b and V_0, respectively, are very similar to their global and local Ising counterparts.

to homogenize; this is expected given that the initial states have similar effective dimension, as they appear random in the eigenbasis of the Floquet operator.

For a random coupling to the environment, measures $\mathcal{N}_{\mathcal{D}}^{\max,\langle\cdot\rangle}$ have a monotonic behavior with respect to IPR. However, in contrast to the behavior of the BLP measure, non-Markovianity increases with the inverse participation ratio. This surprising change can be explained when noticing that the BLP measure depends on the number of pairs of minima and maxima that appear in the fidelity in a given interval, while $\mathcal{N}_{\mathcal{D}}^{\max,\langle\cdot\rangle}$ depend *only* on the amplitude of the fluctuations of $F(t)$. As we take more localized initial environmental states, the size of the fluctuations is increased as the pairs of minima and maxima appear less frequently (shown in Fig. 7), which explains the aforementioned effect. The behavior in the mixed regime, which is also monotonic increasing, has the same explanation. In the chaotic regime, the values of NM also tend to homogenize, having the same explanation as the one given for $V = V_J$ for this regime. Now using $\mathcal{G}(t)$ as indicator, all measure schemes in all regimes yield almost constant NM with respect to the IPR (right panels of Fig. 8). This behavior is expected for the chaotic regime; what remains to be explained is its emergence in the integrable and mixed regimes. To do this, we can find an upper bound for the change of $\mathcal{N}_{\mathcal{G}}^{\max}$ in the whole interval of localization; we shall call this $\Delta\mathcal{N}_{\mathcal{G}}$. From Eq. (7), $\mathcal{N}_{\mathcal{G}}^{\max} = \ln(F(t_f)) - \ln(F(\tau))$, where t_f and τ are the maximum and the minimum attained to the maximization required by the definition. Now, since the logarithm is a monotonic function, the measure $\mathcal{N}_{\mathcal{D}}^{\max}$ is attained to the same times, allowing us to write $\mathcal{N}_{\mathcal{G}}^{\max} = \ln(\mathcal{N}_{\mathcal{D}}^{\max} + F(\tau)) - \ln(F(\tau)) \approx \ln(\mathcal{N}_{\mathcal{D}}^{\max}) + F(\tau)/\mathcal{N}_{\mathcal{D}}^{\max} - \ln(F(\tau))$. Therefore, the total change is $\Delta\mathcal{N}_{\mathcal{G}} = \Delta\ln(\mathcal{N}_{\mathcal{D}}^{\max}) + \Delta(F(\tau)/\mathcal{N}_{\mathcal{D}}^{\max}) - \Delta\ln(F(\tau))$. The last term can be ignored since $F(\tau)$ is typically very similar for any value of localization. The second term is negative since $\mathcal{N}_{\mathcal{D}}^{\max}$ changes faster than $F(\tau)$ and its absolute value is smaller than the first term which is positive. Therefore, $\Delta\mathcal{N}_{\mathcal{G}}^{\max}$ is upper bounded by $\Delta\ln(\mathcal{N}_{\mathcal{D}}^{\max})$ and its numerical values for the integrable and mixed regime are 0.4 and 0.08 respectively. There is a similar explanation for $\mathcal{N}_{\mathcal{G}}^{\langle\cdot\rangle}$ using typical values of the average instead of the minima.

We finish this section by summarizing the results and commenting on practical consequences of the relations we found between non-Markovianity and IPR. The integrable regime shows the richest behavior when we use a structured coupling to the environment. In our case, we observed a wide variety which includes up to two different behaviors for the two hemispheres of the Poincaré sphere. In general, the different measures behave differently and depend on the details of the fidelity. However, the IPR determines coarsely the value of the non-Markovianity. As mentioned in Sec. II B, measure $\mathcal{N}_{\mathcal{D}}^{\langle\cdot\rangle}$ is directly related to the task of storing information safely; we can see that to perform such a task with a high probability of success, we need an environment in the integrable regime, a structured interaction, and states with

intermediate localization. When the environment is in the chaotic regime, the behavior is not so rich, as the coherent states are quite delocalized, and the non-Markovianity seems to be self averaging. In the mixed regime of the environment, we have an intermediate behavior.

B. Underlying structure

In Ref. [24], the authors show that non-Markovianity, via long time fluctuations of fidelity, is able to resolve complex phase space structures of the environment using initial coherent states. In particular, the fractal nature of the phase space is clearly visible in the mixed regime. We investigated the spin chain in a similar way, using spin coherent states as initial environmental states, studying now the measures of NM and the IPR as functions of the parameters of the spin coherent states. Our goal is to study the visible structures and how they change during the transition from integrability to chaos.

In the integrable regime (top of Fig. 9), the values of the NM measures mimic the behavior of the IPR close to the equator of the Poincaré sphere ($\vartheta = \pi/2$); close to the poles, the situation is different. The equator of the Poincaré sphere corresponds to low localized states, and this in turn leads to local minimums for all examined measures of NM. When moving toward the poles, which are very localized states, one finds a local maximum, and then in the vicinity of the pole, a local minimum, for all cases except for $\mathcal{N}_{\mathcal{D}}^{\max}$ near the north pole. The difference arises from the different asymptotic fidelities of the chosen high localized states. This picture deepens the understanding of the behavior already seen in Figs. 2 and 6.

For the mixed regime, the features on the NM measures are mainly governed by the IPR. High localization leads to local maximums in the measure $\mathcal{N}_{\mathcal{D}}^{\max}$ and local minimums for the RHP measure. For the BLP measure, there is also an interesting feature. The local maximum of IPR, located around $\vartheta \approx \varphi \approx 2.5$, leads to a local minimum on the NM which is partially surrounded by a maximum. This behavior is actually similar to the one at the poles in the integrable regime. In the chaotic regime, the relation of the measures with the localization practically vanishes.

Regarding the transition from integrability to chaos, using the BLP and RHP measures, there is not a notable change in the size of the structures as it does for environments with a classical analog [24,25]. This might be due to the absence of such structures, or, that simply due to the relative size of the coherent states in this system, they are not able to resolve small structures. More quantitatively, the fluctuations of the spin coherent states in the Poincaré sphere (chosen to have radius one) scale as $\sim N^{-1}$ [26], i.e., as $[\ln_2(\dim \mathcal{H})]^{-1}$, while for coherent states in the torus fluctuations scale as $(\dim \mathcal{H})^{-1}$ [27].

The situation is different when using $\mathcal{N}_{\mathcal{D}}^{\max}$. In the transition to chaos, a finer structure emerges. Although such features do not appear classical, in the sense of the appearance and breaking of KAM tori, it is clear that there is a finer granularity than is typically expected in this transition; these structures are robust with respect to changes in parameters and times of

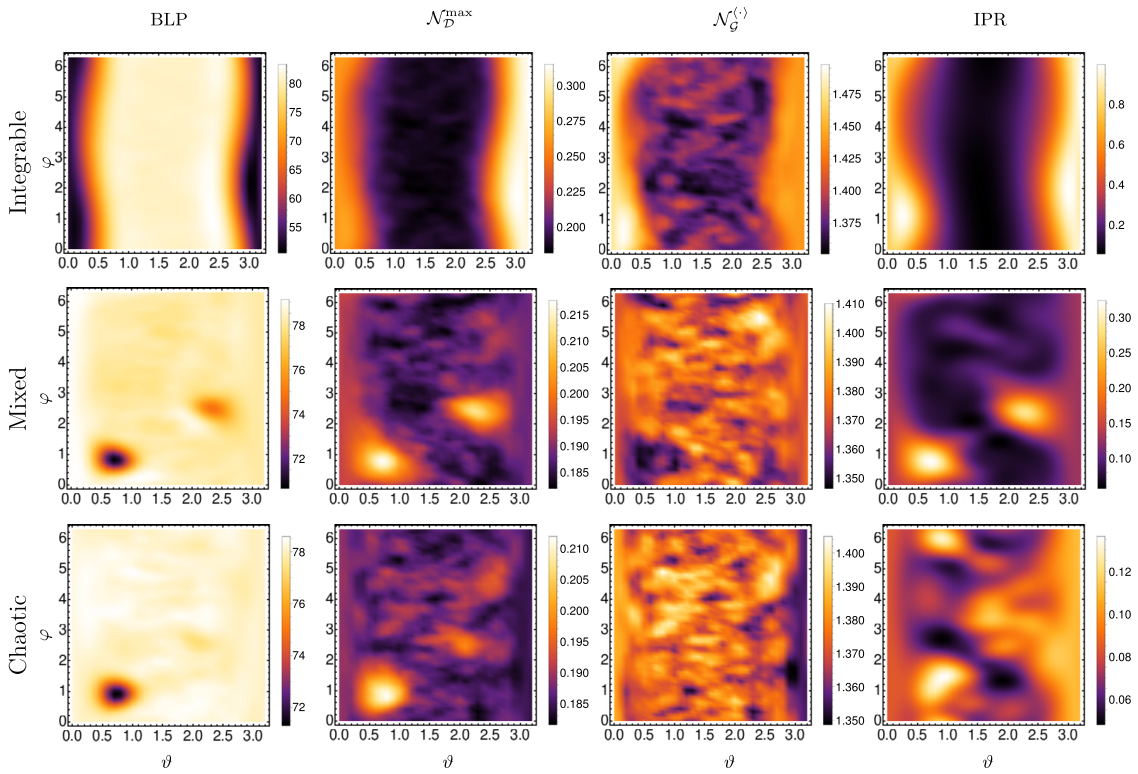

FIG. 10. Density plots of the NM measures and the IPR for the chain with eight qubits, using random potentials $V = V_{\mathrm{GUE}}$ averaged over 40 matrices. Figures show an emerging fine structure in the transition from integrability to chaos in $\mathcal{N}_{\mathcal{G}}^{(\cdot)}$. The structures observed in the NM measures are correlated (or anticorrelated) with the IPR.

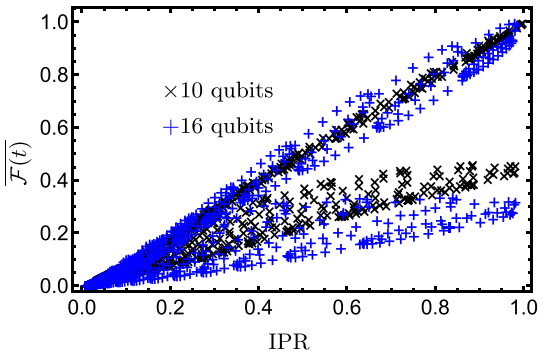

FIG. 11. Relation of the IPR and the averaged square root of the asymptotic fidelity, $\overline{\mathcal{F}(t)}$, for 10 and 16 qubits. The figure shows the splitting in the NM vs IPR relation, explaining both the peculiar behavior of the results shown in Fig. 6 and the spreading of the non-Markovianity measures, for a fixed IPR, as the dimension is increased.

integration. We consider this one of the central results of this work.

Let us now comment on the results using $V = V_{\mathrm{RMT}}$, shown in Fig. 10. In the integrable regime, measures $\mathcal{N}_{\mathcal{D}}^{\max}$ and $\mathcal{N}_{\mathcal{G}}^{\langle\cdot\rangle}$ completely mimic the behavior of the IPR, while the BLP measure is anticorrelated with the IPR. Such behavior is a consequence of the way fidelity contributes to the different measures. Recall that the BLP measure depends mainly on the frequency with which the pairs of minima and maxima occur in $\mathcal{D}(t)$, while schemes $\mathcal{N}_{\mathcal{K}}^{\max}$ and $\mathcal{N}_{\mathcal{K}}^{\langle\cdot\rangle}$ depend mainly on the amplitude. In the mixed and chaotic regimes, the situation is similar: The IPR is correlated with $\mathcal{N}_{\mathcal{D}}^{\max}$ and anticorrelated with BLP. However, for $\mathcal{N}_{\mathcal{G}}^{\langle\cdot\rangle}$ the landscapes appear to have almost no correlation with IPR.

It is also important to underline that the measures $\mathcal{N}_{\mathcal{G}}^{\langle\cdot\rangle}$ and $\mathcal{N}_{\mathcal{D}}^{\max}$ show a nonfractal structure in the transition to chaos, as in the results using V_J.

Results using RHP measure are very similar to the ones for BLP; the ones for $\mathcal{N}_{\mathcal{D}}^{\langle\cdot\rangle}$ resemble the ones for $\mathcal{N}_{\mathcal{D}}^{\max}$, and the results using $\mathcal{N}_{\mathcal{G}}^{\max}$ reveal only a random landscape for all regimes.

C. Generality of the results

This section is devoted to a discussion the validity of the main results presented above for a larger number of qubits and for different cutoff times.

We first discuss three key features, namely (i) the decreasing behavior of the BLP and RHP measures for high localized states (shown in Figs. 2 and 5); (ii) the same property for measures $\mathcal{N}_{\mathcal{K}}^{\max}$ and $\mathcal{N}_{\mathcal{K}}^{\langle\cdot\rangle}$, but only for the hemisphere which contains the states with low asymptotic fidelity (Fig. 6); and (iii) the peculiar behavior of measures based on $\mathcal{D}(t)$ (also shown in Fig. 6), which exhibits a clear change on the slope as localization is increased. Let us now comment how these observations behave as the dimension of the environment is increased, and for sake of brevity only for measures $\mathcal{N}_{\mathcal{K}}^{\max}$ (shown in Fig. 12). The results show that the patterns are preserved; however, as the dimension increases the data becomes diffused, i.e., for each value of IPR there is a wider

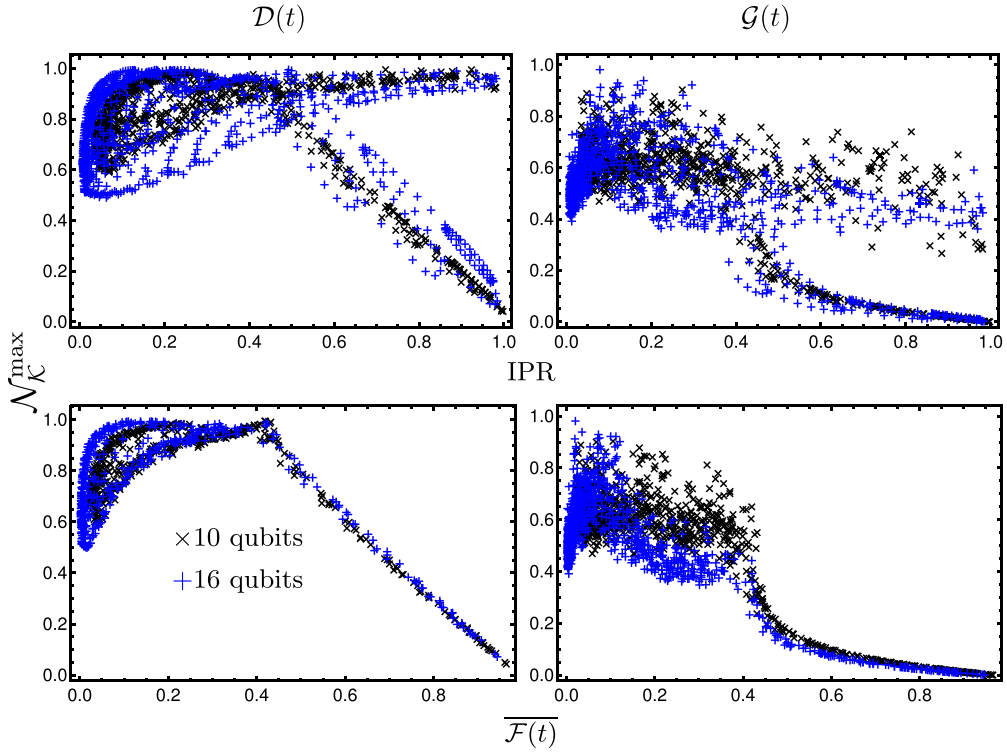

FIG. 12. Relation of the NM with the IPR and with the averaged asymptotic fidelity $\overline{\mathcal{F}(t)}$, for 10 and 16 qubits using $V = V_J$ (compare with Fig. 6). The figures show the data spreading of the relation NM versus IPR when the dimension is increased (upper row). Such feature is not present in the relation of NM versus $\overline{\mathcal{F}(t)}$ (lower row). We have the same situation.

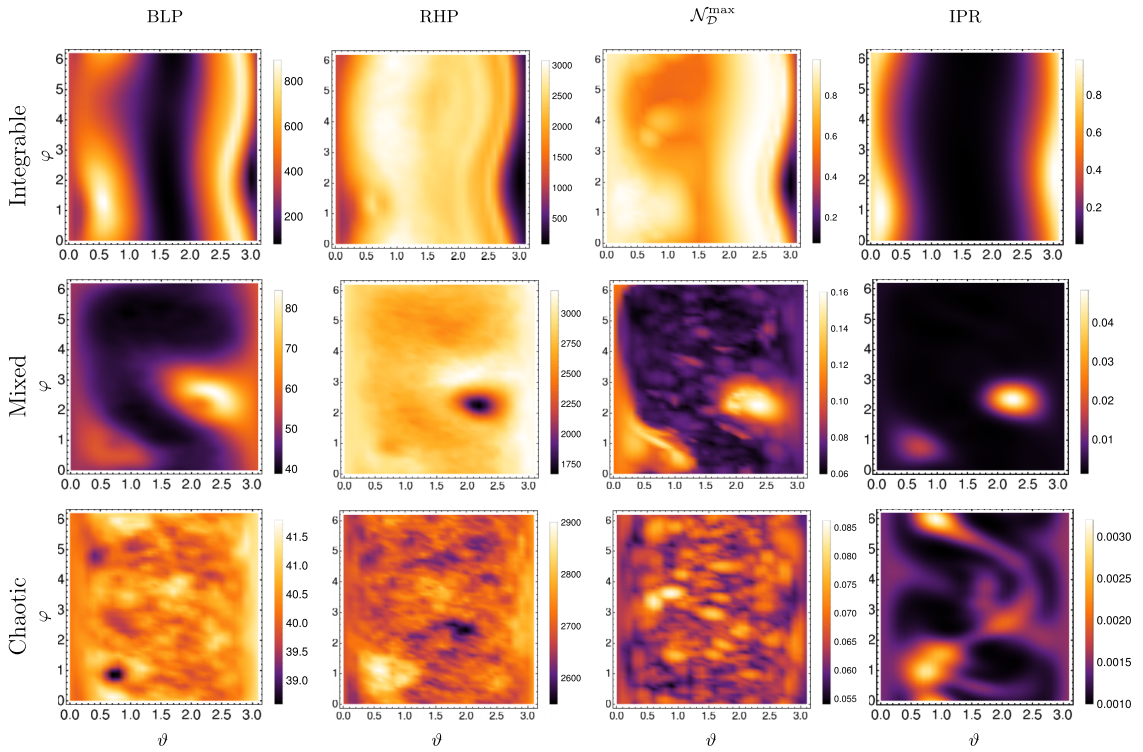

FIG. 13. Density plots of the measures of NM and of the IPR for the chain with 16 qubits and $V = V_J$. As in the case of the chain with 10 qubits, the fine structures in $\mathcal{N}_{\mathcal{D}}^{\max}$ is present. The local maximums in the IPR also dictate where are the dominant structures of local maximums or minimums in the NM.

range of NM. This is due to the relation between asymptotic fidelity $\overline{\mathcal{F}(t)}$ and IPR (shown in top panel of Fig. 11), which is linear (for each hemisphere of the Poincaré sphere) but spreads out for a larger number of qubits.

It is interesting that this observation also reveals the origin of the above-mentioned splitting of the relation between localization and non-Markovianity, due to the different values of asymptotic fidelities of high localized states. Therefore, by plotting the relation of NM versus $\overline{\mathcal{F}(t)}$ (shown in the bottom panel of Fig. 12), it can be seen that the splitting and the spreading of the data are removed, revealing that the relation of NM is simpler as a function of the effective dimension of the Hilbert space of the initial states.

Next, we shall study the emergent structures in the computed measures for the system with a higher dimension (we used a spin chain with 16 qubits). It yields basically the same behavior as for the 10 qubits case (shown in Fig. 13), but there is an emergence of smaller, finer features in the landscapes of measure $\mathcal{N}_{\mathcal{D}}^{\max}$ ($\mathcal{N}_{\mathcal{G}}^{\langle\cdot\rangle}$), which has basically an identical landscape. We conclude that such fine structures become smaller as the dimension is increased. A general characteristic of the landscapes, especially in the integrable and mixed regimes, is that the local maximums in the IPR determines the most visible structures in the NM. They appear as local maximums or minimums depending on the chosen measure and/or in the asymptotic averaged fidelity of the coherent states of the region.

We finalize this section by discussing the validity of our observations for other cutoff times. In Fig. 14, we show the values of all the measures treated in this paper for the integrable case and for one state of the environment, as a function of the cutoff time. Measures BLP and RHP are normalized by t_{cut} to avoid their trivial linear dependence. The figure shows that all measures saturate quickly to its asymptotic value, except $\mathcal{N}_{\mathcal{G}}^{\max}$, which saturates more slowly than others but more quickly with respect to the system size. We discussed only

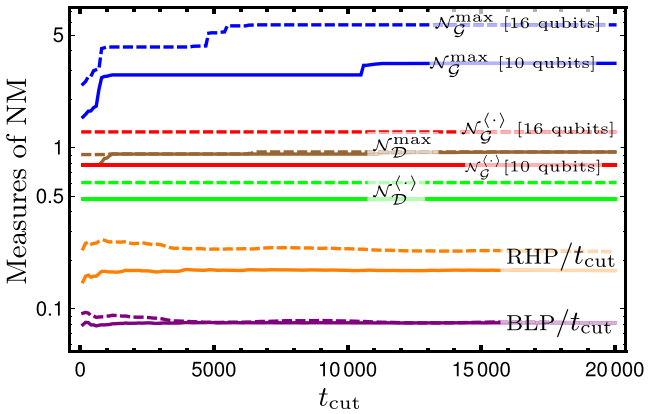

FIG. 14. Measures of NM as a function of the cutoff time, using the coherent state $|\vartheta = 2.8, \varphi = 4.8\rangle$ for 10 (solid lines) and 16 (dashed lines) qubits in the integrable regime. BLP and RHP measures are normalized by t_{cut} to remove their linear dependence on t_{cut}; it is clear from this plot that without such normalization they grow mainly linearly with time. The figure shows that the cutoff time used throughout the paper is appropriate to understand the results for asymptotic times.

the results for one state in one regime since the exploration for other cases gives very similar results.

V. CONCLUSIONS

We performed numerical calculations of the non-Markovianity of a qubit coupled to an environment modeled by a unitary kicked spin chain in a coherent state. Several dynamical regimes of the chain, couplings between qubit and environment, and measures of non-Markovianity were considered. Additionally, the inverse participation ratio of the environment (with respect to the coupled environment) was calculated.

We explored the relation of NM versus IPR and showed that the schemes $\mathcal{N}_{\mathcal{K}}^{\max}$ and $\mathcal{N}_{\mathcal{K}}^{\langle\cdot\rangle}$ proposed in Ref. [11] have important and potentially useful differences with respect to the more common measures BLP and RHP. We showed that that the first mentioned schemes reveal the asymptotic fidelity of the environmental state, leading to two clearly different behaviors of the measures in function of the IPR. Regarding the validity of the former results, we showed that the relations between non-Markovianity and localization for larger environments remain the same. However, self averaging was not observed. A central result of the paper is the identification of a maximum of the NM for intermediately localized environmental states, when using distinguishability as indicator. Such a scenario could be used to protect classical information more efficiently [11].

In the second part of the work, we presented a study of the NM and the IPR as functions of the parameters of the Poincaré sphere in which the initial coherent environmental states live. We concluded that there are structures mainly depicted by the IPR in all dynamical regimes; these are robust under the election of the interaction Hamiltonian and the dimension of the environment. We have shown that although such structures are not classical-like (in the sense that they do not present KAM behavior), they become finer in the transition to chaos when using measures $\mathcal{N}_{\mathcal{D}}^{\max}$ and $\mathcal{N}_{\mathcal{D}}^{\langle\cdot\rangle}$. Such features remain stable with respect to the cutoff time, indicating that they are not random fluctuations, and become finer as the dimension increases.

ACKNOWLEDGMENTS

We acknowledge the support by CONACyT and DGAPA-IN-111015, as well useful discussions with Heinz-Peter Breuer, Diego Wisniacki, and Thomas Gorin.

APPENDIX: DYNAMICAL REGIMES

The spin chain has well-known dynamical regimes in the sense of random matrix theory. The analysis of the spectra (the eigenphases of the Floquet operator) has been done for the chaotic regime and for 16 qubits in Ref. [22].

In this appendix, we present a brief analysis for the integrable regime for 12 qubits and for completeness also for the chaotic and mixed regimes, following the aforementioned work. In order to show the correspondence of the eigenphases of the Floquet operator with the results of random matrix theory, we have to identify the subspaces corresponding to the good quantum numbers of the system. We then compute the distribution of the distance among the nearest neighbor eigenphases [named $P(s)$] in each symmetry sector. The homogeneous spin chain has a symmetry under translation of spins; i.e., the Hamiltonian remains invariant if we take the spin i to $i+1$. Thus we will use the eigenspectra corresponding to the eigenspaces of the translation operator T for the analysis of $P(s)$.

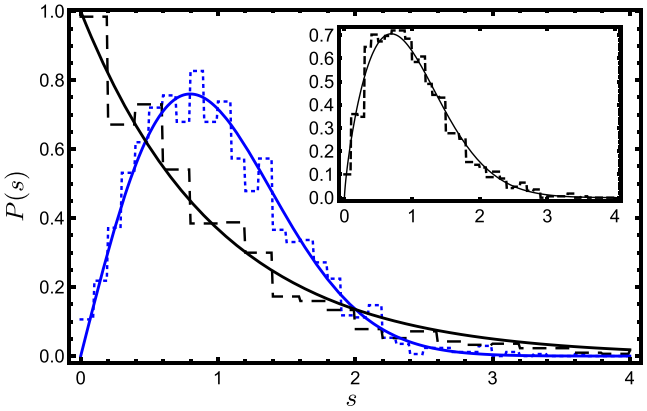

FIG. 15. The figure shows the nearest neighbor spacing distributions $P(s)$ of the spin chain with 12 qubits for two values of the control parameter. In the main figure, the dotted blue curve shows the $P(s)$ for the chaotic regime, and the dashed black shows that for the integrable regime. The solid black curve shows the $P(s)$ for the Poissonian orthogonal ensemble and the solid blue shows it for the circular orthogonal ensemble. In the inset, the dashed curve shows the $P(s)$ for the mixed regime and the solid curve shows that for the Brody distribution with $b = 0.77$; see Ref. [28]. There is good agreement on all regimes with the predictions of random matrix theory.

The symmetry operator acts in the computational basis $|\alpha_0,\ldots,\alpha_{N-1}\rangle$ $(\alpha_j \in \{0,1\})$, as $T|\alpha_0,\ldots,\alpha_{N-1}\rangle = |\alpha_{N-1},\alpha_0,\ldots,\alpha_{N-2}\rangle$. Since $T^N = \mathbb{I}$, its eigenvalues are simply $\exp(2\pi ik/N)$ with k an integer between 0 and $N-1$. Therefore, the Hilbert space is foliated into N subspaces $\mathcal{H} = \oplus_{k\in\mathbb{Z}_N}\mathcal{H}_k$. The chain also has a reflection symmetry given the symmetry operator R, which transforms $R|\alpha_0,\ldots,\alpha_{N-1}\rangle = |\alpha_{N-1},\ldots,\alpha_0\rangle$. This symmetry commutes with the T in the subspace identified by $k=0$, and for even N, also in $k = N/2$; for simplicity these subspaces are removed from the calculation. Figure 15 shows the averaged nearest neighbor spacing distribution over the relevant subspaces, and the ansatz corresponding to the different dynamical regimes [28]. For the integrable regime, we plot the Poisson distribution e^{-s}; for the chaotic, we plot the Wigner surmise; finally, for the mixed regime, we present the Brody distribution [29],

$$P_q(s) = (q+1)s^q\Gamma\left(\frac{q+2}{q+1}\right)^{q+1} e^{-s^{q+1}\Gamma\left(\frac{q+2}{q+1}\right)^{q+1}}.$$

The Brody parameter is denoted by q and takes the ansatz from the integrable case ($q=0$) to the Gaussian orthogonal ensemble ($q=1$), fitting smoothly with the nearest spacing distribution of the chain in the transition to chaos.

[1] J. von Neumann, Wahrscheinlichkeitstheoretischer aufbau der quantenmechanik, Nachr. Ges. Wiss. Goettingen **1927**, 245 (1927).

[2] P. A. M. Dirac, The quantum theory of the emission and absorption of radiation, Proc. R. Soc. London, Ser. A **114**, 243 (1927).

[3] G. Lindblad, On the generators of quantum dynamical semigroups, Commun. Math. Phys. **48**, 119 (1976).

[4] A. Kossakowski, On quantum statistical mechanics of non-hamiltonian systems, Rep. Math. Phys. **3**, 247 (1972).

[5] V. Gorini, A. Kossakowski, and E. C. G. Sudarshan, Completely positive dynamical semigroups of n-level systems, J. Math. Phys. **17**, 821 (1976).

[6] I. de Vega and D. Alonso, Dynamics of non-Markovian open quantum systems, Rev. Mod. Phys. **89**, 015001 (2017).

[7] F. Verstraete, M. M. Wolf, and I. J. Cirac, Quantum computation and quantum-state engineering driven by dissipation, Nat. Phys. **5**, 633 (2009).

[8] J. Nokkala, F. Galve, R. Zambrini, S. Maniscalco, and J. Piilo, Complex quantum networks as structured environments: Engineering and probing, Sci. Rep. **6**, 26861 (2016).

[9] Á. Rivas, S. F. Huelga, and M. B. Plenio, Quantum non-Markovianity: Characterization, quantification, and detection, Rep. Prog. Phys. **77**, 094001 (2014).

[10] H.-P. Breuer, E.-M. Laine, J. Piilo, and B. Vacchini, Colloquium: Non-Markovian dynamics in open quantum systems, Rev. Mod. Phys. **88**, 021002 (2016).

[11] C. Pineda, T. Gorin, D. Davalos, D. A. Wisniacki, and I. García-Mata, Measuring and using non-Markovianity, Phys. Rev. A **93**, 022117 (2016).

[12] P. M. Poggi, F. C. Lombardo, and D. A. Wisniacki, Driving-induced amplification of non-Markovianity in open quantum systems evolution, EPL **118**, 20005 (2017).

[13] T. Prosen, A new class of completely integrable quantum spin chains, J. Phys. A **31**, L397 (1998).

[14] T. Prosen, Exact time-correlation functions of quantum Ising chain in a kicking transversal magnetic field: Spectral analysis of the adjoint propagator in Heisenberg picture, Prog. Theor. Phys. Suppl. **139**, 191 (2000).

[15] H.-P. Breuer, E.-M. Laine, and J. Piilo, Measure for the Degree of Non-Markovian Behavior of Quantum Processes in Open Systems, Phys. Rev. Lett. **103**, 210401 (2009).

[16] Á. Rivas, S. Huelga, and M. Plenio, Entanglement and Non-Markovianity of Quantum Evolutions, Phys. Rev. Lett. **105**, 050403 (2010).

[17] S. Lorenzo, F. Lombardo, F. Ciccarello, and G. M. Palma, Quantum non-Markovianity induced by Anderson localization, Sci. Rep. **7**, 42729(EP) (2017).

[18] L. Benet, T. H. Seligman, and H. A. Weidenmüller, Quantum Signatures of Classical Chaos: Sensitivity of Wave Functions to Perturbations, Phys. Rev. Lett. **71**, 529 (1993).

[19] G. P. Basharin, A. N. Langville, and V. A. Naumov, The life and work of A. A. Markov, Linear Algebra Appl. **386**, 3 (2004).

[20] I. Bengtsson and K. Życzkowski, *Geometry of Quantum States: An Introduction to Quantum Entanglement* (Cambridge University Press, Cambridge, UK, 2006).

[21] A. Goussev, R. A. Jalabert, H. M. Pastawski, and D. Ariel Wisniacki, Loschmidt echo, Scholarpedia **7**, 11687 (2012).

[22] C. Pineda and T. Prosen, Universal and nonuniversal level statistics in a chaotic quantum spin chain, Phys. Rev. E **76**, 061127 (2007).

[23] F. Haake, *Quantum Signatures of Chaos* (Springer-Verlag, New York, 2006).

[24] I. García-Mata, C. Pineda, and D. A. Wisniacki, Quantum non-Markovian behavior at the chaos border, J. Phys. A **47**, 115301 (2014).

[25] M. Žnidarič, C. Pineda, and I. García-Mata, Non-Markovian Behavior of Small and Large Complex Quantum Systems, Phys. Rev. Lett. **107**, 080404 (2011).

[26] A. B. Klimov and S. M. Chumakov, *A Group-Theoretical Approach to Quantum Optics: Models of Atom-Field Interactions* (Wiley-VCH, New York, 2009).

[27] I. García-Mata, C. Pineda, and D. Wisniacki, Non-Markovian quantum dynamics and classical chaos, Phys. Rev. A **86**, 022114 (2012).

[28] T. A. Brody, J. Flores, J. B. French, P. A. Mello, A. Pandey, and S. S. M. Wong, Random-matrix physics: Spectrum and strength fluctuations, Rev. Mod. Phys. **53**, 385 (1981).

[29] T. A. Brody, A statistical measure for the repulsion of energy levels, Lett. Nuovo Cimento **7**, 482 (1973).

Bibliography

[AHFB15] Christian Arenz, Robin Hillier, Martin Fraas, and Daniel Burgarth. Distinguishing decoherence from alternative quantum theories by dynamical decoupling. *Physical Review A - Atomic, Molecular, and Optical Physics*, 92(2):22102, 2015.

[AKM14] Markus Aspelmeyer, Tobias J. Kippenberg, and Florian Marquardt. Cavity optomechanics. *Rev. Mod. Phys.*, 86:1391–1452, Dec 2014.

[ARHP14] Ángel Rivas, Susana F Huelga, and Martin B Plenio. Quantum non-markovianity: characterization, quantification and detection. *Rep. Prog. Phys.*, 77(9):094001, 2014.

[BP07] H.P. Breuer and F. Petruccione. *The Theory of Open Quantum Systems*. OUP Oxford, 2007.

[BvL05] Samuel L. Braunstein and Peter van Loock. Quantum information with continuous variables. *Rev. Mod. Phys.*, 77:513–577, Jun 2005.

[CDG19] Gustavo Montes Cabrera, David Davalos, and Thomas Gorin. Positivity and complete positivity of differentiable quantum processes. *Physics Letters A*, 383(23):2719–2728, 2019.

[Cho75] Man-Duen Choi. Completely positive linear maps on complex matrices. *Linear Algebra and its Applications*, 10(3):285 – 290, 1975.

[CLP07] N J Cerf, G Leuchs, and E S Polzik. *Quantum Information with Continuous Variables of Atoms and Light*. Imperial College Press, 2007.

[CTZ08] Hilary A Carteret, Daniel R Terno, and Karol Zyczkowski. Dynamics beyond completely positive maps: Some properties and applications. *Physical Review A - Atomic, Molecular, and Optical Physics*, 77(4), 2008.

[Cul66] W. J Culver. On the Existence and Uniqueness of the Real Logarithm of a Matrix. *Proceedings of the American Mathematical Society*, 17(5):1146–1151, 1966.

[Den89] L. V. Denisov. Infinitely Divisible Markov Mappings in Quantum Probability Theory. *Theory Prob. Appl.*, 33(2):392–395, 1989.

[EL77] D. E. Evans and J. T. Lewis. *Dilations of Irreversible Evolutions in Algebraic Quantum Theory*, volume 24 of *Communications of the Dublin Institute for Advanced Studies: Theoretical physics*. Dublin Institute for Advanced Studies, 1977.

[EW07] J. Eisert and M. M. Wolf. Gaussian Quantum Channels. In *Quantum Information with Continuous Variables of Atoms and Light*, pages 23–42. Imperial College Press, feb 2007.

[Exn85] Pavel Exner. *Open Quantum Systems and Feynman Integrals*, volume 36. Springer Netherlands, Dordrecht, 1985.

[FPMZ17] S. N. Filippov, J. Piilo, S. Maniscalco, and M. Ziman. Divisibility of quantum dynamical maps and collision models. *Phys. Rev. A*, 96(3):032111, 2017.

[GKL13] A. D. Greentree, J. Koch, and J. Larson. Fifty years of Jaynes–Cummings physics. *J. Phy. B*, 46(22):220201, 2013.

[Gor76] V. Gorini. Completely positive dynamical semigroups of N-level systems. *J. Math. Phys.*, 17(5):821, 1976.

[GSI88] Hermann Grabert, Peter Schramm, and Gert-Ludwig Ingold. Quantum Brownian motion: The functional integral approach. *Physics Reports*, 168(3):115–207, oct 1988.

[GTW09] Alexei Gilchrist, Daniel R. Terno, and Christopher Wood. Vectorization of quantum operations and its use. *arXiv*, page 12, 2009.

[GVAW+03] Frédéric Grosshans, Gilles Van Assche, Jérôme Wenger, Rosa Brouri, Nicolas J. Cerf, and Philippe Grangier. Quantum key distribution using gaussian-modulated coherent states. *Nature*, 421:238, Jan 2003.

[HHHH09] R. Horodecki, P. Horodecki, M. Horodecki, and K. Horodecki. Quantum entanglement. *Rev. Mod. Phys.*, 81(2):865–942, 2009.

[Hol01] Alexander S Holevo. *Statistical Structure of Quantum Theory*, volume 67 of *Lecture Notes in Physics Monographs*. Springer Berlin Heidelberg, Berlin, Heidelberg, 2001.

[Hol07] A S Holevo. One-mode quantum Gaussian channels: Structure and quantum capacity. *Problems of Information Transmission*, 43(1):1–11, mar 2007.

[Hol08] A S Holevo. Entanglement-breaking channels in infinite dimensions. *Problems of Information Transmission*, 44(3):171–184, 2008.

[HR06] S. Haroche and J.-M. Raimond. *Exploring the Quantum: Atoms, Cavities, and Photons*. Oxford University Press, USA, 2006.

[HSP10] Klemens Hammerer, Anders S. Sørensen, and Eugene S. Polzik. Quantum interface between light and atomic ensembles. *Rev. Mod. Phys.*, 82:1041–1093, Apr 2010.

[HZ12] T. Heinosaari and M. Ziman. *The Mathematical Language of Quantum Theory: From Uncertainty to Entanglement*. Cambridge University Press, 2012.

[JC63] E. T. Jaynes and F. W. Cummings. Comparison of quantum and semiclassical radiation theories with application to the beam maser. *Proc. IEEE*, 51:89, 1963.

[KBDW83] Karl Kraus, A. Böhm, J. D. Dollard, and W. H. Wootters. *States Effects Operators*, volume 190 of *Lecture Notes in Physics*. Springer Berlin Heidelberg, Berlin, Heidelberg, 1983.

[KC09] A. B. Klimov and S. M. Chumakov. *A Group-Theoretical Approach to Quantum Optics: Models of Atom-Field Interactions*. Wiley-VCH, 2009.

[KG97] Robert Karrlein and Hermann Grabert. Exact time evolution and master equations for the damped harmonic oscillator. *Physical Review E*, 55(1):153–164, 1997.

[Kos72a] A. Kossakowski. On necessary and sufficient conditions for a generator of a quantum dynamical semigroup. *Bull. Acad. Pol. Sci.*, 20(12):1021, 1972.

[Kos72b] A. Kossakowski. On quantum statistical mechanics of non-hamiltonian systems. *Rep. Math. Phys.*, 3(4):247 – 274, 1972.

[LB99] Seth Lloyd and Samuel L. Braunstein. Quantum computation over continuous variables. *Phys. Rev. Lett.*, 82:1784–1787, Feb 1999.

[Lin76] G. Lindblad. On the generators of quantum dynamical semigroups. *Comm. Math. Phys.*, 48(2):119–130, 1976.

[Lin00] Göran Lindblad. Cloning the quantum oscillator. *Journal of Physics A: Mathematical and General*, 33(28):5059–5076, 2000.

[LRW+18] Ludovico Lami, Bartosz Regula, Xin Wang, Rosanna Nichols, Andreas Winter, and Gerardo Adesso. Gaussian quantum resource theories. *Phys. Rev. A*, 98:022335, Aug 2018.

[MP12] Esteban A Martinez and Juan Pablo Paz. Supplementary material for the paper " Dynamics and thermodynamics for linear quantum open systems. *Phys. Rev. Lett.*, 2012.

[NC11] Michael A. Nielsen and Isaac L. Chuang. *Quantum Computation and Quantum Information: 10th Anniversary Edition*. Cambridge University Press, New York, NY, USA, 10th edition, 2011.

[PGD+16] C. Pineda, T. Gorin, D. Davalos, D. A. Wisniacki, and I. García-Mata. Measuring and using non-Markovianity. *Phys. Rev. A*, 93:022117, 2016.

[Red65] A. G. Redfield. The Theory of Relaxation Processes. In *Advances in Magnetic and Optical Resonance*, volume 1, pages 1–32. Academic Press, jan 1965.

[RFZB12] T. Rybár, S. N. Filippov, M. Ziman, and V. Bužek. Simulation of indivisible qubit channels in collision models. *J. Phys. B*, 45(15):154006, 2012.

[RH12] Ángel Rivas and Susana F. Huelga. *Open Quantum Systems*. SpringerBriefs in Physics. Springer Berlin Heidelberg, Berlin, Heidelberg, 2012.

[RPZ18] Ł. Rudnicki, Z. Puchała, and K. Zyczkowski. Gauge invariant information concerning quantum channels. *Quantum*, 2:60, April 2018.

[RSW02] M. B. Ruskai, S. Szarek, and E. Werner. An analysis of completely-positive trace-preserving maps on M2. *Lin. Alg. Appl.*, 347(1):159 – 187, 2002.

[Sti06] W. Forrest Stinespring. Positive Functions on C*-Algebras. *Proceedings of the American Mathematical Society*, 6(2):211, feb 2006.

[Tun85] Wu-Ki. Tung. *Group theory in physics*. World Scientific, 1985.

[VDD01] F. Verstraete, J. Dehaene, and B. DeMoor. Local filtering operations on two qubits. *Phys. Rev. A*, 64(1):010101, 2001.

[VSL+11] B. Vacchini, A. Smirne, E.-M. Laine, J. Piilo, and H.-P. Breuer.

Markovianity and non-markovianity in quantum and classical systems. *New J. Phys.*, 13(9):093004, 2011.

[VV02] F. Verstraete and H. Verschelde. On quantum channels. *Unpublished*, 2002.

[WC08] M. M. Wolf and J. I. Cirac. Dividing quantum channels. *Comm. Math. Phys.*, 279(1):147–168, 2008.

[WECC08] M. M. Wolf, J. Eisert, T. S. Cubitt, and J. I. Cirac. Assessing non-Markovian quantum dynamics. *Phys. Rev. Lett.*, 101(15):150402, 2008.

[Wol11] Mm Wolf. Quantum channels & operations: Guided tour. *Lecture notes available at http://www-m5. ma. tum. . . .*, 2011.

[WPGP+12] Christian Weedbrook, Stefano Pirandola, Raúl García-Patrón, Nicolas J. Cerf, Timothy C. Ralph, Jeffrey H. Shapiro, and Seth Lloyd. Gaussian quantum information. *Reviews of Modern Physics*, 84(2):621–669, may 2012.

[ZB05] M. Ziman and V. Bužek. Concurrence versus purity: Influence of local channels on Bell states of two qubits. *Phys. Rev. A*, 72(5):052325, 2005.